University of Alberta

SYNTHESIS, STRUCTURES AND REACTIONS OF
HYDROTRIS(PYRAZOLYL)BORATE COMPLEXES OF DIVALENT
AND TRIVALENT LANTHANIDES

by

KUBURAT OLUBANKE SALIU

A thesis submitted to the Faculty of Graduate Studies and Research
in partial fulfillment of the requirements for the degree of

DOCTOR OF PHILOSOPHY

CHEMISTRY

© KUBURAT OLUBANKE SALIU

FALL 2009
Edmonton, Alberta

Examining Committee

Josef Takats, Chemistry

Jonathan G. C. Veinot, Chemistry

Steven H. Bergens, Chemistry

Roderick E. Wasylishen, Chemistry

Suzanne M. Kresta, Chemical and Materials Engineering

David J. Berg, Chemistry, University of Victoria.

To my husband,

Abd Jaleel Aderemi who travelled across the Atlantic Ocean

to Canada to stay with me and support me

my daughter,

Firdaws Ayomide and her future siblings

and my parents

Mr. A. A. Saliu (late) and Mrs. S. O. Saliu,

who raised me and educated me despite all odds.

ABSTRACT

The synthesis and reactions of hydrotris(pyrazolyl)borate, $(Tp^{R,R'})$ supported ytterbium(II) borohydride and lanthanide(III) dialkyl (Ln = Yb, Lu) complexes were investigated. The lanthanide(III) dialkyl complexes were found to undergo both hydrogenolysis reaction and protonolysis reaction with terminal alkynes.

Reaction of $[(Tp^{tBu,Me})YbH]_2$ (**1**) with NH_3BH_3 and $(Tp^{tBu,Me})YbI(THF)$ (**2**) with $NaBH_4$ afforded the corresponding mono-ligand complexes, $(Tp^{tBu,Me})Yb(BH_4)$ (**3**) and $(Tp^{tBu,Me})Yb(BH_4)(THF)$ (**4**), respectively. Compounds **3** and **4** represent rare examples of lanthanide(II) tetrahydroborate complexes. IR spectroscopy data, in the B-H stretching region are consistent with the κ^3-BH_4 bonding mode found in the solid state of compound **4** and the corresponding deuterium labelled BD_4 analogue of **4** shows the expected IR isotope shifts.

Mono-ligand lanthanide dialkyl complexes, $(Tp^{R,R'})Ln(CH_2SiMe_2R'')_2(THF)_{0/1}$ (**5-9**) were synthesized from the homoleptic $Ln(CH_2SiMe_2R'')_3(THF)_2$ (Ln = Yb, Lu; R'' = Me, Ph) complexes by two alternative and complementary methods: alkyl abstraction with the thallium salts of the ligands, $TlTp^{R,R'}$ and protonolysis using the acid form of the ligands, $HTp^{R,R'}$. Hydrogenolysis of the dialkyl complexes $(Tp^{Me2})Ln(CH_2SiMe_3)_2(THF)$ (**7a**, Yb; **8a**, Lu) afforded the corresponding tetranuclear hydride complexes, $[(Tp^{Me2})LnH_2]_4$ (**11**, Yb; **12**, Lu). Similarly, hydrogenolysis of $(Tp)Yb(CH_2SiMe_3)_2(THF)$ (**9**) afforded the hexanuclear hydride $[(Tp)YbH_2]_6$ (**13**). When treated with a variety of terminal alkynes, the dialkyl complexes, $(Tp^{R,Me})Ln(CH_2SiMe_3)_2(THF)$ (**14a**, Y;

8a, Lu), gave the corresponding bis-alkynide complexes, "(Tp^{R,Me})Ln(CCR″)$_2$" (**15-27**). The structures of the complexes depend on the steric size of both the alkyne substituents and the substituent on position 3 of the pyrazolyl ring. Except for the bulkiest substituents, the compounds are dimeric with two asymmetric μ_2-alkynide bridging groups and a coupled alkynide unit bridging the two lanthanide centers via an unusual enyne bonding motif.

The synthesis of Lu(CH$_2$Ph-4-R)$_3$(THF)$_3$ (R = H, **28a**; R = Me, **28b**) was achieved by salt metathesis reactions between KCH$_2$Ph-4-R and LuCl$_3$. Variable temperature NMR studies in THF shows that the formation of these complexes is accompanied by a small amount of the anionic ′ate′ K[Lu(CH$_2$PH-4-R)$_4$(THF)$_n$] (**30**) complexes, which can be prepared independently by reaction of pure Lu(CH$_2$Ph-4-R)$_3$(THF)$_3$ with one equiv. of KCH$_2$Ph-4-R. One of the coordinated THF of **28a** could be removed by trituration with toluene to give Lu(CH$_2$Ph-4-R)$_3$(THF)$_2$ (**29a**). Protonolysis reaction with HTp$^{R,R′}$ afforded the corresponding dibenzyl complexes, (Tp$^{R,R'}$)Ln(CH$_2$Ph-4-R)$_2$(THF)$_n$ (**31-33**).

X-ray crystal structures of complex **4**, the dialkyl complexes **5b**, **6b**, **7** and **8**; dihydride complexes **11**, **12** and **13**; bis-alkynide complexes **15**, **16**, **17**, **21**, **22** and **24** as well as the tribenzyl compounds **28a** and **29a** and dibenzyl complexes **31-33** were determined. The solution behaviour, solid state structures and structural diversity of these complexes are discussed.

ACKNOWLEDGEMENTS

Life without friends would have been a great bore, thus, I would like to acknowledge the following special friends who have contributed chemically or otherwise to make this dream a reality; Adetokunbo Bakinson, Sulayman Olade-po, Olutayo Ogunwemimo, Georgina Blasetti, the Adegokes, the Abolades, the Adedosus, the Olatubosuns, the Owolabis, Dr A. G. A. Bello, Dr Banmeke and a host of others too numerous to mention here.

Finally, I would like to thank my family, the Bellos and the Salius for all their support and encouragement throughout the course of this study.

TABLE OF CONTENTS

Chapter 1

Introduction and Literature Review

Chapter 2

Ytterbium(II) Tetrahydroborate Complexes Supported by

tris(3-*tert*-butyl-5-methylpyrazolyl)borate Ligand:

Synthesis and Characterization

Chapter 3

Scorpionate Supported Lanthanide Dialkyl and Dihydride Complexes

(Ln = Yb, Lu): Synthesis and Characterization

Chapter 4

Synthesis, Characterization and Structural Variation of Lanthanide

Bis-Alkynide Complexes.

4.2 Synthesis of Lanthanide Bis-alkynide Complexes; $[(Tp^{Me2})Ln(CCR'')_2]_2$

Chapter 5

Lanthanide Benzyl Complexes; Lutetium Tribenzyl and Scorpionate

Supported Lanthanide Dibenzyl Complexes.

Chapter 6

Conclusions and Future Works

List of Tables

Chapter 1

Chapter 2

Chapter 3

Chapter 4

Chapter 5

List of Figures

Chapter 1

Chapter 2

Chapter 3

Chapter 4

Chapter 5

List of Schemes

Chapter 1

Chapter 3

Chapter 4

Chapter 5

Chapter 6

LIST OF ABBREVIATIONS AND SYMBOLS

Ad	adamant-1-yl
Å	Angström
Anal.	analytical
atm	atmospheres
av.	average
bipy	bipyridine
br.	broad
^{t}Bu	*tertiary*-butyl, $C(CH_3)_3$-
ca.	circa (approximately)
cald.	calculated
Cp	cyclopentadienyl
Cp*	pentamethylcyclopentadienyl
deg.	degree
eq.	equation
equiv.	equivalent
fac	facial
FT-IR	Fourier Transform Infrared
GC-MS	gas chromatography-mass spectrometry
HMBC	heteronuclear multiple bond correlation
HMQC	heteronuclear multiple quantum coherence
HMDSO	hexamethyldisiloxane
Hz	Hertz

h	hour(s)
J	coupling constant
K	Kelvin
Ln	lanthanide: Sc, Y, La-Lu
Me	methyl,CH_3-
mer	meridional
mg	milligram(s)
MHz	megahertz
mL	millilitres
mmol	millimoles
m/z	mass to charge ratio
m	meta-
NMR	nuclear magnetic resonance
o	ortho-
ppm	parts per million
Ph	phenyl
py	pyridine
Pz	pyrazolyl
″t″	pseudo-triplet
THF	tetrahydrofuran
Tn	thienyl
Tp	hydrotris(pyrazolyl)borate
Trit′	tris(3,5-di-tert-butylphenyl)methyl
v	very
VT	variable temperature

List of Compounds and Code Numbers
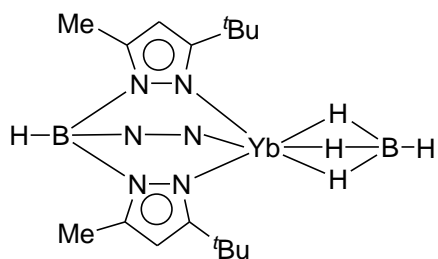
3
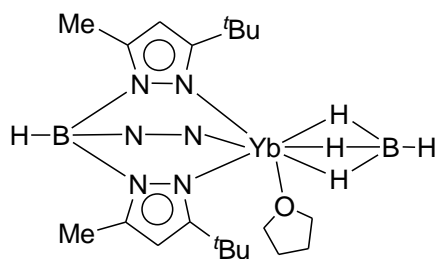
4
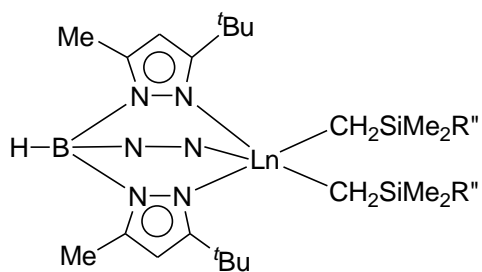
Ln = Yb, **5**; Lu, **6**; R″ = Me, Ph
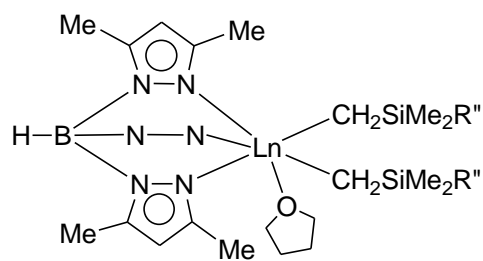
Ln = Yb, **7**; Lu, **8**; R″ = Me, Ph
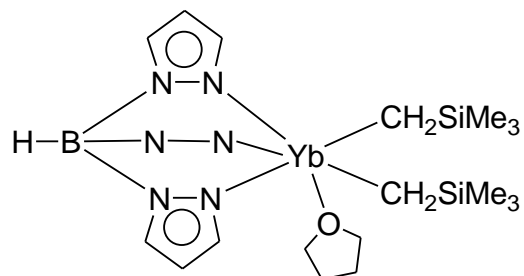
9
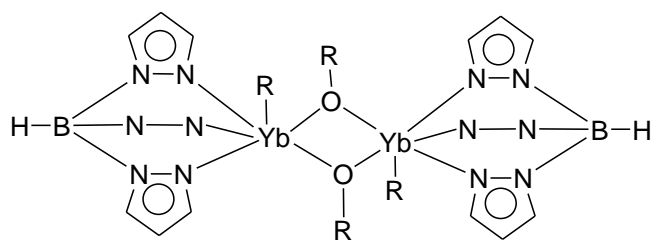
R = CH₂SiMe₃, **10**

Ln = Yb, **11**; Lu, **12**.

13
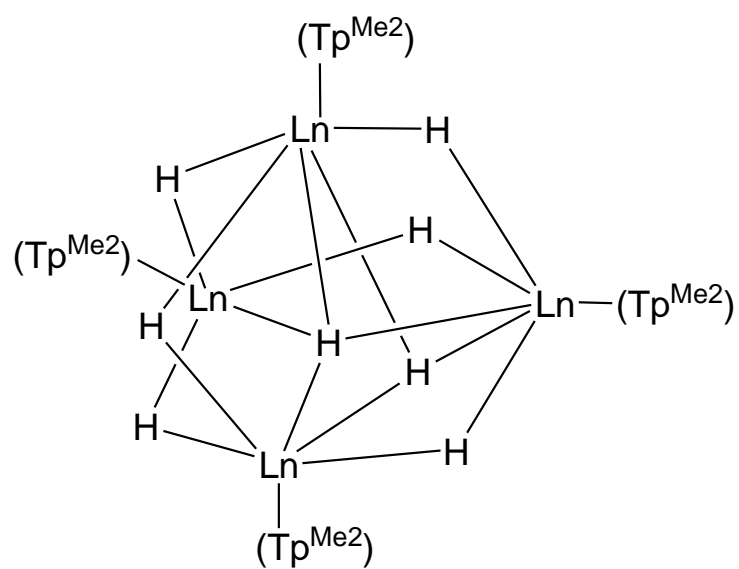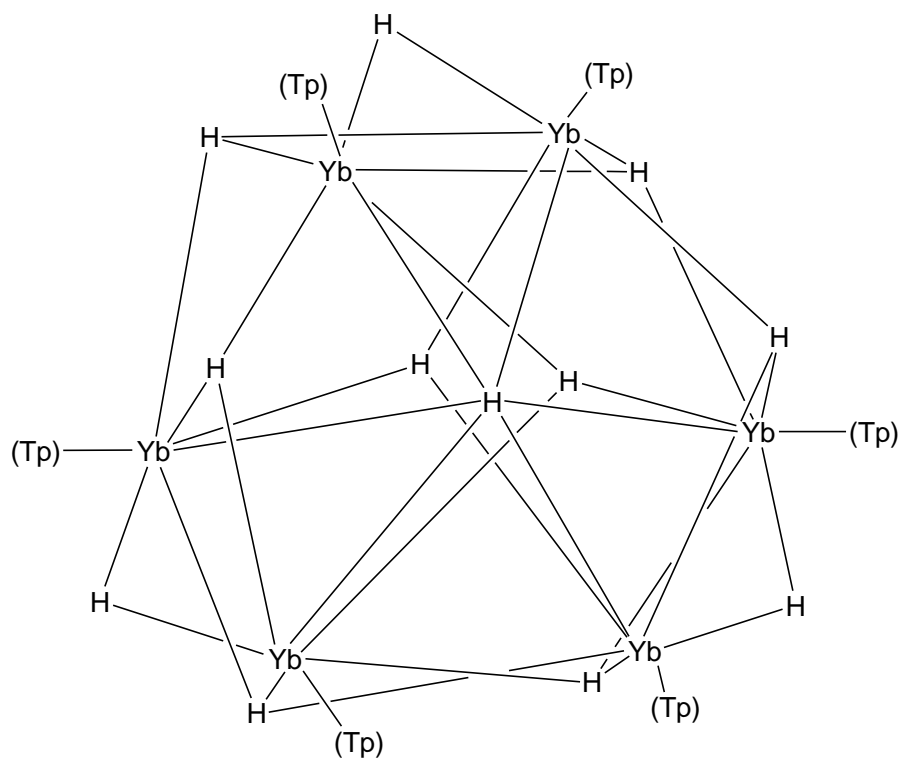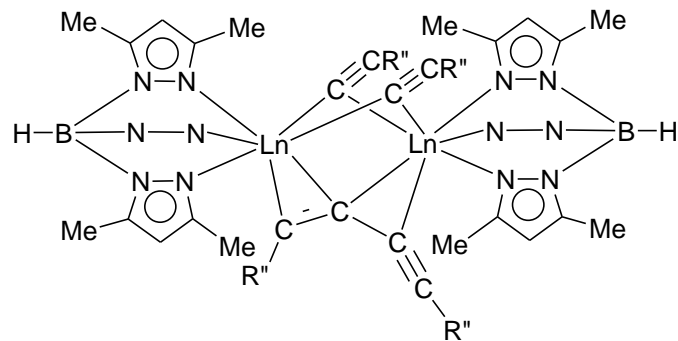
R″ = Ph, **15**; SiMe₃, **17**; ^{t}Bu, **19**; Ad, **21**; Ln = Y.

R″ = Ph, **16**; SiMe₃, **18**; ^{t}Bu, **20**; Ln = Lu.
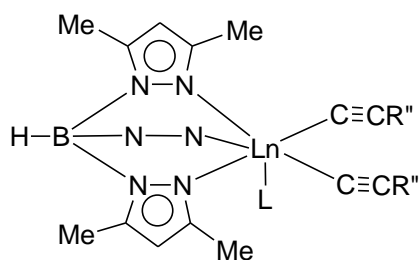
R = ^{t}Bu, L = 2,2′-bipy, **22**; Ln = Lu.

R = Trit′, L = THF, Ln = Y, **23**; Lu, **24**.
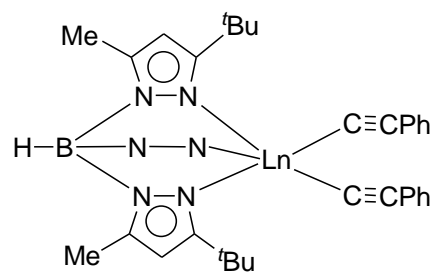
Ln = Y, **26**; Lu, **27**.
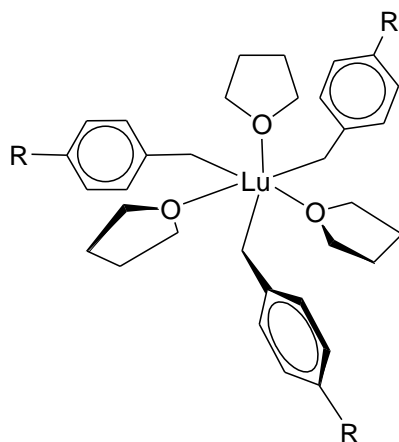
R = H, **28a**; Me, **28b**.
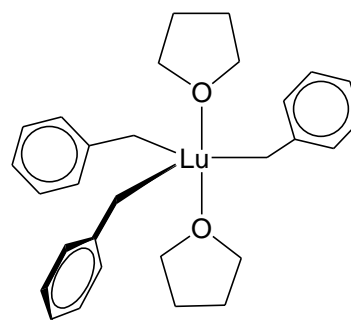
29a
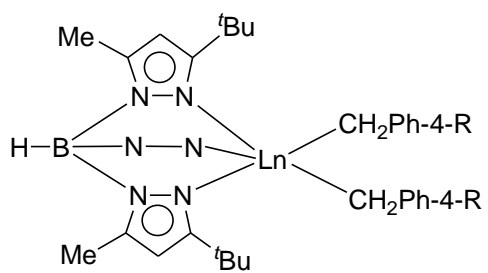
R = Me, Ln = Y, **31b**

R = H, **32a**; Me, **32b**; Ln = Lu.
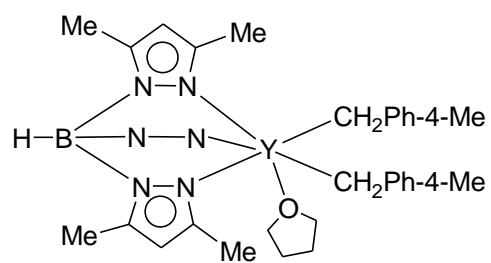
33b

Chapter 1

Introduction and Literature Review

1.1 The Lanthanides

Lanthanum and the 14 elements which follow it constitute a class of chemically similar elements collectively referred to as the lanthanides, which are generally denoted by the symbol Ln. They are also commonly referred to as the rare earths. This name, which was originally used due to the fact that the elements were initially obtained as oxides (earths) from relatively rare minerals, is rather a misnomer as they are really neither rare nor earths. With the exception of the radioactive promethium which does not occur naturally, the lanthanides are relatively abundant in the earth's crust with the least abundant lanthanide, lutetium, being even more abundant than iodine.[1,2,3]

The isolation of yttria, a mineral which was later revealed to contain at least ten new elements, (yttrium, terbium, erbium, ytterbium, scandium, holmium, thulium, gadolinium, dysprosium and lutetium) by the Finnish chemist, Johann Gadolin in 1794 was the hallmark of the discovery of the lanthanides.[1] This was followed by the independent isolation of another new oxide, ceria, by M. H Klaproth, and by J. J. Berzelius and W. Hisinger. This oxide was also found to contain the oxides of cerium, lanthanum, praseodymium, samarium and uranium.[1] A major problem encountered in the early studies of these elements is their separation, this is because of their similar properties which thus meant multi-step fractional recrystallization and/or solvent extraction was needed to achieve complete separation.

1.1.1 Properties of Lanthanides.

The lanthanides are f-block elements and their ground state electronic configuration corresponds to the gradual filling of 4f-orbitals on going from lanthanum (Z = 57 i.e., $[Xe]4f^05d^16s^2$) to lutetium (Z = 71 i.e., $[Xe]4f^{14}5d^16s^2$). Due to their core-like nature (because of their poor shielding and small radial extension) the 4f-orbitals are largely uninvolved in bonding and this is responsible for the similarities in the chemical properties of the lanthanides. This, to a large extent is also responsible for the differences in the chemical properties of the lanthanides when compared with those of typical transition metals in which the valence d-electrons participate actively in their chemical interactions. Although strictly transition metals, scandium and yttrium are often included in treatment of lanthanides because of their chemical similarities to the lanthanides.

A major consequence of the core-like nature of the 4f orbital electrons is that the bonding of the lanthanides is essentially ionic in all non-zero oxidation state. Thus, unlike in transition metal complexes in which ligand field effects influence the geometry and coordination number, in lanthanide complexes where ligand field effects are relatively unimportant, these parameters are determined by the number, size and charge of the ligands.[4] Thus, magnetic and spectroscopic properties of the lanthanides show very little dependence on the nature and number of the ligands. Similarly, the colors of their complexes are for the most part not affected by the nature and/or number of ligands present. Another consequence of the ionic bonding is the pervasiveness of ligand redistribution reactions which often complicate the chemistry of the elements.[5] The most common oxidation

state for the lanthanides is +3, corresponding to loss of the 5d and 6s electrons. Since the 4f electrons have poor radial extension and are poorly shielding, there is a steady decrease in the size of Ln^{3+} ions from 1.032Å (La^{3+}; [Xe] $4f^0$) to 0.861Å (Lu^{3+}; [Xe] $4f^{14}$) for coordination number 6, as the lanthanide series is traversed. This phenomenon is known as the lanthanide contraction.[6,7] Although the +3 oxidation state is the commonest for the lanthanides, the divalent and tetravalent states are accessible for some of them. The tetravalent state is found mostly in cerium compounds, Ce^{4+} ([Xe]$4f^0$) although it is also observed in praseodymium and terbium compounds albeit to a lesser extent due to their strongly oxidizing nature. For many years, the divalent state was the exclusive domain of samarium (Sm^{2+}, [Xe]$4f^6$), europium (Eu^{2+}, [Xe]$4f^7$) and ytterbium (Yb^{2+}, [Xe]$4f^{14}$). Recently, this has been expanded to include the more reducing neodymium (Nd^{2+}, [Xe]$4f^4$), dysprosium (Dy^{2+}, [Xe]$4f^{10}$) and thulium, (Tm^{2+}, [Xe]$4f^{13}$).[8,9] Although the ability of these elements to exist in other oxidation state apart from +3 is often attributed to special stability of empty (Ce^{4+}; $4f^0$), half-filled (Eu^{2+} and Tb^{4+}; $4f^7$) and filled (Yb^{2+}; $4f^{14}$) shells, this explanation does not account for the existence of Pr^{4+} ($4f^1$), Nd^{2+} ($4f^4$), Sm^{2+} ($4f^6$), Dy^{2+} ($4f^{10}$) and Tm^{2+}($4f^{13}$).

Unlike in transition metal compounds, formally two electron processes such as oxidative addition, reductive elimination, etc. are not possible with the lanthanides because no single metal appears to exist in both divalent and tetravalent oxidation state, although one electron processes are known.[10]

1.2   Ligand System in Organolanthanide Chemistry.

Due to the highly ionic nature of lanthanide-ligand bonds and the large size of the metals, successful isolation of lanthanide complexes is dependent on the proper choice of ligands. Ligands of choice should be those with sufficient bulk to prevent solvent coordination, dimerization or ligand redistribution at the large lanthanide centres.

While a ligand of sufficient steric bulk is necessary, it is important to bear it in mind that the bulk should not be such as to shut down the reactivity at the lanthanide centre which is the goal of the synthesis in the first place. In addition, the ligand should be capable of forming strong ionic bonds, i.e., essentially sigma-donor type ligands.

1.2.1   Cyclopentadienyl Ligands

The most ubiquitous ligand used in synthetic organolanthanide chemistry is the cyclopentadienyl ligand and its various substituted and modified forms. While offering easy access to well-defined, monomeric lanthanide organometallic complexes, the steric requirements of lanthanides are such that in most cases, two cyclopentadienyl units are required to sterically saturate the lanthanide centers, especially for larger lanthanide centers, thus limiting only one valence site for another reactive ligand, Figure 1.1.

The use of this ligand has led to an appreciable development in the organometallic chemistry of the lanthanides,[3] however, the limitation of the reactive

site to mostly one has triggered the search for new ancillary environments for the lanthanides.[11,12]
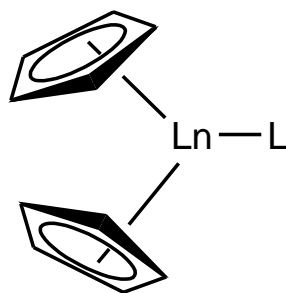
Figure 1.1: Schematic of "$(C_5H_5)_2LnL$" Type Complexes.

1.2.2   Other Ligand Systems

Not surprisingly, the majority of other ligands that have been used in organolanthanide chemistry are those based on hard N and O donor atoms due to the high oxophilicity of the lanthanides (hard acid). This area of organolanthanide chemistry is currently attracting a lot of attention and efforts in this regard have been reviewed comprehensively.[12,13,14] A brief survey of these ligands is given in Scheme 1.1.

Several ligands based on hard donor atoms have been used and interesting chemistry uncovered in most cases. Examples of these ligands include monoanionic, bidentate N-N and N-O donor ligands such as the amidinates,[15] the guanidinates,[16] and several modifications[17] aminotropoiminates,[18] the β-diketiminates (nacnac),[19] salicylaldiminates[20] and dianionic ligands based on N-N (diamides),[21,22] O-O (dialkoxides, silsequioxanes) donors.[23,24] In terms of occupied coordination sites and electron donation, the tridentate ligands are the closest to

5

the cyclopentadienyls, however the charge on the ancillaries can vary from neutral to dianionic. Examples of neutral ancillaries include the facially coordinating tri-azacyclononane heterocycle and the tris(pyrazolyl)methane ligands, both of which

Cyclopentadienyl-based ligands; R = H, alkyl groups E^- $E = NR, PR, C_5R_5$

Amidinates
R = alkyl, aryl, NR_2 etc.

β-Diketiminates

Salicyaldiminates

E = O, MAC
E = NH, DAC

Tris(pyrazolyl)methane

Tris(pyrazolyl)borate
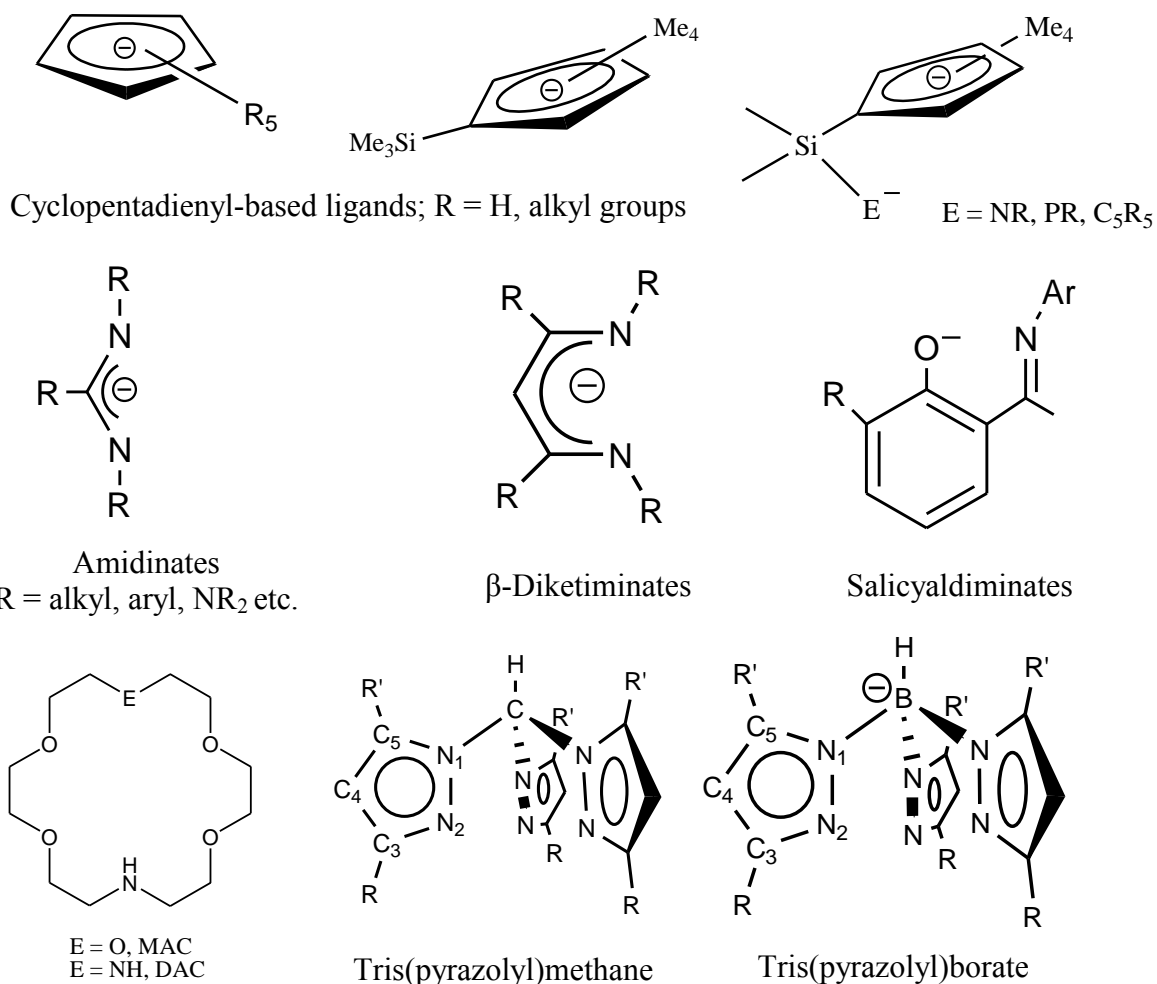
Scheme 1.1: Selection of Ligand Systems in Organolanthanide Chemistry.

are based on the N-N-N framework.[25,26] The monoanionic ligands used vary widely depending on the nature of the donor atoms. Examples includes the charged analogue of the tris(pyrazolyl)methane ligands, the tris(pyrazolyl)borates,[27] modified amidinate ligands,[28,29] both of which are based

6

on the N-N-N framework. Others include N-O-N (arylsiloxide),[30] P-N-P (ami-dodiphosphines),[31] N-P-N (diamido phosphine), which includes examples of mono anionic and dianionic type ligands.[32] Higher denticity ligands used includes examples from Berg's group on their use of deprotonated azacrowns. The ligands used include mono-aza-18-crown-6 (MAC) ligand[33] as well as di-aza-18-crown-6 (DAC) ligand,[34] which are mono-and di-anionic, respectively. Although these ligands have expanded the interesting chemistry of the lanthanides, in most cases their applications have been limited to the group 3 metal and the later lanthanides. The sterically loaded tris(pyrazolyl)borate ligands have however been shown to be very effective ancillaries capable of suppressing ligand redistribution for elements throughout the periodic table,[35] including the lanthanides,[36] without necessarily shutting off the reactivity at the lanthanide center.

1.2.3 Poly(pyrazolyl)borate Ligands ("Scorpionates")

First reported in 1966 by Trofimenko, the pyrazolylborate ligands constitute a class of highly versatile ancillary ligand system in coordination and organometallic chemistry,[27,37] and, in fact they are probably the most popular ancillary ligand used in lanthanide chemistry after cyclopentadienyl ligands. They are essentially borohydride anions in which two $(R_2BPz_2)^-$, three $(RBPz_3)^-$ or four $(BPz_4)^-$ [R = H, alkyl; Pz = pyrazolyl group] of the hydrides have been replaced with pyrazolyl groups. Based on Trofimenko's suggestion, the abbreviations used for these ligands are $Bp^{R,R'}$ for dihydrobis(pyrazolyl)borate, $Tp^{R,R'}$ for hydro-tris(pyrazolyl)borate and $PzTp^{R,R'}$ for the tetrakis(pyrazolyl)borate, respectively;

7

and R and R′ represent the 3- and 5- substituents of the pyrazolyl ring, respective-ly.[38] The versatility of these ligands stems from the large variety of substituents that can be introduced into the position 3 and 5 of the pyrazolyl rings, thus mod-ifying the steric size of the ligand. Based on the uninegative charge of the $Tp^{R,R`}$ ligands, when coordinated in the κ^3 fashion, they are formally analogous to the cyclopentadienyl fragment. Tables 1.1 and 1.2 shows general and steric compari-son of $Tp^{R,R′}$ and C_5R_5 ligands, respectively.

Table 1.1: General Comparison of C_5R_5 and $Tp^{R,R′}$ Ligands.[28, 39]

Common Features		
Electrons donated (number)	6	6
Coordination sites occupied	3	3
Charge	-1	-1
Differentiating Features		
Electrons donated (type)	π-MOs	3-σ lone pairs
Substitutable positions	5	10
Cone angle	≤ 146°	≥184°
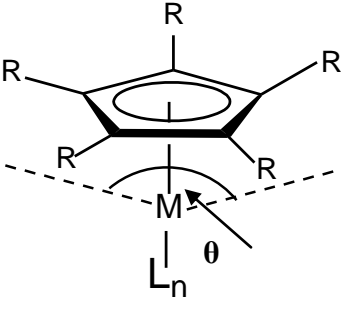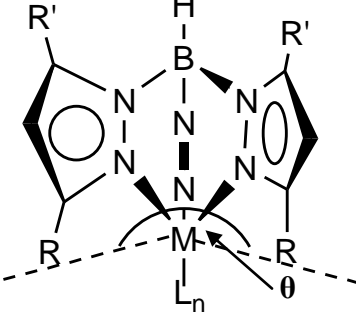
1.3 Cyclopentadienyl Lanthanide Chemistry

1.3.1 Trivalent Lanthanides Chemistry

The first well-characterized organolanthanide complexes prepared were the tris(cyclopentadienyl) complexes, $(C_5H_5)_3Ln$.[39,40,41] Preparation of heteroleptic chloro-dimers, $[(C_5H_5)_2Ln(\mu\text{-}Cl)]_2$ was successful only for the later lanthanides (Ln = Sm, Gd, Dy, Ho, Er, Yb and Lu). For the early lanthanides (La, Ce, Pr and Nd), this ligand combination proved insufficient to satisfy the steric requirement of the larger lanthanides, hence only the tris(cyclopentadienyl) complexes,

Table 1.2: Steric Comparison of C_5R_5 and $Tp^{R,R'}$ Ligands.

R	Cone Angles(°)[*]	
H	136	184
Me	185	239
^tBu	–	243

[*] θ = cone angle

(C$_5$H$_5$)$_3$Ln, were obtained, presumably due to ligand redistribution.[5,42] The isolation of these heteroleptic species was achieved for the early, larger lanthanide by the use of the more sterically demanding bis(trimethylsilyl)cyclopentadienyl ligand, C$_5$H$_3$(SiMe$_3$)$_2$.[43]

The structures of the complexes reflect the variation in sizes of the lanthanide metals. For the tris(cyclopentadienyl) complexes, (C$_5$H$_5$)$_3$Ln, the compounds are polymeric in nature with coordination number decreasing with the size of the lanthanide metal, from 11 (La and Pr), to 9 (Yb) to 7 (Lu) with intermediate coordination numbers in between, Figure 1.2.

Ln = La, Pr
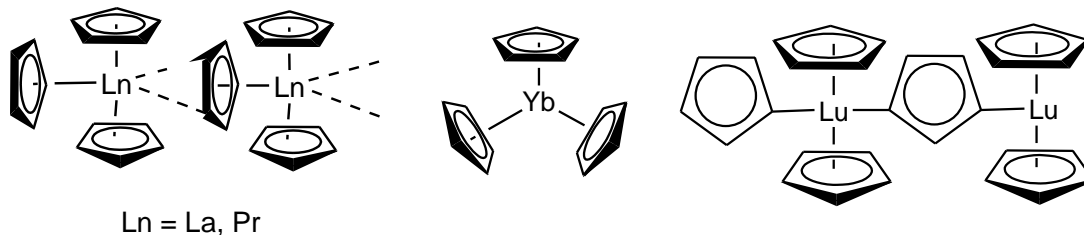
Figure 1.2: Structures of (C$_5$H$_5$)$_3$Ln.

By utilizing the bulky pentamethylcyclopentadienyl ligand, C$_5$Me$_5$, (Cp*), the first monomeric bis(cyclopentadienyl) halide complex of an early lanthanide was isolated by Evans and co-workers via salt metathesis reaction giving the ionic complex, [Li(C$_4$H$_8$O$_2$)$_2$][(C$_5$Me$_5$)$_2$NdCl$_2$].[44] The salt free chloride, (C$_5$Me$_5$)$_2$NdCl(THF) and amide, (C$_5$Me$_5$)$_2$NdN(SiMe$_3$)$_2$ complexes were isolated a year later by Andersen *et al.*[45] With the sterically bulky C$_5$Me$_5$, complexes of the type [(C$_5$Me$_5$)$_2$Ln(μ-Cl)]$_2$ are too crowded to form symmetrically bridging dimers as observed in the case of less bulky ligands such as C$_5$H$_5$, C$_5$H$_3$R$_2$ etc. This

results in the formation of asymmetrically bridging dimers (*vide infra*).[46] With the more reactive methyl co-ligand, isolation of complexes of the type $(C_5H_4R)_2LnMeL$ is limited to the smaller lanthanide centers (R = H, Me; Ln = Sc, Yb, Lu; L = pyridine, THF).[47,48,49] Attempts to remove the coordinated THF led to either formation of the dimeric species $[(C_5H_5)_2Ln(\mu\text{-Me}]_2$ (Ln = Yb, Lu) or decomposition into unidentified species (Ln = Sc).[44] For the larger lanthanides (Ln = Gd, Ho, Er, Tm), the compounds were always obtained as the dimer, $[(C_5H_5)_2Ln(\mu\text{-Me}]_2$. The first neutral bis(pentamethylcyclopentadienyl) lanthanide methyl compound, $(C_5Me_5)_2LuCH_3(Et_2O)$,[50] was obtained in several steps and the reaction was reported to be dependent on both solvent and alkali metal. The best and most reliable reaction sequence is shown in eq. 1.1. The solvent free compound, $(C_5Me_5)_2LuCH_3$ could also be obtained by treating with triethylamine followed by evacuating under vacuum, eq. 1.1. $(C_5Me_5)_2LnMe$ (Ln = Yb, Lu)

$$Cp*_2LuCl_2Li(Et_2O)_2 \xrightarrow[\text{- 2LiCl}]{2CH_3Li/THF} Cp*_2Lu(CH_3)_2Li(THF)_3 \xrightarrow[\text{vacuum}]{75^\circ C} Cp*_2Lu(CH_3)_2Li \xrightarrow[\text{- LiAl(CH}_3)_4]{2Al(CH_3)_3}$$

$$Cp*_2Lu(CH_3)_2Al(CH_3)_2 \xrightarrow[-40^\circ C]{ether} Cp*_2Lu(CH_3)(Et_2O) \xrightarrow[\text{vacuum}]{NEt_3} Cp*_2LuCH_3 \qquad 1.1$$
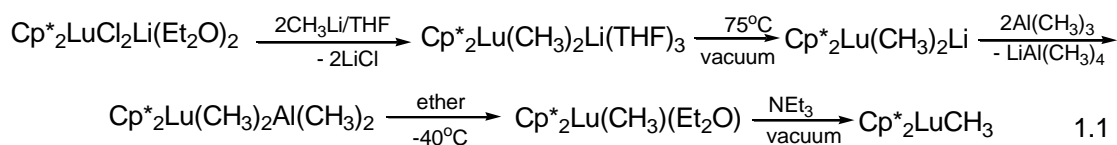
compounds crystallize as weakly bonded dimers which are in rapid equilibrium with the sterically unsaturated monomers, Figure 1.3.[51] Monomeric $(C_5Me_5)_2YMe(THF)$ was obtained and the structure confirmed in the solid state.[52] Hydrogenolysis of $(C_5Me_5)_2LuMe$ gave the hydride, $(C_5Me_5)_2LuH$ which also exist as a weakly coordinating dimer in rapid equilibrium with the monomeric species in solution. Both the alkyl and hydride compounds display interesting

reactivities towards a variety of substrates including benzene, toluene, di-ethylether, pyridine and tetramethylsilane.[53]

Synthesis of mono-C_5R_5 lanthanide complexes generally require more careful synthetic approaches due to the tendency of the mono ligand species to undergo ligand redistribution reaction to give the more thermodynamically stable bis-C_5R_5 derivatives. Furthermore, isolation of the corresponding lanthanide alkyl complexes is often complicated by formation of ′ate′ type complexes due to the salt elimination strategy commonly employed.

Bruno and co-workers demonstrated the effect of varying the size of the halide on the isolation of mono-C_5Me_5 lanthanide dihalide complexes.[54] By

R = H, Me; Ln = Y, Yb

(a)

Ln = Yb, Lu

(b)
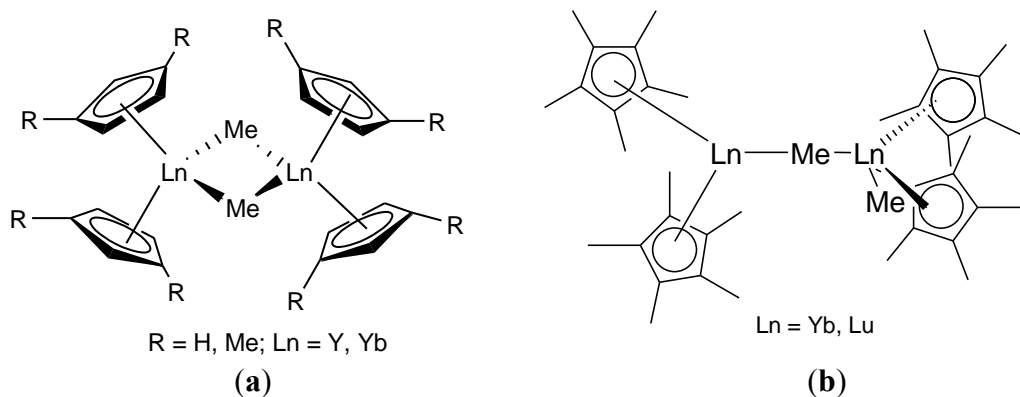
Figure 1.3: Structures of $[(C_5H_3R_2)_2Ln(\mu\text{-Me})]_2$ (**a**) and $[(C_5Me_5)_2Ln(\mu\text{-Me})]_2$ (**b**).

utilizing the bulky C_5Me_5/iodide combination, mono(pentamethylcyclopentadienyl)lanthanide diiodide, $(C_5Me_5)LnI_2$ (THF)$_3$(Ln = Ce, La) was isolated whereas the smaller chloro ligand yielded only the ′ate′ complex, $[Li(ether)_2][(C_5Me_5)_2CeCl_2]$.

The importance of Ln-C containing species is well documented. Reaction of the $(C_5Me_5)LnX_2(THF)_n$ (Ln = La, X = I, n = 3; Ln = Ce, X = OAr, n = 0) complexes with MR (M = Li or K; R = $CH(SiMe_3)_2$) species affords the corresponding monomeric, mono C_5Me_5 lanthanide dialkyl species, $(C_5Me_5)Ln(CH(SiMe_3)_2)_2$.[55,56] $(C_5Me_5)La(CH(SiMe_3)_2)_2$ was characterized both in solution and in the solid state and it represents the first salt free and solvent free mono-C_5Me_5 lanthanide dialkyl complex. Reaction of $(C_5Me_5)Y(OAr)_2$ and $Li(CH(SiMe_3)_2)$ afforded the mixed alkyl-alkoxide species $(C_5Me_5)Y(OAr)(CH(SiMe_3)_2)$ (Ar = 2,6-di-*tert*-butylC$_6$H$_4$), which undergoes hydrogenolysis to give the hydride dimer, $[(C_5Me_5)Y(OAr)\mu\text{-}H]_2$.[57] The stability of $(C_5Me_5)La(CH(SiMe_3)_2)_2$ and $(C_5Me_5)Y(OAr)(CH(SiMe_3)_2)$ was attributed to the presence of β-Si-C-Ln agostic interactions, as evidenced by the elongation of the C-Si bonds.[58] The isolation of these mono-C_5Me_5 dialkyl species is limited to the very bulky alkyl co-ligand, bis(trimethylsilyl)methyl as shown above and this generally has lower reactivity when compared with other alkyl groups such as the methyl (CH_3), trimethylsilylmethyl (CH_2SiMe_3), benzyl ($CH_2C_6H_5$), etc.

By using the less bulky alkyl ligand, CH_2SiMe_3, and the smallest lanthanide metal, lutetium, $(C_5Me_5)Lu(CH_2SiMe_3)_2(THF)$ was obtained by direct protonolysis of $Lu(CH_2SiMe_3)_3(THF)_2$ by $H(C_5Me_5)$.[59] The coordinated THF could be easily replaced by DME and 2,2′-bipyridine to give the corresponding DME and bipyridyl complexes, $(C_5Me_5)Lu(CH_2SiMe_3)_2(L)$ (L = DME, 2,2′-bipy). The bipyridyl complex, $(C_5Me_5)Lu(CH_2SiMe_3)_2(bipy)$, undergoes σ-bond metathesis reaction with various substrates: with one or two equivalents of 2,6-diisopropyl

aniline the corresponding mono- and bis-amide compounds were obtained, with phenyl acetylene, a dimeric compound containing both coupled and terminal alkynide moieties was obtained and characterized in the solid state. In the presence of coordinating solvent such as THF and pyridine, the terminal bis-alkynide compound, $(C_5Me_5)Lu(CCPh)_2(bipy)L$ (L = THF, pyridine) was obtained, Scheme 1.2. The stability of these complexes may be attributed to presence of the bipyridine ligand.[59]
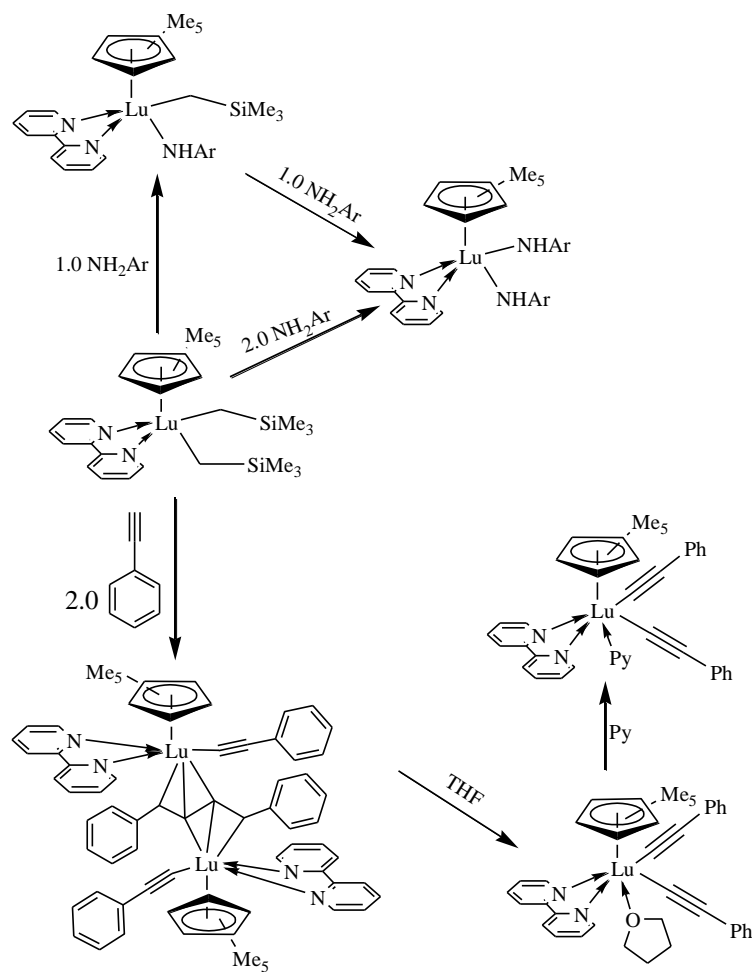
Scheme 1.2: Reactions of $(C_5Me_5)Lu(CH_2SiMe_3)_2(2,2'$ bipy) With Various Substrates.

The dibenzyl complex of gadolinium, $(C_5Me_5)Gd(CH_2Ph)_2(THF)$, was prepared by the salt metathesis of *in-situ* prepared $(C_5Me_5)GdBr_2(THF)$ with KCH_2Ph and it was characterized in the solid state.[60]

More success with synthesis of lanthanide dialkyls was achieved by using modified bulkier "(C_5Me_5)" ligands. Thus, protonolysis of $Ln(CH_2SiMe_3)_3(THF)_2$ with $C_5HMe_4SiMe_2R$ (R = Me, Ph,C_6F_5; Ln = Y; [61] and R = Me; Ln = Sc, Y, Gd, Dy, Ho, Er, Tm and Lu)[62] gave the corresponding dialkyl complexes. These complexes were found to be active catalysts for the polymerization of polar monomers such as *tertiart*-butyl acrylate and acrilonitrile.[61]

When compared with the metallocene hydride complexes of the lanthanides, "$(C_5R_5)_2LnH$" the corresponding dihydrides, "$(C_5R_5)LnH_2$" are rather rare. Early attempts to prepare such complexes via hydrogenolysis of $(C_5Me_5)Lu(CH_2SiMe_3)(CH(SiMe_3)_2)(THF)$ or $(C_5Me_5)_2Lu(CH_2CMe_3)_2(THF)$ did not afford any isolable hydride species even though a reaction was reported to occur due to the formation of free alkanes.[63] Recently, tetranuclear lanthanide hydride clusters of the form $[\{(\eta^5\text{-}C_5Me_4SiMe_3)Ln(\mu\text{-}H)_2\}_4(THF)_n]$ (Ln = Sc, Y, Gd, Dy, Ho, Er, Tm and Lu ; n = 0, 1, 2)[64] have been isolated either from hydrogenolysis or treatment of the corresponding dialkyl complexes, $(C_5Me_4SiMe_3)Ln(CH_2SiMe_3)_2(THF)$ with $PhSiH_3$. In the case of lutetium, hydrogenolysis of the dialkyl compound was reported to give a mixture of hydride species.[64] However, reaction of the lutetium dialkyl compound, $(C_5Me_4SiMe_3)Lu(CH_2SiMe_3)_2(THF)$ with phenylsilane yielded first, the mixed alkyl/hydride dimer $[(C_5Me_4SiMe_3)Lu(CH_2SiMe_3)(\mu\text{-}H)(THF)]_2$ which then

15
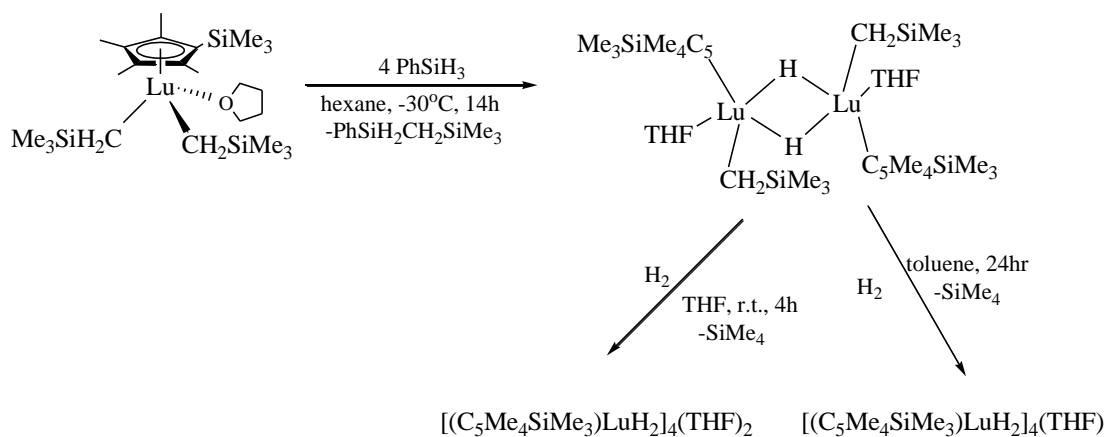
Scheme 1.3: Synthesis of Lutetium Polyhydride Complexes.

undergo hydrogenolysis to give the desired hydride compound, Scheme 1.3.[65] These hydrides have exquisite reactivities towards unsaturated molecules such as CO, CO_2, styrene, cyclohexadiene, alkynes as well as nitriles.[66]

1.3.2   Divalent Lanthanide Chemistry

Unlike the trivalent species, the chemistry of divalent lanthanide complexes was for many years the exclusive domain of Sm, Eu and Yb. The standard electrode potentials in aqeous solution for the Ln^{3+}/Ln^{2+} couple are -1.5V, -0.35V and -1.1V for Sm, Eu and Yb, respectively.[67,68] Thus in terms of reducing power, Sm^{2+} ion is the most reactive whereas Eu^{2+} is the least reactive. Sterically however, Yb^{2+} is the smallest, therefore its compounds are generally easier to handle and better behaved than the corresponding Sm^{2+} compounds. Although only Yb^{2+} is diamagnetic and therefore allow easy monitoring of reactions by NMR, Sm^{2+} compounds are also easily studied by NMR. In fact, it is the only lanthanide which gives sharp NMR signals in both +2 and +3 oxidation states; it gives relatively

sharp signals when compared with other trivalent lanthanide species. The appearance of sharp signal in the NMR spectra of Sm(II) and Sm(III), despite a magnetic moment of 3.4-3.8 μ_B for Sm(II) and 1.3-1.9 μ_B for Sm(III) is attributed to the short electron spin relaxation time.[69]

This area of organolanthanide chemistry has however, recently been expanded to include the more reducing lanthanide(II) ions of Nd(II), Dy(II) and Tm(II).[8,9] The aqueous standard electrode potentials for the Ln^{3+}/Ln^{2+} couple are -2.3V, -2.5V and -2.6V for Tm, Dy and Nd, respectively.[67,68]

1.3.3 $(C_5R_5)_2Ln$ Complexes.

Bis(cyclopentadienyl)Yb(II), $(C_5H_5)_2Yb$, was first synthesized by the reduction of cyclopentadiene with ytterbium metal in liquid ammonia.[41] Ammonia free synthetic routes have since been devised.[70] The analogous samarium compound was initially prepared by reducing $(C_5H_5)_3Sm$ with $KC_{10}H_8$.[71] More recently, these compounds were isolated by Kagan and co-workers via salt metathesis reaction between $LnI_2(THF)_x$ and NaC_5H_5.[72] These compounds are insoluble in hydrocarbons and common ether solvents, thus their chemistry remained unexplored and no structural information is available. The use of C_5Me_5 ligand has led to a spectacular growth in the organometallic chemistry of divalent lanthanides as in the case of early transition metals and the actinides. Being bulkier than the parent unsubstituted C_5H_5, C_5Me_5 imparts greater stability to organometallic systems. Also, the high degree of substitution confers more solubility as well as crystallinity to these systems thus making the exploration of their chemistry possible.

The complexes are easily prepared by salt metathesis of $LnX_2(THF)_2$ (Ln = Yb, X = Br; Ln = Sm, X= I) with alkali metal cyclopentadienide in ether solvents.[73,74] $(C_5Me_5)_2Sm(THF)_2$ adopts a pseudo-tetrahedral geometry defined by the centroids of the two C_5Me_5 units and the oxygen atoms of the THF ligands.[74] Desolvation of $(C_5Me_5)_2Sm(THF)_2$ by heating under vacuum at 75°C is very facile and affords the solvent free compound, $(C_5Me_5)_2Sm$.[75] Attempts to desolvate the ytterbium complex were unsuccessful and at 90°C, only one of the coordinated solvents could be removed to give the mono THF compound, $(C_5Me_5)_2Yb(THF)$.[76] Surprisingly, the solid state structure of the solvent free samarium compound is nearly identical to that of the THF solvate with the arrangement of the C_5Me_5 moieties deviating significantly from the expected 180° (parallel) arrangement. The $(C_5Me_5)_2$-centroid-Sm-$(C_5Me_5)_2$ centroid angle is 140.1°. The analogous ytterbium complex also has a bent structure in the gas phase with a $(C_5Me_5)_2$-centroid-Yb-$(C_5Me_5)_2$-centroid angle of 156°.[77] The observed bent structures are similar to that seen in some alkaline metal dihalide complexes in the gas phase and the bent structure was rationalized on the basis of polarization effects.[78] The same explanation was invoked for the $(C_5Me_5)_2Ln$ complexes. The bent structure optimizes the polarization of the large lanthanide centers by the two anionic C_5Me_5 ligand and therefore, better overall electrostatic bonding for the two C_5Me_5 rings. An alternative argument, which was used to account for the bent structure in the analogous transition metal complexes, involves the interaction of metal d-orbitals with other ligands.[79] An explanation of this nature requires the participation of the 4f-orbitals or the high energy 5d and 6s orbitals and thus is

energetically unfavourable. This unexpected structure of $(C_5Me_5)_2Ln$ (Ln = Sm, Yb) was believed to contribute to the observed unusual and unique reactivities of these compounds, especially samarium compound.

$(C_5Me_5)_2Sm(THF)_2$ displays extremely high reactivity towards a variety of substrates, Scheme 1.4. It reduces CO to give a compound containing four Sm(III) centers and six CO molecules.[80] The reaction involves the reduction of six CO molecules by four electrons followed by reductive homologation to give two ketenecarboxylate units. Slow evaporation of a solution of $(C_5Me_5)_2Sm$ under an inert atmosphere of N_2 gave the first lanthanide dinitrogen complex with dinitrogen ligand side on bound to two $(C_5Me_5)_2Sm$ units.[81] With diphenylacetylene,
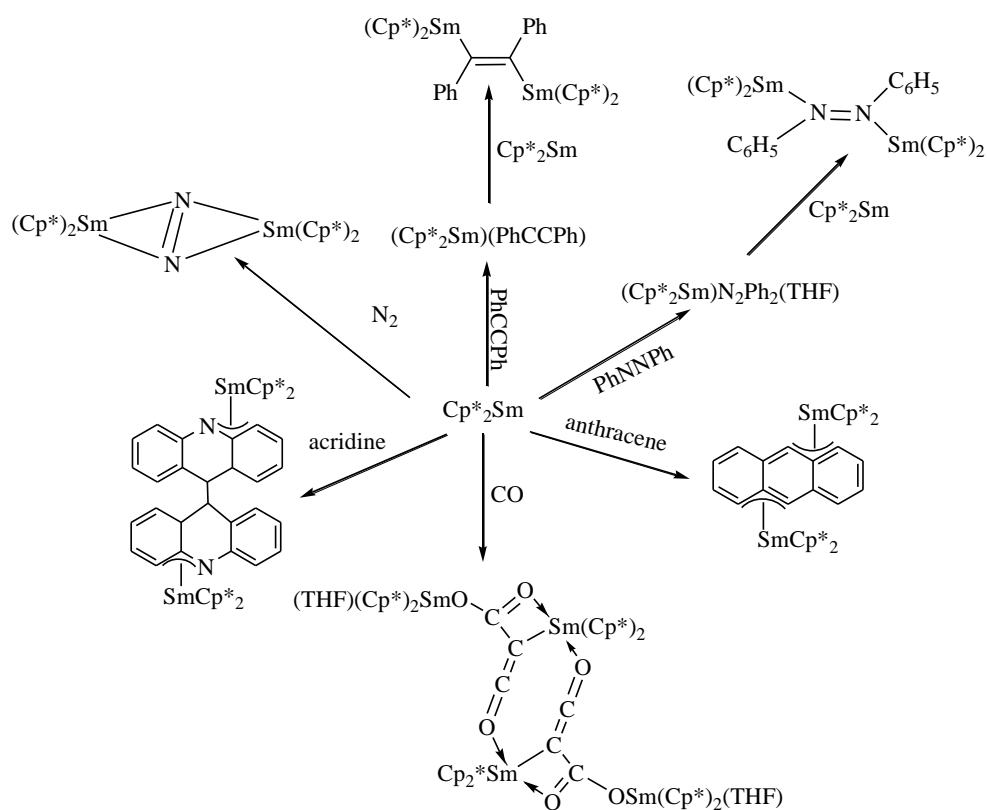
Scheme 1.4: Reactions of $(C_5Me_5)_2Sm$ With Various Substrates.

19

the reaction gave a black compound with an enediyl structure [(C$_5$Me$_5$)$_2$Sm](C$_6$H$_5$)C=C(C$_6$H$_5$)[Sm(C$_5$Me$_5$)$_2$], a rather unusual color for a Sm(III) compound.[82] On further reaction with CO, stereospecific formation of a tetracyclic hydrocarbon was observed.[83] In the presence of hydrogen, (C$_5$Me$_5$)$_2$Sm reacts with diphenylacetylene to give the samarium (III) hydride, [(C$_5$Me$_5$)$_2$SmH]$_2$ and *trans* stilbene.[84] It also react with azobenzene in 1:1 or 2:1 molar ratio to give dark green (C$_5$Me$_5$)$_2$Sm(PhNNPh)(THF) and [(C$_5$Me$_5$)$_2$Sm]$_2$(PhNNPh), respectively.[85] Although there is no report of the direct reaction of (C$_5$Me$_5$)$_2$Sm with dioxygen, it reacts with oxygen containing substrates such as NO, N$_2$O, 1,2-epoxybutane and pyridine *N*-oxide to yield a dinuclear Sm(III) compound containing a bridging oxo ligand.[86] In all compounds having the (C$_5$Me$_5$)$_2$Sm(μ-L)Sm(C$_5$Me$_5$)$_2$ structure, the arrangement of the four (C$_5$Me$_5$)$_2$ centroids is dependent on the size of the bridging ligands. For small ligands, the arrangement adopted by the four (C$_5$Me$_5$)$_2$ centroids is tetrahedral, whereas bulky ligand confers a square planar geometry.[87] This is illustrated for [(C$_5$Me$_5$)$_2$Sm]$_2$(μ-O), Figure 1.4(**a**) and [(C$_5$Me$_5$)$_2$Sm]$_2$(PhNNPh), Figure 1.4(**b**). (C$_5$Me$_5$)$_2$Sm(THF)$_2$ also react

(a)   (b)
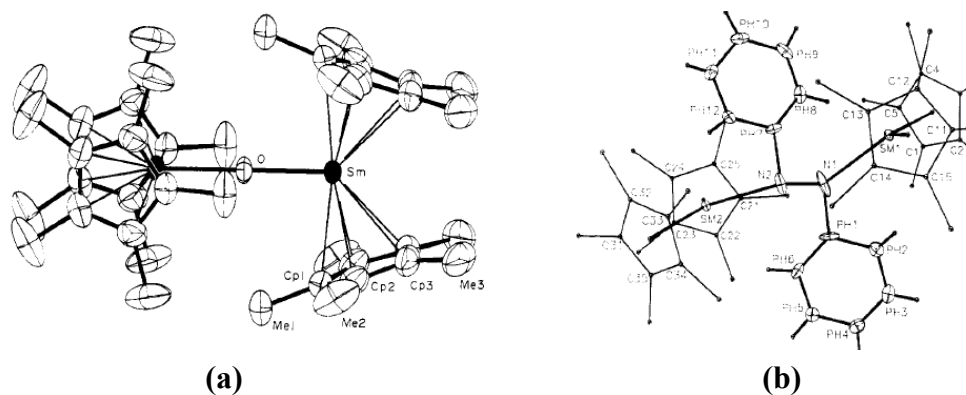
Figure 1.4: Structures of [(C$_5$Me$_5$)$_2$Sm]$_2$(μ-O), (**a**) and [(C$_5$Me$_5$)$_2$Sm]$_2$N$_2$(C$_6$H$_5$)$_2$, (**b**).

with unsaturated molecules like alkenes and polycyclic aromatic hydrocarbons to give η^3-allyl complexes, $(C_5Me_5)_2Sm(\eta^3\text{-}CH_2CHCHR)$.[88] Unlike the rich reductive chemistry displayed by $(C_5Me_5)_2Sm$, the Yb analogue has limited reactivity, this is in line with the lower reducing power of Yb^{2+} ion cf. with Sm^{2+} ion.[67,68]

The chemistry of divalent neodymium, dysprosium and thulium is still very much in its infancy compared with that of their samarium and ytterbium counterparts. The first isolated molecular complexes of these elements are the diiodides, LnI_2L_x (Ln = Tm, Dy, L = DME, x = 3; Ln = Nd, L = THF, x = 5).[89,90,91] The compounds were all characterized in the solid state and display significant reductive properties similar to and surpassing that of samarium in some cases.[90]

The synthesis of the more interesting organometallic compounds of these very reactive divalent lanthanides is not trivial, being hampered by the facile oxidation of the lanthanides to the more stable trivalent state. Reaction of $TmI_2(THF)_x$ solution with 2 equiv. of $K(C_5Me_5)$ in Et_2O under N_2 atmosphere led immediately to the reduction of dinitrogen to give the dinuclear Tm(III) dinitrogen complex, $(C_5Me_5)_2Tm(\mu\text{-}N_2)Tm(C_5Me_5)_2$.[92] This shows that dinitrogen is not sufficiently inert to the highly reducing Tm(II) center, Figure 1.5. Repeating the

(a)   (b)
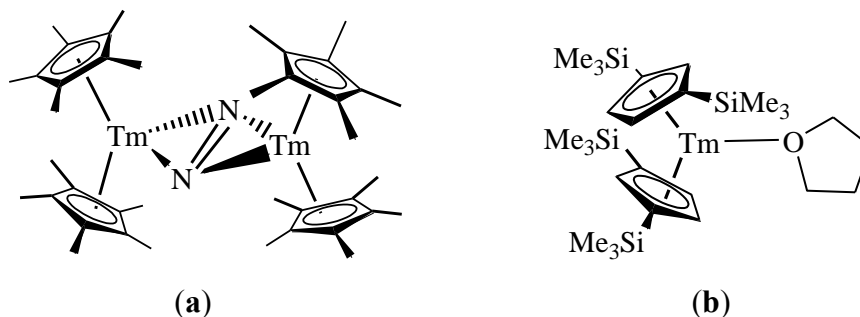
Figure 1.5: Structures of $[(C_5Me_5)_2Tm]_2(\mu\text{-}N_2)$, (**a**) and $[(C_5H_3(SiMe_3)_2)_2]Tm(THF)$, (**b**).

21

reaction under argon atmosphere gave cleavage of the C-O bond of the Et_2O solvent and giving a compound having both ethoxide and oxide moieties.[94]

By proper combination of ligand, solvent and inert atmosphere however, the first metallocene complex of Tm^{2+}, $(C_5H_3(SiMe_3)_2Tm(THF)$, was isolated, Figure 1.5.[93] Attempt to synthesize the dysprosium analogue under nitrogen gave the dysprosium (III) dinitrogen complex.[93]

The chemistry of lanthanide metals based on the cyclopentadienyl ligand system has been well developed; however, the often necessary requirement of two cyclopentadienyl ligands to satisfy the steric demand of the large lanthanide center, especially in the case of the lanthanide (II) ions, has greatly limited the type of chemistry that is achievable.

1.4 Tris(pyrazolyl)borate Lanthanide Chemistry.

1.4.1 Trivalent Lanthanide chemistry

The first forays into lanthanide pyrazolylborate complexes date back to the late 1960's,[37b] although, the first published report was that from Bagnall and Takats *et al*. on Tp_3Ln, in 1976.[94] The synthesis was achieved by simply mixing aqueous solutions of the reactants, eq. 1.2. Despite the aqueous synthesis, the isolated complexes are anhydrous and they do not act as Lewis acids, thus further coordination of donor solvents do not occur as was found in the case of Cp_3Ln. This observation is in accord with the ability of the bulky Tp ligand to satisfy the steric requirements of the large lanthanide ions.

$$\text{LnCl}_3(\text{H}_2\text{O})_n + \text{KTp} \xrightarrow{\text{H}_2\text{O}} \text{Tp}_3\text{Ln} + 3\text{KCl} \qquad 1.2$$
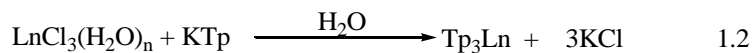
The structure of the Yb complex was determined in the solid state by single crystal X-ray crystallography. The Yb center is eight coordinate with a bicapped trigonal prismatic coordination geometry, Figure 1.6(**a**)[95] and also in solution as shown by paramagnetic NMR. The same structure was assigned to the other late lanthanides on the basis NMR data.[96] The structure of the late lanthanides was later confirmed by Apostolidis and co-workers,[97] who also confirmed that the structures of the early lanthanides differ from that of the late lanthanides, as was first postulated based on IR spectroscopy and solubility properties.[98] The early lanthanides were found to be 9 coordinate with tricapped trigonal prismatic geometry, Figure 1.6. Thus, like the tris(cyclopentadienyl) analogues, and as would be expected based on lanthanide contraction, coordination number decreases as the series is traversed from early to late lanthanides.

Reaction of 2 equiv. of KTp or NaTp with late lanthanide trichlorides in aqueous solution led to the isolation of $\text{Tp}_2\text{LnCl}(\text{L})$ (L = H_2O or pyrazole; Ln = Y, Tb).[99] In THF, $\text{Tp}_2\text{ErCl}(\text{THF})$ [37b] was obtained. Typical of organolanthanide chemistry, extension of this synthesis to early lanthanides was complicated by ligand redistribution reactions.[5,42] Although Wong and Sun reported the isolation of the solvent free neodymium complex, Tp_2NdCl, it readily reacted with moisture to form the water adduct, $\text{Tp}_2\text{NdCl}(\text{H}_2\text{O})$ which was structurally characterized.[100] Isolation of Tp_2LnX type complexes for larger lanthanide metals was achieved by using bidentate X ligands such as β-diketonates, oxalates and carboxylates.[99-101]

23

Thus, the use of the unsubstituted Tp ligand also has the limitation of allowing the isolation of complexes with high coordination number only, despite its steric bulk. Use of substituted pyrazolylborate ligands, $Tp^{R,R'}$ (R and R' $\neq$ H) is expected to overcome the problems encountered with the unsubstituted Tp ligand.

(a)   (b)
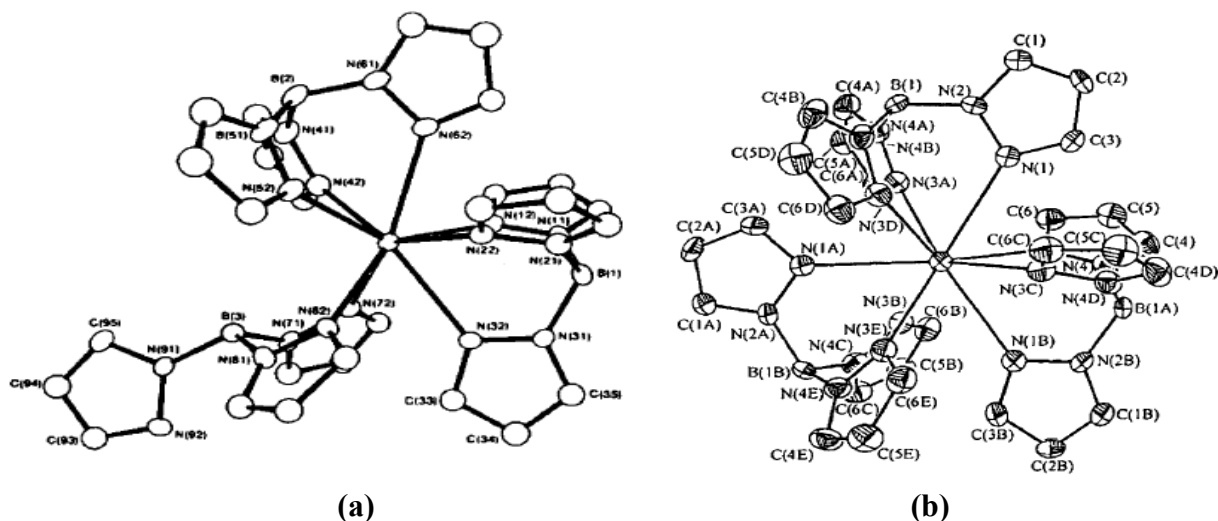
Figure 1.6: Structures of Tp_3Ln ; Tp_3Yb, (**a**) Tp_3Pr, (**b**).

The use of the tris(3,5-dimethylpyrazolyl)borate, Tp^{Me2}, ligand by Sella and co workers allowed the isolation of complexes of type $(Tp^{Me2})_2Ln(OTf)$ (Ln = La, Ce, Pr, Nd, Sm, Eu, Gd, Ho, Yb).[102] The large lanthanides (La, Ce, Pr and Nd) are 7-coordinate with η^1 bound triflate ion, whereas the smaller lanthanides forms 6-coordinate cationic compound with the triflate ion as the counter-ion. This observation is in line with expectations arising from the lanthanide contraction. Although the bis-$Tp^{R,R'}$ complexes are unique, it would be more interesting if mono $Tp^{R,R'}$ complexes could be made as they could take part in interesting reactions which were previously not known.

Initial attempts to isolate mono Tp$^{R,R'}$ lanthanide complexes were plagued by ligand redistribution reactions. Reaction of 1 equiv. of KTp or NaTp with lanthanide trichloride gave TpLnCl$_2$(THF)$_{1.5}$ (Ln = Er, Y).[103] More than two decades later, synthesis and characterization of the monomeric mono-Tp complexes, TpLnX$_2$(THF)$_2$, (Ln = Y, X = Cl, Br; Ln = Nd, X = I) was reported by Bianconi *et al*. and the structure of the neodymium compound was reported.[104] The related ytterbium dichloride was obtained as a dimer, [TpYbCl$_2$(THF)]$_2$, with bridging chloride ligands.[105] Most reports on mono-Tp$^{R,R'}$ complexes have included those with bulky substituents at the 3-position of the pyrazole since these suppress ligand redistribution reactions. Using the more bulky Tp^{R,Me} ligands, Bianconi *et al*. reported the synthesis of half sandwich yttrium complexes (Tp^{Me2})LnX$_2$(THF) (Ln = Y, X = Cl; Ln = Nd, X = I)[104,106] and Piers and co-workers have successfully isolated mono-Tp^{R,Me} scandium dichloride complexes, (Tp^{R,Me})ScCl$_2$(THF)$_n$ (R = ^{t}Bu, n = 0; R = Me, n = 1).[107] Apostolidis and co-workers have extended this to praseodymium, plutonium, neodymium and ytterbium.[108] They showed that with the larger lanthanides, the complexes are dimeric whereas the corresponding ytterbium complex is monomeric in the solid state, reflecting the differences in the sizes of the lanthanide metals. These early works were however focused mostly on the smaller lanthanide and group 3 metal centers and often, attempts to crystallize the compounds over prolonged period of time have been shown to result in the formation of the dimethylpyrazole adducts, (Tp^{Me2})LnX$_2$(3,5-Me$_2$PzH)(THF), and in some cases formation of the ionic species [(Tp^{Me2})LnX$_3$][3,5-Me$_2$PzH$_2$] have been observed.[104,108] To extend it to the larger lanthanides, there is need for addi-

25

tional co-ligands. Sun and Wong showed that in contrast to the THF adducts, use of substituted bipyridine as co-ligand allowed the isolation and structural characterization of $(Tp^{Me2})NdCl_2(L)$ (L = 4,4′-di-*tert*-butyl-2,2′-bipyridine).[100] Marques *et al.* reported on the synthesis of $(Tp^{Me2})LnCl_2(L)$ complexes (Ln = Y, La; L = 2,2′-bipyridine, 1,10-phenanthroline).[109] The structure of $(Tp^{Me2})LaCl_2(2,2′-bipy)$ is shown in Figure 1.7.
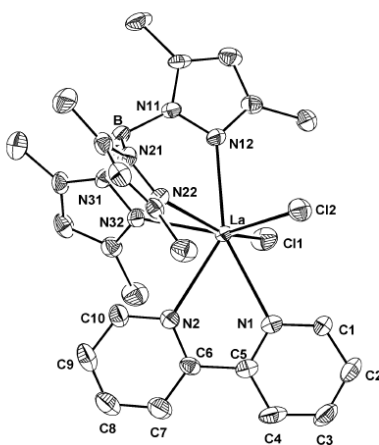
Figure 1.7: Structure of $(Tp^{Me2})LaCl_2(2,2′-bipy)$.

Initial derivatization of these $(Tp^{R,R'})LnX_2(L)$ complexes also proved frustrating. Reaction of the yttrium dichloride complex, $(Tp^{Me2})YCl_2(THF)$, with lithium alkyl reagents, LiR, was reported to afford the corresponding yttrium dialkyl compounds, $(Tp^{Me2})YR_2(THF)$ (R = CH_2SiMe_3, Ph).[106] However, Piers and co-workers reported that their attempts to prepare the analogous scandium dialkyl compounds $(Tp^{R,Me})Sc(CH_2SiMe_3)_2(THF)_{0/1}$ (R = Me, ^tBu) by the same approach (salt metathesis) resulted in isolation of products contaminated with various amounts of $LiTp^{R,Me}$. In contrast, protonolysis reaction, between *in-situ* generated

scandium trialkyl, $Sc(CH_2SiMe_3)_3(THF)_2$, and the acid form of the ligands, $H(Tp^{R,Me})$, did afford the desired complexes.[107]

1.4.2 Divalent Lanthanide Chemistry

1.4.2.1 Bis-$Tp^{R,R'}$ Complexes

Unlike the trivalent pyrazolylborate lanthanide chemistry, the development of the divalent analogues is relatively recent. Evans and co-workers first reported the synthesis of bis-hydrotris(pyrazolyl)borate lanthanide(II) complexes, $(Tp^{R,R'})_2Ln$ complexes (R = R'= H and R = R' = Me; Ln = Eu, Sm, Yb),[110] but none of the compounds reported were structurally characterized. Marques and co-workers also reported on the synthesis of $Tp_2Ln(THF)_2$ complexes of Sm, Eu and Yb. [111] Initial synthesis of the bis(3,5-dimethylyrazolyl)borate compounds, $(Tp^{Me2})_2Ln$ by the reaction of the lanthanide dihalides, $LnI_2(THF)_n$ (Ln = Sm, Eu, Yb) with $K(Tp^{Me2})$, eq. 1.3, was plagued by separation problems due to the highly insoluble nature of the compounds thus, making separation of the product from the potassium halide by-product impossible.

$$LnI_2(THF)_n + 2\ K(Tp^{Me2}) \xrightarrow[\text{-2 KI}]{\text{THF}} (Tp^{Me2})_2Ln \qquad\qquad 1.3$$
$$Ln = Sm,\ Eu,\ Yb$$
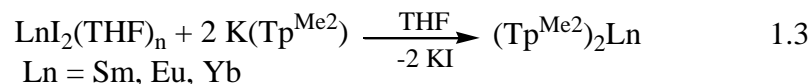
Both the europium and ytterbium compounds were obtained pure by sublimation, the samarium compound was however reported to decompose under the condition of sublimation.[110] Thus, an alternative approach used the sodium salt of the Tp^{Me2} ligand, since the by-product of this reaction, NaI, is more soluble in THF than KI and hence separation can be easily achieved. This approach was used

27

independently by Takats *et al.*[112] and Sella and co-workers[113] to obtain the desired complexes and X-ray quality crystals of the complexes were obtained either by slow diffusion[112] or temperature gradient sublimation[113] Use of other $Tp^{R,R'}$ ligands allowed the isolation of $(Tp^{R,R'})_2Ln$ (Ln = Sm, Yb; R = Ph, Tn; R′ = H)[114,115] complexes, which are soluble and therefore could be easily characterized in solution to compare the solution structures to the solid state structures. The complexes are all six-coordinate with two κ^3 bonded Tp^{Me2} ligands and the coordination geometry around the lanthanide center is best described as distorted octahedron with the two tridentate Tp^{Me2} ligands adopting a staggered conformation about the B-Ln-B axis.[112,113] Despite its insolubility, $(Tp^{Me2})_2Sm$ was found to react readily with a variety of reducible substrates. Reaction with one or two equivalents of azobenzene gave the same complex, $(Tp^{Me2})_2Sm(PhN=NPh)$ irrespective of the stoichiometry of the reaction.[112] This is in contrast to $(C_5Me_5)_2Sm$ which formed both 1:1, $(C_5Me_5)_2Sm(\eta^2\text{-}N_2Ph_2)(THF)$, and 2:1, $((C_5Me_5)_2Sm)_2(N_2Ph_2)$, complexes.[85] This difference in reactivity was attributed to the bulkier nature of the Tp^{Me2} ligand compared to C_5Me_5. The compound also reacted with benzophenone, fluorenone and phenanthrenequinone to give intensely colored solutions of $(Tp^{Me2})_2Sm(OCPh_2)$, $(Tp^{Me2})_2Sm(\eta^1\text{-}OC_{13}H_8)$ and $(Tp^{Me2})_2Sm(\eta^2\text{-}O_2C_{14}H_8)$, respectively.[116] The intense colors of the solutions, NMR spectra as well as crystallographic data confirm the radical anion nature of the coordinating ligands. The solid state structure of $(Tp^{Me2})_2Sm(OCPh)_2$ is shown in Figure 1.8(**a**).[117] With less bulky substrates such as benzaldehyde and pyrazine, $(Tp^{Me2})_2Sm$ reacts to give bimetallic complexes $((Tp^{Me2})_2Sm)_2(\mu\text{-}OCH(Ph)\text{-}CH\text{-}(Ph)O)$ and

$(Tp^{Me2})_2Sm)_2(\mu\text{-}(C_4H_4N_2)_2$, respectively. With 2,6-di-*tert*-butyl-para-benzoquinone and 3,5-di-*tert*-butyl-ortho-benzoquinone, the samarium(III) complexes, $(Tp^{Me2})Sm(para\text{-}^tBu_2quinone)$ and $(Tp^{Me2})Sm(ortho\text{-}^tBu_2quinone)$ were obtained and structurally characterized.[115, 118] With unsubstituted 1,4-benzoquinones, both mono-$(Tp^{Me2})Sm(para\text{-}quinone)$ and bimetallic $[(Tp^{Me2})Sm]_2(\mu\text{-}para\text{-}quinone)$ complexes were obtained; the latter complex was formed by further reduction of the quinone to the dianionic state by another molecule of $(Tp^{Me2})_2Sm$.[116] $(Tp^{Me2})_2Sm$ reacts with dioxygen at low temperature to give the first lanthanide superoxo complex, $(Tp^{Me2})_2Sm(O_2)$, eq. 1.4. Evidence for

(a) (b) (c)
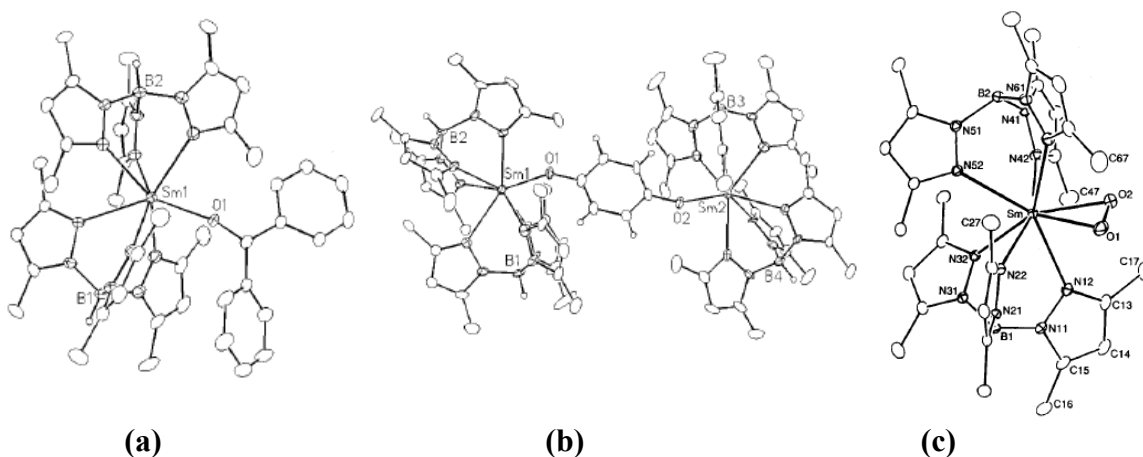
Figure 1.8: $(Tp^{Me2})_2Sm(OCPh_2)$, (**a**) ; $(Tp^{Me2})_2Sm(\mu\text{-}C_6H_4O)$, (**b**) and $(Tp^{Me2})_2Sm(\eta^2\text{-}O_2)$, (**c**).

the coordination of the O_2^- moiety was obtained from UV and Raman spectroscopies on the basis of ^{16}O and ^{18}O isotope substitution experiments and single crystal X-ray crystallography.[119]

$$(Tp^{Me2})_2Sm + O_2 \xrightarrow[\text{toluene}]{-78^oC} \text{red solution} \xrightarrow[\text{r.t.}]{\text{warm up}} (Tp^{Me2})_2Sm(O_2) \qquad 1.4$$
$$\text{purple solid} \hspace{6cm} \text{pale-green solid}$$
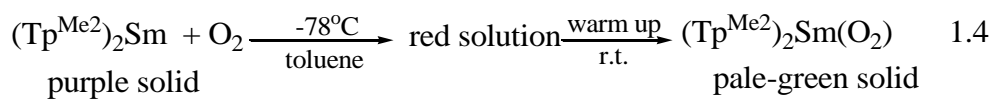
Unlike the pentamethylcyclopentadienyl analogue, $(Tp^{Me2})_2Sm$ does not react with $HC\equiv CPh$, $HC\equiv CH$, $PhC\equiv CPh$, CO or $CH_3CH=CH_2$.[115]

Reaction of the potassium salt of the bulky $Tp^{tBu,Me}$ ligand with LnI_2 in 2:1 molar ratio affords the homoleptic complexes $(Tp^{tBu, Me})_2Ln$ (Ln = Sm, Yb).[120] Unlike the $(Tp^{Me2})_2Ln$ analogue, the steric demand of the *tert*-Butyl groups prevents the formation of symmetric six coordinate structures. In the solid state, one of the $Tp^{tBu,Me}$ ligands coordinates in the classical κ^3 coordination mode whereas the other one is coordinated via two pyrazolyl nitrogen atoms and an agostic B-H-Ln interaction, Figure 1.9.[120]

(a)   (b)
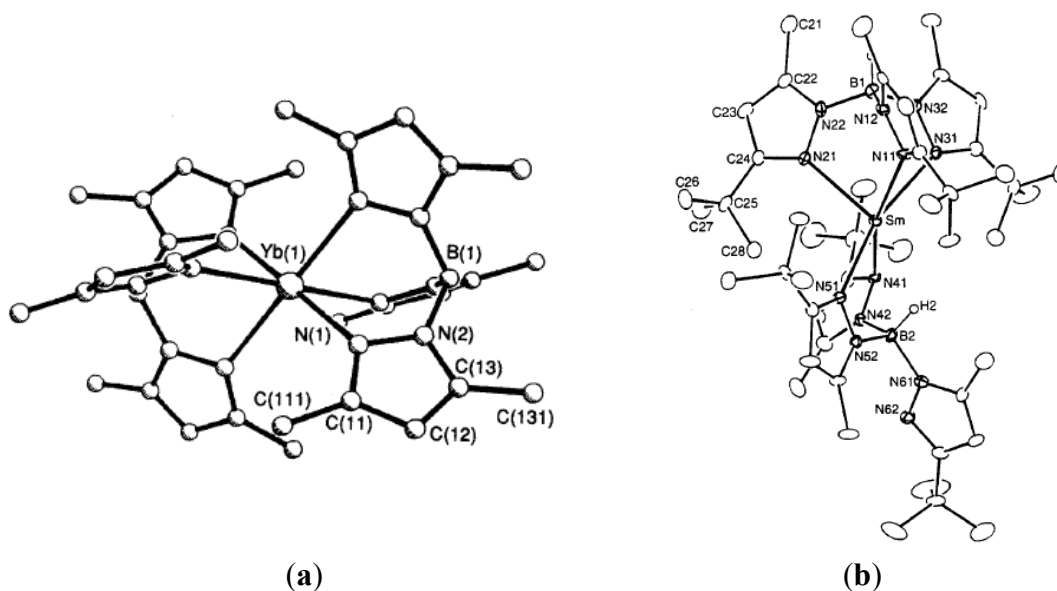
Figure 1.9: Structures of $(Tp^{R,R`})_2Ln$: $(Tp^{Me2})_2Yb$, **(a)** $(Tp^{tBu,Me})_2Sm$, **(b)**.

1.4.2.2   Mono $Tp^{R, R`}$ Complexes

Initial attempts to prepare mono $Tp^{R,R'}$ complexes of divalent lanthanides have all focused on bulky 3,5-disubstituted ligands in order to suppress the ligand

redistribution reaction which is more problematic for the larger lanthanide(II) centers. There has been no reports of mono ligand lanthanide(II) complexes bearing the parent unsubstituted Tp ligand. Use of the more bulky Tp^{Me2} ligand afforded the isolation of (Tp^{Me2})YbI(THF)$_2$ complex. Attempts to derivatize this compound were unsuccessful leading only to the isolation of the insoluble (Tp^{Me2})$_2$Yb complex.[115] In contrast, the use of the more bulky Tp^{tBu,Me} ligand readily allowed the isolation of half sandwich complexes of samarium(II) and ytterbium(II) by simple salt metathesis reactions, eq. 1.5. The compounds were characterized in solution and in the solid state.[121,122]

$$\text{LnI}_2(\text{THF})_n + \text{K}(\text{Tp}^{tBu,Me}) \xrightarrow[\text{-KI}]{\text{THF}} (\text{Tp}^{tBu,Me})\text{LnI}(\text{THF})n \qquad 1.5$$
$$\text{Ln} = \text{Sm, Yb} \qquad\qquad\qquad \text{Ln} = \text{Sm, n} = 2$$
$$\text{Ln} = \text{Yb, n} = 1$$
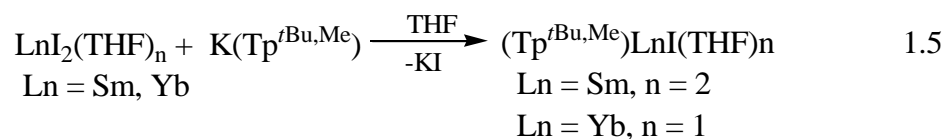
The coordinated THF could be easily removed in the case of the samarium compound to make the solvent free compound, (Tp^{tBu,Me})SmI [115,121] whereas in the case of the ytterbium, this is achieved with great difficulty and formation of the solvent free compound is accompanied by decomposition.[121] This observation was rationalized on the basis of the difference in charge/radius ratio of the lanthanide centers, the smaller ytterbium center having the higher charge/radius ratio and thus stronger interaction with the coordinated THF. This parallels the observation in the (C$_5$Me$_5$)$_2$Sm(THF)$_2$ and (C$_5$Me$_5$)$_2$Yb(THF)$_2$ complexes in which the former easily undergoes desolvation to afford the solvent free compound whereas the latter looses only one of the coordinated THF under identical conditions.[75,76] Other donor molecules such as pyridines and substituted isonitrile could be substituted

for the coordinated THF.[121] The use of 3-mesityl substituted pyrazolylborate ligand Tp^{Ms}, also allowed the isolation of half sandwich complexes of ytterbium. Reaction of $TlTp^{Ms,R}$ with YbI_2 at low temperatures allowed the isolation of $(Tp^{Ms,R})YbI(THF)_2$, complexes (R = H, Me). With R = H, carrying out the reaction at room temperature leads to the isomerisation of the ligand to give $(Tp^{Ms*})YbI(THF)_2$, (in which one of the pyrazolyl groups has the Ms group on position 5 of the pyrazolyl ring) however, the 5-Me substituted ligand, $Tp^{Ms,Me}$, does not isomerize.[117]

Attempts to replace the iodide in $(Tp^{tBu,Me})YbI(THF)$ by alkyl groups using lithium, sodium or Grignard reagents were mostly unsuccessful.[115,121b] However, by using potassium reagents, successful derivatization was achieved; this was believed to be driven by the insolubility of the KI by-product which shifts the position of the equilibrium in favour of the desired products. [115,121b,122] Not surprisingly, the ytterbium complex was more amenable to derivatization whereas derivatives of the samarium complex are limited to bulky co-ligands such as $-CH(SiMe_3)_2$, $-N(SiMe_3)_2$ and the triethyl borane ligand, $-BHEt_3$.[115] All attempts to prepare the samarium(II) analogues of $(Tp^{tBu,Me})Yb(OMes)(THF)$ [123] and $(Tp^{tBu,Me})Yb(CH_2SiMe_3)(THF)$[115] resulted in ligand redistribution and formation of $(Tp^{tBu,Me})_2Sm$.[120] This observation reflects the differences in the size of the lanthanide(II) centres and thus even though the pyrazolylborate ligand is bulky, it is less effective in saturating the larger samarium(II) center.

Very recently, the synthesis of the half sandwich iodide complex of thulium(II), $(Tp^{tBu,Me})TmI(THF)$ has been achieved using a similar approach as that

of the samarium and ytterbium analogues.[124] The derivatization of the thulium iodide complex (Tp^{tBu,Me})Tm(I)(THF) shows similar behaviour to that of the samarium analogue, replacement of the iodide with other ligands was successful only with bulky co-ligands such as –CH(SiMe$_3$)$_2$, –N(SiMe$_3$)$_2$ and –BHEt$_3$. Attempts to make (Tp^{tBu,Me})Tm(CH$_2$SiMe$_3$)(THF) resulted in ligand redistribution and gave (Tp^{tBu,Me})$_2$Tm.[124]

Hydrogenolysis of (Tp^{tBu,Me})YbCH$_2$SiMe$_3$(THF) affords the ytterbium(II) hydride dimer, [(Tp^{tBu,Me})YbH]$_2$ which was characterized in the solid state as the first well-defined, discrete lanthanide(II) hydride complex.[125] The hydride reacts with different types of substrates including insertion of unsaturated substrates like CO, alkynes, etc. as well as by σ-bond metathesis reactions with acidic substrates, Scheme 1.5.
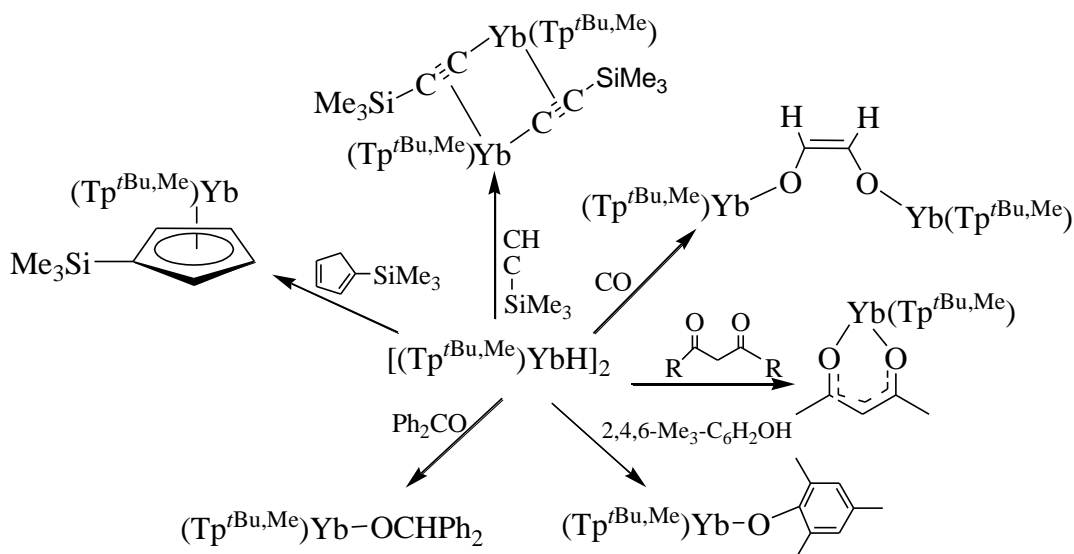
Scheme 1.5: Reactions of [(Tp^{tBu,Me})YbH]$_2$ With Various Substrates.

1.5   Scope of the Thesis

The goal of the research project described herein is to further explore the organometallic chemistry of the lanthanides based on the tris(pyrazolyl)borate ligand framework. The thesis is divided into six chapters. The first chapter is a review of the literature which gives a general introduction to lanthanides, their properties and chemistry. Although divalent lanthanide chemistry of tris(pyrazolyl)borate has been well studied, Chapter 2 reports the synthesis and structure of ytterbium(II) tetrahydroborate complexes as a way of introducing the author to organolanthanide chemistry. Chapter 3 describes the synthesis, structures and reactivities of trivalent lanthanide dialkyl and dihydrides complexes. As an alternative to the usual salt metathesis, preparation of these complexes via protonolysis is discussed. An alternative and complementary route via alkyl abstraction is also presented. In Chapter 4, the reaction of the lanthanide dialkyl compounds towards a variety of terminal alkynes is presented. The variation of structure as a function of steric crowding around the lanthanide center will also be discussed. Results of catalytic dimerization of terminal alkynes by the lanthanide dialkyl complexes will also be mentioned briefly. The synthesis and structures of lanthanide tribenzyl complexes as well as the mono $(Tp^{R,R'})$ supported lanthanide dibenzyl complexes will be covered in Chapter 5. Chapter 6 concludes the thesis with suggestions for future works.

1.6 References

1. Kaltsoyannis, N.; Scott, P. In *The f–Elements*; Oxford Chemistry Primers 76; Oxford University Press, 1999; pp 1–26.

2. Cotton, S. A. In *Lanthanide and Actinide Chemistry*; Woollins, D.; Crabtree, B.; Atwood, D.; Meyer, G., Eds.; Inorganic Chemistry; John Wiley & Sons, Chichester, UK., 2006.

3. Edelmann, F. T. In *Comprehensive Organometallic Chemistry* III; Crabtree, R. H.; Mingos, D. M. P., Eds.; Elsevier, Oxford, *Vol. 401*, **2006**, pp. 1–199.

4. Raymond, K. N.; Eigenbrot, C. W., Jr. *Acc. Chem. Res.* **1980**, *13*, 276–283.

5. Marks, T. J. *Prog. Inorg. Chem.* **1978**, *24*, 51–107.

6. Seitz, M; Oliver, A. G.; Raymond, K. N. *J. Am. Chem. Soc.* **2007**, *129*, 11153–11160.

7. Cotton, F. A.; Wilkinson, G.; Murillo, C. A.; Bochmann, M. *Advanced Inorganic Chemistry*, 6th Edn. Wiley New York **1999**, Chapter 19; pp 1108–1109.

8. Evans, W. J. *Inorg. Chem.* **2007**, *46*, 3435–3449.

9. Bochkarev, M. N. *Coord. Chem. Rev.* **2004**, *248*, 835–851.

10. Elschenbroich, C. *Organometallics* 3rd ed.; WILEY–VCH Verlag GmbH & Co. KGaA, Weinheim: Germany, 2006, pp 610–611.

11. Edelmann. F. T. *Angew. Chem. Int. Ed. Engl.* **1995**, *34*, 2466–2488.

12. Piers, W. E.; Emslie, D. J. E. *Coord. Chem. Rev.* **2002**, *233–234*, 131–155.

13. Edelmann, F. T.; Freckmann, D. M. M.; Schumann, H. *Chem. Rev.* **2002**, *102*, 1851–1896.

14. Mountford, P.; Ward, B. D.; *Chem. Commun*. **2003**, 1797–1803. (Feature Article Review).

15. Duchateau, R.; van Wee, C. T.; Meetsma, A.; Teuben, J. H. *J. Am. Chem. Soc*. **1993**, *115*, 4931–4932.

16. Bailey, P. J.; Pace, S.; *Coord. Chem. Rev*. **2001**, *214*, 91–141.

17. (a) Zhou, Y.; Yapp, G. P. A.; Richeson, D. S. *Organometallics* **1998**, *17*, 4387–4391. (b) Lu, Z.; Yapp, G. P. A.; Richeson, D. S. *Organometallics* **2001**, *20*, 706–712. (c) Luo, Y.; Yao, Y.; Shen, Q.; Yu, K.; Weng, L. *Eur. J. Inorg. Chem*. **2003**, 318–323. (d) Trifonov, A. A.; Lyubov, D. M.; Fedorova, E. A.; Fukin, G. K.; Schumann, H.; Mühle, S.; Hummert, M.; Bochkarev, M. N. *Eur. J. Inorg. Chem*. **2006**, 747–756. (e) Trifonov, A. A.; Fedorova, E. A.; Fukin, G. K.; Bochkarev, M. N. *Eur. J. Inorg. Chem*. **2004**, 4396–4401. (f) Trifonov, A. A.; Lubyov, D. M.; Fukin, G. K.; Boranov, E. V.; Kurskii, Y. A. *Organometallics* **2006**, 25, 3935–3942.

18. Roesky, P. W. *Chem. Ber*. **1997**, *130*, 859–862.

19. (a) Piers, W.E.; Hayes, P. G.; McDonald R. *J. Am. Chem. Soc.* **2002**, *124*, 2132–2133. (b) Hayes, P. G.; Piers, W. E.; Lee, L. W. M.; Knight, L. K.; Parvez, M.; Elsegood, M. R. J.; Clegg, W. *Organometallics* **2001**, *20*, 2533–2544.

20. Emslie, D. J. H.; Piers, W. E.; McDonald, R. *J. Chem. Soc. Dalton Trans*. **2002**, 293–294. (b) Emslie, D. J. H.; Piers, W. E.; Parvez, M.; McDonald, R. *Organometallics* **2002**, *21*, 4226–4240.

21. (a) Gountchev, T. I.; Tilley, T. D. *Organometallics* **1999**, *18*, 2896–2905.

(b)   Gountchev, T. I.; Tilley, T. D. *Organometallics* **1999**, *18*, 5661–
5667.

22. Görlitzer, H. W.; Spiegler, M.; Anwander, R. *Eur. J. Inorg. Chem.* **1998**,
1009–1014.

23. Herrmann, W. A. Anwander, R.; Dufaud, V.; Scherer, W. *Angew. Chem.
Int. Ed.* **1994**, *33*, 1285–1286.

24. Annand, J. A.; Aspinal, H. C.; Steiner, A. *Inorg. Chem.* **1999**, *38*, 3941–
3943.

25. Hajela, S.; Schaefer, W. P.; Bercaw, J. E. *J. Organomet. Chem.* **1997**, *532*,
45–53.

26. Tredget, C. S.; Lawrence, S. C.; Ward, B. D.; Howe, R. G.; Cowley, A. R.;
Mountford, P. *Organometallics* **2005**, *24*, 3136–3148.

27. (a) Trofimenko, S. *Scorpionates: The coordination Chemistry of
Polypyrazolylborate Ligands*, Imperial College Press, London, 1999. (b)
Pettinari, C. *Scorpionates II: Chelating Borane Ligands,* Imperial College
Press, London, 2008.

28. Bambirra, S.; van Leusen, D.; Meetsma, A.; Hessen, B. Teuben, J. H.
Chem. Commun. **2003**, 522–523.

29. Bambirra, S.; Bouwkamp, M.; Meetsma, A.; Hessen, B. *J. Am. Chem.
Soc.* **2004**, *126,* 9182–9183.

30. Shao. P.; Berg, D. J.; Bushnell, G. W. *Inorg. Chem.* **1994**, *33*, 6334–6339.

31. (a) Fryzuk, M. D.; Haddad, T. S.; Rettig, S. J. *Organometallics* **1992**, *11*,
2967–2969. (b) Fryzuk, M. D.; Haddad, T. S. *J. Am. Chem. Soc.* **1988**,

110, 8263–8265.(c) Fryzuk , M. D.; Haddad, T. S.; Rettig, S. J. *Organometallics* **1991**, *10*, 2026–2036.

32. Fryzuk, M. D.; Yu, P.; Patrick, B. O. *Can. J. Chem.* **2001**, *79*, 1194–1200.

33. Lee, L.; Berg, D. J.; Einstein, F. W.; Batchelor, R. J. *Organometallics* **1997**, *16*, 1819–1821.

34. (a) Lee, L.; Berg, D. J.; Bushnell, G. W. *Inorg. Chem*. **1994**, *33*, 5302–5308. (b) Lee, L.; Berg, D. J.; Bushnell, G. W. *Organometallics* **1995**, *14*, 8–10.

35. (a) Parkin, G. *Adv. Inorg. Chem*. **1995**, *42*, 291–393. (b) Kitajima, N. ; Tolmann, W. B. *Prog. Inorg. Chem.* **1995**, *42*, 419–531.

36. (a) Santos, S.; Marques, N. *New J. Chem*. **1995**, *19*, 551–571 (b) Marques, N.; Sella, A.; Takats, J. *Chem. Rev.* **2002**, *102*, 2137–2160.

37. (a) Trofimenko, S. *J. Am. Chem. Soc.* **1966**, *88*, 1842–1844. (b) Trofimenko, S. *J. Am. Chem. Soc.* **1967**, *89*, 3170–3177.

38. Trofimenko, S. *Chem. Rev*. **1993**, *93*, 943–979.

39. Birmingham, J. M.; Wilkinson, G. *J. Am. Chem. Soc.* **1956**, *78*, 42–44.

40. Manastyrskyj, S.; Dubeck, M. *Inorg. Chem*. **1964**, *3*, 1647–1648.

41. Fischer, E. O.; Fischer, H. *J. Organomet. Chem.* **1965**, *3*, 181–187.

42. Magnin, R. E.; Manastyrskyj, S.; Dubeck, M. *J. Am Chem. Soc*. **1963**, 85, 672–676.

43. Lappert, M. F.; Singh, A.; Atwood, J. L.; Hunter, W. E. *J. Chem. Soc. Chem. Commun*. **1981**, 1190–1191.

44. Wayda, A. L.; Evans, W. J. *Inorg. Chem.* **1980**, *19*, 2190–2191.

45. Tilley, T. D.; Andersen, R. A. *Inorg. Chem.* **1981**, *20*, 3267–3270.

46. Evans, W. J.; Peterson, T. T.; Rausch, M. D.; Hunter, W. E.; Zhang, H.; Atwood, J. L. *Organometallics* **1985**, *4*, 554–559.

47. (a) Holton, J.; Lappert, M. F.; Ballard, D. G. H.; Pearce, R.; Atwood, J. L.; Hunter, W. E. *J. Chem. Soc. Chem. Commun.* **1976**, 480–481. (b) Holton, J.; Lappert, M. F.; Ballard, D. G. H.; Pearce, R.; Atwood, J. L.; Hunter, W. E. *J. Chem. Soc. Dalton Trans.* **1979**, 54–61.

48. (a) Ely, N. M.; Tsutsui, M. *J. Am. Chem. Soc.* **1975**, *97*, 1280–1281. (b) Ely, N. M.; Tsutsui, M. *Inorg. Chem.* **1975**, *14*, 2680–2687.

49. (a) Evans W. J.; Dominguez, R.; Hanusa, T. P. *Organometallics* **1986**, *5*, 263–270. (b) Evans, W. J.; Meadows, J. H.; Hunter, W. E.; Atwood, J. L. *J. Am. Chem. Soc.* **1984**, *106*, 1291–1300.

50. Watson, P. L. *J. Am. Chem. Soc.* **1982**, *104*, 337–339.

51. Watson, P. L.; Parshall, G. W. *Acc. Chem. Res.* **1985**, *18*, 51–56, and references therein.

52. de Haan, K. H.; de Boer, J. L.; Teuben, J. H.; Smeets, W. J. J.; Spek, A. L. *J. Organomet. Chem.* **1987**, *327*, 31–38.

53. Watson, P. L. *J. Chem. Soc. Chem. Commun.* **1983**, 276–277.

54. Hazin, P. N.; Hufman, J. C.; Bruno, J. W. *Organometallics* **1987**, *6*, 23–27.

55. van der Heijden, H.; Schaverien, C. J.; Orphen, A. G. *Organometallics* **1989**, *8*, 255–258.

56. (a) Heeres, H. J.; Meetsma, A.; Teuben, J. H. *J. Chem. Soc., Chem.*

Commun. **1988**, 962–963. (b) Heeres, H. J.; Meetsma, A.; Teuben, J. H. ; Rogers, R. D. *Organometallics* **1989**, *8*, 2637–2646.

57. Schaverien, C. J. *Organometallics* **1994**, *13*, 69–82.

58. Klooster, W. T.; Brammer, L.; Schaverien, C. J.; Budzelaar, P. H. M. *J. Am Chem. Soc.* **1999**, *121*, 1381–1382.

59. Cameron, T. M.; Gordon, J. C.; Scott, B. L. *Organometallics* **2004**, *23*, 2995–3002.

60. Mendel, A.; Magul, J. *Z. Anorg. Allg. Chem.* **1996**, *622,* 1913–1919.

61. Hultzsch, K. C.; Spaniol T. P.; Okuda, J. *Angew. Chem. Int. Ed.* **1999**, *38*, 227–230.

62. Cui, D. M.; Nishiura, M.; Hou, Z. *Macromolecules* **2005**, *38*, 4089–4095.

63. van der Heijden, H.; Pasman, P.; de Boer, E. J. M.; Schaverien, C. J. *Organometallics* **1989**, *9*, 1459–1467.

64. Hou, Z.; Nishiura, M.; Shima, T. *Eur. J. Inorg. Chem.* **2007**, 2535–2545.

65. Tardif, O.; Nishiura, M.; Hou, Z. *Organometallics* **2003**, *22*, 1171–1173.

66. (a) Shima, T.; Hou, Z. *J. Am. Chem. Soc.* **2006**, *128*, 8124–8125. (b) Cui, D.; Tardif, O.; Hou, Z. *J. Am. Chem. Soc.* **2004**, *126*, 1312–1313. (c) Tardif, O. Hashizuma, D.; Hou, Z. *J. Am. Chem. Soc.* **2004**, *126*, 8080–8081.

67. Morss, L. R. *Chem Rev.* **1976**, *76*, 827–841.

68. Varlashkin, P. G.; Peterson, J. R. *J. Less–Common Met.* **1983**, *94*, 333–341.

69. (a) Evans, W. J.; Bloom, I.; Hunter, W. E.; Atwood, J. L. *J. Am. Chem. Soc.*

1981, *103*, 6507–6508. (b) Satterlee, J. D**.** *Concepts in Magnetic Resonance,* 1990, *2,* 119-129.

70. Evans W. J. *Polyhedron* **1987**, *6*, 803–835 (and references there in).

71. Watt, G. W.; Gillow, E. W. *J. Am. Chem. Soc.* 1969, 91, 775–776.

72. Namy, J. L.; Girard, P.; Kagan, H. B. *Nouv. J. Chim*. **1981**, *5*, 479–484.

73. Tilley, T. D.; Anderson, R. A.; Spencer, B. Ruben, H,; Zalkin, A.; Templeton, D. H. *Inorg. Chem*. **1980**, *19*, 2999–3003.

74. Evans, W. J.; Grate, J. W.; Choi, H. W.; Bloom, I,; Hunter, W. E. Atwood, J. L. *J. Am. Chem. Soc.* **1985**, *107*, 941–946.

75. Evans, W. J.; Hughes, L. A.; Hanusa, T. P. *J. Am. Chem. Soc.* **1984**, *106*, 4270–4272.

76. Watson, P. L. *J. Chem. Soc. Chem. Commun*. **1980**, 652–653.

77. Andersen, R. A.; Boncella, J. M.; Burns, C. J.; Green, J. C. Hohl, D.; Rösch, N. *J. Chem. Soc. Chem. Commun*. **1986**, 405–407.

78. Büchler, A.; Stauffer, J. L.; Klemperer, W. *J. Am. Chem. Soc.* **1964**, *86*, 4544–4550.

79. Prout, K.; Cameron, T. S.; Forder, R. A.; Critcheley, S. R. Denton, B. R.; Rees, G. V. *Acta Crystallogr*. *Sect. B.* **1974**, *30*, 2290–2304.

80. Evans, W. J.; Grate, J. W.; Hughes, L. A.; Zhang, H.; Atwood, J. L. *J. Am. Chem. Soc.* **1985**, *107*, 3728–3730.

81. Evans, W. J.; Ulibarri, T. A.; Ziller, J. W. *J. Am. Chem. Soc.* **1988**, *110*, 6877–6879.

82. Evans, W. J.; Bloom, I.; Hunter, W. E.; Atwood, J. L. *J. Am Chem. Soc*.

1983, *105*, 1401–1403.

83. Evans, W. E.; Hughes, L. A.; Drummond, D. K.; Zhang, H.; Atwood, J. L. *J. Am. Chem. Soc.* **1986**, *108*, 1722–1723.

84. Evans, W. J.; Bloom, I.; Hunter, W. E.; Atwood, J. L. *J. Am. Chem. Soc.* **1983**, *105*, 1401–1403.

85. (a) Evans, W. J.; Drummond, D. K.; Bott, S. G.; Atwood, J. L; *Organometallics* **1986**, *5*, 2389–2391. (b) Evans, W. J.; Drummond, D. K.; Chamberlain, L. R.; Doedens, R. J.; Bott, S. G.; Zhang, H.; Atwood, J. L. *J. Am. Chem. Soc.* **1988**, *110*, 4983–4994.

86. Evans, W. J.; Grate, J. W.; Bloom, I.; Hunter, W. E.; Atwood, J. L. *J. Am. Chem. Soc.* **1985**, *107,* 405–409.

87. Evans, W. J.; Keyer, R. A.; Ziller, J. W. *J. Organomet. Chem*. **1993**, *450,* 115–120.

88. (a) Evans, W. J.; Ulibarri, T. A.; Ziller, J. W. *J. Am. Chem. Soc.* **1990**, *112*, 2314–2324. (b) Evans, W. J. Gonzales, S. L. Ziller, J. W. *J. Am. Chem. Soc.* **1994**, *116*, 2600–2608.

89. (a) Bochkarev, M. N.; Fagin, A. A.; *Chem.–Eur. J.* **1999**, *5*, 2990–2992. (b) Bochkarev, M. N.; Fedushkin, I. L.; Fagin. A. A. Petrovskaya, T. W.; Ziller, J. W.; Broomhall–Dillard, R. N.; Evans, W. J. *Angew. Chem. Int. Ed*. *Engl*. **1997**, *36,* 133–135.

90. Evans, W. J.; Allen, N. T.; Ziller, J. W. *J. Am. Chem. Soc.* **2000**, *122*, 11749–11750.

91. Bochkarev, M. N.; Fedushkin, I. L.; Dechert, S.; Fagin, A. A. Schumann,

H. *Angew. Chem. Int. Ed. Engl.* **2001**, *40*, 3176–3178.

92. Evans, W. J.; Allen, N. T.; Ziller, J. W. *J. Am. Chem. Soc.* **2001**, *123*, 7927–7928.

93. Evans, W. J.; Allen, N. T.; Ziller, J. W. *Angew. Chem. Int. Ed. Engl.* **2002**, *41*, 359–361.

94. Bagnall, K. W.; Tempest, A. C.; Takats, J.; Masino, A. P. *Inorg. Nucl. Chem. Lett.* **1976**, *12*, 555–557.

95. Stainer, M. V. R.; Takats, J. *Inorg. Chem.* **1982**, *21*, 4050–4053.

96. Stainer, M. V. R.; Takats, J. *J. Am. Chem. Soc.* **1983**, *105*, 410–415.

97. Apostolidis, C.; Rebizant, J; Kanellakopulos, B.; von Ammon, R.; Dornberger, E.; Muller, J.; Powietzka, B.; Nuber, B. *Polyhedron* **1997**, *16*, 1057–1068.

98. Stainer, M. V. R. Lanthanide Polypyrazolylborate Complexes. Ph.D. Thesis, University of Alberta, July 1981.

99. (a) Reger, D. L.; Linderman, J. A.; Lebioda, L. *Inorg. Chim. Acta* **1987**, *139*, 71–73. (b) Reger, D. L. Linderman, J. A.; Lebioda, L. *Inorg. Chem.* **1988**, *27*, 3923–3929. (c) Reger, D. L.; Knox, S. J.; Linderman, J. A.; Lebioda, L. *Inorg. Chem.* **1990**, *29*, 416–419.

100. Sun, C–D.; Wong, W. T. *Inorg. Chim. Acta* **1997**, *255*, 355–360.

101. (a) Moss, M. A. J.; Jones, C. J.; Edwards, A. J. *J. Chem. Soc. Dalton Trans.* **1989**, 1393–1400. (b) Moss, M. A. J.; Jones, C. J. *Polyhedron* **1990**, *9*, 697–702. (c) Moss, M. A. J.; Jones, C. J. *J. Chem. Soc. Dalton Trans.* **1990**, 581–591. (d) Moss, M. A. J.; Jones, C. J. *Polyhedron* **1989**, *8*,

2367–2370.

102. Liu, S. Y.; Maunder, G. H.; Sella, A.; Stephenson, M.; Tocher, D. A. *Inorg. Chem*. **1996**, *35*, 76–81.

103. Masino, A. P. Lanthanide Complexes. Ph.D. Thesis, University of Alberta, August, 1978.

104. Long, D. P.; Chandrasekaran, A.; Day, R. O.; Bianconi, P. A.; Rheingold, A. L. *Inorg. Chem*. **2000**, *39*, 4476–4487.

105. Rabe, G. W.; Zhang–Presse, M.; Riederer, F. A.; Rheingold, A. L. *Acta Crystallogr*. **2006**, *E62*, m3149–m3151.

106. Long, D. P.; Bianconi, P. A. *J. Am. Chem. Soc*. **1996**, *118*, 12453–12454.

107. Blackwell, J. A.; Lehr, C.; Sun, Y.; Piers, W. E.; Pearce–Batchilder, S. D.; Zaworotko, M. J.; Young, V. G. J. *Can. J. Chem*. **1997**, *75*, 702–711.

108. Aposttolidis, C.; Carvalho, A.; Domingos, A.; Kanellakopulos, B.; Maier, R.; Marques, N.; Pires de Matos, A.; Rebizant, J. *Polyhedron* **1999**, *18*, 263–272.

109. Roistershtein, D.; Domingos, A.; Pereira, L. C. J.; Ascenso, J. R.; Marques, N. *Inorg. Chem*. **2003**, *42*, 7666–7673.

110. Moss, M. A. J.; Kresinski, R. A.; Jones, C. J.; Evans, W. J.; *Polyhedron* **1993**, *12* 1953–1955.

111. Domingos, Â, Marçalo, J. Marques, N. Pires De Matos, A. Galvão, A, ; Isolani, P. C.; Vicentini, G.; Zimmer, K. *Polyhedron* **1995**, *14*, 3067–3076.

112. Takats, J.; Zhang, X. W.; Day, V. W.; Eberspacher, T. A.

Organometallics **1993**, *12*, 4286–4288.

113. Maunder, G. H.; Sella, A.; Tocher, D. A. *J. Chem. Soc. Chem. Commun.* **1994**, 885–886.

114. Hiller, A. C.; Zhang, X. W.; Maunder, G. H.; Liu, S. Y.; Eberspacher, T. A.; Metz, M. V.; McDonald, R.; Domingos, A.; Marques, N.; Day, V. W.; Sella, A.; Takats, J. *Inorg. Chem*. **2001**, *40*, 5106–5116.

115. Zhang, X. W. Synthesis and Reactions of Hydrotris(pyrazolyl) borate Complexes of Divalent Lanthanides. Ph.D Thesis, University of Alberta, Edmonton AB. Canada, August, 1995.

116. Domingos, Â.; Lopes, I.; Waerenborgh, J. C.; Marques, N.; Lin, G. Y.; Zhang, X. W.; Takats, J.; McDonald, R.; Hillier, A. C.; Sella, A.; Elsegood, M. R. J.; Day. V. W. *Inorg. Chem.* **2007**, *46*, 9415–9424.

117. Lopes, I.; Dias, R.; Domingos, A.; Marques, N. *J. Alloy Compds.* **2002**, *344*, 60–64.

118. Takats, J. *J. Alloys Compds*. **1997**, *249*, 52–55.

119. Zhang, X. W.; Loppnow, G. R.; McDonald, R.; Takats, J. *J. Am. Chem. Soc.* **1995**, *117*, 7828–7829.

120. Zhang, X. W.; McDonald, R.; Takats, J. *New. J. Chem*. **1995**, *19*, 573–585.

121. (a) Maunder, G. H. Sella, A.; Tocher, D. A. *J. Chem. Soc. Chem. Commun.* **1994**, 2689–2690. (b) Maunder G. H. Chemistry of the Lanthanides with Pyrazolylborate Ligands. Ph.*D* Thesis, University College London, June, **1996**.

122. Hassinoff, L.; Takats, J.; Zhang, X. W.; Bond, P. H.; Rogers, R. D. *J. Am. Chem. Soc.* **1994**, *116*, 8833–8834.

123. Ferrence, G. M.; McDonald, R.; Morissette, M.; Takats, J. *J. Organomet. Chem.* **2000**, *596*, 95–101.

124. Cheng, J.; Takats, J.; Ferguson, M. J.; McDonald, D. *J. Am. Chem. Soc.* **2008**, *130*, 1544–1545.

125. Ferrence, G. M.; McDonald, R.; Takats, J. *Angew. Chem. Int. Ed*. **1999**, *38*, 2233–2237.

Chapter 2

Ytterbium(II) Tetrahydroborate Complexes Supported by tris(3-tert-butyl-5-methylpyrazolyl)borate Ligand: Synthesis and Characterization[*]

2.1 Introduction

The study of complex hydrides, particularly those of the lightest elements, has received fresh impetus in recent years arising from their potential as hydrogen storage media.[1] But complex hydrides have long been of interest to synthetic chemists because of their effectiveness as reagents.[2] In the case of transition metals and lanthanides, significant catalytic reactivity has been uncovered, and as a result there has been intense interest in the details of their structure and bonding. Borohydrides (tetrahydroborates), in particular, are known to adopt a variety of bonding modes when coordinated to such heavier elements, and these studies have shown that the structures adopted depend on both steric and electronic factors.[3,4]

Less numerous than their transition metal, and even actinide counterparts, lanthanide borohydrides have been known for a long time, starting with the earliest reports by Zange, Rossmanith, and Mirsaidov, [5,6,7] of such species as $Ln(BH_4)_3(THF)_n$ complexes (Ln = Y, Sm, Eu, Gd, Tb, Dy, Ho, Er, Tm, Yb, Lu), as well as several mixed ligand examples featuring compounds such as mixed halide tetrahydroborate complexes, $LnCl(BH_4)_2$ (Ln = Y, Sm, Gd, Ho, Dy) and $LnCl_2(BH_4)$ (Ln = Sm, Er, Yb). In these early studies, which have been well-

---

[*] A slightly modified version of this chapter has been published. Saliu, K.O.; Maunder, G.; Ferguson, M. J.; Sella, A.; Takats, J. *Inorg. Chim. Acta.* **2009**, *362*, 4616-4622.

summarized by Marks,[3] structural details were sorely lacking and bonding modes were for the most part inferred from vibrational spectroscopy. Better characterized examples have emerged recently thanks to the work of Ephritikhine *et al.*[8] The use of cyclopentadienyl ancillaries has resulted in the isolation of a variety of well-defined, monomeric mono- and bis-tetrahydroborates such as $[(C_5H_5)_2Ln(BH_4)(THF)_n]$ (n = 0, Ln = Sc; n = 1, Ln = Sm, Er, Yb, Lu),[9] $[(C_5Me_5)_2Nd(BH_4)(THF)]$,[10] $[(C_5H_3(TMS)_2)_2Ln(BH_4)(THF)_n]$ (n = 0, Ln = Sc; n = 1, Ln = Y, La, Pr, Nd, Sm, Yb),[11] $[(C_5H_4CH_2CH_2OMe)_2Ln(BH_4)]$ (Ln = Y, La, Pr, Nd, Sm, Gd),[12] $[(C_5Me_4{}^iPr)_2Sm(BH_4)(THF)]$,[13] $(C_5H^iPr_4)Ln(BH_4)_2(THF)$ (Ln = Sm, Nd),[14] and $(C_5Me_4{}^nPr)Ln(BH_4)_2(THF)$ (Ln = Sm, Nd).[15] There appears to be only one report in the literature describing well characterized lanthanide(II) te-trahydroborate complexes, $Ln(BH_4)_2L_4$ (Ln = Eu, Yb ; L C_5H_5N, CH_3CN),[16] and there are no example of mono-ligand Ln(II) tetrahydroborate complexes. The rari-ty of such compounds can be attributed to the large size of the Ln^{2+} ions together with the lack of starting materials containing ancillary ligands of sufficient bulk to suppress ligand redistribution reactions.

Sterically loaded pyrazolylborates have been shown to be very effective ancillaries capable of suppressing ligand redistribution for elements throughout the periodic table,[17] including the lanthanides.[18] Earlier works from this laboratory have shown that the use of the sterically bulky (3-*tert*-butyl-5-methylpyrazolyl)borate, $(Tp^{tBu,Me})$ ligand, allowed the isolation of low coordina-tion number complexes of the divalent lanthanide metals such as $(Tp^{tBu,Me})YbQ(THF)_n$ (Q = I, CH_2SiMe_3, $CH(SiMe_3)_2$, $N(SiMe_3)_2$, OAr (Ar = 2, 4,

6-trimethylbenzene) n = 0 or 1),[19,20] as well as the hydride dimer, [(Tp^{tBu,Me})YbH]$_2$,[21] which has been shown to display extensive reactivity towards a variety of substrates including protic substrates such as alcohols, dipivaloylmethane, amines, terminal alkynes and unsaturated substrates such as internal alkynes, CO and a host of others[21]. The availability of the hydride dimer, [(Tp^{tBu,Me})YbH]$_2$, **1**,[21] and the half sandwich iodide, (Tp^{tBu,Me})YbI(THF), **2**,[19] affords two alternative and complementary methods for the synthesis of mono-ligand ytterbium(II) tetrahydroborate complexes supported by the bulky hydrotris(3-^{t}Bu, 5-Me pyrazolyl)borate, (Tp^{tBu,Me}), ligand.

The preparation of the ytterbium borohydride complex, (Tp^{tBu,Me})Yb(BH$_4$)(THF), was initially carried out by Graham Maunder at UCL,[22] however, the interest to revisit the synthesis was three fold: 1. The lack of structural details on the compound; even though spectroscopic evidence supported the formulation as the monomeric (Tp^{tBu,Me})Yb(BH$_4$)(THF) complex, it would be valuable to determine the actual bonding mode of the borohydride ligand to allow for comparison with other known ytterbium(II) complexes. 2. The availability of the hydride dimer, [(Tp^{tBu,Me})YbH]$_2$ **1**,[21] was expected to serve as a source of the solvent free analogue of the compound to allow for structural comparison. 3. Finally, it served as a way of introducing the author to the synthesis and the spectroscopic techniques used in organolanthanide chemistry.

2.2 Synthetic Aspects

2.2.1 Synthesis and Characterization of (Tp^{tBu,Me})Yb(BH$_4$) (3)

Addition of two equiv. of H$_3$BNMe$_3$ to a deep red benzene solution of the hydride [(Tp^{tBu,Me})YbH]$_2$, **1**, showed no immediate reaction. However, the color of the solution changed slowly from deep red to orange and finally yellow orange over the course of 2 days, eq. 2.1. Simple work up of the reaction mixture afforded the compound as a free flowing and moisture sensitive yellow powder in good yield. It was later discovered that the compound can be prepared also by the reaction of (Tp^{tBu,Me})YbI(THF), **2**, with NaBH$_4$ in acetonitrile. The latter method has the advantages of shorter reaction time and the possibility of a large scale reaction (see Experimental Section). Compound **3** is soluble in common organic solvents such as pentane, hexane, toluene, benzene, and ether type solvents. However, in THF, it converts to the THF solvated compound, (Tp^{tBu,Me})Yb(BH$_4$)(THF), **4** (*vide infra*).

$$[(Tp^{tBu,Me})YbH]_2 + 2\ H_3BNMe_3 \xrightarrow[\text{48Hrs}]{\text{RT, C}_6\text{H}_6} 2\ (Tp^{tBu,Me})Yb(BH_4) + 2\ NMe_3 \qquad 2.1$$

$$\textbf{1} \qquad\qquad\qquad\qquad\qquad\qquad \textbf{3}$$
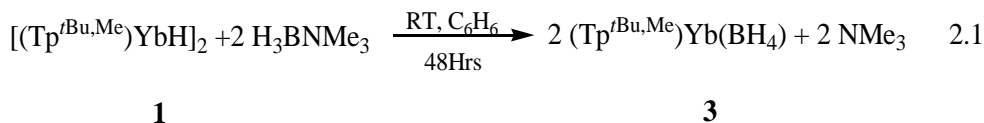
The compound has been characterized by IR and NMR (^{1}H, ^{13}C and ^{11}B) spectroscopies. However, all attempts to obtain elemental analysis failed to give satisfactory results, even when crystalline material was used; higher than expected C, H and lower than expected N values were obtained on each attempt. On the basis of NMR spectroscopy however, the compound is authentic as formulated. The consistently poor elemental analysis values may be attributed to contamination by hydrocarbon solvent impurities. It is noted that similar elemental analysis problem

was encountered by Shore and co-workers with their ytterbium(II) tetrahydrobo-rate compounds, $L_4Yb[(\mu\text{-}H_3\text{-}BH)]_2$.[16]

The IR spectrum of compound **3**, Figure 2.1, displays three bands in the B–H region at 2552 cm^{-1}, 2472 cm^{-1} (strong, singlet) and 2293 & 2236 cm^{-1} (strong, doublet with a splitting of 57cm^{-1}). The band at 2552 cm^{-1} is
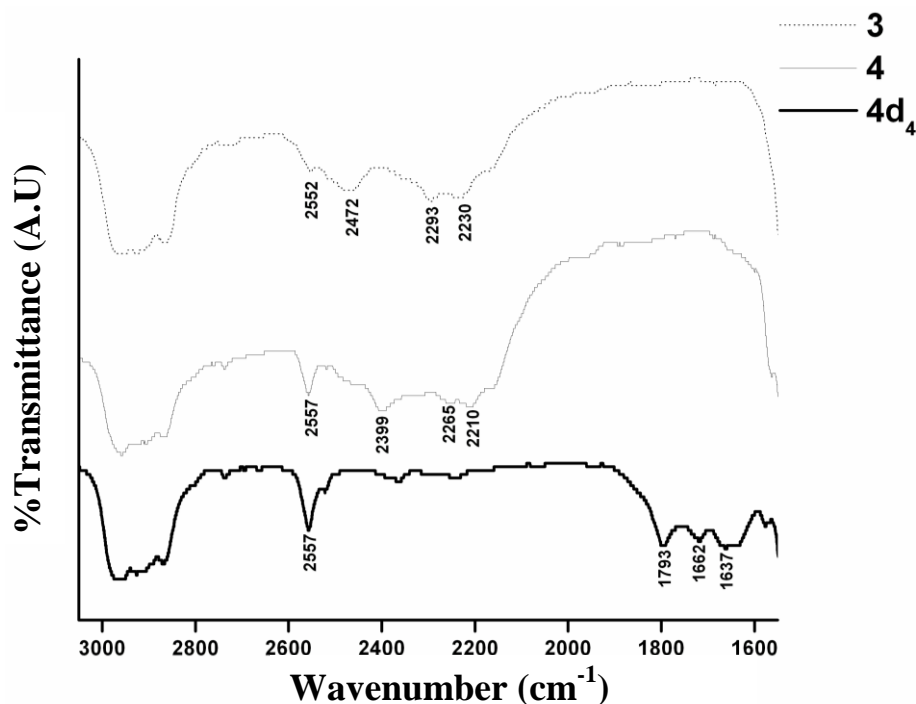
Figure 2.1: FT-IR Spectra of Compounds **3**, **4** and **4-d_4** in the 3000-1600 cm^{-1} Region. The vertical scales for compounds **3** and **4** were magnified by a factor of 2 and 4, respectively, for better visualization.

typical of terminal B–H stretch of κ^3 pyrazolylborate ligands.[23] The other peaks are characteristic of a tridentate tetrahydroborate ligand[3] with the high frequency band assigned to the terminal B–H and the doublet assigned to the bridging B–H stretches, respectively.

51

The ^{1}H NMR spectrum of **3** displays a single set of signals for the pyrazo-lylborate ligand, in the expected 27:9:3 ratio, indicative of a symmetrical Tp^{tBu,Me} ligand environment in solution. The protons of the tetrahydroborate
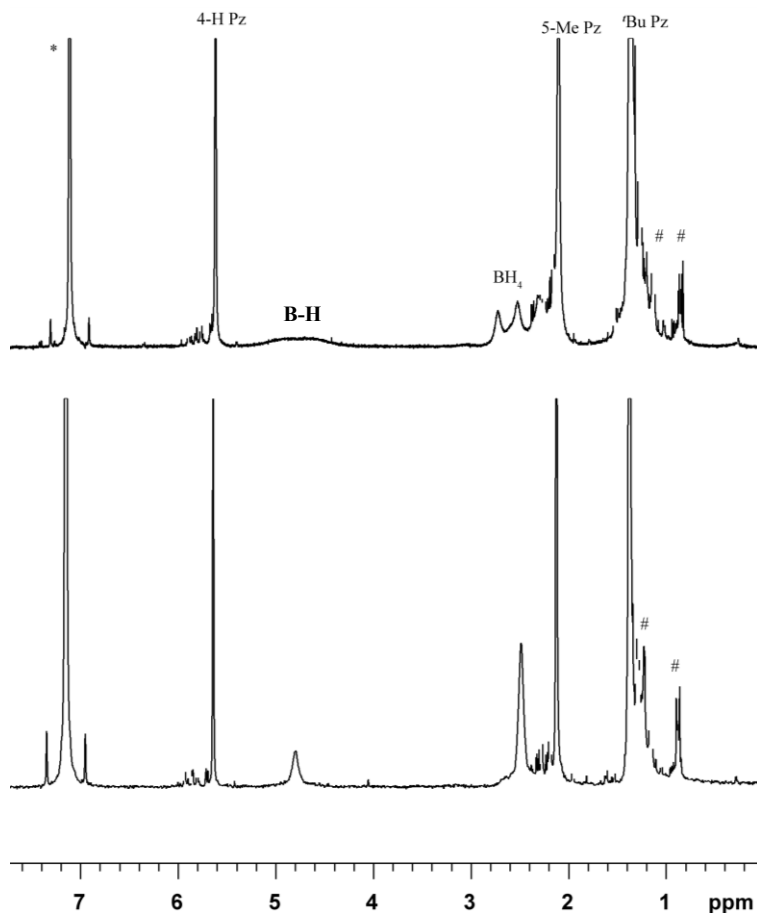
Figure 2.2: ^{1}H NMR Spectra (400 MHz, 25°C) of Compound **3** in C$_6$D$_6$. ^{1}H (top) and ^{1}H{^{11}B} (bottom). The vertical scale has been increased to show the BH$_4$ signals, thus the ^{t}Bu, Me and 4-H signals of the pyrazolyl groups are trun-cated. In this spectrum and all subsequent ones, * denotes residual solvent peak and # denotes hydrocarbon impurities.

ligand appear as a broad 1:1:1:1 quartet centered at 2.44 ppm with J_{B-H} of 82 Hz, indicating, as usual, rapid bridge-terminal hydrogen exchange in the BH$_4$ ligand.[3] This quartet collapsed to a singlet in the boron-decoupled ^{1}H NMR, Figure 2.2. The ^{11}B NMR spectrum, Figure 2.3, shows two signals in the intensity ratio 1:1 at

ca. -8 ppm and -28 ppm. In the proton-coupled ^{11}B NMR spectrum, the high field signal became a well–defined quintet with J_{B-H} of 82 Hz, whereas the low field signal showed no resolvable coupling, just slight broadening. Thus, the high field and low field signals are assigned to the boron atoms of the tetrahydroborate ligand and of the ancillary pyrazolylborate ligand, respectively. The [11]B chemical shift of the latter ligand is similar to the values found in other $(Tp^{tBu,Me})YbQ(THF)_{0/1}$ complexes $(Q = I^-, -CH_2SiMe_3$ and ArO^-).[19,20,24]
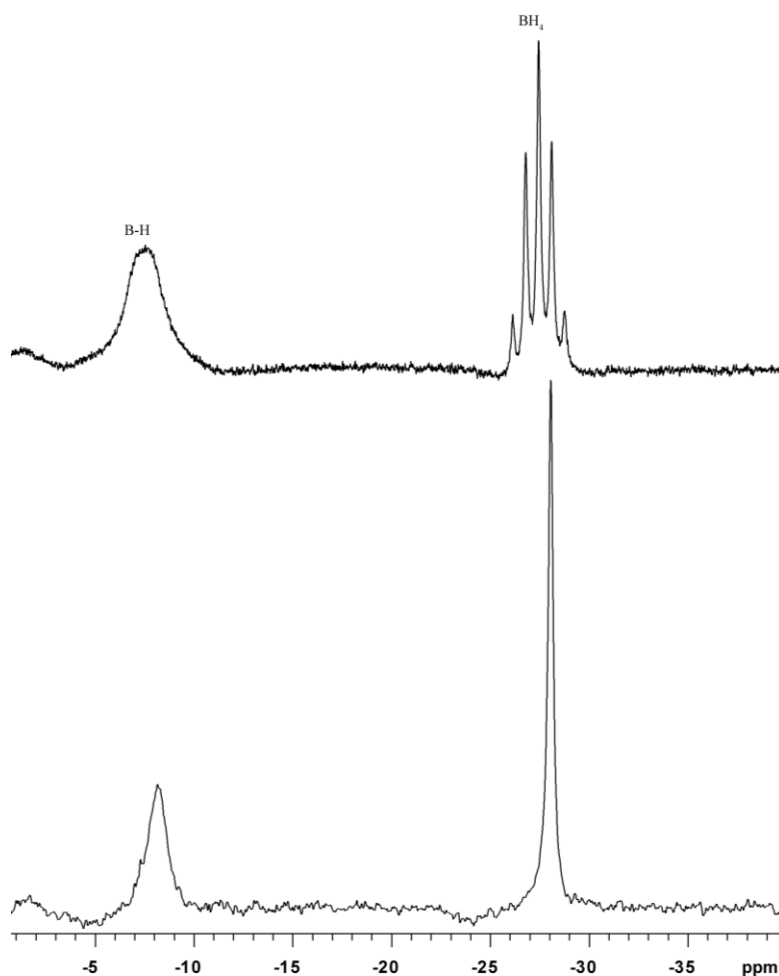
Figure 2.3: ^{11}B NMR Spectra (128 MHz, 25°C) of $(Tp^{tBu,Me})Yb(BH_4)$ (**3**) in C_6d_6; [11]B (top) and [11]B{[1]H} (bottom).

To corroborate the spectroscopic deductions, X-ray quality crystals were grown from a dilute pentane solution. Unfortunately the crystals obtained were those of the THF adduct, $(Tp^{tBu,Me})Yb(BH_4)(THF)$, **4**. Further attempts to obtain ssingle crystals of **3** proved unsuccessful, giving either poor quality crystals or the ligand redistribution product, $(Tp^{tBu,Me})_2Yb$.[25]

2.2.2 Synthesis and Characterization of $(Tp^{tBu,Me})Yb(BH_4)(THF)$ (4)

The THF adduct, **4**, could be prepared more conveniently by salt metathesis using $(Tp^{tBu,Me})YbI(THF)$ and an alkali metal borohydride, such as $NaBH_4$ or KBH_4 according to eq. 2.2

$$(Tp^{tBu,Me})YbI(THF) + MBH_4 \xrightarrow[-MI]{Solvent} (Tp^{tBu,Me})Yb(BH_4)(THF) \quad 2.2$$

<div align="center">

2   **4**

Solvent = THF or CH_3CN
M = K or Na

</div>
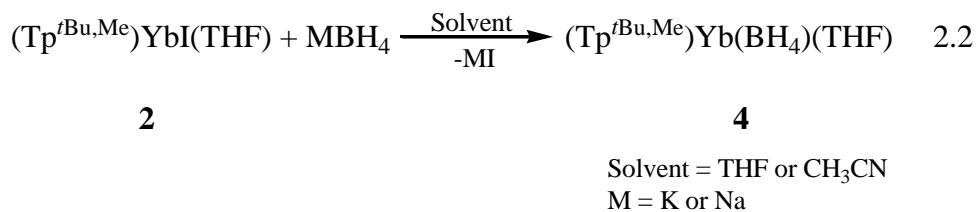
Although on paper the procedure is a simple mixing of two reagents, the course of the reaction is strongly affected by the choice of alkali metal borohydride, the duration of the reaction, and by the choice of solvent. In addition, monitoring the progress and extent of the reaction by ^{11}B NMR spectroscopy initially proved problematic since the [11]B signature of the pyrazolylborate ligand of product **4** is coincident with that of the half-sandwich starting material **2**. Once this was realized, the extent of the reaction could be determined by making appropriate correction to the integration of the overlapping pyrazolylborate peaks of **4** and $(Tp^{tBu,Me})YbI(THF)$, **2**, based on that of the borohydride signal of **4** and the 1:1

ratio of the two signals in the product, **4**.

In THF and with KBH_4 the maximum conversion to **4** was ca. ~ 66% after a 5 day reaction time; longer reaction time led to decomposition and gave unidentified, complex mixtures. Over the same time period complete conversion was obtained with the more THF soluble $NaBH_4$. Not surprisingly, the solubility of the alkali metal borohydride in THF is a major factor. To speed up the reaction, a more polar solvent in which the alkali metal borohydrides are more soluble and in which the half sandwich starting material, $(Tp^{tBu,Me})YbI(THF)$, **2**, is stable was sought. The choice of solvent was aided by two independent contributions, from Shore *et al.* who have found that acetonitrile is a good solvent for the synthesis of lanthanide(II) borohydrides[16] and Desrocher *et al.* who demonstrated the use of acetonitrile for the synthesis of a nickel(II) borohydride complex bearing 3,5-dimethyl(pyrazolyl)borate ligand.[26]

The reaction of $(Tp^{tBu,Me})YbI(THF)$ with $NaBH_4$ in acetonitrile at room temperature was complete in ~19 hrs and gave **4** in good yield after a simple work up. Compound **4** was characterized by IR and NMR spectroscopy, and its solid-state structure determined by single crystal X-ray diffraction. Similar to the observation made on **3**, elemental analysis results were consistently poor even when X-ray quality crystals were used.

The IR spectrum of **4**, in the B-H stretching region, showed bands at 2557 cm^{-1}, 2399 cm^{-1} and a doublet centered at 2238 cm^{-1}, with a splitting of 56 cm^{-1}. The first band corresponds to the B–H stretch of the pyrazolylborate ligand[23] while the other two are characteristic of tridentate tetrahydroborate ligand,[3] Figure 2.1.

The corresponding **4-*d*** analogue showed the expected shifts in the IR spec-

trum, 1793 (s, B–D_t of BD_4, (v_H/v_D = 1.34)), 1662 and 1637 (d, B–D_b of BD_4;

splitting 25 cm^{-1} (v_H/v_D = 1.36)), Figure 2.1. The band positions of **4** are at lower
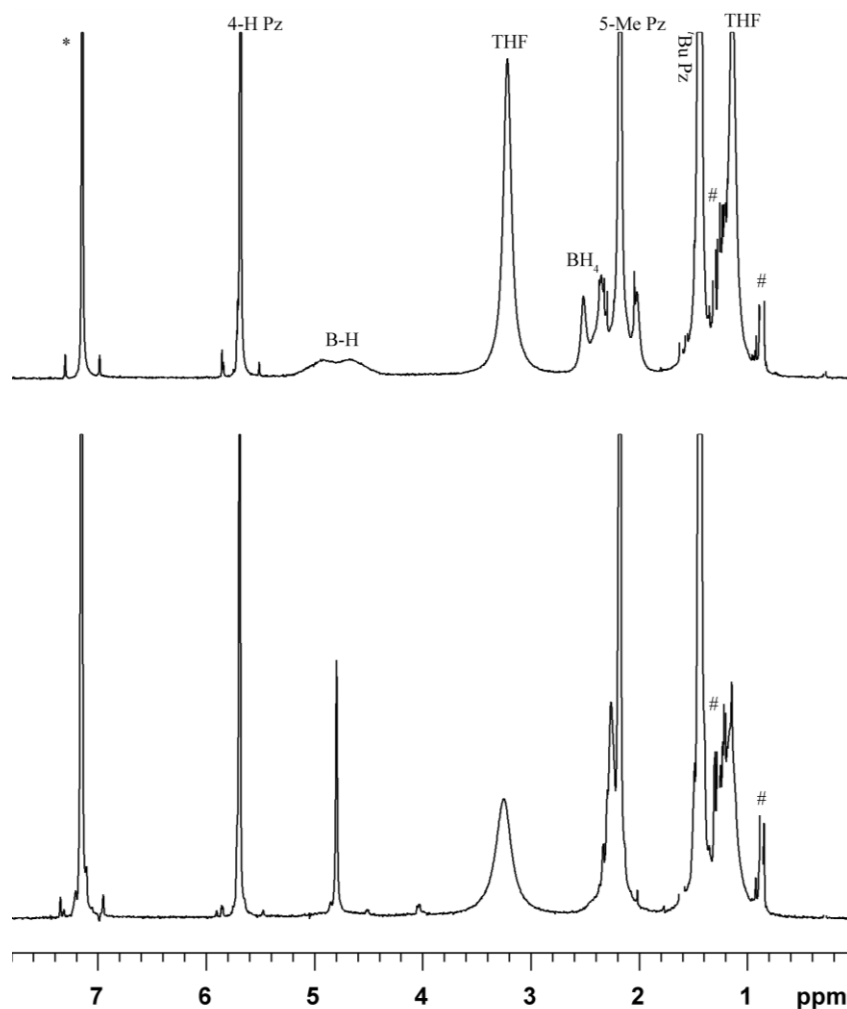
Figure 2.4: ^{1}H NMR Spectra (400 MHz, 25°C) of (Tp^{tBu,Me})Yb(BH$_4$)(THF) (**4**) in C$_6$d$_6$. ^{1}H (top) and ^{1}H{^{11}B}(bottom). (Note that one of the BH$_4$ quartet over-laps with the 5-Me signal of the Tp^{tBu,Me} ligand).

frequency than those of **3** and suggest a weaker Yb-BH$_4$ interaction in **4** as a result

of the presence of the additional THF ligand.

The ^{1}H NMR spectrum of **4** is similar to that of **3** with the exception of

signals due to the coordinated THF ligand and a slight shift by ca. 0.2 ppm of the

BH_4 signal to high field. The BH_4 hydrogens appear as a broad quartet centered at

2.28 ppm with J_{B-H} coupling of 80 Hz, Figure 2.4.

The ^{11}B NMR spectrum exhibits two peaks in intensity ratio 1:1 at ca. -8

ppm and -30 ppm for the pyrazolylborate and tetrahydroborate ligands, respective-

ly. The high field signal is a quintet with J_{B-H} coupling of 80 Hz in the ^{1}H coupled

^{11}B NMR spectrum, Figure 2.5.
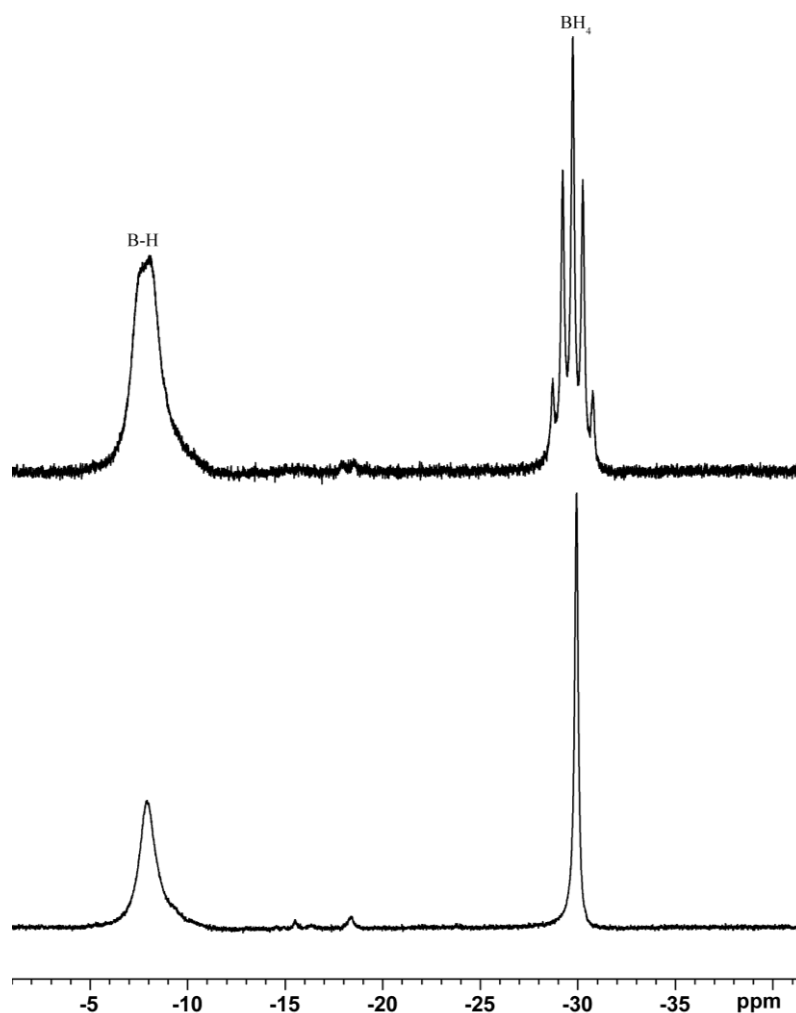
Figure 2.5: ^{11}B NMR Spectra (128 MHz, 25°C) of $(Tp^{tBu,Me})Yb(BH_4)(THF)$ (**4**) in C_6d_6; ^{11}B (top) and ^{11}B{^{1}H}(bottom).

The ^{1}H NMR of BD$_4$ analogue of **4,** is identical to that of **4** except for the absence of the broad quartet due to the BH$_4$ ligand. This appeared in the ^{2}H NMR as a broad signal at ca. 2.20 ppm. The ^{11}B NMR also displayed two peaks of intensity ratio 1:1 at ca. -8 and -30 ppm for the pyrazolylborate and tetradeuterioborate ligands, respectively. The low field peak broadened slightly in the ^{1}H coupled ^{11}B NMR spectrum while the high field peak remained unaffected; however, this peak sharpens in the ^{2}H decoupled ^{11}B NMR spectrum.

In an attempt to understand the nature of, or at least slow down the dynamic process involved in the bridge-terminal exchange of the BH$_4$ hydrogens, variable temperature ^{1}H and ^{11}B NMR studies were carried out. As the temperature was lowered, the broad quartet in the ^{1}H NMR spectrum, associated with the BH$_4$ ligand gradually coalesced giving a broad featureless band. This is consistent with previous observations by Marks *et al.* who observed similar behavior for Zr(BH$_4$)$_4$ and Hf(BH$_4$)$_4$,[27] they rationalized their observations on the basis of "thermal" decoupling of the ^{11}B from the ^{1}H nuclei due to more efficient quadrupolar relaxation of the ^{11}B nucleus as the temperature is lowered.[28] In order to effectively remove the quadrupolar effect of the ^{11}B nucleus on the ^{1}H nucleus, variable temperature ^{1}H NMR study was carried out on **4** in THF-d_8 with ^{11}B decoupling. The dynamic process remained fast on the NMR timescale for the entire temperature range studied (25°C to –90°C) as indicated by the appearance of a single peak for the BH$_4$ ligand. A corresponding variable temperature ^{11}B NMR experiment was also consistent with the above observation, showing gradual broadening as the temperature was lowered resulting in a broad peak at –90°C and all the coupling,

again, essentially being "washed out". These observations are not peculiar to the tetrahydroborate ligand, it has been observed in other boron hydride species.[29]

Attempts to remove the coordinated THF from **4** and **4d_4** by either successive triturations with non–coordinating solvents and / or prolonged drying under high vacuum were unsuccessful. This is similar to observations made on other (Tp^{tBu,Me})YbQ(THF) complexes, such as (Tp^{tBu,Me})YbI(THF), **2**[19,22] (Tp^{tBu,Me})Yb(CH$_2$SiMe$_3$)(THF),[24] (Tp^{tBu,Me})Yb(OC$_6$H$_2$Me$_3$-2,4,6)(THF).[20] Whereas the samarium analogue of compound **2**, (Tp^{tBu,Me})SmI(THF)$_2$ readily loses both THF molecules to give the THF free compound, (Tp^{tBu,Me})SmI[24,22] compound **2** was found to lose THF only under forcing conditions and was accompanied by partial decomposition to give a rather delicate THF free species.[22] This parallels the observation made on the pair of (C$_5$Me$_5$)$_2$Ln(THF)$_2$ (Ln = Sm, Yb); the samarium complex readily loses the two THF molecules,[30] while the ytterbium analogue loses only one under similar condition and attempts to remove the final THF were unsuccessful.[31] This difference in lability of THF can be attributed to the difference in the charge/radius ratio of the two metal centers, binding of the coordinated THF molecule is stronger with the smaller ytterbium(II) cation than with the larger samarium(II) center.

2.2.3 Solid State Structure of (Tp^{tBu,Me})Yb(BH$_4$)(THF) (4)

The solid state structure of **4**, determined by single crystal X-ray diffraction, is in accord with the IR and NMR data. The ORTEP plot of **4** is given in Figure 2.6, selected bond lengths and bond angles are given in Table 2.1.

X–ray analysis revealed a monomeric complex in which the ytterbium center is bonded to a κ^3-pyrazolylborate, κ^3-tetrahydroborate ligand and the oxygen atom of a THF molecule. As in other complexes of the type $(Tp^{tBu,Me})YbQ(THF)$,[19,20,24] the κ^3-pyrazolylborate occupies a position opposite to that of the anionic ligand, in this case the triply bridging κ^3-tetrahydroborate,
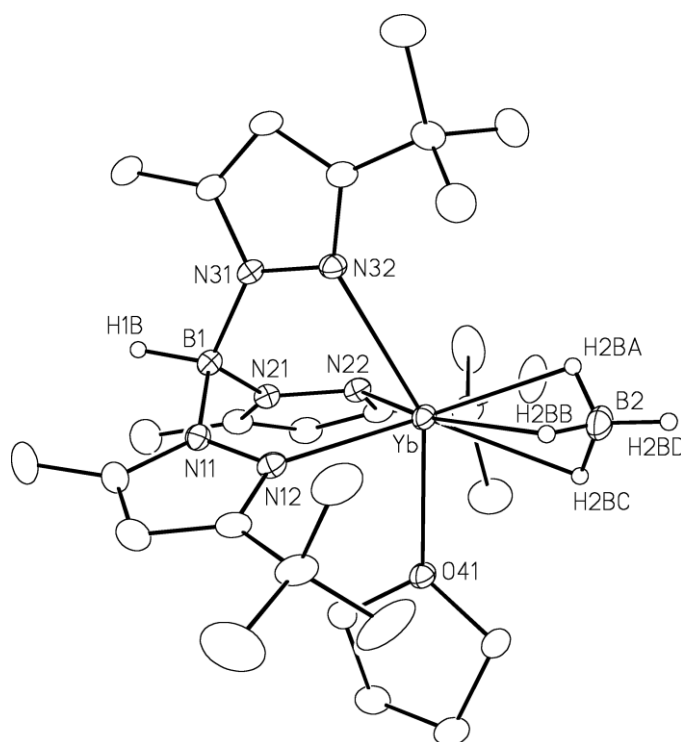
Figure 2.6: ORTEP View of $(Tp^{tBu,Me})Yb(BH_4)(THF)$ (**4**).
In this ORTEP and all subsequent ones, non-hydrogen atoms are
represented by Gaussian ellipsoids at the 20% probability level.

presumably to minimize electrostatic repulsion between the anionic boron centers; the non-bonding B1-Yb-B2 angle being 166.90(13)°. The THF ligand sits in the cleft formed by the ^tBu substituents of two pyrazolyl groups.

To draw analogy and to facilitate structural comparison with the related

Table 2.1: Selected bond lengths and angles in (Tp^{tBu,Me})Yb(BH$_4$)(THF) (**4**).

Yb–O41	2.463(2)	O41–Yb–N12	83.20(8)
Yb–N12	2.454(3)	O41–Yb–N22	81.25(8)
Yb–N22	2.454(3)	O41–Yb–N32	147.54(8)
Yb–N32	2.526(3)	O41–Yb–B2	95.41(12)
Yb–H2BA	2.26(5)	N12–Yb–N22	94.06(9)
Yb–H2BB	2.32(5)	N12–Yb–N32	73.93(9)
Yb–H2BC	2.37(4)	N22–Yb–N32	77.80(9)
Yb----B1	3.343(4)	N12–Yb–B2	131.27(16)
Yb----B2	2.596(5)	N22–Yb–B2	134.16(16)
B1–H1B	1.16(4)	N32–Yb–B2	116.97(13)
B2–H2BA	0.96(5)	B1–Yb–B2	166.90(13)
B2–H2BB	1.05(5)		
B2–H2BC	1.12(4)		
B2–H2BD	1.01(5)		

(Tp^{tBu,Me})YbQ(THF)[19,20,24] complexes, although formally seven coordinate, pound **4** may be regarded as five coordinate if the κ^3-tetrahydroborate ligand is considered to occupy one coordination position. As with these other complexes, the coordination geometry is perhaps best described as distorted trigonal bipyramidal (tbp) with two pyrazolyl nitrogens (N12 and N22) and B2 forming the equatorial plane, and the third nitrogen (N32) and the THF oxygen (O41) occupying the axial positions. In line with this description, the N12–N22–Yb–B2 atoms are almost planar, with the largest deviation being that of Yb, 0.08(2) Å.

The coordinated THF ligand is not far from being orthogonal to the equa-

torial plane with N12–Yb–O41, N22–Yb–O41 and O41–Yb–B2 angles of 83.20(8)°, 81.25(8)° and 95.41(8)°, respectively. Ligand constraint from the κ^3-pyrazolylborate ligand necessarily results in distortions from regular tbp geometry, with compression of the equatorial N12–Yb–N22 angle from 120° to 94.06(9)° and a corresponding opening of the non-bonding N12–Yb–B2 and N22–Yb–B2 angles to 131.27(16)° and 134.16(16)°, respectively. Most significantly, the axial N32–Yb–O41 angle (147.54(8)°), is far from the ideal tbp angle of 180°. Similar type of distortions were seen in the related $(Tp^{tBu,Me})YbQ(THF)$[19, 20,24] complexes but were less severe, reflecting their true five coordinate nature.

As a reflection of its axial position and opposite to the strongly bonded THF ligand, the Yb–N32 distance is about 0.07Å longer than the other Yb−N bonds, otherwise the Yb–N bond lengths are similar to those found in other $(Tp^{tBu,Me})YbQ(THF)$[19,20,24] complexes. The Yb−O41 bond length of 2.463(2)Å is comparable to 2.447(6)Å and 2.484(3)Å found in **2**[19] and $(Tp^{tBu,Me})Yb(CH_2SiMe_3)(THF)$,[24] respectively but slightly longer than the 2.415(5)Å value in $(Tp^{tBu,Me})Yb(OC_6H_2Me_3–2,4,6)(THF)$.[20]

The metal-boron distance has been shown to correlate with the bonding mode of the tetrahydroborate ligand,[32] and based on this, an ionic radius of ~1.6 ± 0.1 Å and 1.36 ± 0.06 Å was assigned to bidentate and tridentate tetrahydroborate ligand, respectively.[33] The Yb-B distance of 2.592(5) Å in **4** is consistent with a tridentate tetrahydroborate bonding mode. This distance is somewhat shorter than 2.666(6) Å found in the higher coordination number $(CH_3CN)_4Yb\{(\mu\text{-}H)_3BH\}_2$[16] complex. The distance also compares favorably with 2.470(8) Å and 2.460(10)Å

found in [*meso*-(CH$_3$)$_2$Si[3-(CH$_3$)$_3$SiC$_5$H$_3$]$_2$Yb[(μ–H$_3$)BH](THF)[34] and Yb(BH$_4$)$_2$(OC$_6$H$_2$-^{t}Bu$_3$-2,4,6)(THF)$_2$,[35] respectively, after allowing for the difference of ca. 0.15Å in ionic radii between Yb(II) and Yb(III).[36] However, as expected, this distance is shorter than 2.800(24) Å found in (MeOCH$_2$CH$_2$C$_5$H$_4$)$_2$Yb(BH$_4$),[37] a compound known to have bidentate tetrahydroborate ligand. The average Yb–H distance of 2.32(5) Å in **4** is comparable to the values seen in the divalent lanthanide complexes (CH$_3$CN)$_4$Yb[(μ–H)$_3$BH]$_2$,[16] (2.44(5) Å) and (Tp^{tBu,Me})Tm(μ–HBEt$_3$)(THF),[38] (2.40(8) Å) and in the Yb(III) complex [*meso*-(CH$_3$)$_2$Si[3-(CH$_3$)$_3$SiC$_5$H$_3$]$_2$Yb[(μ–H$_3$)BH](THF),[34] (2.18(5) Å), again after correction for the difference in size of Yb(III) in the latter complex.

Attempts to make the samarium and thulium analogues of **3** and **4** proved unsuccessful. Reaction of (Tp^{tBu,Me})LnI(THF)$_2$ (Ln = Sm, Tm) with NaBH$_4$ in either acetonitrile or THF gave mixtures of the known (Tp^{tBu,Me})$_2$Ln, [25,38] as shown by NMR spectroscopy, and other unidentified products.

2.3 Conclusions

The availability of the ytterbium hydride dimer, [(Tp^{tBu,Me})YbH]$_2$, **1**, and the half-sandwich ytterbium iodide complex, (Tp^{tBu,Me})YbI(THF), **2**, provides effective routes for the synthesis, isolation and characterization of the first mono-ligand Ln(II) tetrahydroborate complexes, (Tp^{tBu,Me})Yb(BH$_4$), **3** and (Tp^{tBu,Me})Yb(BH$_4$)(THF), **4**. The compounds were characterized by IR and multi-nuclear NMR spectroscopies and, in the case of **4** single crystal X-ray diffraction studies confirmed the tridentate bonding mode of the tetrahydroborate ligand. No

solid state structure is available for **3**; however, spectroscopic evidences support its formulation as the solvent free analogue of **4**. Failure to isolate similar samarium and thulium compounds parallels the difficulties encountered in isolating samarium(II) and thulium(II) analogues of otherwise well-behaved ytterbium(II) pyrazolylborate species. This suggests that the larger samarium and thulium centers are much more susceptible to ligand redistribution processes, and the isolation of such species will either require extremely delicate handling, or the use of a more encumbered ancillary ligand.

2.4 Experimental Section

2.4.1 General Techniques and Solvents

The compounds described herein are extremely air and moisture sensitive, thus all operations were performed under inert (nitrogen/helium or argon) atmospheres using a combination of Schlenk-line and glove-box (Vacuum Atmosphere Company) techniques. Glassware was dried at 250°C prior to use. Solvents (THF, toluene, benzene) were distilled from Na/K alloy/benzophenone ketyl under nitrogen and degassed by three freeze-pump-thaw cycles before use. Pentane was distilled from CaH_2 under nitrogen. Anhydrous acetonitrile (99.8%) was purchased from Aldrich and used without further purification. Deuterated solvents (C_6D_6, toluene-d_8 and THF-d_8; Cambridge Isotope Laboratories) were dried over Na/K alloy/benzophenone ketyl, degassed by three freeze-pump-thaw cycles and vacuum transferred prior to use.

2.4.2 Physical Measurements

NMR samples were prepared in the glove box and sealed under vacuum. Proton chemical shifts are recorded relative to external TMS standard and were referenced to residual protons in deuterated solvents (THF–d_8, 1.73; toluene-d_8, 2.09; benzene-d_6; 7.15ppm), ^{11}B chemical shifts were reported relative to external $F_3B \cdot Et_2O$. ^{1}H and ^{11}B NMR spectra were recorded at 400 or 500 MHz and 128 or 160 MHz, respectively, on Varian Inova 400 or 500 FT spectrometers. Elemental microanalysis was performed on Carlo Erba (Thermo Fisher Scientific) CHNS–O EA1108 Elemental Analyzer, IR spectra were recorded on Nicolet Magna 760 FTIR Spectrometer with Nic-Plan FTIR Microscope by the Analytical and Instrumentation Laboratory, University of Alberta.

2.4.3 Starting Materials and Reagents

Borane-trimethylamine complex, KBH_4, $NaBH_4$ and $NaBD_4$ were purchased from Aldrich and used as received. $[(Tp^{tBu,Me})YbH]_2$,[21] **1**, $(Tp^{tBu,Me})YbI(THF)$, **2**,[19] and $(Tp^{tBu,Me})SmI(THF)_2$,[24] were synthesized according to published procedures.

2.4.4 Synthetic Procedures

$(Tp^{tBu,Me})Yb(BH_4)$ (3)

Method 1: In an inert atmosphere drybox hydride. $[(Tp^{tBu,Me})YbH]_2$, 67mg, 56 μmol) was dissolved in about 5 mL of benzene in a small round bottom flask resulting in an orange-red solution. To this solution was added dropwise a color-

less solution of trimethylamine-borane (8.0 mg, 112 μmol) in the same solvent (2 mL). The mixture was allowed to stir at room temperature for 48 h during which time the color gradually changed from deep orange-red to orange yellow and finally to yellow. The solvent was removed under reduced pressure giving a yellow residue which was recrystallized from pentane to give **3** as yellow powder (60 mg, 98 μmol) in 88% isolated yield. Single crystals, suitable for X-ray diffraction were obtained by cooling a pentane solution to –30 ºC for 2 days. However, these crystals proved to be the THF adduct, presumably as a result of the presence of THF vapor in the atmosphere of the dry box.

Subsequent attempts to obtain good quality crystals of the THF-free compound, **3** failed.

Method 2: To a yellow-orange solution of $(Tp^{tBu,Me})YbI(THF)$ (0.50 g, 0.63 mmol) dissolved in 10 mL of anhydrous acetonitrile was added solid $NaBH_4$ (0.071 g, 1.89 mmol) in several portions. Gradual dissolution of the solid was accompanied by deepening of the color of the solution. The solution was then allowed to stir at RT overnight (ca 19 h). Solvent was stripped under reduced pressure, leaving a deep orange, oily residue. Extraction with toluene gave a yellow solution and white precipitate (NaI and excess $NaBH_4$). After centrifugation, the supernatant solution was decanted and the solvent removed under reduced pressure to afford a yellow solid which was recrystallized from pentane giving **3** as yellow powder (0.287g, 0.47mmol) in 75% isolated yield. Anal. Calc. for $C_{24}H_{44}B_2N_6Yb$: C, 47.15; H, 7.25; N, 13.75. Found: C, 48.82; H, 7.68; N, 12.73. (This was the best of several elemental analysis attempts.)

66

^{1}H NMR (400 MHz, C$_6$D$_6$, 27°C): δ 5.65 (3H, s, 4-*H* Pz), 4.80 (1H, s, Tp B-*H*), 2.44 (4H, q, J_{B-H} = 82 Hz, B*H*$_4$), 2.13 (9H, s, 5-C*H*$_3$ Pz), 1.39 (27H, s, C(C*H*$_3$)$_3$)- Pz). ^{13}C{^{1}H} NMR (100 MHz, C$_6$D$_6$ 27°C): δ 164.49 (3-*C* Pz), 145.67 (5-*C* Pz), 103.26 (4-*C* Pz*)*, 32.11 (3-*C*(CH$_3$)$_3$ Pz), 31.74 (C(*C*H$_3$)$_3$-Pz), 13.56 (5-*C*H$_3$ Pz). ^{11}B NMR (128 MHz, C$_6$D$_6$, 27°C) δ -8.31 (1B, broad singlet Tp *B*-H), -28.07 (1B, quintet, J_{B-H} = 82Hz, *B*H$_4$). ^{11}B{^{1}H} -8.31 (1B, br, *B*-H Tp), -28.07 (1B, s, *B*H$_4$). IR (microscope, cm^{-1}): 2552 (sh, Tp-BH), 2472 (s, B-H$_t$ of BH$_4$), 2293 and 2236 (d, B-H$_b$ of BH$_4$; 57cm^{-1} splitting).

(Tp$^{t\text{Bu,Me}}$)Yb(BH$_4$)(THF) (4)

Method 1: To a yellow solution of (Tp$^{t\text{Bu,Me}}$)YbI(THF) (0.55 g, 0.69 mmol) in THF (approx. 10 mL) was added 0.080g (2.07 mmol) of solid NaBH$_4$ in several portions. No immediate change was observed. The mixture was allowed to stir at RT for 5 days during which time the amount of solid gradually decreased. The mixture was centrifuged to remove excess NaBH$_4$ and the solvent was stripped from the supernatant to obtain a yellow oily residue. The oily residue was triturated with hexane, resulting in a yellow solid which was extracted with 10 mL toluene to give a yellow orange solution and white solid (NaI). The supernatant solution was concentrated to about 2 mL, layered with hexane, and kept at -30 ˚C to afford **2** as a yellow solid (0.38g, 0.56 mmol) in 80% yield.

Method 2 **:** To a yellow-orange solution of (Tp$^{t\text{Bu,Me}}$)YbI(THF) (0.58g, 0.73mmol)   in about 10 mL anhydrous acetonitrile was added 0.071g (1.82 mmol) of solid NaBH$_4$ in several portions. The solid gradually dissolved and the

color became a deeper yellow-orange. The solution was allowed to stir at RT overnight (ca. 19 h). Solvent was stripped in vacuum to obtain a deep orange oily residue which was then extracted with THF to obtain a yellow solution and white precipitate (excess $NaBH_4$). After centrifugation, the supernatant solution was taken to dryness to afford a yellow solid. The solid was extracted with toluene and again centrifuged. The supernatant solution was decanted from solid NaI and taken to dryness. Recrystallization from toluene/pentane gave **4** as a yellow solid (0.41g, 0.60mmol) in 82% isolated yield. Anal. Calc. for $C_{28}H_{52}B_2N_6YbO$: C, 49.21; H, 7.67; N, 12.30. Found: C, 46.81; H, 7.15; N, 11.78. (This was the best of several elemental analysis attempts).

^1H NMR (400 MHz, C_6D_6): δ 5.70 (3H, s, 4-*H* Pz), 4.80 (1H, s, Tp B-*H*), 3.22 (4H, br, THF), 2.28 (4H, q, J_{B-H} = 80Hz, B*H*$_4$), 2.18 (9H, s, 5-C*H*$_3$ Pz), 1.44 (27H, s, C(C*H*$_3$)$_3$) Pz) 1.21 (4H, br, THF). $^{13}C\{^1H\}$ NMR (100 MHz, C_6D_6, 27°C): δ 163.68 (3-*C* Pz), 145.24 (5-*C* Pz), 103.16 (4-*C* Pz*)*, 68.82 (α-C THF), 32.18 (*C*(CH$_3$)$_3$ Pz), 31.45 (C(*C*H$_3$)$_3$ Pz), 25.49 (β-C THF), 13.50 (5-*C*H$_3$ Pz). ^{11}B NMR (128 MHz, C_6D_6, 27°C) δ -7.97 (1B, broad singlet *B*-H Tp), -29.83 (1B, quint, J_{B-H} = 80Hz, *B*H$_4$). $^{11}B\{^1H\}$ -7.97 (1B, br, *B*-H Tp), -29.83 (1B, s, *B*H$_4$). ^{171}Yb NMR (70 MHz, C_6D_6, 27°C): δ 587.02. IR (microscope, cm^{-1}): 2557 (s, Tp-BH), 2399 (br), B–H$_t$ of BH$_4$), 2265 and 2210 (d, B-H$_b$ of BH$_4$; 56 cm^{-1} splitting).

$(Tp^{tBu,Me})Yb(BD_4)(THF)$ ($4d_4$)

The deuterated analogue of **4** (**4d_4**) was made following the same procedure as for the hydrido analogue, using 0.55g, (0.69 mmol) of **2** and 0.08g, (1.9

mmol) of NaBD$_4$. The mixture was worked up as for **4** to obtain 0.325g, (0.47 mmol) of **4d$_4$** as a yellow-orange solid in 70% isolated yield.

^{1}H NMR (400 MHz, C$_6$D$_6$, 27°C): δ 5.70 (3H, s, 4-*H* Pz), 4.80 (1H, s, Tp B-*H*), 3.22 (4H, br, THF), 2.18 (9H, s, 5-C*H$_3$* Pz), 1.44 (27H, s, 3-C(C*H$_3$*)$_3$) Pz) 1.21 (4H, br, THF). ^{2}H{^{1}H} NMR (61.40 MHz, C$_6$H$_6$, 27°C): δ 2.18 (s, br) ^{13}C{^{1}H} NMR (100 MHz, C$_6$D$_6$, 27°C): δ 160.32 (3-*C* Pz), 144.08 (5-*C* Pz), 101.23 (4-*C* Pz*)*, 68.82 (THF α-C), 31.90 (3-*C*(CH$_3$)$_3$ Pz), 31.40 (C(*C*H$_3$)$_3$ Pz), 25.59 (THF β-C), 13.57 (5-*C*H$_3$ Pz). ^{11}B NMR (128 MHz, C$_6$D$_6$, 27°C) -7.92 (1B, br, *B*–H Tp), -30.08 (1B, s, *B*D$_4$). IR (microscope, cm^{-1}): 2557 (s, Tp B-H, 1793 (s), B-D$_t$ of BD$_4$, (υ_H/υ_D = 1.34) 1662 and 1637 (B-D$_b$ of BD$_4$; splitting 25cm^{-1}). (υ_H/υ_D = 1.36).

Reaction of (Tp^{tBu,Me})SmI(THF) with NaBH$_4$

To a dark green solution of (Tp^{tBu,Me})SmI(THF)$_2$ (0.52 g, 0.62 mmol) in acetonitrile (about 10 mL) was added solid NaBH$_4$ (0.072g, 1.86 mmol) in several portions. The color of the reaction mixture changed immediately to blue-black. The mixture was then left to stir at RT for ~19hrs. The mixture was worked up as for **2** above to obtain a blue–black solid which was identified by ^{1}H and ^{11}B NMR spectroscopy as the known (Tp^{tBu,Me})$_2$Sm.

^{1}H NMR (500 MHz, C$_6$D$_6$, 27°C): δ 7.30 (27H, s, 3-C(C*H$_3$*)$_3$) Pz), 3.98 (9H, br s, 5-C*H$_3$* Pz), 2.80 (3H, s, br, 4-*H* Pz), 2.28 (3H, s, 4-*H* Pz), 1.90 (9H, s, 5-C*H$_3$* Pz), -0.96 (27H, s, 3-C(C*H$_3$*)$_3$) Pz). ^{11}B NMR (159.8 MHz, C$_6$D$_6$ 27°C) δ -21.07 (br s Tp, *B*-H), -51.49 (br s, Tp *B*-H).

2.4.5 X–Ray Crystallographic Studies

Crystals for X–Ray analysis were obtained as described in the Experimental Section. The crystals were manipulated in the glove box, coated with Paratone-N oil, and transferred to a cold gas stream on the diffractometer. Complete X–ray structure determination for compound **4** was carried out by Dr. M. J. Ferguson at the X–ray Crystallographic Laboratory, Department of Chemistry University of Alberta. Summary of data collection and Structure refinement for compound **4** is given in the Structure Report, TAK0406.

2.5   References

1. Orimo, S.; Yakamori, Y.; Elseo, J. R.; Züttel A. Jensen, C. M. *Chem. Rev.* **2007**, *107*, 4111–4132.

2. Hlatky,G. G.; Crabtree, R. H. Coord. *Chem. Rev.* **1985**, *65*, 1–48.

3. Marks, T. J.; Kolb, J. R. *Chem. Rev.* **1977**, *77*, 263–293.

4. (a) Ephritikhine, M. *Chem. Rev.* **1997**, *97*, 2193–2242. (b) Ephritikhine, M. *New J. Chem.* **1992**, *16*, 451–469.

5. Zange, E. *Chem. Ber.* **1960**, *93,* 652–657.

6. Rossmanith, K.; Macalka, H. *Monatsh Chem.* **1963**, *94,* 295–305.

7. (a) Mirsaidov, U.; Kurbonbekov, A.; Rotenberg, T. G.; Dzhuraev, K. *Inorg. Mater. (USSR),* **1978**, *14*, 1340–1342. (b) Mirsaidov, U.; Kurbonbekov, A. *Dokl. Akad. Nauk. Tadzh. SSR* **1979**, *22*, 313–314. (c) Mirsaidov, U.; Rakhimova, A.; Dymova, T. N. *Dokl. Akad. Nauk. SSSR* **1977**, *236*, 120–123. (d) Mirsaidov, U. *Russ. J. Inorg. Chem.* **1977**, *22*, 1555–1556. (e) Mirsaidov, U.; Rakhimova, A.; Dymova, T. N. *Inorg. Mater. (USSR),* **1979**, *15*,1248–1251. (f) Mirsaidov, U.; Shaimuradov, I. B. Khikmatov, M. *Russ. J. Inorg. Chem.* **1986,** *31*, 753–754.

8. (a) Cendrowski-Guilaume, S. M.; Nierlich, M.; Lance, M.; Ephritikhine, M. *Organometallics* **1998**, *17*, 786–788. (b) Arliguie, T.; Lance, M.; Nierlich, M.; Ephritikhine, M. *J. Chem. Soc. Dalton Trans.* **1997**, 2501–2504.

9. (a) Mancini, M.; Bougeard, P.; Burns, R. C.; Mlekus, M.; Sayer, B. G.; Thompson, J. I. A.; McGlinchey, J. *Inorg. Chem.* **1984**, *23*, 1072–1078. (b) Marks, T. J.; Grynkewich, G. W. *Inorg. Chem.* **1976**, *15*, 1302–1307.

(c) Schumann, H.; Genthe, W.; Picardt, J. *Organometallics* **1982**, *1*, 1194–1200.

10. Visseaux, M.; Chenal, T.; Roussel, P.; Mortreux, A. *J. Organomet. Chem.* **2006**, *691*, 86–92.

11. Lappert, M. F.; Singh, A.; Atwood, J. L.; Hunter, W. E. *J. Chem. Soc. Chem. Commun.* **1983**, 206–207.

12. Deng, D.; Zheng, X.; Qian, C.; Sun, J.; Zheng, L. *J. Organomet. Chem.* **1994,** *466*, 95–100.

13. Schumann, H.; Keitsch, M. R.; Mühle, S. H. *Acta. Crystllogr*. **2000**, *C56*, 48–49.

14. Barbier Baudry, B.; Blacque, O.; Hafid, A.; Nyassi, A.; Sitzmann, H. ; Visseaux, M. *Eur. J. Inorg. Chem.* **2000**, 2333–2336.

15. Bomet, F.; Visseaux, M.; Barbier-Baudry, D.; Hafid, A.; Vigier, E.; Kubicki, M. M. *Inorg. Chem.* **2004**, *43*, 3682–3690.

16. White, III, J. P.; Deng, H.; Shore, S. G. *Inorg. Chem*. **1991**, *30*, 2337–2342.

17. (a) Trofimenko S. Scorpionates: *The coordination Chemistry of Poly-pyrazolylbortae Ligands*, Imperial College Press, London, **1999**. (b) Pettinari, C. *Scorpionates II*: *Chelating Borane Ligands,* Imperial College Press, London, **2008**. (c) Parkin, G. *Adv. Inorg. Chem*. **1995**, *42*, 291–393. (d) Kitajima, N.; Tolmann, W. B. *Prog. Inorg. Chem.* **1995**, *34,* 419–531.

18. (a) Carvalho, A.; Domingos, A.; Gaspar, P.; Marques, N.; Pires de Matos,

A.; Santos, I. *Polyhedron* **1992**, *11,* 1481–1488. (b) Santos, I.; Marques,

N. *New J. Chem.* **1995**, *19*, 551–571. (c) Marques, N.; Sella, A.; Takats, J.

Chem. Rev. **2002**, *102*, 2137–2160.

19. Hasinoff, L.; Takats, J.; Zhang, X. W. ; Bond, A. H.; Rogers, R. D. *J.

Am. Chem. Soc.* **1994**, *116,* 8833–8834. (b) Maunder, G. H.; Sella, A.;

Tocher, D. A. *J. Chem. Soc. Chem. Commun.* **1994**, 2689–2690.

20. Morissette, M.; Haufe, S.; McDonald, R.; Ferrence, G. M.; Takats, J.

Polyhedron **2004**, *23*, 263–271.

21. Ferrence, G. M.; McDonald, R.; Takats, J. *Angew. Chem. Int. Ed.* **1999**,

38, 2233–2237. (b) Ferrence, G. M; Takats, J. *J. Organomet. Chem.* **2002**,

647, 84–93.

22. Maunder G. H. Chemistry of the Lanthanides with Pyrazolylborate

Ligands. Ph.D Thesis, University College London, June, **1996**.

23. (a) Trofimenko, S.; Calabrese, J. C.; Kochi, J. K.; Wolowiec, S.;

Hulsebergen, F. B.; Reedijk, J. *Inorg. Chem.* **1992**, *31*, 3943–3950. (c)

Takats, J. *J. Alloy Compd.* **1997**, *249,* 52–55.

24. Zhang, X. W. Synthesis and Reactions of Hydrotris(pyrazolyl) borate

Complexes of Divalent Lanthanides. Ph.D Thesis, University of Alberta,

Edmonton, AB., August, **1995**.

25. (a) Saliu, K. O.; Takats, J.; Ferguson, M. J.; *Acta Crystallogr.* **2009**, *E65*,

m643-m644. (b) Zhang, X. W.; McDonald, R.; Takats, J. *New J. Chem.*

1995, *19*, 573–585.

26. Desrocher, P. J.; Lelievre, S.; Johnson, R. J.; Lamb, B. T.; Phelps, A. L.;

Cordes, A. W.; Gu, W.; Cramer, S. P. *Inorg. Chem*. **2003**, *42,* 7945–7950.

27. (a) Beall, H.; Bushweller, C. H. *Chem. Rev.* **1973**, *73*, 465–486. (b) Marks, T. J. Shimp, L. A. *J. Am. Chem. Soc.* **1972**, *94*, 1542–1550.

28. (a) Emsley, J. W.; Feeney, J.; Sutcliffe, L. H. *High Resolution Nuclear Magnetic Resonance Spectroscopy, Vol I and II,* Pergamon Press, **1965** (b) Eaton, G. R.; Lipscomb, W. N. *NMR Studies of Boron Hydrides and Related Compounds*. W. A. Benjamin Inc, New York, **1969**.

29. (a) Bushweller, C. H.; Beall, H.; Grace, M.; Dewkett, W. J.; Bilofski, H. S. *J. Am. Chem. Soc.* **1971**, *93*, 2145–2149. (b) Grace, M.; Beall, H.; Bushweller, C. H. *J. Chem. Soc. D.* **1970**, 701. (c) Marynick, D.; Onak, T. *J. Chem. Soc. A.* **1970**, 1160–1161.

30. Evans, W. J.; Hughes, L. A.; Hanusa, T. P. *J. Am Chem. Soc*. **1984**, *106*, 4270–4272.

31. Tilley, T. D.; Anderson, R. A.; Spencer, B. Ruben, H.; Zalkin, A.; Templeton, D. H. *Inorg. Chem.* **1980**, *19*, 2999–3003.

32. Bernstein, E. R.; Hamilton, W.C.; Keiderling, T. A.; La Placa, S. J.; Lippard, S .J.; Mayerle, J. J. *Inorg. Chem.* **1972**, *11*, 3009–3016.

33. Edelstein, N. *Inorg. Chem.* **1981**, *30*, 297–299.

34. Khvostov, A.V.; Nesterov, V. V.; Bulychev, B. M.; Sizov, A. I. Antipin, M. Yu. *J. Organomet. Chem*. **1999**, *589*, 222–225.

35. Yuan, F.; Yang, J.; Xiong, L. *J. Organomet. Chem.* **2006**, *691*, 2534–2539.

36. Shannon, R. D. *Acta Crystallogr.* **1976**, *A32*, 751–767.

37. Deng, D.; Zheng, X.; Qian, C. *Acta Chim. Sin.* **1992**, *50*, 1024–1033.

38. Cheng, J.; Takats, J.; Ferguson, M. J.; McDonald, R. *J. Am. Chem. Soc.* **2008**, *130*, 1544–1545.

Chapter 3

Scorpionate Supported Lanthanide Dialkyl and Dihydride Complexes (Ln = Yb, Lu): Synthesis and Characterization[*]

3.1 Introduction

There has been a considerable interest in the isolation of discrete lanthanide compounds bearing lanthanide carbon sigma bonds due to their usefulness both in stoichiometric and catalytic transformations.[1,2] While this area has been dominated by bis-cyclopentadienyl mono-alkyl type complexes, (Cp_2LnR), for a long time, there has been a resurgence of interest in the isolation of mono-ligand dialkyl complexes of the type $(Ligand)LnR_2L_n$ bearing two reactive lanthanide-carbon sigma bonds.[3] Such complexes can provide entry into lanthanide-alkyl mono- and di-cations, arguably more active than their neutral analogues as olefin polymerization catalysts.[4] Toward this end, application of non-cyclopentadienyl ligands is currently attracting considerable attention.[3,5] The application of these ligands have, however been mostly limited to group 3 and the later lanthanides and only recently has this area been extended to the entire lanthanide series by the works of Hou, using bulky cyclopentadienyl ligands [6,7] and Hessen, using

---

[*] This Chapter describes the work of the author; a more comprehensive account which includes the range of lanthanide metals has appeared: Cheng, J.; Saliu, K.; Kiel, G. Y.; Ferguson, M. J.; McDonald, R.; Takats, J. *Angew. Chem. Int. Ed.* **2008**, *47*, 4910–4913.

amidinate ligands.[8] The paucity of this important class of compounds is associated with the problems encountered during their isolation which is not unconnected to the large steric requirement of the mid- and early lanthanide and lack of suitable starting materials.

Literature survey revealed that the chemistry of "$(Tp^{R,R'})Ln(CH_2SiMe_2R'')_2$" type complexes was virtually unexplored. Prior to the work reported here, such complexes were limited to the group 3 metals. Bianconi and Long reported the synthesis of $(Tp^{Me2})YR_2(THF)$ via salt metathesis reaction between $(Tp^{Me2})YCl_2(THF)$ and two equiv of LiR (R = CH_2SiMe_3, Ph)[9]. Piers and co-workers reported the synthesis and characterization of $(Tp^{R,Me})Sc(CH_2SiMe_3)_2(THF)_n$ (R = Me, n = 1; R = ^tBu, n = 0) using both salt metathesis and protonolysis approaches.[10] The long hiatus in this area was rather surprising in view of the well documented ability of the tris(pyrazolyl)borate ligand to suppress ligand redistribution for elements throughout the periodic table,[11] including the lanthanides.[12] The goal of this research was to expand the range of known $(Tp^{R,R'})LnR_2$ complexes and to explore the possibility to convert them to the still very rare mono ligand lanthanide dihydride complexes, $LLnH_2$.

3.1.1 Synthesis of "$LLnR_2$" Type Complexes

The commonest method of making lanthanide-carbon containing species, salt metathesis, has been shown to be often complicated by the formation of ′ate′ complexes. These complexes are formed by retaining the alkali metal halide by-

product of salt elimination, thus contaminating the desired reaction product. This is especially important for larger lanthanides, eq. 3.1.

$$(\text{Ligand})\text{LnX}_2 + 2\ \text{MR} \xrightarrow{-\text{MX}} [(\text{Ligand})\text{LnR}_2\text{X}]^{\ominus}[\text{M(solvent)n}]^{\oplus} \qquad 3.1$$
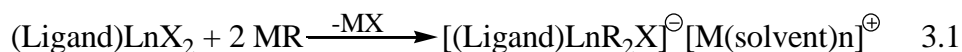
In order to circumvent the problem of 'ate' complexes formation, an attractive alternative method to salt metathesis is protonolysis.

Protonolysis of $\text{Ln}(\text{CH}_2\text{SiMe}_3)_3(\text{THF})_2$ was used successfully by both Hou[6,7] and Hessen[8] in their synthesis of the full range of lanthanide cyclopentadienyl and amidinate dialkyl complexes, Scheme 3.1.
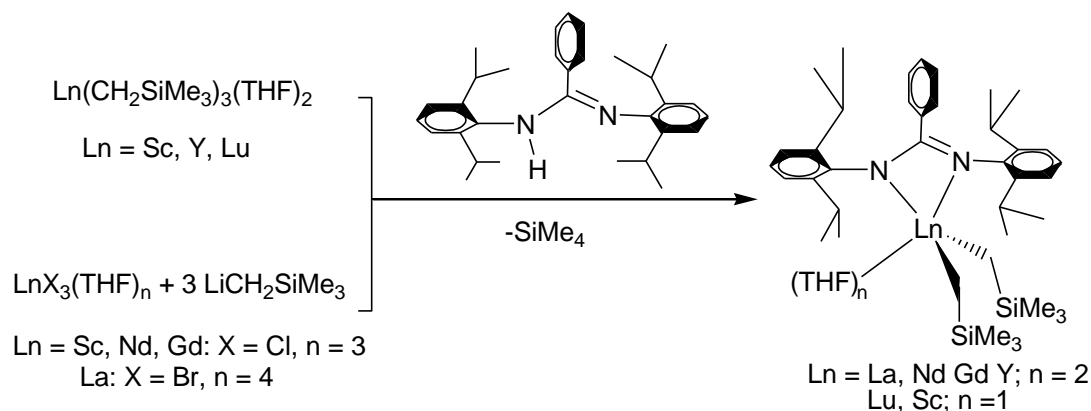
Scheme 3.1 Preparation of Amidininate Supported Lanthanide Dialkyl Complexes.

As mentioned, Piers *et al*[10] also used the protonolysis approach to prepare scorpionate supported scandium dialkyls, eq. 3.2. In this study, it was

$$\text{Sc}(\text{CH}_2\text{SiMe}_3)_3(\text{THF})_2 + \text{H}(\text{Tp}^{R,Me}) \xrightarrow[- \text{SiMe}_4]{\text{toluene or hexanes}} (\text{Tp}^{R,Me})\text{Sc}(\text{CH}_2\text{SiMe}_3)_2(\text{THF})_x \qquad 3.2$$
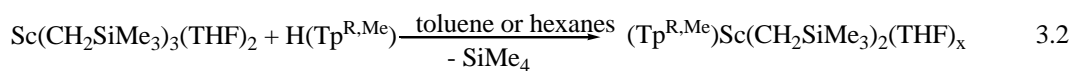
generated in-situ

R = Me, x = 1
R = ᵗBu, x = 0

shown that salt metathesis of $(\text{Tp}^{R,Me})\text{ScCl}_2(\text{THF})$ (R = Me, ᵗBu) with $\text{LiCH}_2\text{SiMe}_3$ was accompanied by displacement of the scorpionate ligand,

giving undesired $Li(Tp^{R,Me})$ by-product. In the case of Tp^{Me2} ligand, about 10% $LiTp^{Me2}$ was formed, whereas in the case of $Tp^{tBu,Me}$ ligand, the major product of the reaction was $Li(Tp^{tBu,Me})$. This observation thus implies the superior performance of the protonolysis protocol.

Another potential route to LMR_{n-1} complexes is alkyl abstraction from MR_n precursors, eq. 3.3. Although this method has not been applied to lanthanide alkyls prior to our work, this synthetic protocol was successfully used by

$$MR_n \xrightarrow{M'L} LMR_{n-1} + "M'R" \qquad\qquad 3.3$$

Parkin to prepare scorpionate supported Mg^{13} and Al^{14} alkyls and more recently by Jordan for analogous Zr^{15} and Hf^{16} benzyl complexes, Scheme 3.2.
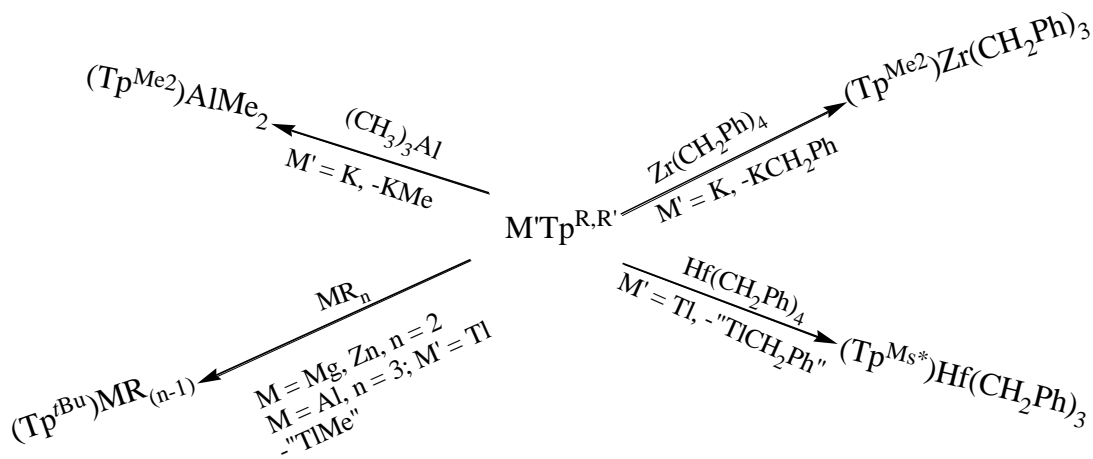
Scheme 3.2 Alkyl Abstraction by $M'(Tp^{R,R'})$ Reagents from MR_n Complexes.

3.1.2 Synthesis and Characterization of $H(Tp^{R,Me})$ (R = Me, ^{t}Bu)

Full details of the synthesis and characterization of the acid form of the popular $Tp^{tBu,Me}$ ligand have not yet been reported even though it has previously been used.

Following the suggestion of Parkin,[17] treating a methylene chloride solution of the thallium salt, $Tl(Tp^{tBu,Me})$ with H_2S at -78° afforded the compound as white crystalline solid in good yield, Scheme 3.3. Later, it was discovered that adaptation of Trofimenko's original method, glacial acetic acid treatment of an aqueous suspension of the potassium salt, $K(Tp^{tBu,Me})$, also gave the acid form as a white crystalline solid in very good yield. Clearly, the latter method is far preferable as it avoids the use of toxic thallium salt.

Unfortunately, attempts to synthesize the corresponding $H(Tp^{Me2})$ by either method proved problematic either due to contamination of the compound by the thallium salt (H_2S reaction) or very poor, erratic yield (from acetic acid reaction). A very recent preparation by the acetic acid route showed that by using very small amount of water the yield can be improved (see Experimental Section)
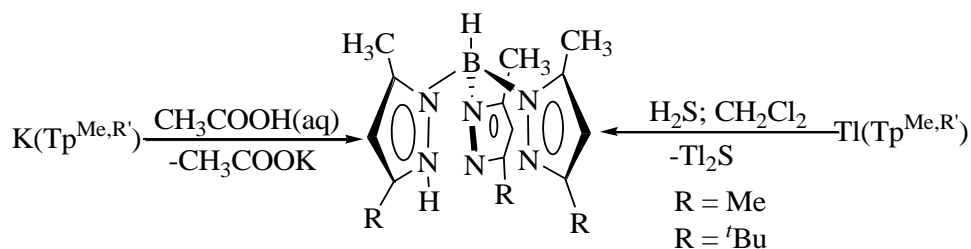
Scheme 3.3 Synthesis of $H(Tp^{tBu,Me})$.

$H(Tp^{tBu,Me})$ was characterized by NMR (^1H, $^{13}C\{^1H\}$, and ^{11}B) and IR spectroscopies, elemental analysis and its structure was confirmed in the solid state by single crystal X-ray crystallography. The structure is shown in Figure 3.1.

The room temperature ^{1}H and ^{13}C NMR spectra are very simple, showing single set of signals for the pyrazolyl hydrogen and carbons atoms, the proton signals are in the expected 27:9:3 ratio for the 3-tBu, 5-Me and 4- hydrogen, respectively. The 5-Me signal appears as a doublet as a result of coupling to the 4-H of the pyrazolyl ring which in turn is a quartet with a coupling constant of $^4J_{HH}$ of 0.65 Hz. In addition, the H(Tp^{tBu,Me}) hydrogen atom appears as a broad singlet significantly downfield, ca. 14 ppm, this signal is both temperature and concentration dependent. The single set of signals observed for the pyrazolyl hydrogen atoms is an indication of a fluxional system at ambient temperature. In an attempt to slow down the fluxional process, variable temperature NMR study was initiated. The compound remained fluxional down to the lowest accessible temperature (-80°C), as shown by the observation of a single set of pyrazolyl peaks. The signals due to pyrazolyl hydrogen atoms showed slight broadening as the temperature is lowered; on the other hand, the N-H signal sharpens and moves to lower field. The sharpening of the N-H signal as temperature is lowered is consistent with thermal decoupling of the proton from the quadrupolar nitrogen nucleus.[18] The shift of the signal to lower field upon lowering the temperature may be rationalized on the basis of increased hydrogen bonding interaction. As the temperature is lowered, the fluxionality is reduced thus bringing the hydrogen atom into the vicinity of both N22 and N32 (*vide infra*). This increases the hydrogen bond interaction and thus results in the deshielding of the hydrogen atom, thus accounting for the shift of the hydrogen signal to low field.

Structurally characterized H(Tp[R,R′]) derivatives are relatively rare, and, the only known examples are those involving tetra-substituted boron, H(pzTp)·H_2O,[19] H[(pz[Me2])Tp[Me2]][20] and H(PhTp[tBu]).[21] Even though there have been reports on the preparation and use of such H(Tp[R,R′]) species containing tri-substituted boron,[10,22] none of these has been structurally characterized. X-ray quality crystals of HTp[tBu,Me] were obtained by cooling a pentane solution to -30°C overnight. An ORTEP drawing of the compound is shown in Figure 3.1. H(Tp[tBu,Me]) crystallizes in the monoclinic space group $P2_1/n$ with four molecules in the unit cell. The N-H proton was both located and refined and is clearly bonded to one of the pyrazolyl nitrogen, N12, thus lengthening the B-N11 bond, 1.575(2) Å compared to 1.537(2) Å and 1.548(2) Å for B-N21 and B-N31, respectively.
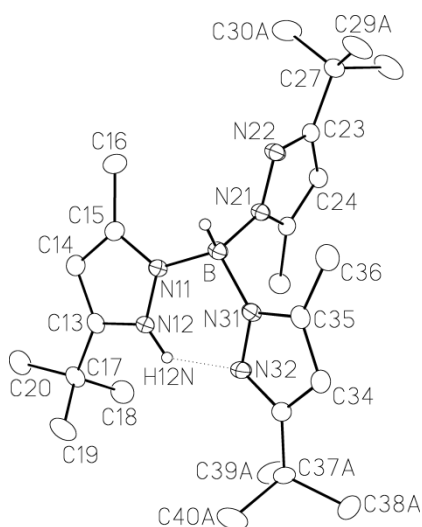
Figure 3.1 Solid State Structure of H(Tp[tBu,Me])

The N12-H12 distance of 0.99(2) Å is longer than the value of 0.84 Å found in H(PhTp[tBu]).[21] The distance to the closest nitrogen atom, N32 is 1.70(2) Å

is shorter than the 2.00 Å found in H(PhTp^{tBu}), indicating a certain degree of hydrogen bond interaction between these atoms.

3.1.3   Ln(CH$_2$SiMe$_2$R″)$_3$(THF)$_2$ (Ln = Yb, Lu; R″ = Me, Ph) Complexes; Some Observations

As mentioned earlier, both the protonolysis approach and the alkyl abstraction protocol requires the availability of the lanthanide trialkyl precursors, Ln(CH$_2$SiMe$_3$)$_3$(THF)$_2$.

The original synthesis of Ln(CH$_2$SiMe$_3$)$_3$(THF)$_x$, as described by Lappert,[23] seemed cumbersome, subsequent works have however indicated that their synthesis, at least for the late, small lanthanide metals is rather straightforward and give isolable Ln(CH$_2$SiMe$_3$)$_3$(THF)$_2$ in good yields. The synthesis also benefits from the commercial availability of LiCH$_2$SiMe$_3$.

Isolable in pure form as solid, Ln(CH$_2$SiMe$_3$)$_3$(THF)$_2$, (Ln = Yb, Lu) are thermally labile and should be used promptly for further derivatization. It was also confirmed in this laboratory that the synthesis of the trialkyls of the early, large lanthanides (Ln = Sm, Nd) is problematic. Thus, utilizing these trialkyls for further derivatization is best accomplished by in situ preparation, not unlike the "one-pot" synthesis used by Hessen[8] to prepare the amidinate supported dialkyl complexes for the full range of the lanthanide.

LiCH$_2$SiMe$_2$Ph is not commercially available, however, Marks[24] and Piers[25] have shown that the –CH$_2$SiMe$_2$Ph moiety imparts more stability and

crystallinity to LMR_n complexes. Thus, $Ln(CH_2SiMe_2Ph)_3(THF)_x$ are potentially desirable precursors for scorpionate supported lanthanide dialkyls.

3.2 Synthesis of $(Tp^{R,R'})Ln(CH_2SiMe_2R'')_2$ Complexes (Ln = Yb, Lu)

The lanthanide dialkyl complexes $(Tp^{tBu,Me})Ln(CH_2SiMe_2R'')_2$ (R'' = Me, Ph; Ln = Yb, **5**; Lu, **6**) and $(Tp^{Me2})Ln(CH_2SiMe_2R'')_2(THF)$ (R'' = Me, Ph; Ln = Yb, **7**; Lu, **8**) are made by two alternative methods as described below. The dialkyl complex $(Tp)Yb(CH_2SiMe_3)_2(THF)$, **9**, was made only by the alkyl abstraction route since the acid form, HTp is not available.

3.2.1 Synthesis via Protonolysis Reaction

$$R' = CH_3, \ n = 1$$
$$R' = {}^{t}Bu, \ n = 0 \qquad 3.4$$
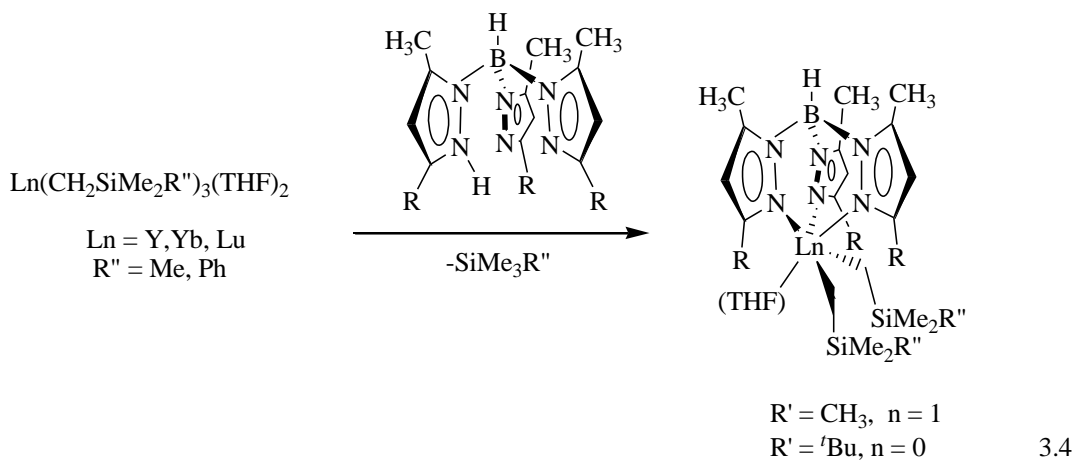
Reaction of the acid form, $H(Tp^{tBu,Me})$, with one equivalent of the lanthanide trialkyl complexes, $Ln(CH_2SiMe_3)_3(THF)_2$ (Ln = Yb, Lu), in hexane at room temperature afforded the lanthanide dialkyl complexes, $(Tp^{tBu,Me})Ln(CH_2SiMe_3)_2$, (Ln = Yb, **5a**; Ln = Lu, **6a**) in very good to excellent yields. The corresponding $(Tp^{tBu,Me})Ln(CH_2SiMe_2Ph)_2$, (Ln = Yb, **5b**; Ln = Lu, **6b**) were prepared in a

similar fashion. In a similar way, reaction of H(Tp^{Me2}) with one equivalent of the corresponding trialkyl complexes afforded the dialkyl compounds (Tp^{Me2})Ln(CH$_2$SiMeR″)$_2$(THF) (R = Me; Ln = Yb, **7a**; Ln = Lu, **8a**: R = Ph; Ln = Yb, **7b**, Ln = Lu, **8b**) in very good yields.

As shown above, the protonolysis reaction affords the complexes in pure form and in very good yields, however, the synthesis of the acid form H(Tp$^{R,R'}$) from the corresponding alkali metal or thallium salts M(Tp$^{R,R'}$), in the case of H(Tp^{Me2}) is not trivial. The latter is difficult to obtain pure and the yield is always very low. Moreover, in the case of the unsubstituted Tp ligand, the acid form is not available. Clearly, an alternative procedure for the synthesis of the unsubstituted ligand dialkyl complexes is needed. An attractive alternative would be to use the more readily available alkali metal salts or the thallium salt of the ligand as alkyl abstraction reagents. As mentioned earlier, there is indeed a precedent for this in the work of Parkin *et al*. for (Tp$^{R,R'}$)MR$_n$ complexes (M = Al, n = 2; M = Mg, n = 1), Scheme 3.2.[13, 14]

3.2.2 Synthesis via Alkyl Abstraction
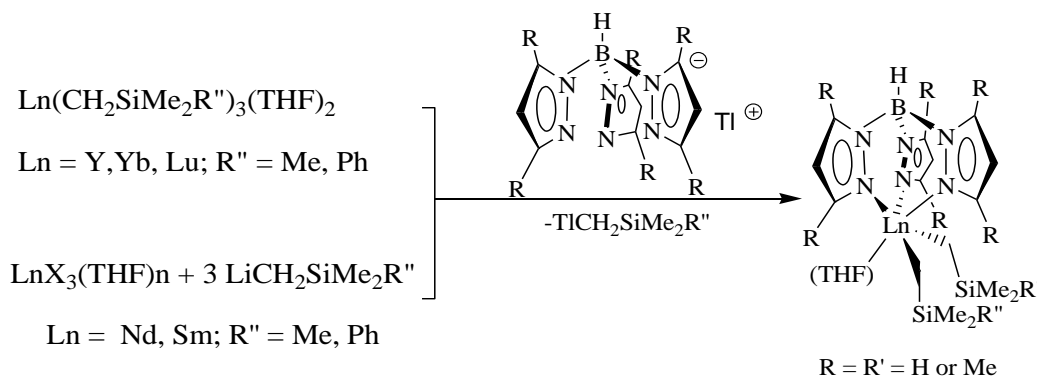
Scheme 3.4 Preparation of (Tp$^{R,R'}$)Ln(CH$_2$SiMe$_2$R″)$_2$(THF) Complexes by Alkyl Abstraction.

Treatment of a THF solution of the respective trialkyl complexes with solid Tl(Tp^{Me2}) at RT immediately results in the formation of black solid precipitate. After about 30 minutes, the black precipitate gathers to give a shiny Tl shot and an almost clear solution. Removal of the Tl shot, followed by simple work up gave the dialkyl complexes (Tp^{Me2})Ln(CH$_2$SiMeR″)$_2$(THF) (R = Me; Ln = Yb, **7a**; Ln = Lu, **8a**: R″ = Ph; Ln = Yb, **7b**, Ln = Lu, **8b**) in excellent yields, Scheme 3.4. In the case of ytterbium, there was formation of a small amount of a purple solid, presumably the highly insoluble (Tp^{Me2})$_2$Yb via redox reaction.[26] The formation of the black precipitate is consistent with initial formation of a Tl(I) alkyl species, which then undergoes decomposition to give the Tl metal.

Tl(I) alkyls have never been isolated or observed spectroscopically, even though they have been postulated as reaction intermediates. They are however believed to decompose by two pathways (i) disproportionation into thallium metal and thallium(III) alkyl, eq. 3.5 and (ii) homolysis of the Tl-R giving thallium metal and alkyl radical coupled products, eq. 3.6.[27]

$$3 \text{ TlR} \longrightarrow 2 \text{ Tl}^0 + \text{TlR}_3 \qquad 3.5$$

$$2 \text{ Tl}^{\text{I}}\text{R} \longrightarrow 2 \text{ Tl}^0 + \text{R-R} \qquad 3.6$$
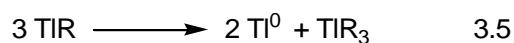
Both mechanisms have been observed, for instance, reaction of thallium iodide with excess MeLi gives 2 equiv of Tl metal and 1 equiv of TlMe$_3$, suggesting that the initially formed TlMe disproportionates to Tl^0 and TlMe$_3$ via eq. 3.5.[28] In contrast, the reaction of TlBr with tolyl magnesium bromide results in the formation of Tl metal and 4,4′dimethylbiphenyl, suggesting that the

reaction proceeds by eq. 3.6.[29] The lack of Tl(CH$_2$SiMe$_2$R″)$_3$ in these preparations suggests that the initially formed "Tl(CH$_2$SiMe$_2$R″)" decomposes via eq. 3.6. Although the observation of small extra-CH$_2$SiMe$_3$ resonances in the NMR spectra of crude reaction products seems to indicate that decomposition of the putative thallium(I) alkyl, "Tl(CH$_2$SiMe$_2$R″)" is not spontaneous. Thus, recrystallization was necessary to obtain pure compounds **7** and **8**. Alternatively, the crude products could be used in hydrogenolysis reaction to obtain the corresponding dihydrides (*vide infra*). The small amount of Tl metal formed in the hydrogenolysis reaction could simply be removed by centrifugation prior to work up.

Alkyl abstraction with the bulky TlTp^{tBu,Me} was very slow. The solution remained black, irrespective of the length of reaction time, and clean product was only obtained in the case of Lu, where the desired compound, (Tp^{tBu,Me})Lu(CH$_2$SiMe$_3$)$_2$, could be isolated in appreciable yield.

On the other hand, the alkyl abstraction protocol also worked well with the unsubstituted pyrazolylborate ligand, Tp. The dialkyl complex (Tp)Yb(CH$_2$SiMe$_3$)$_2$(THF) (**9**) was isolated as a deep-red crystalline solid, an unexpectedly deep color for this Yb(III) complex.

Since for the early, large lanthanides the trialkyl species Ln(CH$_2$SiMe$_2$R″)$_3$(THF)$_x$ (Ln = Nd and Sm) could not be isolated, an "*in-situ*" approach, much like the one-pot synthesis of Hessen,[8] was successfully used by Dr. Jianhua Cheng of this group,[30] to prepare (Tp^{Me2})Ln(CH$_2$SiMeR″)$_2$(THF) (Ln = Nd, Sm; R″ = Me, Ph), Scheme 3.4. The same approach was attempted for lanthanum. Addition of 3 equiv of LiCH$_2$SiMe$_2$R″ to a suspension of LaX$_3$(THF)$_n$

(obtained by stirring the anhydrous LaX_3 overnight in THF) (X = CF_3SO_3, Cl, Br, I) at low temperature (ca. -40°C) in the appropriate solvent resulted in the formation of a clear solution which was then treated with $Tl(Tp^{R,Me})$, (R = ^tBu. Me). The formation of black precipitate, followed by Tl shot formation was observed in all cases. Formation of the Tl shot was very facile, even with the bulky $Tp^{tBu,Me}$ ligand which reacted rather sluggishly with the smaller lanthanide trialkyls (Ln = Y, Yb, Lu). Unfortunately, a mixture of products, in major part being the lithium salt of the ligands, $Li(Tp^{R,Me})$ was obtained after work up. The amount of the lithium salt formed depended on the ligand. With $Tp^{tBu,Me}$ ligand, the product obtained was almost exclusively $Li(Tp^{tBu,Me})$. The formation of $Li(Tp^{R,Me})$ with the larger lanthanum center is perhaps due to the stronger covalent interaction between the lithium ion and the scorpionate ligand. Formation of $Li(Tp^{R,Me})$ also complicated the preparation of $(Tp^{R,Me})Sc(CH_2SiMe_3)_2(THF)_{1/0}$, the amount of $Li(Tp^{R,Me})$ obtained depending on the ligand in question;[10] the bulky $Tp^{tBu,Me}$ ligand giving almost exclusively $LiTp^{tBu,Me}$.

3.3   Characterization of $(Tp^{R,R'})Ln(CH_2SiMe_2R'')_2(THF)_{0/1}$ Complexes

3.3.1 General Methods

The compounds are all air and moisture sensitive but thermally stable. In solution, the compounds were characterized by multinuclear NMR spectroscopy (^1H, ^{13}C and ^{11}B). Their formulation was confirmed by elemental analysis and the connectivity of the atoms established by single crystal X-ray crystallography studies in the case of compounds **6**, **7** and **8**.

3.3.2 $(Tp^{tBu,Me})Ln(CH_2SiMe_2R'')_2$ (Ln = Yb, 5; Lu, 6; R'' = Me, a; Ph, b)

The compounds are soluble in ether type as well as hydrocarbon solvents. The ^1H and $^{13}C\{^1H\}$ NMR spectra of the paramagnetic ytterbium compounds **5a** and **5b** are not very informative, thus their formulation is based on
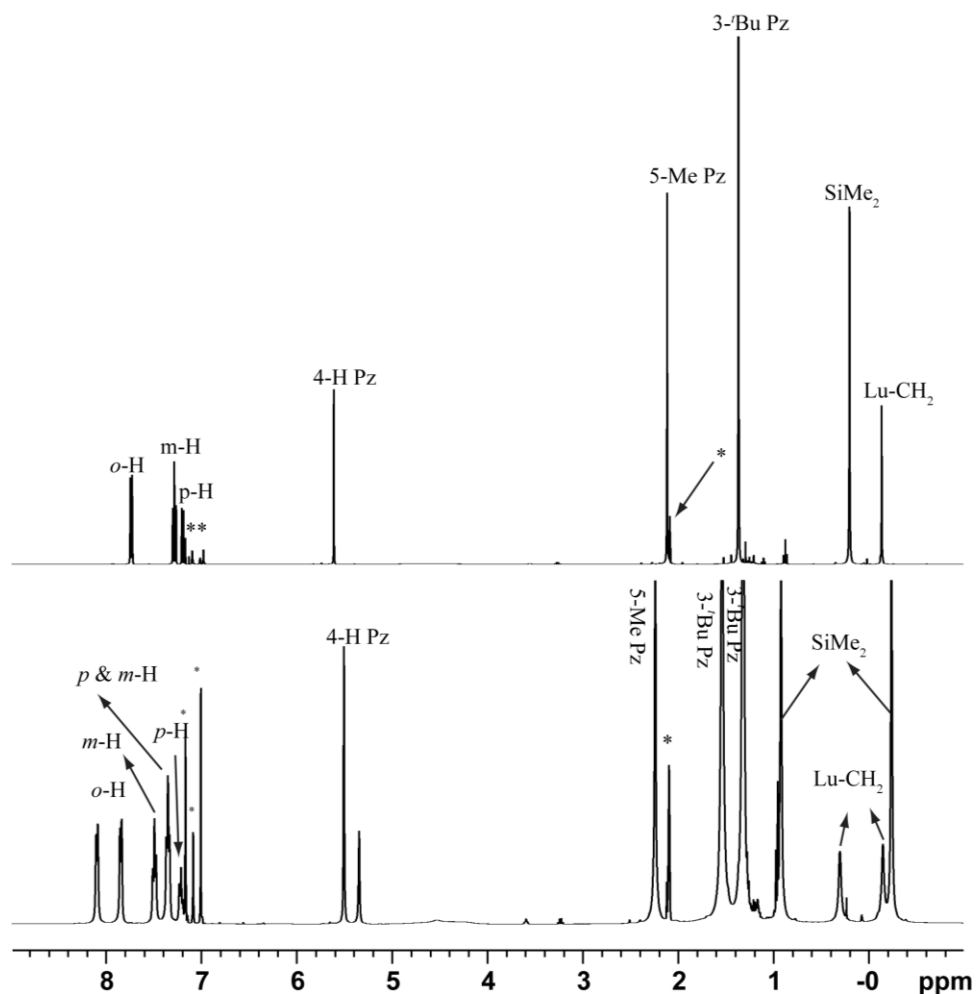
Figure 3.2: Room Temperature (top) and −80°C (bottom) ^1H NMR Spectra of $(Tp^{tBu,Me})Lu(CH_2SiMe_2Ph)_2$ (**6b**) in C_7D_8.

elemental analysis, analogy with the corresponding lutetium compounds **6a** and **6b**, and in the case of **5b**, single crystal X-ray structural analysis. The ambient

temperature ^{1}H and ^{13}C{^{1}H} NMR of the diamagnetic lutetium complexes **6a** and **6b** shows a single set of peaks for the pyrazolylborate ligand as well as the alkyl ligands Figure 3.2. In line with the bulky nature of the Tp^{tBu,Me} ligand, no signals due to coordinated THF solvent were observed.

The appearance of a single set of signals at room temperature is suggestive of dynamic solution behavior. In order to slow down the fluxional process, variable temperature NMR study was carried out. As the temperature was lowered, the pyrazolyl signals broadened and coalesced at about –40°C and then re-emerged as two sets of singlets in a 2:1 ratio. Also, the signals due to the alkyl ligands coalesced at about the same temperature and re-emerged as two set of signals of equal intensity. The single set of peaks observed in the room temperature NMR spectra is consistent with a fluxional 5-coordinate structure. Similar behavior was observed with the yttrium[30] and scandium[10] analogues.

Single crystals of **5b** and **6b** suitable for X-ray diffraction studies were obtained by cooling dilute hexane solutions to -40°C for several days. The compounds are isostructural and an ORTEP drawing of **6b** is shown in Figure 3.3 as a representative structure. Selected metric parameters are listed in Table 3.1.

In the solid state, (Tp^{tBu,Me})Ln(CH$_2$SiMe$_2$Ph)$_2$ (Ln = Yb, **5b**; Lu, **6b**) complexes are five-coordinate and have identical structure as the yttrium[30] and scandium[10] analogues. The metal center is coordinated by the three nitrogen atoms of the pyrazolylborate ligand in the classical κ^3 bonding mode and the two carbon atoms of the alkyl ligand. Further solvent coordination is prevented by the bulky nature of the Tp^{tBu,Me} ligand, which has been described as a tetrahedral enforcer in

90
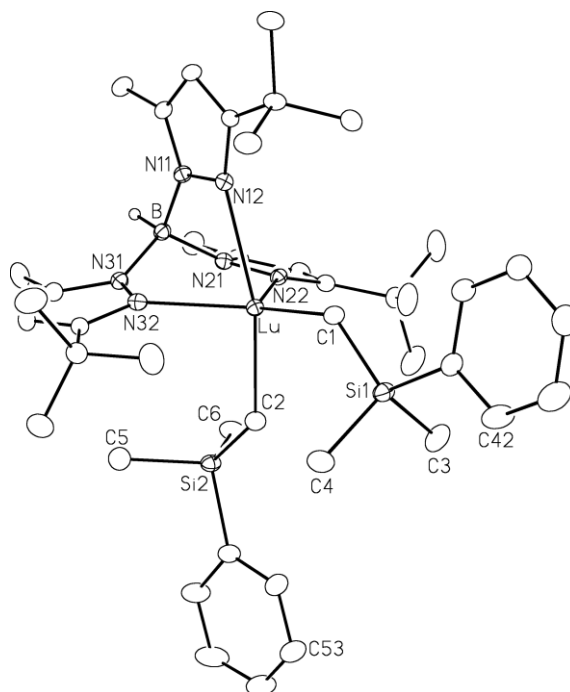
Figure 3.3: ORTEP View of $(Tp^{tBu,Me})Lu(CH_2SiMe_2Ph)_2$ (**6b**).

transition metal chemistry.[31] The coordination geometry around the metal center is best described as distorted trigonal bipyramidal with N12 and C2 occupying the axial sites and N22, N32 and C1 in the equatorial positions, as shown by the respective angles, N12–Lu–C2, 156.70(13)°; C2–Lu---B1, 106.44(14)° and C1–Lu---B1, 155.11(13)°.

As typical of trigonal bipyramidal geometry, the Ln–N22 and Ln–N32 (equatorial) bond distances are shorter than Ln-N12 (axial) bond length by ca. 0.2 Å, although the Ln–C distances are similar. The difference between the average Ln-C 2.36(1) Å, **5b** and 2.35(1) Å, **6b**) distances is approximately equal to the difference in the ionic radii of the lanthanide metals.[32] In complex **5b**, the average Yb-C distance of 2.364(6) Å compares favorably with that found in other 5-coordinate ytterbium compounds containing Yb-C bonds: 2.357(10) in

Table 3.1 Selected Bond Lengths (Å) and Angles (deg) for $(Tp^{tBu,Me})Yb(CH_2SiMe_2Ph)_2$ (**5b**) and $(Tp^{tBu,Me})Lu(CH_2SiMe_2Ph)_2$ (**6b**).

	5b	6b
	Distances	
Ln-N12	2.564(2)	2.557(3)
Ln-N22	2.342(2)	2.320(3)
Ln-N32	2.340(2)	2.319(3)
Ln-C1	2.370(2)	2.354(3)
Ln-C2	2.358(2)	2.353(3)
	Angles	
N12-Ln-N22	73.95(6)	74.28(10)
N12-Ln-N32	73.10(6)	73.48(11)
N12-Ln-C1	105.47(7)	104.93(12)
N12-Ln-C2	156.05(7)	156.70(13)
N22-Ln-N32	98.80(6)	99.77(11)
N22-Ln-C1	127.83(7)	127.42(13)
N22-Ln-C2	90.42(8)	90.50(14)
N32-Ln-C2	92.04(8)	92.37(14)
C1-Ln-C2	98.44(8)	98.32(15)

$Yb(CH_2SiMe_3)_3(THF)_2,$[33] 2.379(4) in $Yb(CH_2{}^tBu)_3(THF)_2.$[34] The isostructural **6b** also have average Lu-C bond of 2.35(1) that compares well with those of other known compounds, for example, 2.361(3) Å in the homoleptic trialkyl complex $Lu(CH_2SiMe_3)_3(THF)_2.$[33]

The axial alkyl ligand sits in the cleft formed by two ^tBu substituents of the two equatorial pyrazolyl groups, thus opening up the equatorial N32–Lu–N22

bite angle (99.77(11)°) compared to the other two, N32–Lu–N12 (73.48(11)°) and

N22–Lu–N12 (74.28(10)°).

The intra-ligand N-Yb-N bond angles in **5b** are marginally smaller than

those in **6b**. This observation can be explained in terms of the difference in the

sizes of the lanthanide centers and the fact that the tripodal Tp ligand provides a

pocket-like environment around the metal. The smaller the metal, the deeper the

pocket and hence the larger the N-M-N angle.

3.3.3 $(Tp^{Me2})Ln(CH_2SiMe_2R'')_2(THF)$ (Ln = Yb 7; Lu, 8; R'' = Me, Ph)

The compounds are soluble in aromatic hydrocarbon as well as ether type

solvents but only sparingly soluble in hydrocarbon solvents. Unlike in the case of

5a and **5b**, the room temperature ^{1}H NMR spectra of the paramagnetic ytterbium

compounds **7a** and **7b** proved quite informative.

As would be expected for a six-coordinate octahedral complex with facial-

ly coordinated tripodal pyrazolylborate ligand exhibiting C_s symmetry, the low

temperature ^{1}H NMR spectrum of the diamagnetic lutetium complexes **8a** and **8b**

shows two sets of signals for the pyrazolyl ring substituents in 2:1 ratio, Figure 3.4.

The signals for the diastereotopic CH_2 groups also appear as two distinct doublets

at –0.31 ppm and –0.47 ppm with $^2J_{HH}$ value of 11.6 Hz and the SiMe$_3$ group ap-

pears as a sharp singlet in the expected region and integrates for 18 protons. In
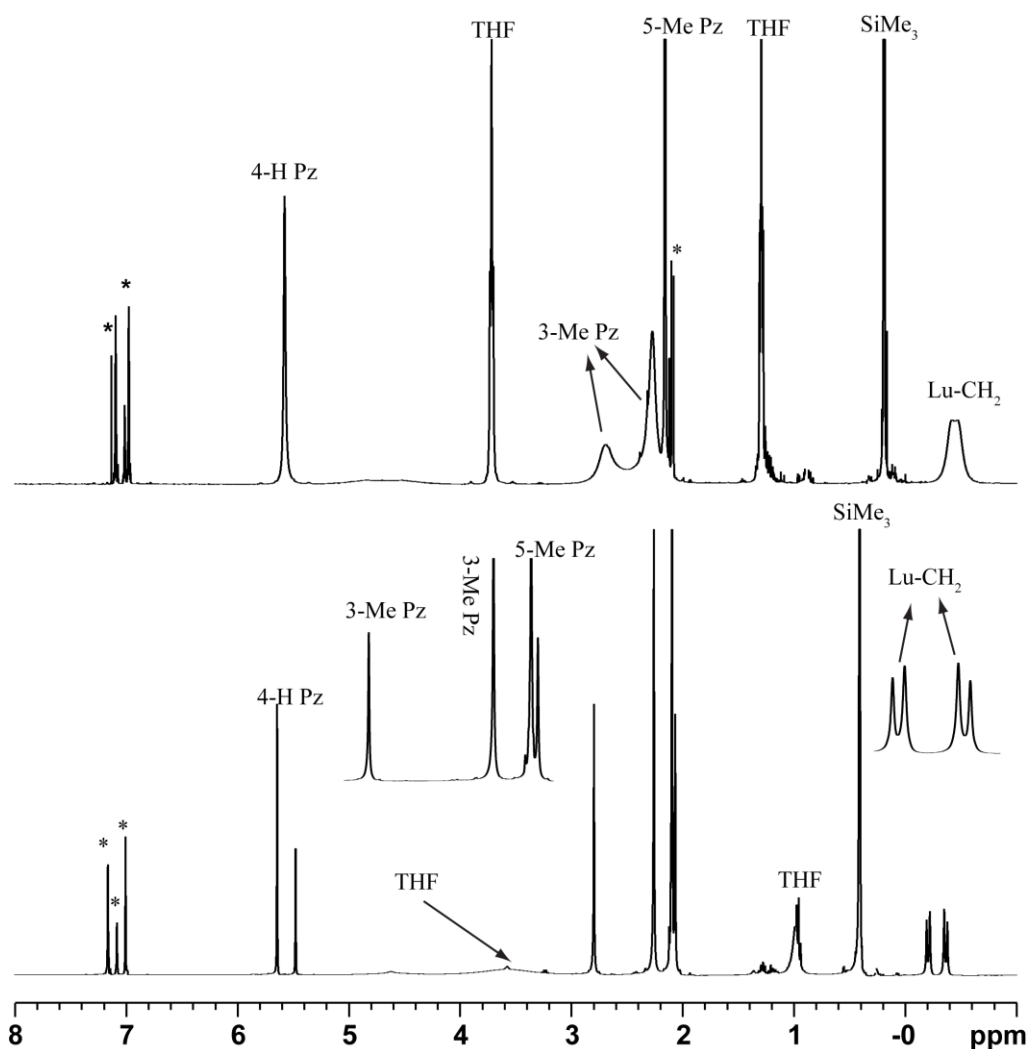
Figure 3.4: Room Temperature (top) and −80°C (bottom) ^{1}H NMR Spectra of (Tp^{Me2})Lu(CH$_2$SiMe$_3$)$_2$(THF) (**8a**) in C$_7$D$_8$.

addition signals due to coordinated THF ligand appear at ca 3.6 ppm and 1.1 ppm for the α–H and β–H, respectively. The presence of THF in these complexes reflects the difference in the steric sizes of the respective ancillary Tp$^{R,R'}$ ligands.

The room temperature ^{1}H NMR of **8a** and **8b** in non-coordinating solvents such as C$_6$D$_6$ or toluene-d_8 exhibit a degree of dynamic behavior in solution. The

94

signal due to the methyl group on the 3 position of the pyrazolyl ring appears in the expected 2:1 ratio, although considerably broadened. The signal for the methyl on 5-position of the pyrazolyl ring gives a single sharp signal, whereas the 4-hydrogen appears as a slightly broadened singlet. This can be explained on the basis of fast exchange of the pyrazolyl substituents at room temperature (*vide infra*). The different degree of broadening displayed by the peaks may be justified on the basis of the chemical shift differences of ca. 0.17, 0.54 and 0.03 ppm between the 4-H, 3-Me and 5-Me signals, respectively. The larger separation between the 3-Me signals requires a faster rate of exchange than that for 4-H which in turns require a faster exchange rate than the 5-Me signals. The resonances due to the lutetium bound alkyl groups are also slightly broadened and the diastereotopic methylene protons appear as a broad peak. The $SiMe_3$ unit appears as a sharp singlet in the case of compound **8a,** Figure 3.4 while the diastereotopic methyl groups of the $SiMe_2$ unit appears as broad singlet for **8b**.

The complexes behave differently in THF. With the exception of the 3-Me signals which appears slightly broadened, the room temperature ^{1}H NMR of **8a** displays three resonances for the pyrazolyl ring substituents in the expected ratio of 9:9:3 for the 3-Me, 5-Me and 4-H, respectively, Figure 3.5. In addition, the resonances due to the alkyl ligands appear as sharp singlets in the expected 4:18 ratio for the CH_2 and $SiMe_3$ groups, respectively. The signals due to the coordinated THF solvent also appeared as well resolved multiplet at ca. 3.61 ppm and 1.78 ppm. Thus, the complexes exhibit an even greater degree of dynamic behavior in THF than in non-coordinating solvents.
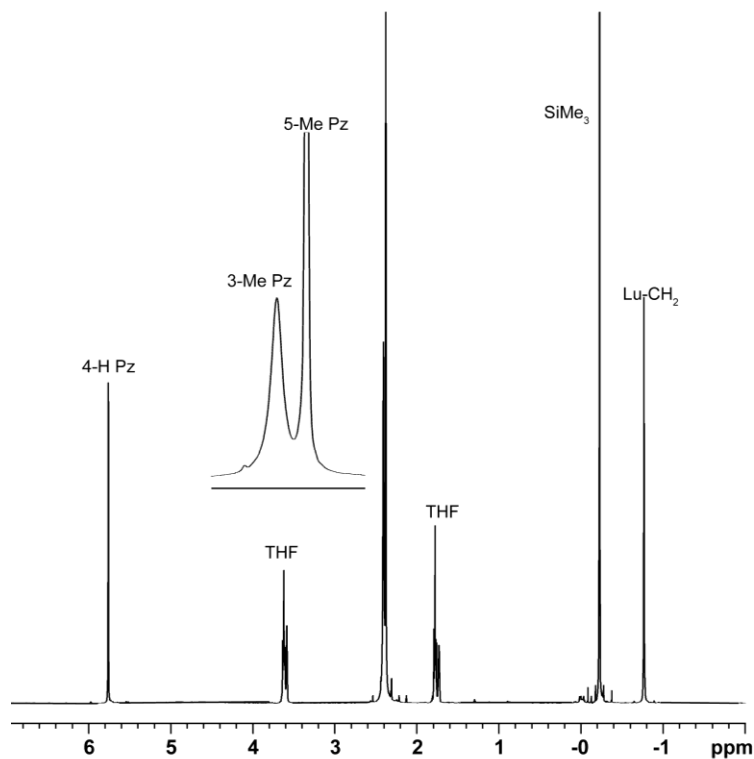
Figure 3.5: Room Temperature ^{1}H NMR Spectrum of $(\text{Tp}^{\text{Me2}})\text{Lu}(\text{CH}_2\text{SiMe}_3)_2(\text{THF})$ (**8a**) in THF-d_8.

This solvent dependent appearance of the ^{1}H NMR signals of these complexes is consistent with THF dissociation and re-coordination equilibrium, eq. 3.7 which in THF-d_8 results in exchange of coordinated and bulk THF, eq. 3.8.

$$(\text{Tp}^{\text{Me2}})\text{Lu}(\text{CH}_2\text{SiMe}_2\text{R})_2(\text{THF}) \underset{\text{or C}_7\text{D}_8}{\overset{\text{C}_6\text{D}_6}{\rightleftarrows}} [\text{"}(\text{Tp}^{\text{Me2}})\text{Lu}(\text{CH}_2\text{SiMe}_2\text{R})_2]\text{"} + \text{THF} \qquad 3.7$$

$$(\text{Tp}^{\text{Me2}})\text{Lu}(\text{CH}_2\text{SiMe}_2\text{R})_2(\text{THF}) \overset{\text{THF-}d_8}{\rightleftarrows} \text{"}(\kappa^2\text{-Tp}^{\text{Me2}})\text{Lu}(\text{CH}_2\text{SiMe}_2\text{R})_2(\text{THF})(\text{THF-}d_8)\text{"}$$

$$\rightleftarrows [(\text{Tp}^{\text{Me2}})\text{Lu}(\text{CH}_2\text{SiMe}_2\text{R})_2(\text{THF-}d_8)(\text{THF})] \rightleftarrows [(\text{Tp}^{\text{Me2}})\text{Lu}(\text{CH}_2\text{SiMe}_2\text{R})_2(\text{THF-}d_8)] \quad 3.8$$
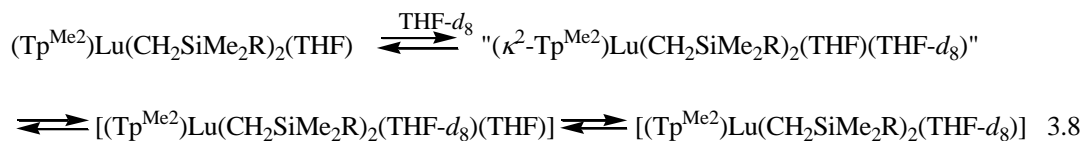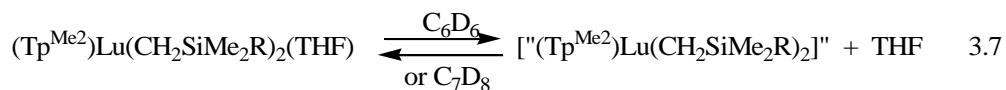
The process is much faster in THF-d_8, where the intermediate could be a (κ^2-Tp^{Me2})Lu(CH$_2$SiMe$_3$)$_2$(THF)(THF-d_8). At any rate, formation of a 5-coordinate THF free intermediate or the above 7-coordinate complex can render the pyrazolyl groups and the diastereotopic CH$_2$ or SiMe$_2$ equivalent leading to the observed simple room temperature ^{1}H NMR spectrum. The effect is more pronounced on the 3-Me and the methylene proton signals since these are the closest to the lutetium center and thus experience a significant amount of steric interaction with other ligands on the lutetium center. Similar behavior was reported for the closely related scandium[10] and yttrium chloride and alkyl complexes,[35,36] (Tp^{Me2})LnX$_2$(THF) (Ln = Sc, Y; X = Cl, –CH$_2$SiMe$_3$). In the scandium dichloride complex, (Tp^{Me2})ScCl$_2$(THF), the room temperature ^{1}H NMR in C$_6$D$_6$ is consistent with a rigid 6-coordinate, octahedral complex with two sets of resonances in 2:1 ratio for the pyrazolyl ring substituents. The yttrium complex (Tp^{Me2})YCl$_2$(THF) on the other hand is fluxional displaying one set of signals for the pyrazolyl ring substituents albeit with slight broadening of the 3-Me signal. This observation is consistent with a faster THF dissociation on the larger yttrium center. The room temperature ^{1}H NMR of the scandium dialkyl complex (Tp^{Me2})Sc(CH$_2$SiMe$_3$)$_2$(THF) in C$_6$D$_6$ displays a single set of signals for both the pyrazolyl ring substituents and the alkyl ligands and this was attributed to fast THF dissociation due to the larger size of the –CH$_2$SiMe$_3$ group compared with the chloride ligand.[10] The yttrium dialkyl compound behaves similarly to the analogous **8a** in benzene (3-Me signal almost broadened into the baseline) and THF-d_8.[36] The difference in the behaviour of (Tp^{Me2})Ln(CH$_2$SiMe$_3$)$_2$(THF) (Ln = Y,

Lu) from their scandium analogue can be attributed to the difference in the size of the respective metal centers.

The paramagnetic Yb compounds **7a** and **7b** both display a solution structure which approximates the observed C_s symmetry in the solid state (*vide infra*). Each gives rise to well separated, and lanthanide shifted resonances in the ^{1}H NMR spectra with a chemical shift range of ca. 433 ppm, Figure 3.6 shows the room temperature ^{1}H NMR spectrum of **7a**. The appearance of a "static" solution structure is due to the larger chemical shift differences between the respective signals, which necessitate a faster rate of exchange to produce averaged signals. In both **7a** and **7b**, the diastereotopic CH_2 protons appear as two well separated broad singlets at ca. -190 ppm and -280 ppm, respectively. Also, the pyrazolyl protons appear in the expected 2:1 ratio, the aromatic protons of **7b** also appear as unresolved singlets. The distinct set of signals in this case is in accordance with the effect of the paramagnetic ytterbium center which gives well separated signals.

Single crystals of compounds **7** and **8** suitable for X-ray diffraction studies were obtained by cooling toluene solutions layered with hexane to -40°C for 2-3 days. In the solid state, the compounds are six-coordinate and have similar structures to the other $(Tp^{Me2})Ln(CH_2SiMe_3)_2(THF)$ analogues (Ln = Sc, Y, Nd and Sm).[10,30] ORTEP drawings of the ytterbium complexes **7a** and **7b** are shown in Figures 3.7 and 3.8, respectively and selected bond lengths and angles are listed in Table 3.2. The lanthanide center is coordinated to a κ^3 bonded Tp^{Me2} ligand, two carbon atoms of the alkyl groups and the oxygen of THF ligand in a distorted octahedral geometry, the distortion from the ideal can be attributed to the constraint
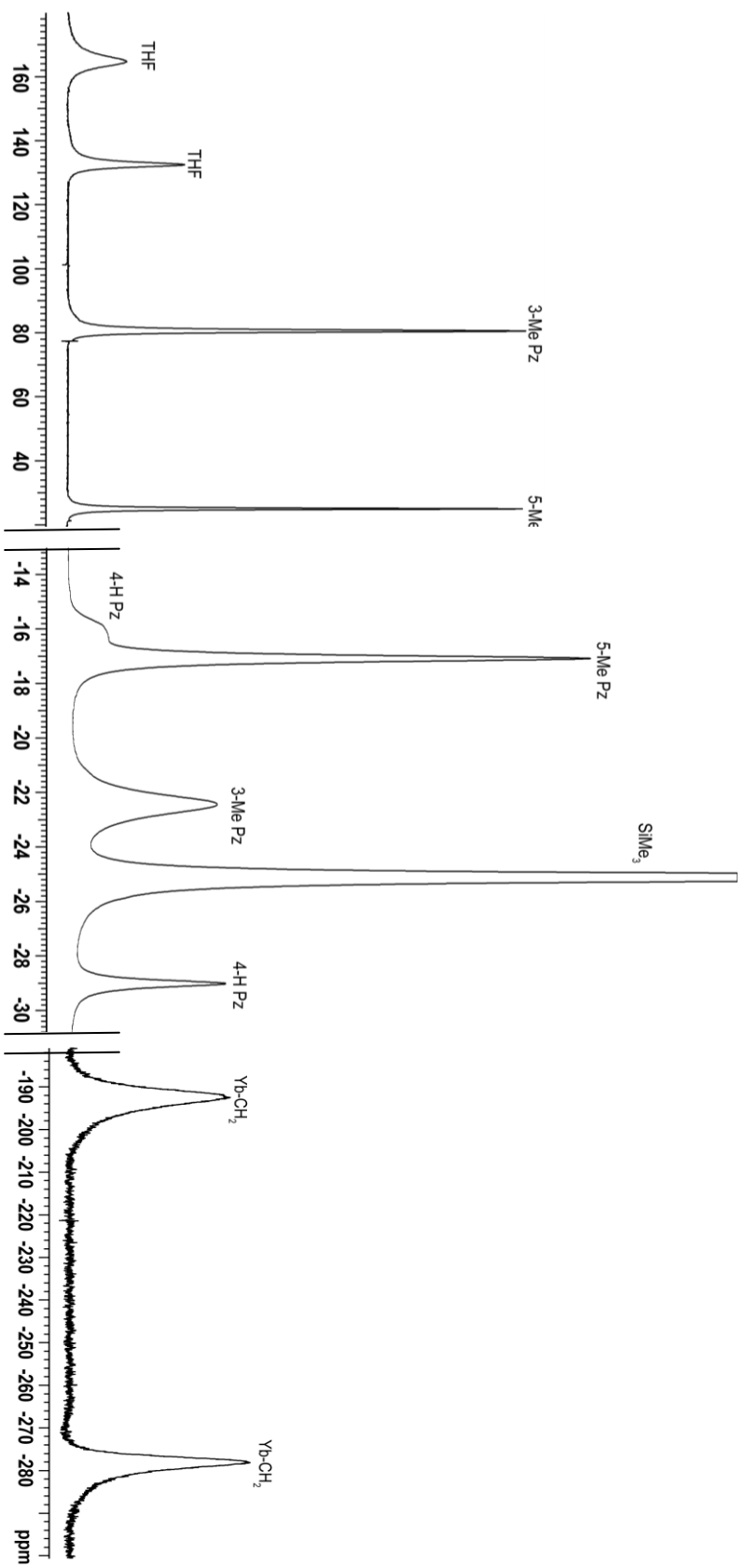
Figure 3.6: Room Temperature ^{1}H NMR Spectrum of $(Tp^{Me2})Yb(CH_2SiMe_3)_2(THF)$ **(7a)** in C_6D_6; the vertical scale of the Yb–CH$_2$ signals region was increased for better visualization.
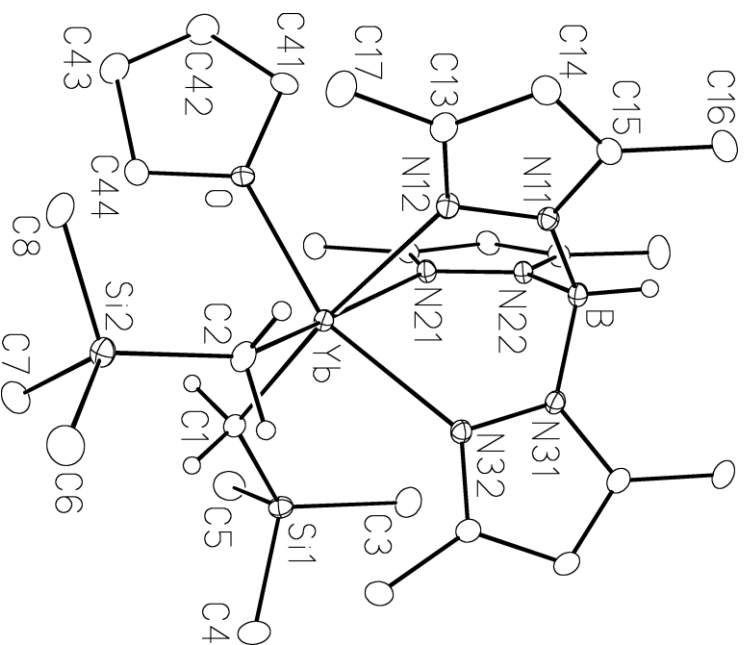
Figure 3.7: ORTEP View of $(Tp^{Me2})Yb(CH_2SiMe_3)_2(THF)$ (**7a**).
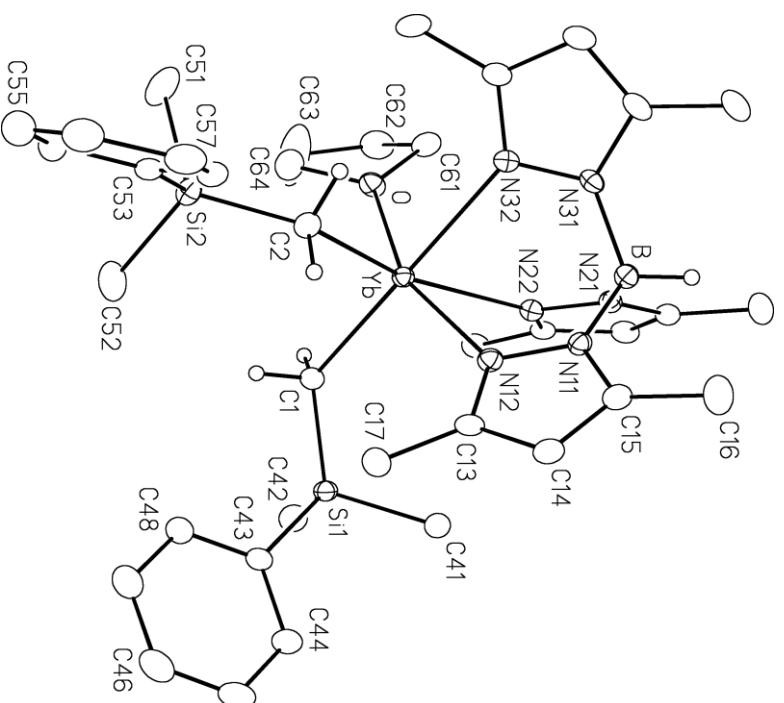
Figure 3.8: ORTEP View of $(Tp^{Me2})Yb(CH_2SiMe_2Ph)_2(THF)$ (**7b**).

100

of the tripodal Tp^{Me2} ligand. The molecular symmetry approaches C_s, with O of the THF ring, Ln, pyrazole (N21, N22) and B almost in a plane, and renders the two CH_2SiMe_3 moieties and the other two pyrazole rings equivalent. The equivalence of these groups is also maintained in solution (*vide supra*). The Ln-N and Ln-C bond lengths in **7** and **8** are longer than those in the corresponding **5** and **6** as expected for the increased coordination number, Table 3.2. The bond distances showed marginal increase as a function of the Ln^{3+} ion size, the smaller than expected difference in the distances probably reflect an increased steric congestion around the smaller lutetium ion. However, the Ln-O, Ln-N and Ln-C bond lengths compares well with the values observed in the analogous $(Tp^{Me2})Ln(CH_2SiMe_3)_2(THF)$ (Ln = Y, Nd, Sm)[30] compounds after accounting for the differences in the ionic radii of the respective Ln(III) ions.[32]

3.3.4 (Tp)Yb(CH₂SiMe₃)₂(THF) Complex (9)

The compound is soluble in ether-type as well as hydrocarbon solvents. Attempts to characterize this delicate compound by spectroscopic means proved frustrating as the ^1H and ^{13}C NMR spectra of the paramagnetic ytterbium compound displayed intense peaks due to hydrocarbon solvent impurities which appear to hide some of the signals of interest. In the ^1H NMR spectrum, only the B-H signal at ca. 19 ppm could be unequivocally assigned based on decoupling experiments for the pyrazolylborate ligand. The other peaks due to the ligand could not be assigned without ambiguity due to the presence of solvent peaks. On the other hand, both the Yb-alkyl groups and the coordinated THF solvent displayed

one set of signals in the expected ratios. The two THF signals appeared at ca. 167

ppm and 80 ppm, for the α and β protons, respectively. For the alkyl groups

Table 3.2: Selected Bond Lengths (Å) and Angles (deg) for
$(Tp^{Me2})Ln(CH_2SiMe_2R'')_2(THF)$ (Ln = Yb, **7**; Lu, **8**; R'' = Me, Ph).

	7a	7b	8a	8b
		Distances		
Ln-O	2.335(2)	2.333(4)	2.314(1)	2.300(4)
Ln-N12	2.443(2)	2.467(5)	2.439(2)	2.473(5)
Ln-N22	2.451(2)	2.484(5)	2.447(2)	2.445(5)
Ln-N32	2.396(2)	2.371(5)	2.375(2)	2.348(5)
Ln-C1	2.377(2)	2.381(7)	2.379(2)	2.366(6)
Ln-C2	2.373(2)	2.396(6)	2.373(2)	2.392(6)
		Angles		
O-Ln-N12	84.18(6)	83.22(17)	84.41(6)	86.3(2)
O-Ln-N22	81.85(6)	86.15(18)	81.99(6)	82.6(2)
O-Ln-N32	158.48(6)	158.92(18)	158.99(6)	159.2(2)
O-Ln-C1	97.69(7)	89.5(2)	97.32(7)	89.5(2)
O-Ln-C2	100.09(8)	101.8(2)	99.73(7)	101.5(2)
N12-Ln-N22	75.24(6)	76.63(18)	81.95(6)	76.6(2)
N12-Ln-N32	78.26(7)	81.09(18)	78.52(6)	81.6(2)
N12-Ln-C1	168.04(8)	171.2(2)	168.14(7)	160.7(2)
N12-Ln-C2	91.73(8)	87.0(2)	91.56(7)	97.4(2)
N22-Ln-N32	81.70(6)	76.60(18)	75.53(6)	76.9(2)
N22-Ln-C1	93.27(8)	98.0(2)	93.04(7)	86.9(2)
N22-Ln-C2	166.64(8)	160.9(2)	166.81(7)	170.4(2)
N32-Ln-C1	97.03(7)	104.6(2)	96.97(7)	104.5(2)
N32-Ln-C2	92.85(7)	91.3(2)	92.95(7)	91.1(2)
C1-Ln-C2	99.53(9)	98.32(15)	99.67(8)	98.44(8)

coordinated to the ytterbium center, the SiMe₃ signal appears at about -18 ppm and integrates for 18 protons and the other peak corresponding to the CH_2 groups appears at -252 ppm, as a broad peak. However, based on elemental analysis results, the compound is authentic as formulated.

Attempts to obtain X-ray quality crystals by cooling a diethyl ether/ hexamethyldisiloxane solution of **9** to -30°C for several days afforded bright red needles which proved to be the dimer, $[(Tp)Yb(CH_2SiMe_3)\{\mu\text{-}OCH_2SiMe_3)]_2$, **10** shown in Figure 3.9.
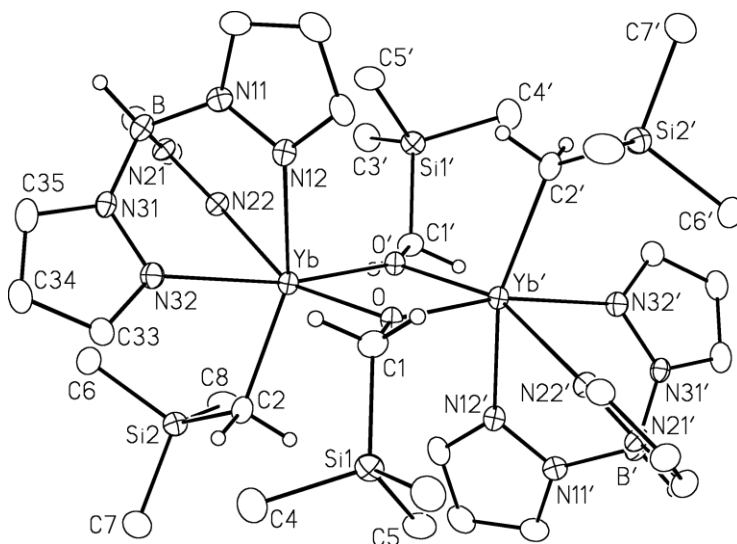
Figure 3.9: ORTEP View of $[(Tp)Yb(CH_2SiMe_3)\{\mu\text{-}OCH_2SiMe_3)]_2$ (**10**).

The formation of **10** must be due to the presence of trace amounts of adventitious oxygen in the glovebox atmosphere. Similar observation was made when the yttrium monoalkyl complex L′Y(CH₂SiMe₃)(THF) (L′ = [2-O-3,5-ₜBu₂-C₆H₂CH₂N(CH₃)(CH₂)]₂ was exposed to a nitrogen atmosphere containing a

103

limited amount of oxygen. The oxygenation product, $L'Y(\mu\text{-}OCH_2SiMe_3)$ was obtained.[37]

Compound **10** crystallizes in the monoclinic space group $P2_1/n$ with two molecules in the unit cell. It is a centrosymmetric dimer with two -OCH_2SiMe_3 groups bridging the two ytterbium centers. Each Yb atom is thus coordinated by a κ^3 bonded Tp ligand, two bridging –OCH_2SiMe_3 groups as well as one terminal –CH_2SiMe_3 moiety in a distorted octahedral arrangement around the metal center. The tris(pyrazolyl)borate ligands and the terminal alkyl groups on different ytterbium centers adopt an anti-arrangement around the core. This is similar to the structure found in the related dichloride complex, $[(Tp)YbCl\{\mu\text{-}Cl)(THF)]_2$,[38] the presence of THF in this compound reflects the difference in the size of the alkyl ligand in compound **10** as opposed the smaller chloride ligand in the former complex. The four membered ring core of the structure is essentially planar as reflected by the ca. 360° sum of the angles around the O of the –OCH_2SiMe_3 group and also by the O'-Yb-O-Yb' torsion angle of 0.0° for the four atoms forming the four membered ring.

Even though the oxygen atoms of the bridging –OCH_2SiMe_3 group appear to be positioned symmetrically between the two ytterbium centers (Yb–O; 2.208(3) Å and Yb–O'; 2.205(3) Å), the bridge is asymmetric as shown by the difference in Yb–O'–C1 and Yb'–O'–C1 angles, which are 116.3(3)° and 137.2(3)°, respectively. This is due to steric crowding between the SiMe$_3$ groups and the pyrazolyl rings. The average Yb-N bond of 2.433(4) Å in **10** is slightly longer than the average value of 2.403(4) Å in $[(Tp)YbCl\{\mu\text{-}Cl)(THF)]_2$, this probably reflects

the crowding around the Yb center in **10**. The observed average Yb–O bond length

of 2.207(2) Å in **10** is shorter than the 2.297(4) in L′Y(CH$_2$SiMe$_3$)(THF). The Yb–

C bond distance of 2.391(5) Å in **10** is within the range of other Yb–C bond dis-

tances.[33, 34].

3.4   Synthesis of "LLnH$_2$" type Complexes

3.4.1 Introduction

Metal hydrides are of great importance for their role in a wide range of

stoichiometric and catalytic reactions, and as such, their importance in chemistry

cannot be overemphasized.[39] Although numerous metallocene monohydride com-

plexes of the rare earth metals of the general form "Cp$_2$LnH" have been synthe-

sized and studied since the first example reported by Evans *et al*. in the 1980s,[40]

the corresponding dihydrides are still rather rare. As mentioned in Chapter 1,

complexes of this type were only recently reported by Hou and co-workers.[41] They

reported an extensive series of monocyclopentadienyl rare earth metal dihydrides,

"[(C$_5$Me$_4$SiMe$_3$)LnH$_2$]"[42] (Ln = Sc, Y, Gd, Dy, Ho, Er, Tm, Lu), which exhibit

remarkable reactivity, far different from that of metallocene monohydrides. These

complexes, which consists of tetrameric lanthanide hydride clusters of the form

[{(η^5-C$_5$Me$_4$SiMe$_3$)Ln(μ-H)$_2$}$_4$(THF)$_n$] (Ln = Sc, Y, Gd, Dy, Ho, Er, Tm and Lu ;

n = 0, 1, 2)[41], were prepared either by hydrogenolysis or treatment of the corre-

sponding dialkyl complexes, (C$_5$Me$_4$SiMe$_3$)Ln(CH$_2$SiMe$_3$)$_2$(THF) with PhSiH$_3$. In

the case of lutetium, hydrogenolysis of the dialkyl compound was reported to give

a mixture of hydride species.[41]   However, by first treating the lutetium dialkyl

complex with phenylsilane followed by hydrogenolysis, the corresponding lutetium dihydride complex was isolated.[41]

Compared to the aforementioned compounds, the development of cyclopentadienyl-free rare earth metal hydrides is still relatively new.5 Dimeric complexes of the form "[(Ligand)$_2$Ln(μ–H)]$_2$" have been reported, with examples including benzamidinate,[43] guanidinate,[44] salicylaldiminate,[25] diamides,[45] bis(phenolate)[46], aminopyridinate[47] etc. ligands. Despite the success of these ligand systems,[48] examples of dihydride species of the form "LLnH$_2$" were unknown prior to this work. The only other known non-cyclopentadienyl lanthanide dihydride complexes are the trinuclear hydrido cluster, [Ln(Me$_3$TACD)H$_2$]$_3$ (Me$_3$TACDH = 1,4,7-trimethyl-1,4,7,10-tetraazacyclododecane; Ln = Y, Ho, Lu), reported very recently by Okuda et $al.$,[49] as well as the mixed alkyl-hydrido cluster, (Ap*Ln)3(μ_2-H)$_3$(μ_3-H)$_2$(CH$_2$SiMe$_3$)(THF)$_2$ (Ap*H = 2,6-diisopropylphenyl)[6-(2,4,6-triisopropylphenyl)pyridin-2-yl]amine; Ln = Y, Lu) prepared by Trifonov and co-workers.[50] The investigation of this class of compounds has been hampered by the difficulty in isolating structurally well defined complexes, a direct consequence of lack of suitable starting materials.

3.4.2 Synthesis of $[(Tp^{Me2})LnH_2]_4$ (Ln = Yb, Lu) and $[(Tp)YbH_2]_6$ Complexes

Reaction of $(Tp^{Me2})Ln(CH_2SiMe_3)_2(THF)$ (Ln = Yb, Lu) with dihydrogen afforded the corresponding dihydride complexes $[(Tp^{Me2})LnH_2]_4$ (Ln = Yb, **11**; Ln = Lu, **12**) albeit under rather forcing conditions, Scheme 3.5.

$$(Tp^{R,R'})Ln(CH_2SiMe_3)_2(THF)$$

H_2; 75-82 atm; Et_2O
R = R' = Me
Ln = Yb, Lu

H_2; 68 atm; Et_2O
R = R' = H
Ln = Yb

$$[(Tp^{Me2})LnH_2]_4 \qquad\qquad [(Tp)LnH_2]_6$$
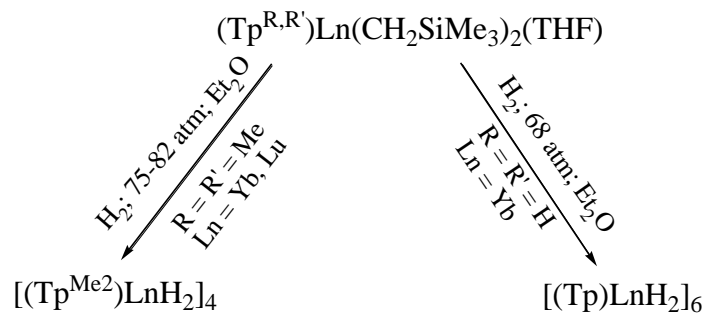
Scheme 3.5 Hydrogenolysis of $(Tp^{R,R'})Ln(CH_2SiMe_3)_2(THF)$ Complexes.

The ytterbium complex undergoes hydrogenolysis to yield the dihydride complex when pressurized with about 1100 psi (75 atm.) of hydrogen gas for 48 h. While the lutetium complex required 1200 psi (82 atm.) and a longer reaction time, 69 h. The higher reaction pressures and longer reaction times (i.e. slower reaction rates) for the scorpionate dialkyls compared to their cyclopentadienyl analogues, 15 psi (1 atm.) and 4-24 h reaction time,[41] are presumably due to a combination of electronic and steric effects. The presence of the hard nitrogen donor scorpionate ligand may induce stronger Ln-C (alkyl) interaction, while the steric bulk of the ligand, centered around the metal, hinders approach of dihydrogen toward the reactive and highly polar Ln-C bonds. Thus, both factors contribute to the more stringent condition required to effect hydrogenolysis of the

(Tp^{Me2})Ln(CH$_2$SiMe$_3$)$_2$(THF) complexes. Similar to the observation made in the preparation of the ytterbium dialkyl complexes, **7a** and **7b**, formation of an insoluble purple solid, presumably (Tp^{Me2})$_2$Yb, was observed during the hydrogenolysis of the ytterbium dialkyl complexes and while attempting to recrystallize the dihydride complex **11**. This possibly reflects easier reduction of "(Tp^{Me2})YbH$_2$", followed by rapid ligand redistribution and precipitation of the highly insoluble (Tp^{Me2})$_2$Yb.

In an effort to investigate the influence of ligands on cluster hydride formation, hydrogenolysis of ($Tp^{tBu,Me}$)Lu(CH$_2$SiMe$_3$)$_2$, **6a** was investigated. Although the alkyl ligands were eliminated, the ^{1}H NMR spectrum of the products showed the presence of a mixture of compounds. This was attributed to possible metalation of the ^{t}Bu substituents. Similar observation was made with the analogous yttrium complex by Dr Cheng. On the other hand, hydrogenolysis of (Tp)Yb(CH$_2$SiMe$_3$)$_2$(THF), **9**, afforded the dihydride (Tp)YbH$_2$, as the hexanuclear complex, [(Tp)YbH$_2$]$_6$, **13**, albeit in a rather poor yield, Scheme 3.5.

3.5   Characterization of (Tp^{Me2})LnH$_2$ and (Tp)YbH$_2$ Complexes

3.5.1   General Methods

The compounds are all air and moisture sensitive but thermally stable, except in the case of **11** which gradually decomposes in solution to give an insoluble purple solid presumed to be the known (Tp^{Me2})$_2$Yb, and other unidentified species. The compounds were studied by multinuclear NMR spectroscopy (^{1}H, ^{13}C and ^{11}B) but only in the case of the tetranuclear **12** was this informative. For the

paramagnetic ytterbium complexes, the NMR spectrum was complex. This obser-

vation probably reflects the instability of **11** in solution. The formulation of the

complexes is however consistent with elemental analysis results and their struc-

ture was confirmed in the solid state by single crystal X-ray crystallography stud-

ies.

3.5.2   [(Tp^{Me2})LnH$_2$]$_4$ Complexes (Ln = Yb,11; Lu, 12)

The compounds are soluble in toluene and THF and moderately soluble in

Et$_2$O. The room-temperature ^{1}H NMR spectrum of the lutetium complex **12** dis-

plays a single set of peaks assignable to the Tp^{Me2} ligand and a single sharp Lu–H

signal at ca. 12 ppm. There are no signals due to coordinated THF,

Figure 3.10.
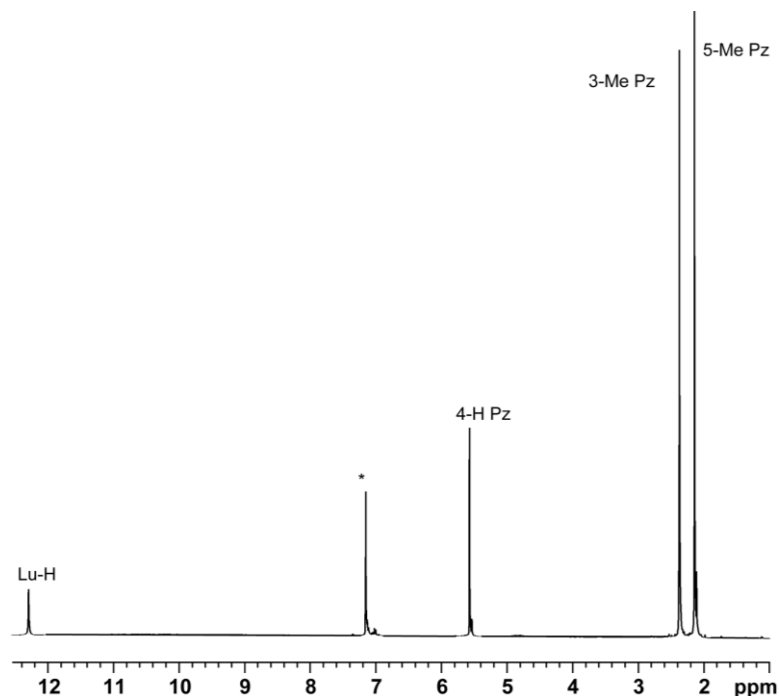
Figure 3.10: Room Temperature ^{1}H NMR Spectrum of
[(Tp^{Me2})LuH$_2$]$_4$ (**12**) in C$_6$D$_6$.

109

Since it is not possible to have a symmetrical environment for all 8 hydride for a tetranuclear cluster, unless it would correspond to a square arrangement of four lanthanide centers, the observation of a single set of signals for the hydrides is indicative of a fluxional process similar to what was observed in other "(Tp^{Me2})LnH$_2$" complexes (Ln = Y, Nd, Sm,).[30] For the yttrium complex, the hydride signal appeared as a quintet at room-temperature consistent with coupling of the hydrides to four equivalent yttrium atoms. Cooling a toluene solution of the yttrium hydride complex down to -80°C only broadened the hydride signal indicating that the compound is still fluxional at this temperature.[51]

X-ray analysis on a single crystal grown from a concentrated THF solution revealed a tetranuclear cluster structure. Despite the fact that the crystals were obtained from a THF solution, the solid state structure contains no coordinated THF molecules. The lack of THF coordination to the lanthanide attests to the bulkier nature of the Tp^{Me2} ligand compared to C$_5$Me$_4$SiMe$_3$, for which up to two THF molecules were retained by the cluster hydrides.[41] The structure of the representative Lu complex is shown in Figure 3.11 along with the Lu$_4$H$_8$ core structure, Figure 3.12 and selected bond distances are listed in Table 3.3.

The structure consists of four Lu ions located on the corners of a slightly distorted tetrahedron. Each Lu is bonded to a κ^3-Tp^{Me2} ligand, and the hydride ligands form bridges between the Lu atoms in three modes: one μ_4-H1 at the center of the Lu$_4$ unit, one face-capping μ_3-H2, and six edge-bridging μ_2-H. The Lu---Lu distances range from 3.4329(2) (Lu3---Lu4) to 3.5931(3) Å

Table 3.3: Selected Bond Distances (Å) of [(Tp^Me2)LnH₂]₄ (Ln = Yb, **11**; Lu, **12**).

Ln--Ln	μ_2–H-Ln		μ_3–H-Ln	μ_4–H-Ln
Yb1--Yb2 3.6196(3)	Yb1-H3 2.05(5)	Yb3-H3 1.96(5)	Yb2-H2 2.34(5)	Yb1-H1 2.17(4)
Yb1--Yb3 3.5611(3)	Yb1-H4 1.98(5)	Yb3-H6 1.97(4)	Yb3-H2 2.15(5)	Yb2-H1 2.21(4)
Yb1--Yb4 3.5628(3)	Yb1-H5 2.01(4)	Yb3-H8 2.07(4)	Yb4-H2 2.25(5)	Yb3-H1 2.11(4)
Yb2--Yb3 3.4810(3)	Yb2-H5 2.13(4)	Yb4-H4 2.08(5)		Yb4-H1 2.16(4)
Yb2--Yb4 3.4982(3)	Yb2-H6 2.10(4)	Yb4-H7 2.13(4)		
Yb3--Yb4 3.4556(3)	Yb2-H7 2.00(4)	Yb4-H8 1.96(4)		
Lu1--Lu2 3.5931(3)	Lu1-H3 1.94(5)	Lu3-H3 2.03(5)	Lu2-H2 2.37(4)	Lu1-H1 2.05(3)
Lu1--Lu3 3.5266(3)	Lu1-H4 2.05(4)	Lu3-H6 1.97(5)	Lu3-H2 2.17(4)	Lu2-H1 2.27(3)
Lu1--Lu4 3.5397(3)	Lu1-H5 2.06(4)	Lu3-H8 2.07(4)	Lu4-H2 2.21(4)	Lu3-H1 2.11(3)
Lu2--Lu3 3.4631(2)	Lu2-H5 2.11(4)	Lu4-H4 2.04(4)		Lu4-H1 2.18(3)
Lu2--Lu4 3.4831(3)	Lu2-H6 2.10(5)	Lu4-H7 2.14(6)		
Lu3--Lu4 3.4329(2)	Lu2-H7 1.88(4)	Lu4-H8 2.01(4)		
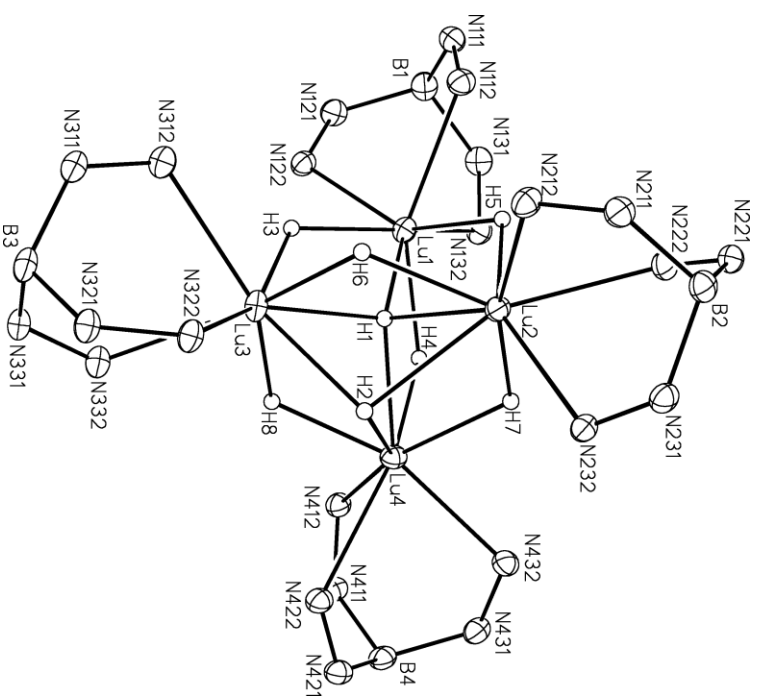
Figure 3.11: ORTEP View of $[(Tp^{Me2})LuH_2]_4$ (**12**) With All of the Pyrazole Carbon Atoms Removed for Clarity.
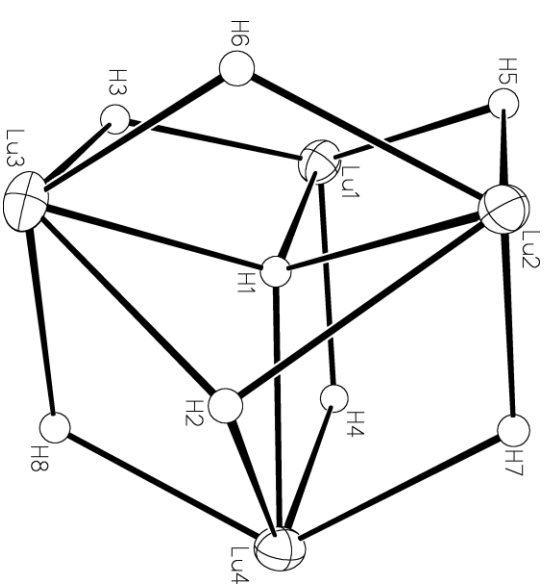
Figure 3.12: View of the Lu_4H_8 Core of **12**.

(Lu1---Lu2), and the shortest separation is associated with the Lu3···Lu4 edge which is bridged by three hydride ligands.

These Lu---Lu distances are more than 0.1 Å larger than in the cyclopenta-dienyl analogue $[(\eta^5\text{-}C_5Me_4SiMe_3)Lu(\mu\text{-}H)_2]_4$ (3.3689 Å–3.4641 Å),[41,52] and this again reflects the bulkier nature of the Tp^{Me2} ligand. The μ_2-H–Lu bond lengths range from 1.88(6) Å (Lu2–H7) to 2.14(6) Å (Lu4–H7), which fall in the range found in other dimeric lutetium hydrido complexes; 2.12(5) Å and 2.06(5) Å found in $[(\eta^5\text{-}C_5Me_4SiMe_3)Lu(CH_2SiMe_3)(\mu\text{-}H)(THF)]_2$, 1.93(6) Å and 2.10(6) Å in $[Lu(\eta^5\text{:}\eta^1\text{-}C_5Me_4SiMe_2NCMe_3)(\mu\text{-}H)(PMe_3)]_2$.[53]

The μ_3-H-Lu distances (Lu3-H2 2.17(4) Å, Lu4–H2 2.21(4), Å Lu2–H2 2.37(4) Å) indicate an asymmetric bridging arrangement with a weaker bond to Lu2. The μ_4- H–Lu bond distances which ranges from 2.05(3) Å (Lu1-H1) to 2.27(3) Å (Lu2-H1) also reflects an asymmetric bonding of the μ_4-H with the weaker bond again, to Lu2. The complexes **11** and **12** are isostructural and have the same Ln$_4$H$_8$ core structure as their yttrium and samarium analogues but slightly different from that of the neodymium analogue in which H8 exhibits a slightly more face-capping than edge-bridging tendency.

3.5.3   [(Tp)YbH$_2$]$_6$ Complex (13)

The compound is soluble in toluene, Et$_2$O as well as THF. Unfortunately, the ^{1}H NMR of this paramagnetic ytterbium compound is not informative and thus the structure is determined only by X-ray crystallography studies.

The compound crystallizes from Et_2O in the trigonal space group as the Et_2O solvate. The molecular structure of $[(Tp)YbH_2]_6$ is shown in Figure 3.13, also shown is the hexanuclear Yb_6H_{12} frame, Figure 3.14.

The compound is isostructural to the Y and Lu analogues. The structure consists of six "(Tp)YbH$_2$" units forming a hexanuclear cluster held together by twelve bridging hydride ligands. The six Yb centers are disposed in a trigonal-antiprismatic arrangement with D_3 point symmetry, which results in one crystallographically unique Yb atom and ″top″ and ″bottom″ equilateral triangular faces formed by Yb, Yb*, Yb″ and Yb′, Yb#, Yb%, respectively.

There are four crystallographically unique hydride ligands. Three of them (H2, H2*, H2″), located on twofold rotational axes, bridge the top/bottom faces in μ_2 fashion on alternating edges. There are two μ_3-bridging hydride ligands on the top/bottom faces (H3, H3″) sitting on a threefold rotation axis, while the remaining six hydride ligands (H1 and related) cap the other faces in a μ_3 fashion; these hydride ligands are not on a symmetry element, but are related by them. The last hydride ligand, H4, binds in a μ_6-H–Ln fashion and is located at the intersection of the threefold and twofold axes. The parallel top/bottom faces are rotated by 10.50° away from being eclipsed. This result in unequal interplane Yb···Yb distances; (3.2400(5) and 3.6360(6) Å for Yb···Yb′ and Yb···Yb#, respectively), the unique Yb···Yb distance within each equilateral triangular face is 3.60545(5). For the same reason, there are two unequal distances to the hydride ligands that bridge the faces between the top/bottom planes (Yb–H1, 2.24(7), Yb–H1# 2.17(7) Å); the distance to H3 is 2.37(6) Å. The shortest Yb-H distance is that to the μ_2 edge-
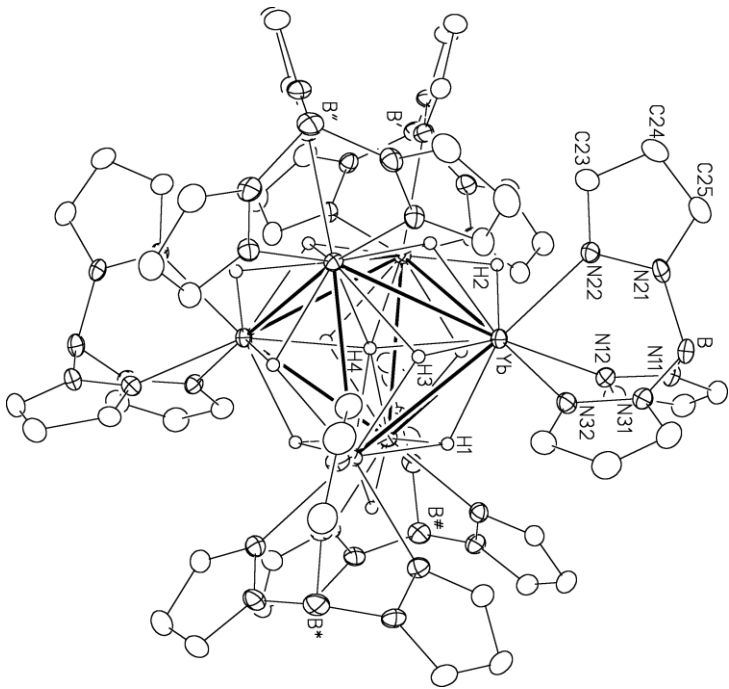
Figure 3.13: ORTEP View of [(Tp)YbH$_2$]$_6$ (**13**).
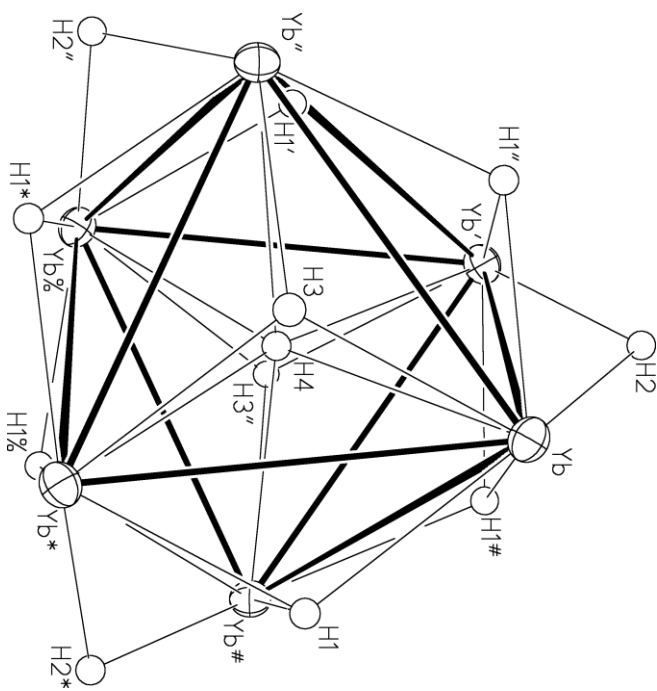
Figure 3.14: View of the Yb$_6$H$_{12}$ Core of **13**.

115

bridging hydride H2 (and symmetry related ligands), 1.99(6) Å, while the distance to μ_6-H4 is significantly longer (2.4894(3) Å) and is also longer than the μ_4-H–Yb distance (2.11(4)–2.21(4) Å) in the tetranuclear cluster **11**.

3.6   Conclusions

The steric protection offered by tris(pyrazolyl)borate ligands allowed the synthesis of lanthanide dialkyl complexes, $(Tp^{R,R'})Ln(CH_2SiMe_2R'')_2$. The complexes were obtained by two alternative and complementary protocols. For the synthesis of $(Tp^{tBu,Me})Ln(CH_2SiMe_2R'')_2$ complexes, the method of choice is the protonolysis of $Ln(CH_2SiMeR'')_3(THF)_2$ with $H(Tp^{tBu,Me})$; a similar approach was used to obtain the yttrium analogues. However, in the case of $(Tp^{Me2})Ln(CH_2SiMe_2R'')_2(THF)$ and $(Tp)Yb(CH_2SiMe_3)_2(THF)$ complexes, alkyl abstraction from $Ln(CH_2SiMe_2R'')_3(THF)_2$ by $Tl(Tp^{R,R'})$ (R = R' = Me; R = R' = H) is the preferred route to these complexes. The alkyl abstraction method is also applicable to the early lanthanides, neodymium and samarium by using a one pot approach similar to that used by Hessen and co-workers.[8] However, attempts to extend the same approach to the largest lanthanide, lanthanum, failed to yield any isolable dialkyl compound. The only isolable products from these reactions are the lithium salts of the tris(pyrazolyl)borate ligand, $Li(Tp^{R,R'})$. For the isolated complexes, $(Tp^{Me2})Ln(CH_2SiMe_2R'')_2(THF)$, the Ln-O, Ln-N and Ln-C bond distances exhibit the usual decrease from early to late lanthanide consistent with the expected decrease in size as a result of lanthanide contraction, Table 3.4.

Table 3.4: Selected Bond Distances (Å) in $(Tp^{Me2})Ln(CH_2SiMe_3)_2(THF)$ (Ln = Nd, Sm, Y, Yb, Lu) Showing the Effect of Lanthanide Contraction.

	R″ = Me			R″ = Ph		
Ln	Ln–C$_{1/2}$	Ln–O	Ln–N$_{xx}$	Ln–C$_{1/2}$	Ln–O	Ln-N$_{xx}$
			2.528(2)			2.504(2)
Nd	2.495(3)	2.4867(15)	2.604(2)	2.523(2)	2.4717(17)	2.596(2)
	2.500(3)		2.632(2)	2.498(2)		2.633(2)
			2.498(2)			2.472(2)
Sm	2.467(3)	2.4603(18)	2.567(2)	2.4936(19)	2.4442(14)	2.565(2)
	2.473(3)		2.599(2)	2.474(2)		2.601(2)
			2.429(2)			2.394(4)
Y	2.418(2)	2.3590(15)	2.491(2)	2.440(5)	2.344(3)	2.517(4)
	2.432(2)		2.492(2)	2.420(5)		2.500(4)
			2.396(2)			2.371(5)
Yb	2.373(2)	2.3350(16)	2.443(2)	2.396(6)	2.333(4)	2.484(5)
	2.377(2)		2.451(2)	2.381(7)		2.467(5)
			2.375(2)			2.348(5)
Lu	2.373(2)	2.3143(14)	2.4398(2)	2.366(6)	2.300(4)	2.445(5)
	2.379(2)		2.447(2)	2.392(6)		2.473(5)

Hydrogenolysis of $(Tp^{R,R'})Ln(CH_2SiMe_3)_2(THF)$ (R = R′ = Me, H) successfully led to the isolation of the first non-cyclopentadienyl lanthanide dihydrides $[(Tp^{R,R'})LnH_2]_n$. The structure of the dihydrides can be described as a

polynuclear cluster framework which is maintained in solution and their nuclearity is dependent on the steric size of the ancillary scorpionate ligand.

3.7   Experimental Section

3.7.1   General Techniques, Solvents and Physical Measurements

As in Chapter 2. In addition, hydrogenolysis was carried out in a Parr Instrument Company (022486) 2000 psi bomb.

3.7.2   Starting Materials and Reagents

Anhydrous $LnCl_3$ (Ln = Y, Yb, Lu) were purchased from Strem Chemicals Ltd. $LiCH_2SiMe_3$ (1.0M solution in pentane) was purchased from Aldrich, the pentane solvent was removed under vacuum and the so obtained solid $LiCH_2SiMe_3$ was used without further purification. H_2 gas (4.5 pp) was purchased from PRAXAIR Canada Inc., and used without further purification. The compounds $LiCH_2SiMe_2Ph$,[25,54] $Tl(Tp^{tBu,Me})$, $Tl(Tp^{Me2})$,[31] $H(Tp^{tBu,Me})$, $H(Tp^{Me2})$,[21,22] $Ln(CH_2SiMe_2R'')_3(THF)_2$ (Ln = Lu, Yb; R'' = Me, Ph)[23,24,25] were prepared by a combination of literature procedures and modification of literature procedures.

3.7.3   Synthesis of the Compounds

$H(Tp^{tBu,Me})$

Method 1: **Reaction of $Tl(Tp^{tBu,Me})$ with H_2S**

A clear, colorless, CH_2Cl_2 (25 mL) solution of $Tl(Tp^{tB,Me})$ (1.8g, 2.87 mmol) was cooled down to -78°C and then pressurized with about 40psi of H_2S

(20 psi twice). There was formation of black precipitate immediately. The mixture was allowed to stir while gradually warming to RT and then stirred at RT for ca. 1 h All volatiles was then removed in vacuum and the black residue was then extracted with pentane (25mL) and all volatiles were then removed in vacuum to obtain (0.968g, 2.28 mmol) of a white solid in 79% isolated yield. Cooling a concentrated pentane solution to -30°C affords colorless crystals suitable for single crystal X-ray studies.

Method 2: Reaction of $K(Tp^{tBu,Me})$ with CH_3COOH.

A suspension of $K(Tp^{tBu,Me})$ (3.0g, 6.49mmol) in 50 mL distilled water was treated with neat glacial acetic acid, 0.37 mL (0.389g, 6.49 mmol), a white emulsion formed immediately and this was stirred for another 2 h, centrifuged, washed with water (about 1L) and then dried under vacuum. The resulting white powder was re-dissolved in about 25mL of pentane, filtered and the supernatant concentrated to about 5mL and cooled to -30°C to obtain white crystalline solid which was dried in vacuum after decanting the supernatant to obtain 2.05g, 0.48 mmol of the compound (75% isolated yield). Anal. Calc. for $C_{24}H_{41}N_6B$: C, 67.92; H, 9.74; N, 19.80. Found: C, 67.95; H, 9.75; N, 19.73.

^{1}H NMR (400 MHz, C_6D_6, 27°C): δ 14.22* (br, 1H, N-*H*) (* concentration and temperature dependent), 5.69 (q, J_{HH} = 0.65Hz, 3H, 4-*H* Pz), 5.10 (br, 1H, B-*H*), 2.18 (d, J_{HH} = 0.65Hz, 9H, 5-C*H*$_3$ Pz). 1.32 (s, 27H, 3-(C*H*$_3$)$_3$C Pz), ^{13}C{^{1}H} NMR (100 MHz, C_6D_6, 27°C): δ 158.63 (s, 3-*C* Pz), 144.87 (s, 5-*C* Pz), 102.56 (s, 4-C Pz), 31.94 (s, (CH$_3$)$_3$*C*), 30.88 (s, (CH$_3$)$_3$C Pz), 12.32 (s, 5-C*H*$_3$ Pz). ^{11}B NMR

(128 MHz, C_6D_6, 27°C): δ -5.77 (d, $^1J_{BH} = 116$ Hz) ^{11}B {^{1}H} NMR δ -5.77 (s). IR (KBr or Nujol) ν_{B-H} 2467 cm^{-1}.

H(Tp^{Me2})

Method 1: Reaction of Tl(Tp^{Me2}) with H_2S.

Following the same procedure for the synthesis of H(Tp^{tB,Me}) using (1.34g, 3.99 mmol) of Tl(Tp^{Me2}) and about 40 mL CH_2Cl_2. The black residue was extracted with benzene, filtered to give a clear colorless supernatant. Removal of solvent from the solution gave (0.92g, 3.10 mmol) of a white solid. ^{1}H NMR showed a mixture of H(Tp^{Me2}) and Tl(Tp^{Me2})

Method 2: Reaction of K(Tp^{Me2}) with CH_3COOH.

A suspension of K(Tp^{Me2}) (1.62g, 4.80 mmol) in 20 mL distilled water was treated with neat glacial acetic acid, 0.28 mL (0.29g, 4.8 mmol), a white emulsion formed immediately and this was stirred for another 1 h, centrifuged, washed with water (about 1L) and then dried under vacuum. The resulting white powder was then washed with 3 mL pentane (10 mL 3ce) and dried in vacuum to obtain 0.206g, 0.69 mmol of the compound (14 % isolated yield).

^{1}H NMR (500 MHz, C_6D_6, 27°C): δ 13.18 (s, 1H, N-*H*), 5.61 (s, 3H, 4-*H*-Pz), 5.10 (br, 1H, B-*H*), 2.20 (s, 9H, 3-C*H*$_3$ Pz), 2.03 (s, 9H, 5-C*H*$_3$ Pz). ^{13}C{^{1}H} NMR (125 MHz, C_6D_6, 27°C): δ 144.89 (s, 3-*C* Pz), 143.52 (s, 5-*C* Pz), 105.59 (s, 4-C Pz), 12.81 (s, 3-C*H*$_3$ Pz), 12.18 (s, 5-C*H*$_3$ Pz). ^{11}B NMR (160 MHz, C_6D_6, 27°C): δ -6.45 (d, $^1J_{BH} = 106.4$ Hz) ^{11}B {^{1}H} NMR δ -6.56 (s).

LiCH$_2$SiMe$_2$Ph

To a slurry of Li powder (1.152g, 166 mmol) in 50mL of toluene was added pieces of Na metal (0.019g, 0.5% in Li) under argon. Me$_2$PhSiCH$_2$Cl (15.36g, 83 mmol) was slowly added to the slurry under argon. The slurry was degassed by three freeze-pump-thaw cycles and after melting and warming to RT, the slurry was heated gently to 120°C at first to allow the toluene to reflux. The temperature was then controlled to ca. 75°C. The mixture was stirred at this temperature for 4 days. The resulting orange-grey mixture was centrifuged and toluene was stripped in vacuum to obtain a brownish solid which was washed several times with hexane to obtain a white solid. Recrystallization from hexanes affords the title compound as white crystalline solid (6.95g, 45 mmol) in 54% isolated yield.

^{1}H NMR (500 MHz, C$_6$D$_6$, RT) δ 7.42 (dd, J = 7.5 Hz, 1.5 Hz, 2H, *o*-H Ph), 7.22 (tt, J = 7.5 Hz, 1.5 Hz, 2H, *m*-H Ph), 7.15 (tt, J = 7.5 Hz, 1.5 Hz, 1H, *p*-H Ph), 0.23 (s, 6H, Si*Me$_2$*), -2.43 (s, 2H, LiC*H$_2$*). ^{13}C{^{1}H} (125 MHz, C$_6$D$_6$, 27°C) δ 142.91 (*ipso*-C Ph), 133.35 (*m*-C Ph), 129.73 (*p*-C Ph), 129.46 (*o*-C Ph), 2.21 (Si*Me$_2$*), -9.11 (br, LiC*H$_2$*).

Yb(CH$_2$SiMe$_3$)$_3$(THF)$_2$

Anhydrous YbCl$_3$ (0.43g, 1.54 mmol) was suspended in about 10mL THF and stirred for ca. 1 h. LiCH$_2$SiMe$_3$ (0.42g, 4.62 mmol) dissolved in about 5 mL THF was added in drops, during addition the suspension dissolved giving a deep red solution which was stirred at RT for another 3 h. THF was stripped under vacuum to obtain a red oily residue which was triturated with about 10 mL hexane,

stirred for about 3 mins and the solvent stripped in vacuum. This process was re-peated once more to obtain a red solid which was then extracted with about 40mL hexane, centrifuged and supernatant was stripped in vacuum to obtain (0.66g, 1.14 mmol) of $Yb(CH_2SiMe_3)_3(THF)_2$ as a white solid in 74% isolated yield.

^{1}H NMR (400 MHz, C_6D_6, 27°C): δ 170 (s, br 8H, THF), 80 (s, br 8H, THF), -40 (s, 27H, Si*Me₃*), -230 (s, br 6H, Yb-C*H₂*).

Lu(CH₂SiMe₃)₃(THF)₂

Following the same approach as for the synthesis of $Yb(CH_2SiMe_3)_3(THF)_2$, $Lu(CH_2SiMe_3)_3(THF)_2$ was synthesized from $LuCl_3$ (0.50g, 1.78 mmol) and $LiCH_2SiMe_3$ (0.50g, 5.33 mmol) to obtain the title com-pound as a white solid (0.78g, 1.34 mmol) 76% isolated yield.

^{1}H NMR (400 MHz, C_6D_6, 27°C): δ 3.96 (m, 8H, α-H THF), 1.31 (m, 8H, β-H THF), 0.28 (s, 27H, Si*Me₃*), -0.91 (s, 6H, Lu-C*H₂*). ^{13}C NMR (100 MHz, C_6D_6, 27°C): δ 70.9 (s, α-C THF), 41.8 (s, Lu-CH₂), 24.0 (s, β-C THF), 4.8 (s, Si*Me₃*).

Yb(CH₂SiMe₂Ph)₃(THF)₂

Anhydrous $YbCl_3$ (0.42g, 1.50 mmol) was suspended in about 10mL THF and stirred overnight for ca. 15 h. The THF solvent was removed under vacuum and the resulting white solid re-suspended in about 25mL of toluene pre-cooled to ca. -30°C and the suspension was stirred for another 25 mins. at this temperature. $LiCH_2SiMe_2Ph$ (0.71g, 4.50 mmol) dissolved in the same solvent was added in

drops; during addition the suspension dissolved giving a clear, colorless solution and a white oily deposit. The mixture was stirred at this temperature for another 3.5 h while slowly warming to 5°C and another 30mins at RT. Toluene was stripped under vacuum to obtain an oily residue which was triturated with about 10mL hexane, stirred for about 3mins and the solvent stripped in vacuum. This process was repeated once more to obtain a white solid which was then extracted with about 70 mL hexane, centrifuged and supernatant was stripped in vacuum to obtain (0.92g, 1.20 mmol) of $Yb(CH_2SiMe_2Ph)_3(THF)_2$ as a red crystalline solid in 82% isolated yield. The compound was characterized by ^{1}H NMR spectroscopy.

^{1}H NMR (C_6D_6, 27°C): δ 160.8 (s (br), 8H, THF), 79.4 (s, 8H, THF), 3.4 (6H, *m*-H Ph), 0.2 (s, 3H, *p*-H Ph), -23.4 (6H, *o*-H Ph), -32.9 (s, 18H, Si*Me$_2$*Ph), -217.8 (s (br), 6H, Yb-C*H$_2$*).

$Lu(CH_2SiMe_2Ph)_3(THF)_2$

Following the same approach as for the synthesis of $Yb(CH_2SiMe_3)_3(THF)_2$, $Lu(CH_2SiMe_3)_3(THF)_2$ was synthesized from $LuCl_3$ (0.50g, 1.78 mmol) and $LiCH_2SiMe_2Ph$ (0.83, 5.34 mmol) to obtain the title compound as a white crystalline solid (1.16g, 1.12mmol) 85% isolated yield. The compound was characterized by NMR spectroscopy, ^{1}H and [13]C{[1]H}.

^{1}H NMR (400 MHz, C_6D_6, 27°C): δ 7.78 (dd, 6H, $^3J_{HH}$ = 8.0, 1.2 Hz, *o*-H Ph), 7.28 (ddd, 6H, $^3J_{HH}$ = 6.8 Hz, 7.6 Hz, 1.2 Hz, *m*-H Ph), 7.18 (tt, 3H, $^3J_{HH}$ = 8.0 Hz, 1.2 Hz, *p*-H Ph), 3.62 (m, 8H,α-H THF), 1.12 (m, 8H, β-H THF), 0.52 (s,

18H, Si*Me₂*Ph), -0.68 (s, 6H, Lu-C*H₂*). ^{13}C NMR (100 MHz, C₆D₆, 27°C): δ 145.97 (*ipso*-C Ph), 134.40 (*m*-C Ph), 129.92 (*p*-C Ph), 129.12 (*o*-C Ph), 70.86 (s, α-C THF), 39.82 (s, Lu-CH₂), 24.90 (s, β-C THF), 3.27 (s, Si*Me₂*Ph).

(Tp^{tBu,Me})Yb(CH₂SiMe₃)₂ (5a)

At room temperature, a colorless hexane solution of HTp^{tBu,Me} (0.34g, 0.81mmol) was added, slowly to a hexane solution (15 mL) of Yb(CH₂SiMe₃)₃(THF)₂ (0.47g, 0.81mmol). The color of the solution changed from red to purple. The purple solution was stirred for 4 h. The volume of the solution was reduced under vacuum, centrifuged and kept at -40°C to give **5a** (0.53g, 0.69mmol, 85% yield) as a purple solid. Anal. Calcd. for C₃₂H₆₂N₆Si₂BYb (**1d**): C, 49.86; H, 8.11 N, 10.90. Found: C, 49.80; H, 8.06; N, 10.55.

(Tp^{tBu,Me})Lu(CH₂SiMe₃)₂ (6a)

Method 1: A procedure analogous to **5a** using Lu(CH₂SiMe₃)₃(THF)₂ (0.58g, 1.00mmol) and HTp^{tBu,Me} (0.42g, 1.00mmol) and stirring overnight gave **6a** (0.75g, 0.97mmol, 97% yield) as a white solid. Anal. Calcd. for C₃₂H₆₂N₆Si₂BLu (**6a**): C, 55.97; H, 9.10; N, 12.24. Found: C, 55.78; H, 9.08; N, 12.04.

^{1}H NMR (C₆D₆, 27°C): δ 5.65 (s, 3H, 4-H Pz), 4.62 (br, 1H, *H*-B), 2.09 (s, 9H, 5-*Me* Pz), 1.46 (s, 27H, 3-(*CH₃*)₃C Pz), 0.16 (s, 18H, Si*Me₃*), -0.27 (s, 4H, Lu-*CH₂*,). ^{13}C NMR (C₆D₆, 27°C): δ 164.96 (s, 5-C Pz, 146.83 (s, 3-C Pz), 104.06 (s, 4-*C* Pz), 46.15 (s, Lu-*C*H₂), 32.35 (s, 3-(CH₃)₃*C* Pz), 31.64 (s, 3-(*CH₃*)₃C Pz),

13.26 (s, 5-*Me* Pz), 4.23 (s, Si*Me₃*). ^{11}B NMR (C₆D₆, 27°C): δ -8.40.

Method 2: Solid of TlTp^{tBu,Me} (0.27g, 0.43mmol) was added in several portions to a clear THF solution (20mL) of Lu(CH₂SiMe₃)₃(THF)₂ (0.25g, 0.43mmol) at room temperature. Immediately, a black mixture resulted which was stirred for 5 h, centrifuged and all the volatiles removed under vacuum. The residue was extracted with hexane (15 mL). After centrifugation, the colorless supernatant solution was concentrated and kept at -40°C to give **6a** (0.25g, 0.32mmol, 75% yield) as a white solid; characterized by NMR spectroscopy.

(Tp^{tBu,Me})Yb(CH₂SiMe₂Ph)₂ (5b)

At room temperature, to a red-orange solution (10 mL hexane) of Yb(CH₂SiMe₂Ph)₃(THF)₂ (0.18g, 0.23mmol) was added with (Tp^{tBu,Me})H (0.097g, 0.229mmol) in several portions. The mixture turned gradually dark and eventually became dark purple. The resulting dark purple solution was stirred for another 4 h, centrifuged and then concentrated to about 5mL under reduced pressure, and kept at -40°C to give **5b** (0.62g, 0.69mmol, 94% yield) as a purple crystalline solid. Single crystals of **5b** suitable for X-ray analysis were obtained by cooling a dilute hexane solution to -30°C for two days. Anal. Calcd. for C₄₂H₆₆BN₆Si₂Yb (**5b**): C, 56.36; H, 7.43; N, 9.39. Found: C, 56.26; H, 7.56; N, 9.49.

(Tp^{tBu,Me})Lu(CH₂SiMe₂Ph)₂ (6b)

A procedure analogous to **5b** using Lu(CH₂SiMe₃)₃(THF)₂ (0.57g, 0.74 mmol) and HTp^{tBu,Me} (0.32g, 0.32 mmol) gave **6b** (0.62g, 0.69mmol, 94% yield)

as white crystalline solid. Single crystals of **6b** suitable for X-ray analysis were obtained by cooling a dilute hexane solution to -40°C for two days. Anal. Calcd. for $C_{42}H_{66}BN_6Si_2Lu$ (**6b**): C, 56.24; H, 7.42; N, 9.37. Found: C, 56.42; H, 7.46; N, 9.63.

^{1}H NMR (400 MHz, C_6D_6, 27°C): δ 7.82 (d, 4H, $^3J_{HH}$ = 7.2 Hz, *o*-H Ph), 7.34 (t, 4H, $^3J_{HH}$ = 7.2 Hz, *m*-H Ph), 7.22 (t, 2H, $^3J_{HH}$ = 7.2 Hz, *p*-H Ph), 5.62 (s, 3H, 4-H Pz), 4.62 (br, 1H, *H*-B), 2.09 (s, 9H 5-*CH$_3$* Pz), 1.38 (s, 27H, 3-(*CH$_3$*)$_3$C Pz), 0.27 (s, 12H, Si*Me$_2$*Ph), -0.053 (s, 4H, Lu-C*H$_2$*). ^{13}C NMR (100 MHz, C_6D_6, 27°C): δ 165.08 (s, 3-*C* Pz), 147.85 (s, Ph), 146.91 (s, 5-*C* Pz), 133.99 (s, Ph), 127.61 (s, Ph), 104.15 (s, 4-*C* Pz), 43.00 (s, Lu-CH$_2$), 32.28 (s 3-(CH$_3$)$_3$*C* Pz), 31.56 (s, 3-*CH$_3$* Pz), 13.28 (s, 5-*CH$_3$* Pz), 2.16 (s, Si*Me$_2$*Ph). ^{11}B NMR (128 MHz, C_6D_6, 27°C): δ -8.40.

^{1}H NMR (400 MHz, C_7D_8, 27°C): δ 7.74 (d, 4H, $^3J_{HH}$ = 7.2 Hz, *o*-H Ph), 7.28 (t, 4H, $^3J_{HH}$ = 7.2 Hz, *m*-H Ph), 7.19 (t, 2H, $^3J_{HH}$ = 7.2 Hz, *p*-H Ph), 5.61 (s, 3H, 4-H Pz), 4.62 (br, 1H, *H*-B), 2.10 (s, 9H 5-*CH$_3$* Pz), 1.37 (s, 27H, 3-(*CH$_3$*)$_3$C Pz), 0.20 (s, 12H, Si*Me$_2$*Ph), -0.13 (s, 4H, Lu-C*H$_2$*).^{13}C NMR (100 MHz, C_6D_6, 27°C): δ 165.01 (s, 3-*C* Pz), 147.74 (s, Ph), 146.87 (s, 5-*C* Pz), 133.99 (s, Ph), 128.17 (s, Ph), 104.11 (s, 4-*C* Pz), 43.19 (s, Lu-CH$_2$), 32.30 (s 3-(CH$_3$)$_3$*C* Pz), 31.57 (s, 3-*CH$_3$* Pz), 13.29 (s, 5-*CH$_3$* Pz), 2.17 (s, Si*Me$_2$*Ph). ^{11}B NMR (128 MHz, C_6D_6, 27°C): δ -5.07.

^{1}H NMR (400 MHz, C_7D_8, -80°C): δ 8.10 (d, 2H, $^3J_{HH}$ = 7.2 Hz, *o*-H Ph), 7.85 (d, 2H, $^3J_{HH}$ = 7.2 Hz, *o*-H Ph), 7.49 (t, 2H, $^3J_{HH}$ = 7.2 Hz, *m*-H Ph), 7.35 (7.49 (t, 2H, $^3J_{HH}$ = 7.2 Hz, *m*-H Ph), 7.35 (t, 1H, $^3J_{HH}$ = 7.2 Hz, *p*-H Ph), 7.20 (t,

1H, $^3J_{HH}$ = 7.2 Hz, *p*-H Ph), 5.51 (s, 2H, 4-H Pz), 5.35 (s, 1H, 4-H Pz), 4.62 (br, 1H, *H*-B), 2.24 (s, 6H 5-*CH₃* Pz), 1.55 (s, 3H 5-*CH₃* Pz,), 1.55 (s, 9H, 3-(*CH₃*)₃C Pz), 1.32 (s, 18H, 3-(*CH₃*)₃C Pz), 0.92 (s, 6H, Si*Me₂*Ph), 0.30 (s, 2H, Lu-C*H₂*), -0.15 (s, 2H, Lu-C*H₂*), -0.24 (s, 12H, Si*Me₂*Ph).

Attempts to prepare (Tp^{tBu,Me})La(CH₂SiMe₃)₂

At -30°C, a solution of LiCH₂SiMe₃ (0.30g, 3.10 mmol) in 5mL THF was added drop-wise to a suspension of La(CF₃SO₃)₃ (0.65g, 1.10 mmol) in 30 mL THF. The suspension dissolved to give a pale-yellow solution, which was stirred for 3 h, after which Tl(Tp^{tBu,Me}) (0.58g, 0.94 mmol) was added in several portions. Almost immediately, a dark solid started to precipitate and after ca. 30 minutes gathered to give a shiny Tl shot and an almost clear solution. The mixture was stirred for 3 h at this temperature, and another 1 h at room temperature, centri-fuged and all the volatiles were removed under vacuum. The resultant oily residue was triturated with pentane (3x10 mL) giving a sticky solid. Pentane was subse-quently removed under vacuum and the residue was again extracted with large volume of pentane (3x40 mL). The volume of pentane was reduced to 4 mL, cooled to -40°C to obtain 0.473g of a white solid which proved to be Li(Tp^{tBu,Me}) by multinuclear NMR.

^{1}H NMR (400 MHz, C₆D₆, 27°C): δ 5.70 (s, 3H, 4-*H*-Pz), 4.99 (s, 1H, B-*H*), 2.31 (s, 9H, 5-C*H₃* Pz), 1.29 (s, 27H, 3-(C*H₃*)₃C Pz). ^{13}C{^{1}H} NMR (100 MHz, C₆D₆, 27°C): δ 160.22 (s, 3-*C* Pz), 143.72 (s, 5-*C* Pz), 101.00 (s, 4-C Pz),

31.93 (s, $(CH_3)_3C$), 30.96 (s, $(CH_3)_3C$ Pz), 12.75 (s, 5-CH_3 Pz,. ^{11}B {^1H} NMR (C_6D_6, 27°C): δ -8.63 (s). ^7Li{^1H} NMR (155.4 MHz, C_6D_6, 27°C) δ 3.23.

Similar results were obtained with LaI_3, $LaBr_3$ or $LaCl_3$

$(Tp^{Me2})Yb(CH_2SiMe_3)_2(THF)$ (7a)

Method 1: Solid of $TlTp^{Me2}$ (0.35g 0.69 mmol) was added in several portions to a clear THF solution (20mL) of $Yb(CH_2SiMe_3)_3(THF)_2$ (0.40g, 0.69 mmol) at room temperature. Almost immediately, a dark solid started to precipitate and after ca. 30 mins gathered to give a shiny Tl shot (ca. 70% collected) and an almost clear-red solution. The mixture was stirred for 4 h, centrifuged and all the volatiles were removed under vacuum. The residue was extracted with toluene (5 mL), centrifuged to obtain a bright red supernatant and a small amount of a mixture of black Tl and purple $(Tp^{Me2})_2Yb$ residue. The supernatant was concentrated to 2 mL, and layered with 3 mL hexane. Cooling the solution to -40°C gave **7a** (0.40g, 0.56 mmol, 80% yield) as an orange-red crystalline solid. Single crystals of **7a** suitable for X-ray analysis were grown by slow diffusion of hexane to a concentrated toluene solution at -40°C.

Method 2: A colorless toluene (3 mL) of HTp^{Me2} (0.20g, 0.67 mmol) was added drop-wise to a toluene solution (10mL) of $Yb(CH_2SiMe_3)_3(THF)_2$ (0.39g, 0.67 mmol) at room temperature. The resulting orange-red mixture was stirred for 4 h at RT. The volume was reduced under vacuum, centrifuged to obtain a bright red supernatant and a small amount of purple $(Tp^{Me2})_2Yb$ residue. The supernatant was concentrated to about 2 mL, layered with pentane, and kept at -40°C to give

(0.34g, 0.47 mmol) of **7a** as an orange-red crystalline solid in 71% isolated yield. Anal. Calc. for $C_{27}H_{52}BN_6OSi_2Yb$ (**7a**): C, 45.24; H, 7.31; N, 11.72. Found: C, 45.29; H, 7.29; N, 11.56.

^{1}H NMR (500 MHz, C_6D_6, 27°C) δ 164.5 (br, 4H, THF), 131.99 (br, 4H, THF), 80.3 (6H, 3-*Me* Pz), 24.9 (s, 3H, 5-*Me* Pz), -15.9 (br, 1H, 4-*H* Pz), -17.0 (br, 6H, 5-*Me* Pz), -22.4 (br, 3H, 3-*Me* Pz), -25.1 (18H, Si*Me₃*), -29.0 (br, 2H, 4-*H*-Pz), −191.5 (br, 2H, Yb-C*H₂*), −278.2 (br, 2H, Yb-C*H₂*); the B-H signal could not be located. ^{13}C NMR (125 MHz, C_6D_6, 27°C) δ 148.0 (v. br), 92.5, 45.1, 41.2, 14.2, -27.4, -32.0. ^{11}B (160 MHz, C_6D_6, 27°C) δ -60.4.

(Tp^{Me2})Lu(CH$_2$SiMe$_3$)$_2$(THF) (8a)

Method 1: A procedure analogous to **7a** using Lu(CH$_2$SiMe$_3$)$_3$(THF)$_2$ (0.50g, 0.86 mmol) and TlTp^{Me2} (0.43g, 0.86 mmol) gave **8a** as a white crystalline solid (0.52g, 0.73 mmol, 85% yield). Single crystals of **8a** suitable for X-ray analysis were grown from toluene/pentane by cooling to -30°C overnight. Anal. Calcd. for $C_{27}H_{52}BN_6OSi_2Lu$ (**8a**): C, 45.12; H, 7.29; N, 11.69. Found: C, 45.28; H, 7.41; N, 11.57.

^{1}H NMR (400 MHz, C_6D_6, 27°C): δ 5.59 (br, 3H, 4-*H* Pz), 4.85 (br, 1H, *H*-B), 3.69 (br, 4H, THF), 2.26, 2.74 (br, 6H+3H, 3-*Me* Pz), 2.11 (s, 9H, 5-*Me* Pz), 1.18 (br, 4H, THF), 0.26 (s, 18H, Si*Me₃*), -0.39 (br, 4H, Lu-C*H₂*). ^{13}C NMR (100MHz, C_6D_6, 27°C): δ 150.20 (s, 3-*C* Pz), 144.96 (s, 5-*C* Pz), 106.21 (s, 4-*C* Pz), 71.07 (s, THF), 35.89 (s, Lu-C*H₂*), 25.20 (s, THF), 13.50 (br, 3-*Me* Pz), 12.97 (s, 5-*Me* Pz), 5.02 (s, Si*Me₃*). ^{11}B NMR (128 MHz, C_6D_6, 27°C): δ -9.05. ^{1}H NMR

(400MHz, THF-d_8, 27°C): δ 5.76 (s, 3H, 4-H Pz), 4.85 (br, 1H, H-B), 3.61 (m, 4H, THF), 2.41 (br, 9H, 3-Me Pz), 2.38 (s, 9H, 5-Me Pz), 1.78 (m, 4H, THF), –0.29 (s, 18H, SiMe_3), –0.77 (s, 4H, Lu-CH_2). ^{13}C NMR (100.54 MHz, THF-d_8, 27°C): δ 150.48 (s, 3-C Pz), 145.71 (s, 5-C Pz), 106.47 (s, 4-C Pz), 68.20 (s, THF), 35.42 (s, Lu-CH_2), 26.36 (s, THF), 15.17 (s, 3-Me Pz), 13.05 (s, 5-Me Pz), 4.79 (s, SiMe_3). ^{11}B NMR (128 MHz, THF-d_8, 27°C): δ

-9.10.

^{1}H NMR (400 MHz, C$_7$D$_8$, 27°C): δ 5.58 (br, 3H, 4-H Pz), 4.85 (br, 1H, H-B), 3.72 (m, 4H, THF), 2.65, (br, 3H, 3-Me Pz), 2.27 (br, 6H, 3-Me Pz), 2.12 (s, 9H, 5-Me Pz), 1.29 (m, 4H, THF), 0.18 (s, 18H, SiMe_3), -0.44 (br, 4H, Lu-CH_2). ^{13}C NMR (100 MHz, C$_7$D$_8$, 27°C): δ 149.72 (br, 3-C Pz), 144.87 (s, 5-C Pz), 106.23 (s, 4-C Pz), 71.07 (s, THF), 35.97 (s, Lu-CH_2), 25.30 (s, THF), 14.76 (br, 3-Me Pz), 12.96 (s, 5-Me Pz), 5.01 (s, SiMe_3).

^{1}H NMR (400 MHz, C$_7$D$_8$, -80°C): δ 5.64 (br, 2H, 4-H Pz), 5.48 (br, 1H, 4-H Pz), 4.85 (br, 1H, H-B), 3.60 (v. br, 4H, THF), 2.80 (s, 3H, 3-Me Pz), 2.26 (s, 6H, 3-Me Pz), 2.10 (s, 6H, 5-Me Pz), 2.07 (s, 3H, 5-Me Pz), 0.97 (br, 4H, THF), 0.41 (s, 18H, SiMe_3), -0.21 (d, $^2J_{HH}$ = 11.6 Hz, 2H, Lu-CH_2), -0.37 (d, $^2J_{HH}$ = 11.6 Hz, 2H, Lu-CH_2).

Method 2: A procedure analogous to **7a** using Lu(CH$_2$SiMe$_3$)$_3$(THF)$_2$ (0.50g, 0.86 mmol) and HTp^{Me2} (0.256g, 0.86 mmol) gave **8a** as a white crystalline solid (0.45g, 0.63 mmol, 73% yield); characterized by NMR spectroscopy.

(Tp^{Me2})Yb(CH$_2$SiMe$_2$Ph)$_2$(THF) (7b)

A procedure analogous to that for **7a** using $Yb(CH_2SiMe_2Ph)_3(THF)_2$ (0.85g, 1.11 mmol) and $Tl(Tp^{Me2})$ (0.56g, 1.11 mmol) gave **7b** (0.80g, 0.89 mmol, 85% yield) as an orange-red crystalline solid. A small amount of an insoluble purple solid, presumably $(Tp^{Me2})_2Yb$, was obtained during work up. Single crystals of **7b**·C_7H_8 suitable for X-ray analysis were grown from toluene/pentane by cooling to -30°C for 2 days. Anal. Calcd. for $C_{44}H_{64}BN_6OSi_2Yb$ (**7b**·C_7H_8): C, 56.64 ; H, 6.91 ; N, 9.01 . Found: C, 56.45; H, 6.90; N, 9.28.

^1H NMR (500 MHz, C_6D_6, 27°C): δ 160.2 (br, 4H, THF), 124.7 (br, 4H, THF), 77.6 (br, 6H, 3-*CH₃* Pz), 25.5 (br, 3H, 5-*CH₃* Pz), 4.1 (s, 2H, *p*-Ph), 1.85 (s, 4H, *m*-Ph), -13.5 (br s, 1H, 4-H Pz), -16.2 (br, 6H, 5-*CH₃* Pz), -16.8 (s, 4H, *o*-Ph), -20.8 (s, 6H, Si*Me₂*Ph), -21.5 (br, 3H, 3-*CH₃* Pz), -27.1 (s, 6H, Si*Me₂*Ph), -28.5 (br s, 2H, 4-H-Pz), −181.7 (2H, br. s, Yb-C*H₂*), -272.7 (2H, br. s, Yb-C*H₂*). $^{13}C\{^1H\}$ NMR (125 MHz, C_6D_6, 27°C): δ 144.2, (v. br), 121.6, 118.9, 117.3, (s, sharp), 112.9, 111.7, 95.1, 46.5, 38.7, -12.4 & -13.3, (br), -26.3, -32.0. ^{11}B NMR (160 MHz, C_6D_6, 27°C) δ -54.0.

$(Tp^{Me2})Lu(CH_2SiMe_2Ph)_2(THF)$ (8b)

A procedure analogous to **7b** using $Lu(CH_2SiMe_2Ph)_3(THF)_2$ (0.50g, 0.65 mmol) and $Tl(Tp^{Me2})$ (0.33g, 0.65 mmol) gave **8b** (0.40g, 0.48 mmol, 73% yield) as a white crystalline solid. Single crystals of **8b**·C_7H_8 suitable for X-ray analysis were obtained from toluene/pentane by cooling to -30°C. Anal. Calcd. for $C_{44}H_{64}BN_6OSi_2Lu$ (**8b**·C_7H_8): C, 56.52; H, 6.90; N, 8.99. Found: C, 55.96; H, 6.96; N, 8.80.

^{1}H NMR (400 MHz, C$_6$D$_6$, 27°C): δ 7.86 (d, 4H, ^{3}J$_{HH}$ = 8 Hz, o-H Ph), 7.31 (t, 4H, ^{3}J$_{HH}$ = 7.2 Hz, m-H Ph), 7.23 (t, 2H, ^{3}J$_{HH}$ = 7.2 Hz, p-H Ph), 5.57 (br, 3H, 4-H Pz), 4.65 (br. 1H, H-B), 3.56 (m, 4H, THF), 2.48 (br, 3H, 3-CH_3 Pz), 2.13 (s, (9H, 5-CH_3Pz) + (6H, 3-CH_3 Pz), 1.22 (m, 4H, THF), 0.37, 0.42 (br, 12H, SiMe_2Ph), -0.24, 0.09 (br, 4H, Lu-CH_2). ^{13}C{^{1}H} NMR (100 MHz, C$_6$D$_6$, 27°C): δ 149.86 (s, $ipso$-C Ph), 148.40 (s, 3-C Pz), 145.00 (s, 5-C Pz), 127.53, 134.14 (s, Ph-C), 106.29 (s, 4-C Pz), 71.02 (s, THF), 32.70 (s, Lu-CH_2), 25.16 (s, THF), 14.69 (s, 3-CH_3 Pz), 12.95 (s, 5-CH_3 Pz), 3.27 (s, SiMe_2Ph). ^{11}B NMR (128 MHz, C$_6$D$_6$, 27°C): δ -8.65.

Attempts to prepare (Tp^{Me2})La(CH$_2$SiMe$_3$)$_2$(THF)

At -30°C, a solution of LiCH$_2$SiMe$_3$ (0.24g, 2.55 mmol) in 5 mL THF was added drop-wise to a suspension of La(CF$_3$SO$_3$)$_3$ (0.52g, 0.89 mmol) in 30 mL THF. The suspension dissolved to give a pale-yellow solution, which was stirred for 3h, after which TlTp^{Me2} (0.42g, 0.84 mmol) was added in several portions. Almost immediately, a dark solid started to precipitate and after ca. 30 mins. gathered to give a shiny Tl shot and an almost clear solution. The mixture was stirred for 3 h at this temperature, and another 1 h at room temperature, centrifuged and all the volatiles were removed under vacuum. The resultant oily residue was triturated with pentane (3x10 mL) giving a sticky solid. Pentane was subsequently removed under vacuum and the residue was again extracted with large volume of pentane (3x40 mL). All volatiles were removed from the resulting pale-yellow extract and the pale-yellow solid residue was then extracted with 10 mL toluene.

The volume of toluene was reduced to 4 mL, and the blue solution layered with 8 mL hexane. Cooling the solution to

-40°C gave (0.45g) of a pale-yellow solid which proved to be a mixture of Li(Tp^{Me2}) (> 90% by ^{1}H and ^{7}Li{^{1}H} NMR spectroscopy) and other unidentified species.

^{1}H NMR (400 MHz, C$_6$D$_6$, 27°C): δ 5.75 (s, 3H, 4-*H* Pz), 2.32 (s, 9H, 3-C*H*$_3$ Pz), 1.73 (s, 9H, 5-C*H*$_3$ Pz), ^{7}Li{^{1}H} NMR (155.4 MHz, C$_6$D$_6$, 27°C) δ 3.19.

Similar results were obtained with LaI$_3$, LaBr$_3$ or LaCl$_3$

(Tp)Yb(CH$_2$SiMe$_3$)$_2$(THF) (9)

Following a procedure analogous to that for **7a** using Yb(CH$_2$SiMe$_3$)$_3$(THF)$_2$ (0.50g, 0.86 mmol) and TlTp (0.36g, 0.86 mmol), at room temperature and crystallization from pentane gave **9** (0.34g, 0.54 mmol, 63% yield) as a deep red crystalline solid. Anal. Calcd. for C$_{21}$H$_{40}$N$_6$BSi$_2$OYb (**9**): C, 39.87; H, 6.37; N, 13.28. Found: C, 39.93; H, 6.37; N, 12.98.

Crystals suitable for X-ray diffraction studies were obtained from a dilute diethyl ether/HMDSO solution, the crystals obtained were however proved to be the dimeric complex [(TpYbCH$_2$SiMe$_3$)$_2${μ-OCH$_2$SiMe$_3$)$_2$], (**10**).

[(Tp^{Me2})YbH$_2$]$_4$ (11)

A sample of (Tp^{Me2})Yb(CH$_2$SiMe$_3$)$_2$(THF) (0.55g, 0.77 mmol) obtained directly from the reaction, without recrystallization was dissolved in Et$_2$O (20 mL) was charged into a glass lined medium-pressure autoclave. The autoclave was

pressurized with H_2 to 1100 psi for 48 h. After releasing the pressure, the solution was centrifuged to obtain a pale pink solution and a mixture of black thallium precipitate and a purple solid, presumably $(Tp^{Me2})_2Yb$. Solvent was stripped under vacuum to obtain a pale pink solid which was extracted with hexane and centrifuged and solvent stripped under reduced pressure to obtain a pale pink solid. *In solution, the solid gradually underwent redox disproportionation to give the purple $[Tp^{Me2}Yb]_2$, and other unidentified species.* X-ray quality crystals were grown from concentrated THF solution at RT as $[Tp^{Me2}YbH_2]_4 \cdot 3.5THF$. (*A crystal was carefully selected from a mixture of $[Tp^{Me2}Yb]_2$ and other unidentified species.*)

$[(Tp^{Me2})LuH_2]_4$ (12)

$(Tp^{Me2})Lu(CH_2SiMe_3)_2(THF)$ (crude) (0.49g, 0.68 mmol) in Et_2O (20 mL) was charged into a glass lined medium-pressure autoclave. The autoclave was pressurized with H_2 to 1200 psi for 69 h. After pressure release, the solution was centrifuged and the solvent was stripped under vacuum to obtain a white solid. The solid was extracted with Et_2O (10 mL), centrifuged and concentrated to ca. 4 mL and then ~5 drops of toluene were added and the solution kept at −30°C overnight to obtain **12**·$3C_7H_8$ as colorless crystals (0.18g, 0.083 mmol, 43% yield). Single crystals of **12**·4.75THF, suitable for X-ray analysis were grown from concentrated THF solution at room temperature. Anal. Calc. for $C_{81}H_{120}N_{24}B_4Lu_4$ (**12**·$3C_7H_8$): C, 44.77; H, 5.57; N, 15.47. Found: C, 44.42; H, 5.72; N, 14.98.

^1H NMR (400 MHz, C_6D_6, 27°C) δ 12.19 (s, 2H, Lu-H), 5.57 (s, 3H, 4-*H* Pz), 4.80 (br, 1H, *H*-B), 2.37 (s, 9H, 3-*Me* Pz), 2.14 (s, 9H, 5-*Me* Pz). ^{13}C NMR

(100 MHz, C_6D_6, 27°C): δ 152.20 (s, 3-*C* Pz), 144.95 (s, 5-*C* Pz), 106.49 (s, 4-*C* Pz), 16.91 (s, 3-*Me* Pz), 13.23 (s, 5-*Me* Pz). ^{11}B NMR (128 MHz, C_6D_6, 27°C): δ -8.21.

[(Tp)YbH$_2$]$_6$ (13)

Method 1: A bright-red Et$_2$O (20 mL) solution of 0.150g, 0.240 mmol of crude (Tp)Yb(CH$_2$SiMe$_3$)$_2$(THF) was treated with excess phenylsilane. Upon addition, the solution gradually turns pale with deposition of black thallium precipitate. The mixture was allowed to stir overnight and centrifuged to obtain black precipitate (Tl) and a pale pink solution. Solvent was stripped from the solution under reduced pressure to obtain a pale pinkish-yellow oily residue. Rigorous trituration of the oily residue with hexane affords 0.090g; 0.231 mmol of **13** as a pinkish yellow solid in 96% isolated yield for the crude product. Recrystallization from concentrated Et$_2$O solution affords the compound as pale pink block crystals in lower yield, ca. 50%.

Method 2: (Tp)Yb(CH$_2$SiMe$_3$)$_2$(THF) (crude) (0.309g, 0.488 mmol) in toluene (10mL) was charged into a glass lined medium-pressure autoclave at room temperature. The autoclave was pressurized with H$_2$ to 1000 psi for 48h. Work-up analogous to above gave **13** (0.35g, 0.902 mmol, 54% yield) as pink block crystals. Single crystals of **13**·3Et$_2$O suitable for X-ray analysis were grown from a concentrated Et$_2$O solution at -40°C. Anal. Calc. for C$_{54}$H$_{72}$N$_{36}$B$_6$Yb$_6$·5 C$_7$H$_8$ C, 38.33; H, 4.05; N, 18.08. Found C, 39.40; H, 4.27; N, 18.84. This was the best of several elemental analysis attempts.

135

3.7.4 X-Ray Crystallographic Studies

Crystals for X-ray analysis were obtained as described in the preparations. The crystals were manipulated in the glove box, coated with Paratone-N oil, transferred to a cold gas stream on the diffractometer. Complete X-ray structure determination for the compounds (except **7a**) were carried out by Dr R. McDonald and Dr. M. J. Ferguson at the X–ray Crystallographic Laboratory, Department of Chemistry University of Alberta. Data for **7a** was collected by Mr. David O. Miller at the Department of Chemistry, Memorial University of Newfoundland. The data refinement and structural solution of **7a** was carried out by Dr. R. McDonald. Data collections were performed at -80°C on a Bruker PLATFORM/SMART 1000 CCD diffractometer, using graphite monochromated Mo Kα radiation ($\lambda = 0.71069$Å). The determination of crystal class and unit cell was carried out by SMART program package.[55] The raw frame data were processed using SAINT[56] and SADABS[57] to yield the reflection data file. The structures were solved by using SHELXS-86 program.[58] Refinements were performed on F^2 anisotropically for all the non-hydrogen atoms by the full-matrix least-squares method using SHELXL-93 program.[59] The SQUEEZE[60] routine of the program PLATON[61] was implemented to remove the contributions of the disordered solvents (toluene in **7b** and **8b;** and Et$_2$O in **10** and **13**, and THF in **11 and 12**) to the observed structure factors. The hydrides in **11, 12** and **13** were located by difference Fourier syntheses and their coordinates and isotropic parameters were refined. Other hydrogen atoms were placed at the calculated positions and were included in the structure calculation without further refinement of the pa-

rameters.

For summary of data collection and structure refinement see the structure reports; **6a** (TAK 0722); **6b** (TAK 0517); **7a** (TAK 0606); **7b** (TAK 0726); **8a** (TAK 0514); **8b** (TAK 0513); **10** (TAK 0704); **11** (TAK 0732); **12** (TAK 0717); **13** (TAK 0720).

3.8 References

1. Edelmann, F. T. In *Comprehensive Organometallic Chemistry* III; Crabtree, R. H.; Mingos, D. M. P., Eds.; Elsevier, Oxford, *Vol. 401*, **2006**, pp. 1–199.

2. Gromada, J.; Carpentier, J-F.; Mortreux, A. *Coord. Chem. Rev*. **2004**, *248*, 397–410.

3. Lyubov, D. M.; Fukin, G. K.; Trifonov, A. A. *Inorg. Chem*. **2007**, *46*, 11450–11456 and references therein.

4. Zeitmentz, P. M.; Ardnt, S.; Elvidge, B. R.; Okuda, J. *Chem. Rev*. **2006**, *106*, 2404–2433 and references therein.

5. Piers, W. E.; Emslie, D. J. A. *Coord. Chem. Rev.* **2002**, *233*, 131–155.

6. Luo, Y. J.; Nishiura, M.; Hou, Z. *J. Organomet. Chem*. **2007**, *692*, 536–544.

7. Cui, D. M.; Nishiura, M. Hou, Z. *Macromolecules* **2005**, *38*, 4089–4095.

8. Bambirra, S.; Bouwkamp, M. W.; Meetsma, A.; Hessen, B. *J. Am. Chem. Soc.* **2004**, *126*, 9182–9183.

9. Long, D. P.; Bianconi, P. A. *J. Am. Chem. Soc.* **1996**, *118*, 12453–12454.

10. Blackwell, J,; Lehr, C.; Sun, Y. M.; Piers, W. E.; Pearce-Batchilder, S. D.; Zaworotko, M. J.; Young, V. G. *Can. J. Chem.* **1997**, *75*, 702–711.

11. (a) Trofimenko, S. Scorpionates: The coordination Chemistry of Poly-pyrazolylbortae Ligands, Imperial College Press, London, 1999. (b) Pettinari, C. Scorpionates II: Chelating Borane Ligands Imperial College Press, London, 2008. (c) Parkin, G. *Adv. Inorg. Chem*. **1995**, *42,* 291–393. (d) Kitajima, N.; Tolmann, W. B. *Prog. Inorg. Chem.* **1995**, *34*, 419–531.

12. (a) Carvalho, A.; Domingos, A.; Gaspar, P.; Marques, N.; Pires de Matos,

A.; Santos, I. *Polyhedron* **1992**, *11*, 1481–1488. (b) Santos, I.; Marques, N.; *New J. Chem*. **1995,** *19*, 551–571. (b) Marques, N.; Sella, A.; Takats, J. *Chem. Rev*. **2002**, *102*, 2137–2160.

13. Han, R.; Parkin, G. *Organometallics* **1991**, *10*, 1010–1029.

14. Looney, A.; Parkin, G. *Polyhedron* **1990**, *9*, 265–276.

15. Lee, H.; Jordan, R. F. *J. Am. Chem. Soc*. **2005**, 127, 9384–9385.

16. Lee, H.; Nienkemper, K.; Jordan. R. F. *Organometallics* **2008**, 27, 5075–5081.

17. Parkin, G. Personal Communications.

18. (a) Pople, J. A. *Mol. Phys.*, **1958**, *1*, 168–174. (b) Muetterties, E. L.; Phillips, W. D. *J. Am. Chem. Soc*. **1959**, *81,* 1084–1088. (c) Roberts, J. D.; *J. Am. Chem. Soc*. **1956**, *78*, 4495–4496.

19. López, C.; Claramunt, R. M; Foces-Foces, C.; Cano, F. H.; Elguero, J. *Rev. Roum. Chim*. **1994**, *39*, 795–805.

20. Bradley, D. C.; Hursthouse, M. B.; Newton, J.; Walker, N. P. C. *J. Chem. Soc., Chem. Commun*. **1984**, 188–190.

21. Kisko, J. L.; Hascall, T.; Kimblin, C.; Parkin, G. *J. Chem. Soc. Dalton Trans*. **1999**, 1929–1935.

22. (a) Trofimenko, S.; *J. Am. Chem. Soc*. **1967***, 89*, 3170–3177. (b) Kresinski, R. A.; *J. Chem. Soc., Dalton Trans*. 1999, 401–406.

23. Lappert, M. F.; Pearce, R. J. *J. Chem. Soc. Chem. Commun*. **1973**, 126.

24. Bruno, J. W.; Smith, G. M.; Marks, T. J.; Fair, C. K.; Shultz, A. J.; Williams, J. M. *J. Am. Chem. Soc*. **1986**, *108*, 40–56.

25. Emslie, D. J. H.; Piers, W. E.; Parvez, M.; McDonald, R. *Organometallics* **2002**, 21, 4226-4240. (b) Emslie, D. J. H.; Piers, W. E.; MacDonald, R. *J. Chem. Soc.*, *Dalton Trans*. **2002**, 293–294.

26. (a) Maunder G. H.; Sella, A; Tocher, D. A. *J. Chem. Soc. Chem. Commun.* **1994**, 885–886. (b) Takats J.; Zhang, X. W.; Day, V. W.; Eberspacher, T. A. *Organometallics* **1993**, *12*, 4286–4288. (c) Hillier, A.C.; Zhang, X. W.; Maunder, G. H.; Liu, S. Y.; Eberspacher, T. A.; Metz, V. M.; McDonald, R.; Domingos, A.; Marques, N.; Day, V. W.; Sella, A.; Takats, J. *Inorg. Chem*. **2001,** *40*, 5110–5116.

27. (a) Lee, A. G. Q. Rev., Chem. Soc. 1970, 24, 310–329. (b) Schwerdtfeger, P.; Boyd, P. D. W.; Bowmaker, G. A.; Mack, H. G.; Oberhammer, H. *J. Am. Chem. Soc*. **1989**, *111*, 15–23.

28. Gilman, H.; Jones, T. G. *J. Am. Chem. Soc*. **1946**, *68*, 517–520.

29. McKillop, A.; Elsom, L. F.; Taylor, E. C. *J. Am. Chem. Soc* **1968**, *90*, 2423–2424.

30. Cheng, J.; Saliu, K.; Kiel, G. Y.; Ferguson, M. J.; McDonald, R.; Takats, J. *Angew. Chem.Int. Ed.* **2008**, *47*, 4910–4913.

31. Trofmenko, S.; Calabrese, J. C.; Kochi, J. K.; Wolowiec, S.; Hulsbergen, F. B.; Reedijk, J. *Inorg. Chem*. **1992**, *31*, 3943–3950.

32. Shannon, R. D. Acta. *Crystallogr. Sect. A* **1976**, *A32*, 751–767.

33. Schumann, H.; Freckmann, D. M. M.; Dechert, S. *Z. Anorg. Allg. Chem*. **2002**, *628*, 2422–2426.

34. Niemeyer, M. *Z. Anorg. Allg. Chem*. **2000**, *626*, 1027–1029.

35. Long, D. P.; Chandrasekaran, A. ; Day, R.O.; Bianconi, P. A.; Rheingold, A. L.; *Inorg. Chem.* **2000**, 39, 4476–4487.

36. Long, D. P. Lanthanide Alkyl and Hydride Complexes Containing the Tris(pyrazolyl)borohydride Ligand and their Activity as Polymerization Catalysts. Ph.D Thesis, University of Massachusetts Amherst, September, 1998.

37. Liu, X.; Cui, D. *Dalton Trans*. **2008**, 3747–3752.

38. Rabe, W. G.; Zhang-Presse, M.; Riederer, F.A.; Rheingold, A. L. *Acta Crystallogr*. **2006**, *E62*, m1349–m1351.

39. Selected reviews on rare earth metal hydride complexes: (a) Okuda, J. *Dalton Trans.* **2003**, 2367–2378. (b) Arndt, S.; Okuda, J. *Chem. Rev.* **2002**, *102*, 1953–1976. (c) Molander, G. A.; Romero, J. A. C. *Chem. Rev.* **2002**, *102*, 2161–2186. (d) Hou, Z.; Wakatsuki, Y. *Coord. Chem. Rev.* **2002**, *231*, 1–22. (e) Hou, Z.; Wakatsuki, Y. in *Science of Synthesis*; T. Imamoto, R. Noyori, Eds.; Thieme, Stuttgart, **2002**, vol. 2, p. 849–942. (f) Hoskin, A. J.; Stephan, D. W. *Coord. Chem. Rev.* **2002**, *233–234*, 107–129. (g) Ephritikhine, M. *Chem. Rev.* **1997**, *97*, 2193–2242. (h) Schumann, H.; Meese-Marktscheffel, J. A.; Esser, L. *Chem. Rev.* **1995**, *95*, 865–986. (i) Schaverien, C. J. *Adv. Organomet. Chem.* **1994**, *36*, 283–362.

40. Evans, W. J.; Meadows, J. H.; Wayda, A. L.; Hunter, W. E. ; Atwood, J. L. *J. Am. Chem. Soc.* **1982**, *104*, 2008–2014.

41. (a) Tardif, O.; Nishiura, M.; Hou, Z. *Organometallics* **2003**, *22*, 1171–1173. (b) Hou, Z.; Nishiura, M.; Shima, T. *Eur. J. Inorg. Chem.* **2007**,

2535–2545.

42. [{(C$_5$Me$_4$SiMe$_2$R)YH$_2$}$_4$(THF)$_2$] (R = Me, Ph) have also been synthe-
sized: Hultzsch, K. C.; Voth, P.; Spaniol, T. P.; Okuda, J. *Z. Anorg. Allg. Chem.* **2003**, *629*, 1272–1276.

43. (a) Duchateau,R.; van Wee, C. T.; Meetsma,A.; Teuben, J. H. *J. Am. Chem. Soc.* **1993**, 115, 4931–4932. (b) Hagadorn, J. R.; Arnold, J. *Organometallics* **1996**, 15, 984–991.

44. (a) Trifonov, A. A.; Fedorova, E. A.; Fukin, G. K.; Bochkarev, M. N. *Eur. J. Inorg. Chem.* **2004**, 4396–4401. (b) Trifonov, A. A.; Skvortsov, G. G.; Lyubov, D. M.; Skorodumova, N. A.; Fukin, G. K.; Baranov, E. V.; Glushakova, V. N. *Chem. Eur. J.* **2006**, *12*, 5320–5327.

45. Gountchev, T. I.; Tilley, T. D. *Organometallics* **1999**, 18, 2896-2905

46. Konkol, M.; Spaniol, T. P.; Kondracka, M.; Okuda, J. *Dalton Trans.* **2007**, 4095–4102.

47. Lyubov, D. M.; Fukin, G. K.; Cherkasov, A. V.; Shavyrin, A. S.; Trifonov, A. A.; Luconi, L.; Bianchini, C.; Meli, A. Giambastiani, G. *Organometallics* **2009**, 28, 1227–1232.

48. Konkol, M.; Okuda, J. *Coord. Chem. Rev.* **2008**, *252*, 1577–1591.

49. Ohashi, M.; Konkol, M.; Rosal, I. D.; Poteau, R.; Maron L.; Okuda, J. *J. Am. Chem. Soc.* **2008**, 130, 6920–6921.

50. Lyubov, D. M.; Döring, C.; Fukin, G. K.; Cherkasov, A. V.; Shavyrin, A. S.; Kempe, R.; Trifonov, A. A. *Organometallics* **2008**, 27, 2905–2907.

51. Cheng, J.; Takats, J. Unpublished Results.

52. Luo,Y.; Baldamus, J.; Tardif, O.; Hou, Z. *Organometallics* **2005**, 24, 4362–4366.

53. Arndt, S.; Voth, P.; Spaniol, T. P.; Okuda, J. *Organometallics* **2000**, *19*, 4690–4700.

54. Piers, W. E.; Kenward, A.; Personal Communication.

55. SMART Software Users Guide, Version 4.21; Bruker AXS, Inc.: Madison, WI, 1997.

56. SAINT, Version 6.02; Bruker AXS, Inc.: Madison, WI 1999.

57. Sheldrick, G. M. SADABS; Bruker AXS, Inc.: Madison, WI 1998.

58. Sheldrick, G. M. *Acta Crystallogr.* **1990**, *A46*, 467-473

59. Sheldrick, G. M. Shelxl-93. Program for crystal structure determination. University of Göttingen, Germany, 1993.

60. Sluis, P. van der; Spek, A. L. *Acta Crystallogr*. **1990**, A46, 194-201.

61. Spek, A. L. *Acta Crystallogr*. **1990**, *A46*, C-34.

Chapter 4

Synthesis, Characterization and Structural Variation of

Lanthanide Bis-Alkynide Complexes

4.1   Introduction

Organolanthanide alkynide complexes are attractive both due to their structural aspects and further reactions. Structurally, they can adopt a variety of bonding modes ranging from terminal (a) to uncoupled asymmetric alkynide bridged dimers (b) to coupled butatrienediyl bridged dimers (c), Scheme 4.1. The particular bonding mode adopted is a subtle interplay of steric crowding around the lanthanide center as well as the steric and electronic properties of the alkynide substituents. In terms of further reactions, they are the precursors for the atom economic[1] dimerization of terminal alkynes to enynes.[2,3,4]

(a)	(b)	(c)
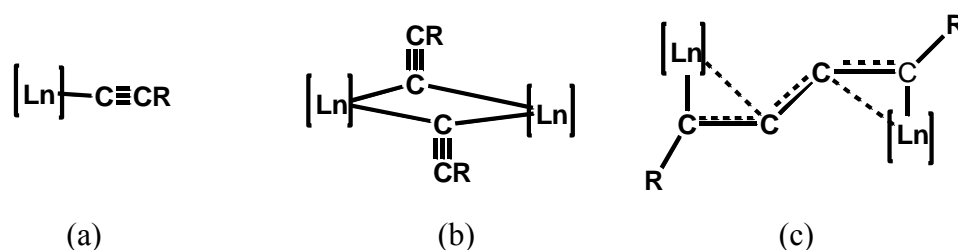
Scheme 4.1: Bonding Modes of Alkynide Ligands.

Organolanthanide alkynide complexes have been known and studied for a long time,[5] well-known examples are however limited to those based on lanthanocene systems, $[(C_5R_5)_2Ln(alkynide)]_n$. For most ancillary ligand systems, the compounds mostly adopt either the asymmetric bridging structure (type b), as found in $[(C_5H_4Me)_2Sm(\mu\text{-}C\equiv C^tBu)]_2,$[6]

[(C₅H₅)₂Er(μ-C≡C'Bu)]₂,[7] [(C₅H₄'Bu)₂Sm(μ-C≡CPh)]₂,[8] [(DAC)Y(μ-C≡CPh)]₂, (DAC = diaza-18-crown-6),[9] [(PCP*)YC≡C(SiMe₃)₂(μ-C≡C(SiMe₃)₂], (PCP* = phenanthrene-fused cyclopentadienyl),[10] [{PhC(NSiMe₃)₂}₂Y(μ-C≡CH)]₂,[11] [(C₅H₄'Bu)₂Ln(μ-C≡CPh)]₂ (Ln = Nd, Gd)[12] or the coupled butatrienediyl bridged dimeric structure (type c), as found in [(C₅Me₅)₂Sm]₂(μ-η²:η²-PhC₄Ph),[13] [(C₅Me₅)₂Ln]₂(μ-η²:η²-RC₄R) (R = Me, 'Bu; Ln = La, Ce),[14] [(C₅Me₅)₂La]₂(μ-η²:η²-RC₄R) (R = Ph, 'Bu).[15] Alkynides adopting the terminal bonding mode, (type a) are still few even though they are known, and for the most part, structural details are absent.[16,17,18] On the other hand, the more interesting bis-alkynide complexes of the type "(Ligand)Ln(alkynide)₂" remain rather rare. The paucity of examples in the above two interesting classes of compounds is due in part to lack of sufficient steric bulk of the alkynide ligands to stabilize the electron deficient lanthanide center, and in the case of the bis-alkynide species, due to lack of appropriate starting materials such as the mono-ligand lanthanide dialkyl complexes of type "(Ligand)LnR₂". The availability of the series of lanthanide dialkyl complexes[19] detailed in Chapter 3 provided a very attractive entry into the synthesis and characterization of the corresponding bis-alkynide complexes via protonolysis with terminal alkynes.

Earlier works by Hessen et al.[20] and Cameron et al.[21] on the protonolysis of [η³:η¹-Me₂TACN(CH₂)₂N'Bu]La(CH₂SiMe₃)₂ (TACN = triazacyclononane) and (Cp*)Lu(CH₂SiMe₃)₂(2,2'-bipy), respectively, with terminal alkynes resulted

in two different structural motifs; a lanthanum bis-alkynide dimer complex with terminal and bridging alkynide ligands and a lutetium bis-alkynide complex, also a dimer, albeit with terminal and coupled alkynide moieties bonded to the two lutetium centers. More recently, Hessen and co-workers reported the synthesis of lanthanide bis-alkynide complexes bearing an amido ligand, $(L)Ln(CCPh)_2$ (Ln = Sc, Y, La); (L = N-{2-pyrolidin-1-ylethyl)-1,4-diazepan-6-amido ligand).[22] In the scandium complex, the alkynide ligands are in terminal disposition (type a), whereas the yttrium and lanthanum complexes are both dimeric with bridging and terminal alkynide moieties, reflecting the difference in the size of scandium compared to yttrium and lanthanum.[23] Another recent report by Cui and co-workers detailed the synthesis of a lutetium bis-alkynide complex supported by an anilido-phosphinimine ligand.[24] In this complex also, both alkynide ligands are terminal. In all of the above complexes, the alkyne used was phenyl acetylene and these appear to be the only lanthanide bis-alkynide complexes reported to date. The effects of alkyne substituent on the course of the reaction and nature of product obtained have not been examined. The aim of this study was to synthesize a series of bis-alkynide complexes supported by the bulky tris(pyrazolyl)borate ligand, $Tp^{R,R}$, and to observe the effect of changing the size of the alkyne substituents on the structures of the resulting bis-alkynide complexes. Their ability to effect the catalytic dimerization of terminal alkynes was also of interest.

4.2. Synthesis of Lanthanide bis-alkynide Complexes; [(Tp^{Me2})Ln(CCR″)$_2$]$_2$ (Ln = Y, Lu; R″ = Ph, SiMe$_3$, ^{t}Bu, Ad)

Reaction of the lanthanide dialkyl complexes, (Tp^{Me2})Ln(CH$_2$SiMe$_3$)$_2$(THF), (Ln = Y, **14a**; Lu, **8a**) with 2 equiv. of terminal alkynes, HC≡CR″, (R″ = Ph, SiMe$_3$, ^{t}Bu, adamantyl) proceeds with excellent yields to give the corresponding dimeric bis-alkynide complexes with the general formula, [(Tp^{Me2})$_2$Ln$_2$(μ-C≡CR″)$_2$(μ-R″CCCCR″)] (R″ = Ph, Ln = Y, **15**; Lu, **16**; SiMe$_3$, Ln = Y, **17**; Lu, **18**; ^{t}Bu, Ln = Y, **19**; Lu, **20**; Ad, Ln = Y, **21**) after simple work up, Scheme 4.2. The evidences for the formulation of the complexes, shown in the scheme are detailed in the following sections. The compounds vary in color from intense red (for R″ = Ph and SiMe$_3$) to yellow (for R″ = ^{t}Bu and adamantyl).

$$(Tp^{R,R'})Ln(CH_2SiMe_3)_2(THF) + 2\ HCCR''$$
$$R'' = Ph, SiMe_3, {}^tBu, Adamantyl$$

↓ -2 SiMe$_4$

$$"(Tp^{R,R'})Ln(CCR)_2(THF)"$$
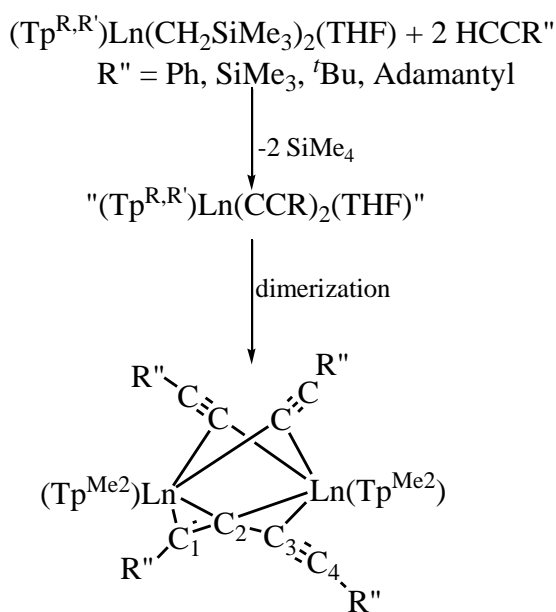
↓ dimerization

Scheme 4.2: Reaction of (Tp^{Me2})Ln(CH$_2$SiMe$_3$)$_2$(THF) Complexes With Terminal Alkynes.

The compounds are air and moisture sensitive but stable at room temperature for a prolonged time under an inert atmosphere.

4.2.1 Characterization of [(Tp^{Me2})Ln(CCR″)$_2$]$_2$ Complexes

Compounds **17**, **18**, **19** and **20** are soluble in aliphatic and aromatic solvents; complexes **15** and **16** are soluble in aromatic solvent but not in pentane or hexane while complex **21** is only sparingly soluble in aromatic solvents and insoluble in aliphatic solvents. Unlike in previous reports where synthesis in THF give the monomeric THF adduct complexes,[2,14] the complexes could be isolated from THF solution as the THF free dimer. However, when dissolved in THF formation of the corresponding monomeric THF adduct species was observed (*vide infra*). The compounds were characterized by standard spectroscopic and analytical techniques (see Experimental Section) and in the solid state by single crystal X-ray diffraction for complexes **15**, **16**, **17** and **21**.

The ^{1}H-NMR and ^{13}C{^{1}H} spectra of the phenyl acetylide complexes, **15** and **16**, are consistent with the presence of two different types of alkynide units. This is shown by the presence of two sets of resonances for the phenyl protons and carbon atoms of the alkynide units. For instance, the room temperature ^{1}H NMR spectrum of **15** shows two set of signals for the pyrazolyl 3-Me and 4-H groups with intensity ratio 2:1, the 5-Me group on the other hand is a sharp singlet, presumably due to accidental signal overlap. One set of aryl protons appear at 6.95, 6.85 and 6.79 ppm, (*m*, *p* & *o*); the other set are at 6.90, 6.67 and 6.66 ppm (*o*, *m* & *p*), respectively with the latter being more poorly resolved than the former. The two sets were differentiated on the basis of 2-D correlation experiments (HMQC and HMBC).

The observation of two sets of resonances is consistent with several possible combinations of alkynide ligands: bridge and terminal, terminal and coupled, or bridged and coupled units. However, the color of these compounds points to the presence of coupled alkyne units. Indeed the lanthanum bis-alkynide complex of Hessen,[20] $\{[\eta^3:\eta^1\text{-}Me_2TACN(CH_2)_2N^tBu]La(CCPh)(\mu\text{-}CCPh)\}_2$, (TACN = triazacyclononane) containing terminal and bridged alkynide moieties is cream colored, whereas, the lutetium bis-alkynide complex of Cameron and co-workers,[21] $[\{Cp^*Lu(CCPh)(bipy)\}_2(\mu\text{-}\eta^2:\eta^2\text{-}PC_4Ph)]$, with coupled alkynide is dark-red, similar to the color of compounds **15** and **16**.

In other to gain more insight into the possible structure of the bis-alkynide complexes, advantage was taken of the known fact that the nature of the bridging units in alkynide dimers can be differentiated on the basis of ^{13}C chemical shift position and in the case of yttrium, from $^{89}Y\text{-}^{13}C$ coupling constant values. Table 4.1 summarizes the typical chemical shift, as well as coupling constants, for the different types of alkynide bonding modes.

The $^{13}C\{^1H\}$ NMR spectrum of **15**, Figure 4.1 shows the diagnostic downfield doublet for the terminal carbon atom (Y-C_t) of a coupled alkynide fragment at 181.12 ppm ($^1J_{YC}$ = 17 Hz), the internal carbon, also a doublet, appears at 133.91 with a much smaller coupling constant of 5.7 Hz, corroborating the presence of a coupled alkynide moiety, already suspected from the intense coloration. The other alkynide unit shows two triplets at 143.84 ($^1J_{YC}$ = 22.3 Hz) and 120.76 ($^2J_{YC}$ = 3.9 Hz) for the α and β carbons, respectively, thus suggesting that the second alkynide unit is bridging. The observation of triplets for the alkynide

149

Table 4.1: Comparison of $^{13}C\{^1H\}$ Data (δ and J_{YC}) for the Different Types of Alkynide Bonding Modes.

compound	δ	mult.	J_{YC}	assign.	ref
Terminal					
Cp*$_2$YC≡CMe(OEt$_2$)*	133.04	d	73.9	C_α	16
	102.32	d	10.8	C_β	
Cp*$_2$YC≡CPh(OEt$_2$)	146.95	d	70.9	C_α	16
	109.59	d	12.9	C_β	
Cp*$_2$YC≡CSiMe$_3$(OEt$_2$)	134.21	d	72.0	C_α	16
	114.19	d	6.1	C_β	
[(PCP)*Y(C≡CSiMe$_3$)$_2$(THF)†	171.2	d	55.5	C_α	10
	no$^\#$	-	-	C_β	
(sCp)Y(C≡CSiMe$_3$)$_2$(THF)	172.46	d	47.8	C_α	10
	111.95	d	8.8	C_β	
Cp*Lu(C≡CPh)$_2$(bipy)(THF)	159.80	s	-	C_α	21
	108.60	s	-	C_β	
(N-O)$_2$Y C≡CSiMe$_3$‡	163.12	d	72.0	C_α	25
	108.91	d	12.5	C_β	
μ^2-Bridging					
[Cp*$_2$La(μ-C≡CMe)]$_2$	156.20	s	-	C_α	14
	117.00	s	-	C_β	
[(DAC)Y(μ-C≡CPh)]$_2$§	150.10	br	-	C_α	9
	no$^\#$	-	-	C_β	
[Cp″Y(μ-C≡CPh)(THF)]$_2$**	138.70	t	22.5	C_α	26
	no$^\#$	-	-	C_β	
{[PhC(NSiMe$_3$)$_2$]$_2$Y(μ-C≡CMe)]$_2$}	136.00	t	21.0	C_α	11
	no$^\#$	-	-	C_β	
{[PhC(NSiMe$_3$)$_2$]$_2$Y(μ-C≡CPh)]$_2$}	141.80	t	21.0	C_α	11
	no$^\#$	-	-	C_β	
Coupled					
[Cp*$_2$La]$_2$[μ-PhC=C=C=CPh]	208.60	s	-	$C_t^{\dagger\dagger}$	14
	117.00	s	-	$C_i^{\S\S}$	
[(DAC)Y]$_2$[μ-PhC=C=C=CPh]	195.60	d	38.4	C_t	9
	169.50	d	4.0	C_i	

* Cp* = C$_5$Me$_5$ δ = chemical shift in ppm

† (PCP)* = Phenanthrene-fused C$_5$Me$_5$. $^\#$no = not observed

‡ (N-O) = Salicyaldiminato Ligand. J_{YC}= coupling constant in Hz

§ (DAC) = diaza-18-crown-6.   multiplicity; d (doublet),

** Cp″ ={Me$_2$Si(C$_5$Me$_4$)(NPh)}   s (singlet), br (broad)

†† C$_t$ = terminal carbon §§C$_i$ = internal carbon
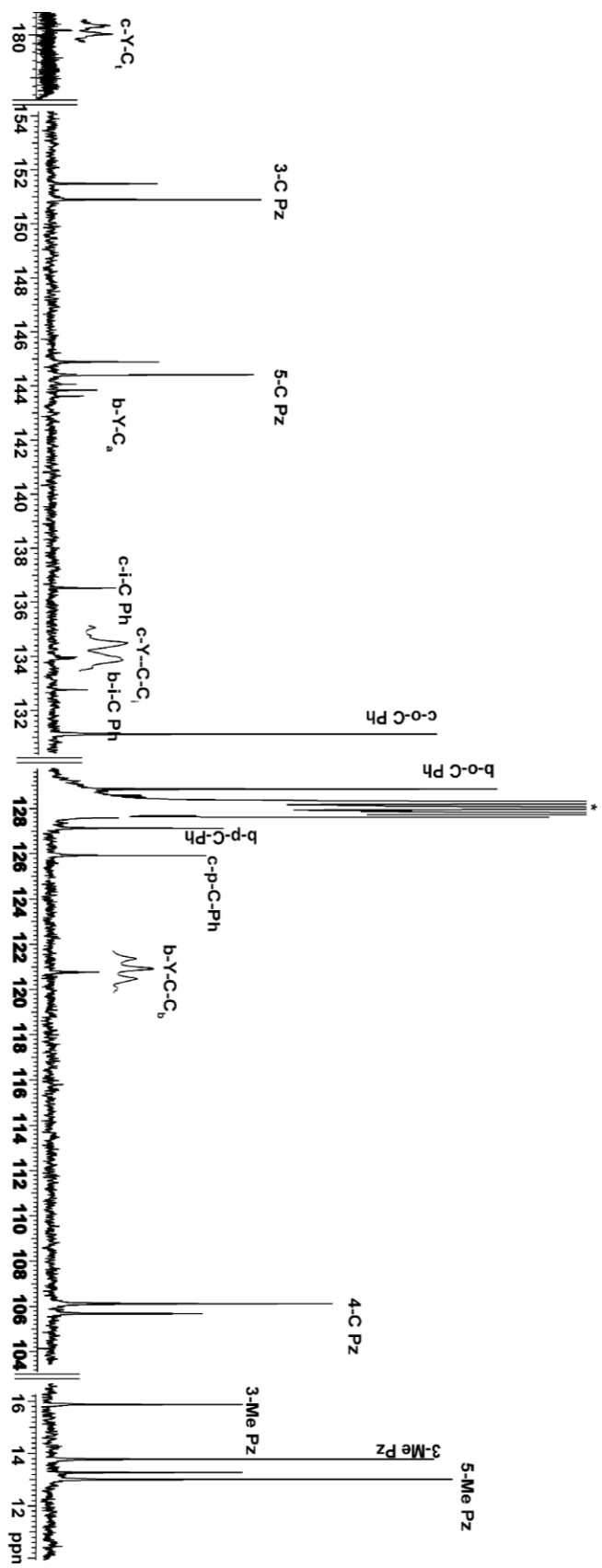
Figure 4.1: $^{13}C\{^1H\}$ NMR Spectrum (100 MHz, C_6D_6) of $[(Tp^{Me2})Y(CCPh)_2]_2$ (**15**)

c = coupled, b = bridging; C_t = terminal carbon, C_i = internal carbon; i = ipso,

o = ortho, p = para, m = meta. (both meta carbons are hidden under solvent C_6D_6 peaks).

151

carbons is due to coupling to two equivalent yttrium atoms, either by symmetry or time-averaging. The smaller Y-C_t coupling constant of 17.0 Hz in **15**, for the phenyl bound carbon atom of the coupled alkynide unit, compared to 38.4 Hz reported for [(DAC)Y]$_2$[PhC=C=C=CPh] will find explanation in the actual solid state structure of the compound (*vide infra*). Table 4.2 lists the $^{13}C\{^1H\}$ NMR data for the alkynide units in these complexes. The low field signal in the $^{13}C\{^1H\}$ NMR spectrum of compound **16** also confirms the presence of the coupled alkynide unit in this complex.

Since one of the aims of this study was to obtain terminal bis-alkynide complexes, more bulky terminal alkynes such as trimethylsilyl acetylene (Me$_3$SiC≡CH), *tert*-butyl acetylene (${}^tBuC≡CH$) and adamantyl acetylene ((Ad)C≡CH), were also investigated. The reaction of 2 equiv of Me$_3$SiC≡CH with the dialkyl compounds (Tp^{Me2})Ln(CH$_2$SiMe$_3$)$_2$(THF) (Ln = Y, **14a**; Lu, **8a**) gave the bis-alkynide complexes **17** and **18**, again, with similar intense coloration as observed for the phenyl acetylide complexes. In the case of ${}^tBuC≡CH$ and (Ad)C≡CH, the compounds obtained, **19** (${}^tBu$, Y), **20** (${}^tBu$, Lu) and **21** (Ad, Y), respectively are less intensely colored and thus may suggest the formation of monomeric species although this cannot be taken as conclusive evidence. The ^1H and $^{13}C\{^1H\}$ NMR signature of these complexes are similar to those of the phenyl acetylide complexes **15** and **16**, Table 4.2. For example, the ^1H NMR spectrum of compound **17** displays two sets of signals in 2:1 ratio for the pyrazolylborate ligand. The presence of two different signals for the SiMe$_3$ groups further supports the proposal that there are two different kinds of alkynide units, Figure 4.2. The

Table 4.2: $^{13}C\{^1H\}$ Data of the Alkynide Moieties in **15**, **16**, **17**, **18**, **19** and **20**.

	coupled unit				bridging unit			
	δ^*	mult.	$J^\#_{YC}$	assign.	δ	mult.	J_{YC}	assign.
15	181.12	d	17.0	C_t	143.84	t	22.3	C_α
	133.91	d	5.7	C_i	120.76	t	3.9	C_β
16	184.88	s	-	C_t	148.60	s	-	C_α
	134.72	s	-	C_i	122.71	s	-	C_β
17	204.00	d	14.9	C_t	173.07	t	21.7	C_α
	158.28	d	4.6	C_i	128.00§§	-	-	C_β
18	204.99	s	-	C_t	177.67	s	-	C_α
	155.61	s	-	C_i	128.00§	-	-	C_β
19	195.50	d	17.2	C_t	127.02	t	23.6	C_α
	126.66	d	8.5	C_i	128.00§§	-	-	C_β
20	198.80	s	-	C_t	132.47	s	-	C_α
	130.21	s	-	C_i	122.71	s	-	C_β

chemical shift in ppm § hidden under the solvent peak

$^\#$coupling constant in Hertz
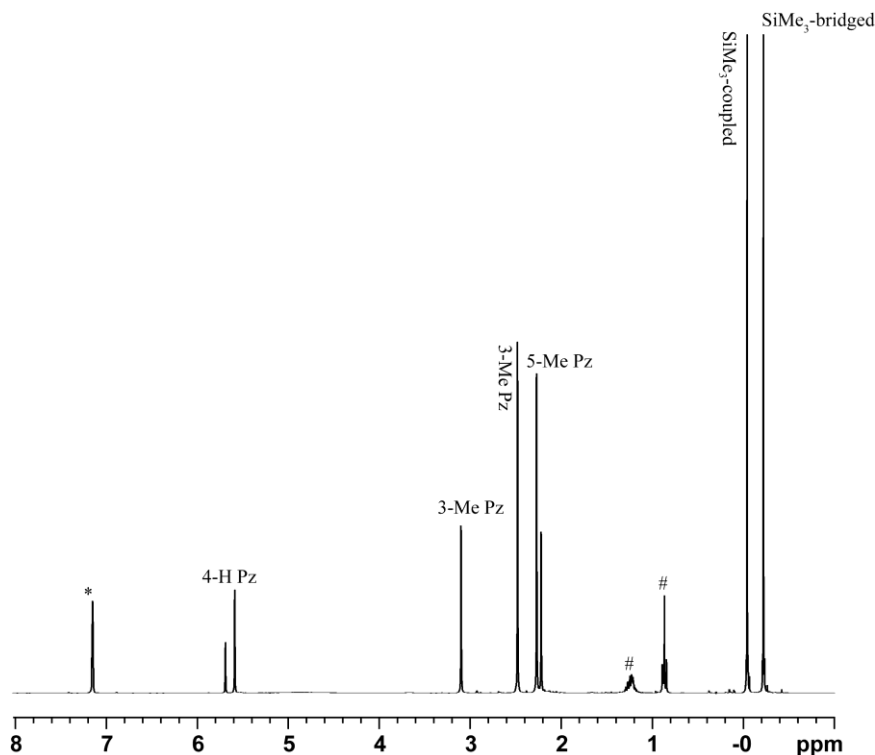
Figure 4.2: ^1H NMR Spectrum (400 MHz, C_6D_6) of [(Tp^{Me2})Y(CCTMS)$_2$]$_2$ (**17**).

153

^{13}C{^{1}H} NMR spectrum of compound **17**, shown in Figure 4.3, is also similar to that of compound **15**. Thus, similar solid state structures are expected. Although compound **21** has similar ^{1}H NMR signature as the other complexes, its extreme insolubility in aromatic solvent made it difficult to obtain good a ^{13}C{^{1}H} NMR spectrum.
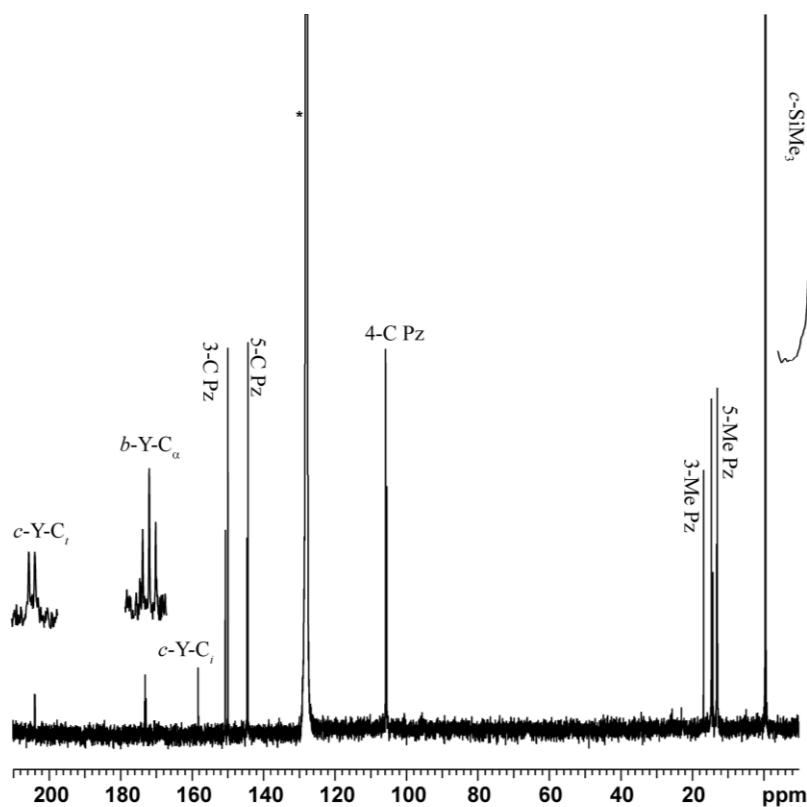
Figure 4.3: ^{13}C{^{1}H} NMR Spectrum (100 MHz, C$_6$D$_6$) of [(Tp^{Me2})Y(CCSiMe$_3$)$_2$]$_2$ (**17**).

4.2.2 Solid State Structures of 15, 16, 17 and 21

The solid state structures were determined by single crystal X-ray diffraction studies. Compounds **15** and **16** crystallize as the toluene solvates; **17**

crystallizes as the hexane solvate and **21** has two molecules of toluene in the crystal lattice. The structures of **15** and **16** are virtually identical and an ORTEP drawing of the yttrium compound, **15**, is shown in Figure 4.4, as a representative example. Also shown is another view in which all the pyrazole carbon atoms are removed for clarity, Figure 4.5. The structures of **17** and **21** are shown in Figures 4.6 and 4.7, respectively. Selected distances are listed in Table 4.3.

The solid state structures revealed that the compounds are dimeric with the two lanthanide centers bridged by two μ^2-alkynide bridges on one hand and a coupled alkynide unit on the other, and the coordination sphere around each metal atom is completed by a classical κ^3 pyrazolylborate ligand. Although the lanthanide centers are both formally 7-coordinate, with each bonded to two carbon atoms each from the bridging and coupled alkynide units, it is best to consider the latter as occupying one-coordination position on each lanthanide. Under this formalism of "six-coordinate" lanthanides, the coordination geometry is a distorted octahedron with the three N-atoms of the tripodal κ^3-Tp^{Me2} ligand occupying one triangular face and the two carbon atoms of the μ^2-bridging alkynides (C5 and C7) and one from the coupled alkynide unit (C2) forming the other triangular face. As a result of both lanthanides sharing the latter triangular face, the pyrazolyl rings of the "top" and "bottom" pyrazolylborate ligands are eclipsed with the coupled alkynide unit nestling between two "top" and "bottom" pyrazolyl rings. The substituents of the μ^2-alkynide bridges are also positioned between two pyrazolyl rings: in **15**, **16** and **17**, the orientation is between alternating "top" and "bottom" rings, whereas in **21** both adamantyl substituents are in clefts formed by a pair of
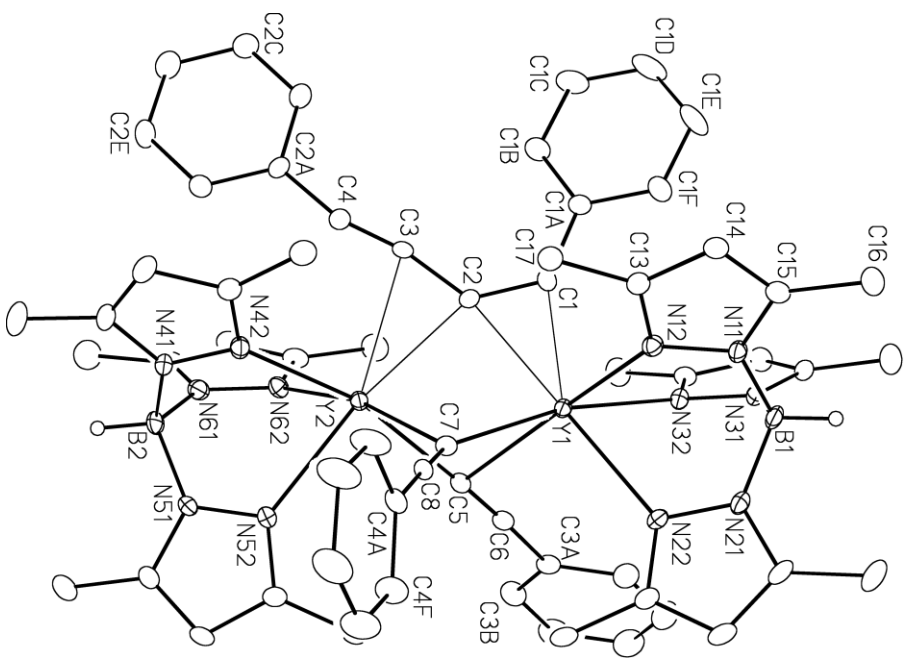
Figure 4.4: ORTEP View of [(Tp^{Me_2})Y(CCPh)$_2$]$_2$ (**15**).
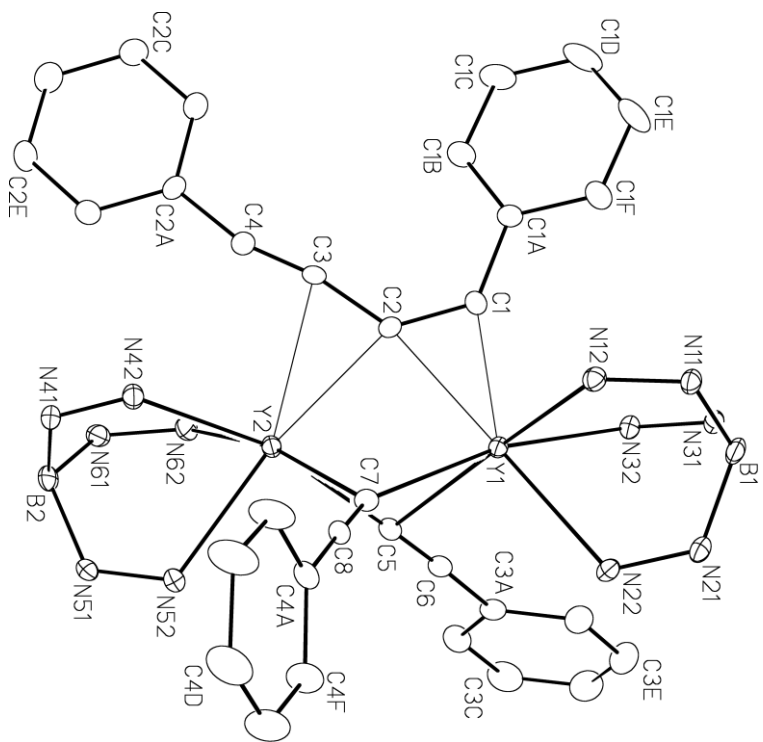
Figure 4.5: ORTEP View of **15** With All the Pyrazole Carbon Atoms Removed for Clarity.
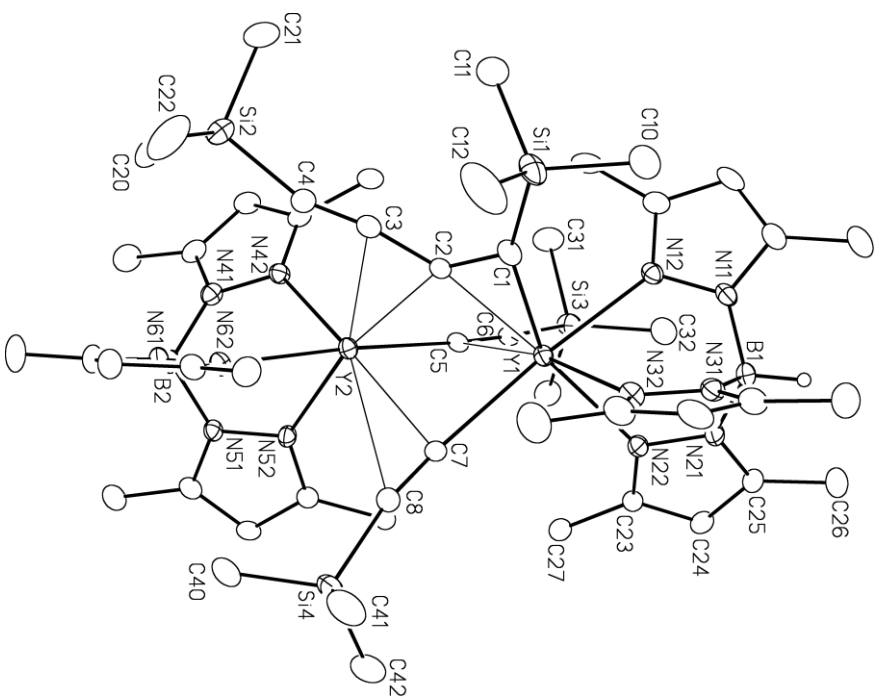
Figure 4.6: ORTEP View of [(Tp^{Me2})Y(CCSiMe$_3$)$_2$]$_2$ (**17**).
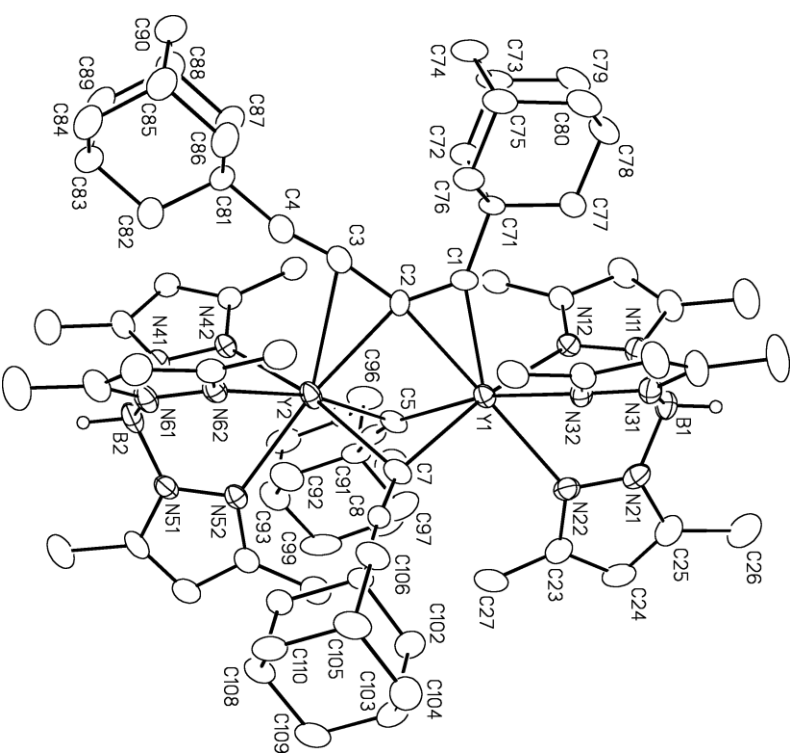
Figure 4.7: ORTEP View of [(Tp^{Me2})Y(CCAd)$_2$]$_2$ (**21**).

Table 4.3: Selected Distances (Å) in $[(Tp^{Me2})Ln(CCR)_2]_2$ Complexes (**15**, **16**, **17** and **19**; Ln = Y, Lu).

Ln-X	15	16[‡‡]	17	21
Ln1-Ln2	3.4103(5)	3.3094(5)	3.5017(7)	3.3476(8)
Ln1-C1	2.283(4)	2.172(7)	2.295(5)	2.336(5)
Ln1-C2	2.480(4)	2.467(5)	2.465(5)	2.478(5)
Ln1-C5	2.617(4)	2.524(5)	2.658(5)	2.552(6)
Ln1-C6	3.095(4)	3.124(5)	2.996(5)	3.666(6)
Ln1-C7	2.581(4)	2.468(5)	2.532(5)	2.565(5)
Ln1-C8	3.662(4)	3.628(6)	3.731(6)	3.687(5)
Ln2-C2	2.531(4)	2.467(5)	2.560(5)	2.497(5)
Ln2-C3	2.691(4)	2.830(10)	2.649(5)	2.732(6)
Ln2-C4	3.167(4)	3.38(2)	3.035(5)	3.310(7)
Ln2-C5	2.506(4)	2.468(5)	2.492(5)	2.507(6)
Ln2-C6	3.708(4)	3.628(6)	3.704(5)	3.253(6)
Ln2-C7	2.531(4)	2.524(5)	2.569(5)	2.523(6)
Ln2-C8	3.399(4)	3.124(5)	3.021(5)	3.312(5)
C1-C2	1.348(5)	1.518(8)	1.339(6)	1.305(6)
C2-C3	1.413(5)	1.217(12)	1.428(7)	1.430(8)
C3-C4	1.209(5)	1.23(3)	1.213(7)	1.241(8)
C5-C6	1.206(5)	1.181(7)	1.213(6)	1.175(7)
C7-C8	1.202(5)	1.181(7)	1.209(6)	1.195(6)

[‡‡] Compound **16** sits on a C_2 axis and the coupled alkynide unit is disordered.

"bottom" pyrazolyl rings not occupied by the adamantyl groups of the coupled alkynide unit.

The average Ln-N bond distances to the pyrazolylborate ligands are 2.44(1), 2.39(1), 2.46(1) and 2.45(1) Å in **15**, **16**, **17**, and **21**, respectively. These values are comparable to 2.47(6) Å and 2.42(7) Å in the starting dialkyl complexes **14a** and **8a**, respectively[19] and require no further comments.

The overall bonding motif between the lanthanide centers and alkynide units is the same for all complexes; however, there are subtle variation in the bonding within each fragment depending on the lanthanide and the alkynide substituents. Consideration of each bridging fragment will shed more light on these subtle differences.

4.2.3   Bonding within the [Ln(μ-CCR)]$_2$ Core

The bonding within the Ln$_2$(μ_2-CCR)$_2$ cores shows subtle variations both as a function of alkynide substituent and lanthanide metals, a schematic of the core structures is shown in Scheme 4.3.
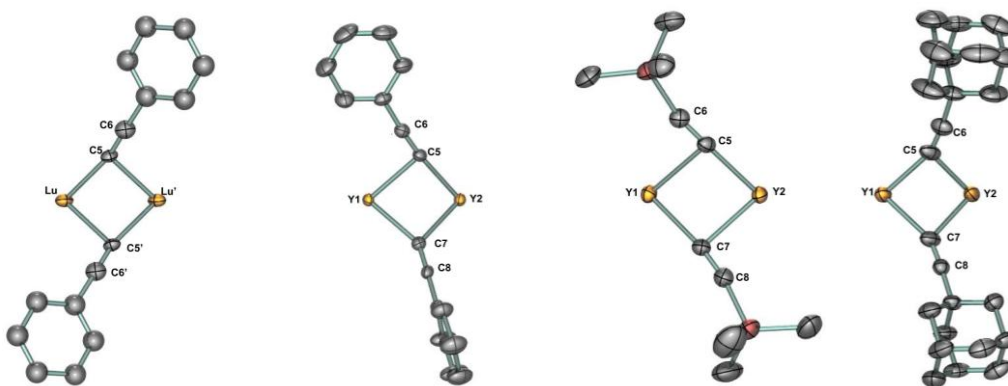
Scheme 4.3: μ_2-Bridging Alkynide Cores in **15**, **16**, **17** and **21**.

159

As usual for μ_2-alkynides bridging two lanthanide centers, the bonding is asymmetric. The magnitude of the asymmetry can be gleaned from the differences in Ln-C$_\alpha$ (i.e., C5 and C7) distances and the corresponding Ln-C$_\alpha$-C$_\beta$ (i.e., Ln-C5-C6 and Ln-C7-C8) angles; these are summarized in Table 4.4. The asymmetry is reflected in both the distances and the angles. The asymmetry in the yttrium complex **15** is different between the two bridging alkynide units, whereas, in the

Table 4.4: Asymmetry Parameters for the μ-CCR Bridges in **15**, **16**, **17** and **21**.

	15	Δ^*	**16**	Δ	**17**	Δ	**21**	Δ
			Distances (Å)					
Ln1-C5	2.617(4)		2.524(5)		2.658(5)		2.552(6)	
		0.11		0.06		0.17		0.05
Ln2-C5	2.506(4)		2.468(5)		2.492(5)		2.507(6)	
Ln1-C7	2.581(4)		2.524(5)		2.532(5)		2.565(5)	
		0.05		0.06		0.04		0.04
Ln2-C7	2.531(4)		2.468(5)		2.569(5)		2.523(6)	
			Angles (deg)					
Ln1-C5-C6	101.7(3)		109.5(4)		93.9(4)		157.5(5)	
		72.2		57.6		82.8		37.9
Ln2-C5-C6	173.9(3)		167.1(4)		176.7(4)		119.6(5)	
Ln1-C7-C8	148.7(3)		109.5(4)		171.3(4)		155.7(5)	
		21.2		57.6		71.4		33.9
Ln2-C7-C8	127.5(3)		167.1(4)		99.9(4)		121.8(4)	

$^*\Delta$ = differences between distances (Δ_{dist}) or angles (Δ_{ang}).

analogous lutetium compound,, **16**, it is the same, as required by symmetry. The increased asymmetry of one of the alkynide bridge in **15**, Δ_{dist} = 0.11 Å compared to 0.06 Å in **16**, may be due to the larger size of yttrium allowing for easier access

of the phenyl substituents to the cleft formed by two pyrazolyl rings. The larger Ln1-Ln2 separation, 3.4103 Å in **15** compared to 3.3094 Å in **16** is in line with this. The asymmetry of the two bridging alkynide units in **17** is also different. The increase in asymmetry of the more asymmetrically bridging alkynide unit, Δ_{dist} = 0.17 Å and Δ_{ang} = 82.8°, is most likely due to the larger size of the SiMe$_3$ substituent. In accord with the steric argument, the Ln1-Ln2 separation in **17** has lengthened to 3.5017(7) Å.

Observation of the C≡C-X angle of the alkynide units also supports this argument. The average values of these angles are 178.4(7)° (**15**); 177.35(4)° (**16**) and 168.35(5)°, (**17**). The angle in **15** and **16** are close to the linear angle of 180° for a regular alkyne. In the case of **17**, the deviation from linearity may be attributed to the bending away of the bulky SiMe$_3$ group from the substituents on the pyrazolyl rings of the Tp^{Me2} ligand to avoid unfavorable steric interaction. The distortion in the distance seen in **17** is comparable to that observed in {(L)Y(CCPh)(μ_2-CCPh)}$_2$, (L = 1,4,6,-trimethyl-*N*-(2-pyrrolidin-1-ylethyl)-1,4,-diazepan-6-amido) (Δ_{dist} = 0.17; although the corresponding Δ_{ang} of 20.0° is much less than the value of 82.8° in **17**), the only other structurally characterized bis-alkynide yttrium complex with asymmetric bridging moiety, but larger than those found in previously reported mono alkynide bridged lanthanide dimers; ([(C$_5$H$_4$Me)$_2$Sm(μ-C≡C^{t}Bu)]$_2$, Δ_{ang} = 39°, Δ_{dist} = 0.00 Å;[27] [(C$_5$H$_5$)$_2$Er(μ-C≡C^{t}Bu)]$_2$, Δ_{ang} = 34°, Δ_{dist} = 0.05 Å;[28] [(C$_5$H$_4$^{t}Bu)$_2$Sm(μ-C≡CPh)]$_2$, Δ_{ang} = 58.2°, Δ_{dist} = 0.06 Å;[8] [{PhC(NSiMe$_3$)$_2$}$_2$Y(μ-C≡CH)]$_2$, Δ_{ang} = 61.4°, Δ_{dist} = 0.05 Å;[11] [(DAC)Y(μ-C≡CPh)]$_2$, Δ_{ang} = 45°, Δ_{dist} = 0.02 Å;[9] (PCP*)Y(μ-C≡C(SiMe$_3$))$_2$, Δ_{ang}

= 45°, Δ_{dist} = 0.01 Å;[10] [(C$_5$H$_4$^{t}Bu)$_2$Nd(μ-C≡CPh)]$_2$, Δ_{ang} = 56.5°, Δ_{dist} = 0.04 Å;[12]

[(C$_5$H$_4$^{t}Bu)$_2$Gd(μ-C≡CPh)]$_2$, Δ_{ang} = 58.5°, Δ_{dist} = 0.07 Å.[12] In all the complexes

however, the asymmetry is such that Ln2-C$_\alpha$ distance is shorter than the corres-

ponding Ln1-C$_\alpha$ distance, Table 4.4.

Asymmetry may also result in additional π-interaction of the lanthanide

metals with the triple bond of the alkynide moiety. Maximum interaction with the

C≡C triple bond requires Ln2-C5-C6 angle of close to 180° and is expected to re-

sult in the elongation of the C≡C bond from the ideal value of ca. 1.208 Å found

in free PhC≡CH.[29] The Ln2-C5-C6 angles of 173.9(3)° in **15** and 176.7(4)° in **17**,

are close to the expected 180° value. These angles are also close to the value of

172° seen in [(C$_6$H$_5$)$_2$AlC≡CC$_6$H$_5$)]$_2$,[30] a compound cited as the closest example

of the π-bonded extreme for a μ-alkynide bridge.[28] The Δ_{dist} value of 0.19 Å in this

compound is larger than the corresponding values in **15**, **16** and **17**, despite the

small size of the aluminum metal compared with the large lanthanide centers in

the former compounds.[23] The large value of Δ_{dist} in this compound is a reflection

of a high degree of asymmetry.

Furthermore, inspection of the β-carbons of the bridging alkynes shows

that they exhibit relatively short contact with the metal centers. The shortest of

these interactions in **15**, Y1-C6 = 3.095 Å, suggests some degree of π-interaction

with this more asymmetrically bridged alkynide ligand. Similar explanation can be

used for the bonding in **17** albeit with a higher degree of asymmetry and thus, in-

creased π-interaction as shown by the shorter Y1-C6 and Y2-C8 distances of

2.996(5) Å and 3.021(5) Å, respectively. Based on the above bonding description,

elongation of the C≡C bond is expected. However contrary to expectation, but similar to observations made previously on other alkynide complexes, [8,11,23,31] the C≡C bonds are rather short. The short C≡C bond lengths of 1.206(5) Å and 1.213(7) Å (C5-C6) and 1.202(5) Å and 1.209(6) Å (C7-C8) for **15** and **17**, respectively, are not significantly different from 1.208 Å found in free PhC≡CH.[29]

The observed Lu-C5-C6 angle of 167.1(4)° in **16** deviates from linearity by ca. 13° and the Lu-C_β distance of 3.124(5) Å in **16** is slightly longer than the corresponding distance in **15**, especially when considering the smaller sized lutetium. The longer Ln-C_β bond in **16** again, reflects the increased crowding around the smaller lutetium center thus making the bridge less asymmetric when compared with the yttrium analogue.

As already mentioned, the orientation of the bridging alkynides substituents in **21** is different from that in the other complexes. Instead of the alternating "top-bottom" orientation, both adamantyl substituents point in the same direction toward Y2. The bonding within the bridge is also less asymmetric, with Δ_{dist} of 0.05 Å and Δ_{ang} of 37.9°. The more symmetric bonding may be described as mainly a σ-interaction between the yttrium centers and C5 of the bridging alkynides, with very little, if any additional π-component, as reflected in the long Y2-C_β distances, of 3.253(6) Å and 3.312(6) Å, as well as the very short C≡C bond lengths of 1.175(7) and 1.195(6) Å for C5-C6 and C7-C8, respectively. The relatively short Y2-C_α distances of 2.507(6) Å and 2.523(6) Å, compared to the Y1-C_α values of 2.552(6) and 2.565(5) Å, indicate a stronger interaction with Y2, similar to what was seen in compounds **15**, **16** and **17**.

The changes observed in $[Y(\mu\text{-CCAd})]_2$ core in **21** must be related to the very bulky nature of the adamantyl group. The inability of the bulky adamantyl group to fit between the pyrazolyl rings favors the less asymmetric bonding. Also, the orientation of the substituents towards Y2 is in line with the less crowded nature of the Tp^{Me2} ligand bonded to it as a result of the coupled alkynide bending away from this ligand due to the enyne motif of the unit (*vide infra*).

4.2.4 Bonding Within the $Ln_2(\mu\text{-RCCCCR})$ Core
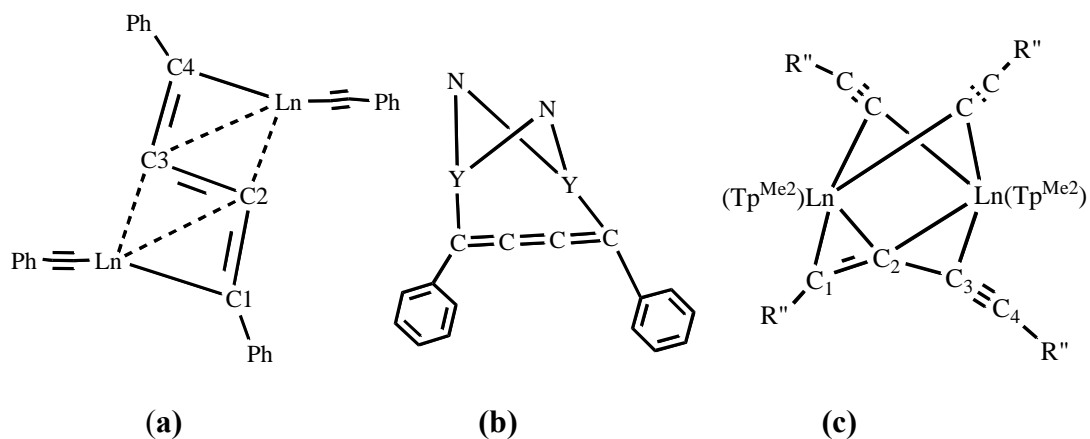
Scheme 4.4: Coupled Alkynide Cores.

The coupled alkynide unit shows two important differences from other structurally characterized lanthanide alkynide dimers bridged by coupled alkynide fragments. First, unlike in the other complexes in which the bridging fragment is a butatriene unit, Scheme 4.4 (a) and (b), the bridging unit in the present case is best considered as an enyne unit, Scheme 4.4(c). This can be clearly seen in the C-C bond distances and C-C-C bond angles within the coupled alkynide units, Table

4.5. For example, in compound **15**, the C1-C2 bond distance of 1.348(5) is clearly a double bond, and the C2-C3 and C3-C4 bond distances of 1.413(5) and 1.209(5), Å, are single (sp^2-sp) and triple bonds, respectively. The seemingly abnormal values of these distances in the lutetium compound, **16**, is a result of the disordered coupled alkynide unit which thus makes C2 to occupy the special position of the two-fold rotational axis.

Table 4.5: Selected Distances (Å) and Angles (deg) within the coupled alkynide units of **15**, **16**, **17** and **21**.

	Distances (Å)			
	15	**16**[§]	**17**	**21**
C1-C2	1.348(5)	1.518(8)	1.339(6)	1.305(6)
C2-C3	1.413(5)	1.217(12)	1.428(7)	1.430(8)
C3-C4	1.209(5)	1.23(3)	1.213(7)	1.241(8)
Ln1-C1	2.283(4)	2.172(7)	2.295(5)	2.336(5)
Ln1-C2	2.480(4)	2.467(5)	2.465(5)	2.478(5)
Ln2-C2	2.531(4)	2.467(5)	2.560(5)	2.497(5)
Ln2-C3	2.691(4)	2.830(10)	2.649(5)	2.732(6)
Ln2-C4	3.167(4)	3.38(2)	3.035(5)	3.310(7)
	Angles (deg.)			
Cx-C1-C2	127.4(4)	130.4(6)	126.5(4)	129.3(5)
C1-C2-C3	128.3(4)	122.3(9)	127.6(5)	123.6(5)
C2-C3-C4	169.7(4)	165.8(14)	166.9(6)	166.9(6)

[§] the seemingly "abnormal" C1-C2 and C2-C3 distances in compound **16** is a result of the disorder in the coupled alkynide unit causing C2 to sit on the two-fold rotational axis.

In addition, the Ln-C distances show that the enyne moiety is bonded rather asymmetrically to the lanthanide centers. The trend in distances is such that Ln1-C1 < Ln1-C2 and Ln2-C2 < Ln2-C3 and implies the same trend in terms of bond strength. The Ln2-C3 distance is long and there is virtually no interaction between Ln2 and C4, Table 4.5. It is worth noting that the longest Ln2-C3 distance is that in the lutetium complex **16**, giving further evidence of increased steric crowding in this smaller lanthanide compound. The asymmetric bonding of the coupled alkynide unit, with stronger bonding to Ln1, is in response to the weaker bonding between Ln1 and the bridging alkynide unit (*vide supra*).

The asymmetric enyne bonding renders ″top″ and ″bottom″ parts of the molecules different and should result in complicated NMR spectra, contrary to the simple spectrum seen. Clearly, the bonding mode of the coupled alkynide unit changes rapidly between Ln1 and Ln2, accompanied by similar oscillation of the μ^2-CCR alkynide bridges thus, giving a time averaged C_{2v} symmetry solution structure and the observed NMR spectra.

Secondly, the coupled alkynide fragment is in a *Z*-conformation in which both alkyne substituents are on the same side of the C_4 chain. Such *Z*-conformation of the coupled fragment has only been reported in the case of $[(DAC)Y(CCPh)]_2$,[9] which exists in solution as an equilibrium mixture of the bridging, $[(DAC)Y(\mu\text{-}C\equiv CPh)]_2$ and the coupled $[(DAC)Y]_2(\mu\text{-}PhC=C=C=CPh)]_2$, Scheme 4.3(b). The preference for *Z*-conformation in the latter compound was attributed to the more flexible nature of the DAC ligand when compared to two C_5Me_5 units. In the present case however, the preference for *Z*

conformation is due to the steric congestion of the two μ^2-bridged alkynide moieties and the bulky tripodal pyrazolylborate ligands. As commented before, the bridging alkynide units sits in the cleft formed by two of the 3-Me substituent on the pyrazolyl rings on one side of the dimer thus leaving only the ligand cleft on the other side for the coupled unit to fit into and therefore accounting for the Z-conformation adopted by the coupled alkynide unit. The formation of enyne as opposed to normally observed butatrienediyl moiety might be due to the fact that such a bonding arrangement would necessarily bring both alkynide substituents into close proximity with the pyrazolyl substituents thereby causing unfavorable steric interactions.

As earlier mentioned in the introduction, formation of coupled product appears to be controlled by a subtle interplay of steric and electronic factors. Previous work by Evans et al. [13] suggested that the presence of a phenyl group was necessary for the coupling reaction. Subsequent to this report, Marks and co-workers[15] showed that the coupling reaction proceeds in the absence of a phenyl group, although its presence may enhance the rate. In the present case, while no kinetic study was carried out, the reaction proceeds irrespective of the substituent to give the coupled product. The electronic effect of the substituents on the course of reaction in the present case seems minimal, leading to the reasonable conclusion that the major driving force for the coupling reaction is most likely steric.

4.3 Synthesis of Monomeric Bis-alkynide Complexes

Both the bridge splitting of $Ln_2(\mu^2\text{-CCR})_2$ dimers as well as the decoupling of coupled alkynide fragments by the addition of THF are well documented.[9,11,21] It was therefore not surprising that a THF solution of the intensely colored complexes became gradually less intense and overtime gave very pale or colorless solution indicating the cleavage of the coupled alkynide unit.

Attempts to break down the dimeric complex **16** with the stronger donor molecule, 2,2′-bipyridine was unsuccessful giving simply a mixture of the complex and 2,2′-bipyridine as observed by the presence of free, uncoordinated bipyridine in the ^{1}H NMR spectrum. Recrystallization gave only the clean starting complex. However, reacting the dialkyl complex **8a** with one equivalent of 2,2′-bipyridine followed immediately by two equivalents of *tert*-butyl acetylene gave the product, $(Tp^{Me2})Lu(CC^tBu)_2(2,2'\text{-bipy})$, **22** in excellent yields. This compound is very pale pink in color, as would be expected for a trivalent lutetium complex with terminal alkynide units; the complex has been characterized by NMR spectroscopy, elemental analysis as well as by single crystal X-ray diffraction.

Reaction of lanthanide dialkyl complexes, $(Tp^{Me2})Ln(CH_2SiMe_3)_2(THF)$ (Ln = Lu, **8a**; Y, **14a**) with two equivalents of the very bulky terminal alkyne, tris(3,5-di-tert-butylphenyl)methyl acetylene, (Trit′C≡CH) gave colorless compounds which on the basis of their NMR signatures are best formulated as the terminal bis-alkynide complexes, $(Tp^{Me2})Ln(CCTrit')_2(THF)$ Ln = Y, **23**; Lu, **24**). Single crystal X-ray diffraction studies confirmed the presence of terminal alkynides in the lutetium compound, **24**, in the solid state.

Since increasing the bulk of the alkyne substituents did not afford the desired bis-terminal alkynide species free of other donor ligand, an alternative that could be used to achieve this is to increase the bulk of the ancillary pyrazolylborate ligand. To do this, we turned to the bulky $Tp^{tBu,Me}$ ligand. This ligand is known for its ability to stabilize unusually low coordination numbers and for this purpose it has been termed a tetrahedral enforcer in transition metal chemistry.[32] Reaction of two equivalents of phenyl acetylene with $(Tp^{tBu,Me})Ln(CH_2SiMe_3)_2$, (Ln = Y, **25a**; Lu, **6a**) gave pale yellow solids of $(Tp^{tBu,Me})Ln(CCPh)_2$ (Ln = Y, **26**; Lu, **27**) in good yields.

4.4   Characterization of $(Tp^{Me2})Ln(C{\equiv}CR'')_2(L)_{0/1}$ Complexes

4.4.1 $(Tp^{Me2})Ln(C{\equiv}CR'')_2(THF\text{-}d_8)$ (Ln = Y, R'' = SiMe₃; Ln = Lu, R'' = Ph)

As mentioned, dissolution of $[(Tp^{Me2})Ln(CCR'')_2]_2$ complexes (Ln = Y, R'' = SiMe₃; Ln = Lu, R'' = Ph), in THF-d_8 gave pale pink and colorless solution, respectively. However, attempts to isolate the presumed terminal alkynide complexes were not successful as intensely colored solids were again obtained upon removing the THF solvent. Thus an equilibrium exist between the dimeric product and the monomeric THF coordinate bis-alkynide complexes in which the alkynide dimer is the stable form in the solid state whereas the monomer is the preferred form in THF solution. A similar observation was made on the pair of analogous bis-alkynide complexes $(PCP^*)Y(CCSiMe_3)_2(THF)$ (solution) and $[(PCP^*)Y(CCSiMe_3)(THF)]_2(\mu\text{-}CCSiMe_3)_2$ (solid).[10] Therefore, these terminal alkynide complexes were characterized only in solution by NMR spectroscopy.

The ^{1}H and ^{13}C{^{1}H} NMR spectra of the THF-d_8 solution is consistent with the formation of bis-alkynide complexes bearing terminal alkynide moieties. The room temperature ^{1}H NMR spectra show one set of resonances each for the phenyl protons of (Tp^{Me2})Lu(CCPh)$_2$(THF-d_8) and SiMe$_3$ protons of (Tp^{Me2})Lu(CCSiMe$_3$)$_2$(THF-d_8) as well as the pyrazolyl protons. In the ^{13}C NMR spectrum of the yttrium compound (Tp^{Me2})Y(CCSiMe$_3$)$_2$(THF-d_8), Figure 4.8, the α and β carbons appear as doublets at 170.0 ppm ($^1J_{YC}$ = 53.5 Hz) and 107.0 ppm ($^1J_{YC}$ = 10.2 Hz), respectively. These values are similar to those reported for (PCP)Y(CCSiMe$_3$)$_2$(THF), 171.2ppm ($^1J_{YC}$ = 53.6 Hz) and other terminal alkynide complexes, Table 4.1.
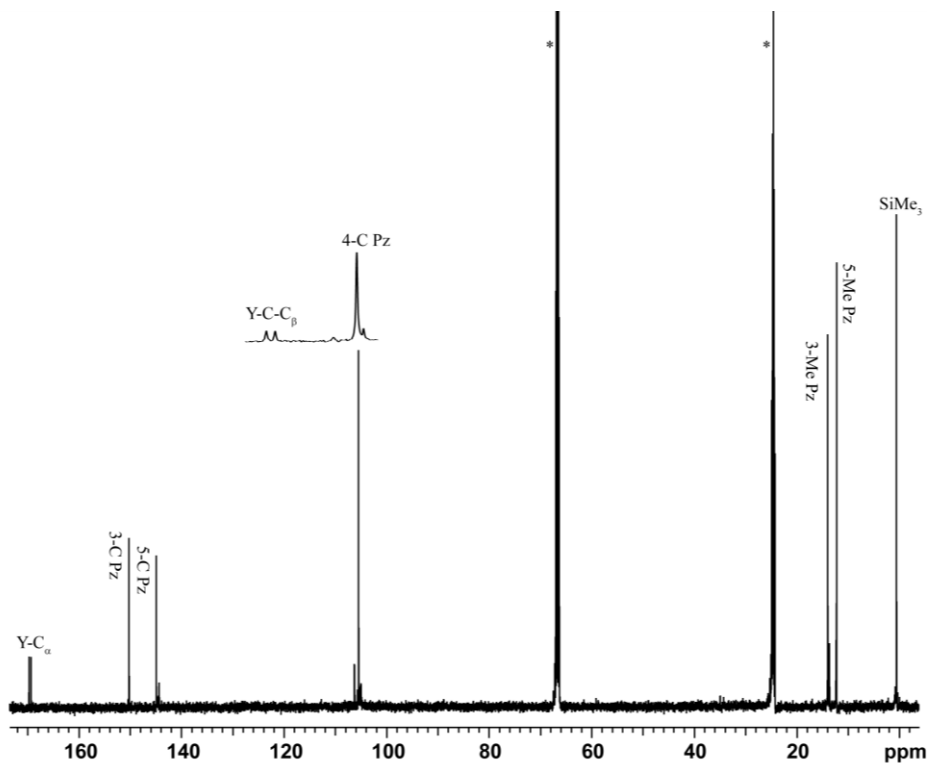
Figure 4.8: ^{13}C{^{1}H} NMR Spectrum (100 MHz, THF-d_8) of [(Tp^{Me2})Y(CCTMS)$_2$]$_2$ (**17**) i.e., (Tp^{Me2})Y(CCTMS)$_2$(THF-d_8).

4.4.2 $(Tp^{Me2})Lu(C\equiv C^tBu)_2(2,2'-bipy)$ (22)

The compound is insoluble in hydrocarbon solvents and very sparingly soluble in aromatic solvents. Although soluble in THF, attempts to obtain NMR in C_6D_6/THF-d_8 led to a mixture of complexes and free bipyridine, as seen by ^1H NMR spectroscopy. The ^1H NMR in C_6D_6 at RT shows two set of signals in 2:1 ratio for the pyrazolylborate protons and the signals due to the coordinated bipyridine ligands also gave distinct signals for each proton. The $^{13}C\{^1H\}$ NMR spectrum exhibited similar features (see Experimental Section). The appearance of the spectra is consistent with a rigid C_s symmetry structure observed in the solid state.
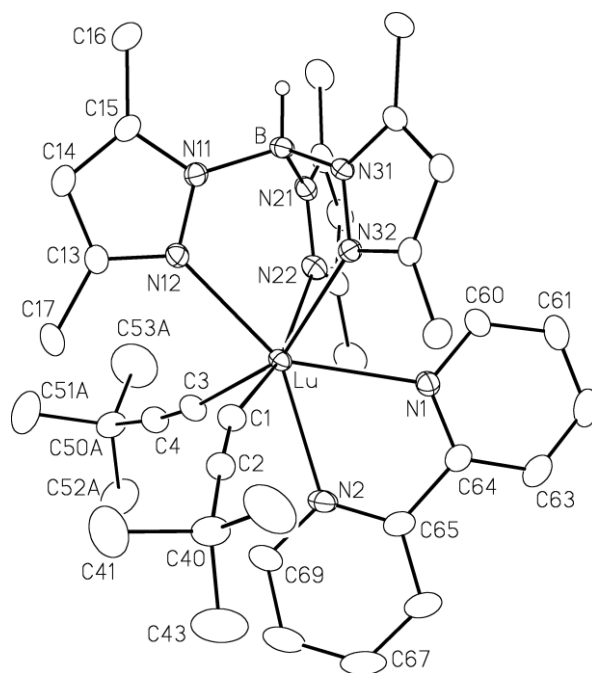
Figure 4.9: ORTEP View of $(Tp^{Me2})Lu(CC^tBu)_2(2,2'-bipy)$ (**22**).

The compound crystallizes with two molecules of benzene in the unit cell and single crystal X-ray diffraction studies confirmed its formulation as the monomeric bis-alkynide complex, $(Tp^{Me2})Lu(C\equiv C^tBu)_2(2,2'-bipy)$, **22** with the two

alkynide ligands in terminal disposition. The molecular structure of **22** is shown in Figure 4.9 and selected metrical parameters are listed in Table 4.6.

The lutetium center is 7-coordinate with one κ^3-Tp^{Me2} ligand, two alkynide carbon atoms and the two nitrogen atoms of the bipyridyl ligand. The geometry around the metal center is best described as a distorted capped octahedron with N12, N22 and N32 of the tripodal ligand occupying one of the triangular faces, the other expanded face is formed by the two carbons and N1 (bipy) while N2 caps the latter face of the octahedron.

Table 4.6: Selected Distances (Å) and angles (deg) in (Tp^{Me2})Lu(CC^{t}Bu)$_2$(2,2′-bipy) **(22)**.

Distances (Å)		Angles (deg.)	
Lu-N12	2.433(2)	N1-Lu-N2	63.90(9)
Lu-N22	2.404(3)	N1-Lu-C1	111.79(11)
Lu-N32	2.454(2)	N1-Lu-C3	117.97(11)
Lu-C1	2.378(3)	C1-Lu1-C3	105.54(12)
Lu-C3	2.384(3)	N2-Lu-C1	77.21(11)
Lu-N1	2.529(3)	N2-Lu-C3	79.09(12)
Lu-N2	2.460(3)	N12-Lu-N22	76.87(9)
C1-C2	1.310(5)	N12-Lu-N32	75.94(8)
C3-C4	1.199(5)	N22-Lu1-N32	77.19(8)
		Lu-C1-C2	162.9(3)
		Lu-C3-C4	169.3(3)
		C1-C2-C40	177.2(4)
		C3-C4-C50	173.2(4)

The Lu-N distances of Lu-Tp^{Me2} ranges from 2.404(3) Å to 2.454(2) Å with an average value of 2.43(5) Å. This distance is similar to 2.42(7) Å found in the starting dialkyl complex, (Tp^{Me2})Lu(CH$_2$SiMe$_3$)$_2$(THF),[19] and those found in other 7-coordinate Tp^{Me2} lanthanide complexes: 2.600(4) Å in (Tp^{Me2})LaCl$_2$(bipy);[33] 2.55(3) Å in (Tp^{Me2})NdCl$_2$(L) (L = 4,4'-di-*tert*-butyl-2,2'-bipiridyl)[34] and 2.52(7) Å in (Tp^{Me2})$_2$Nd(O$_3$SCF$_3$),[35] after accounting for the difference in ionic radii of the respective lanthanides.[23] The average Lu-C bond lengths of 2.381(3) Å is comparable to 2.376(3) in **8a** and 2.390(7) Å found in (C$_5$Me$_5$)Lu(C≡CPh)$_2$(bipy)(py).[21] Although the Ln-C(alkynide) bond is expected to be shorter than the Ln-C(alkyl) bond distance, the similarity of the Ln-C bond distance of **22** with that in **8a** can be accounted for by the higher coordination number and thus more congested lutetium center in **22**. The bipyridyl ligand is bonded in an asymmetric fashion to the lutetium center as reflected by the Lu-N bond distances: Lu-N1 2.529(3) Å; Lu-N2 2.460(3). The average Lu-N(bipy) bond distance of 2.50(4) Å is comparable to the 2.699(5) Å and 2.63(5) Å found in (Tp^{Me2})LaCl$_2$(bipy)[33] and (Tp^{Me2})NdCl$_2$(L),[34] (L = 4,4'-di-*tert*-butyl-2,2'-bipiridyl) respectively, again, after taking into account the differences in ionic radii.[23]

4.4.3   (Tp^{Me2})Ln(C≡CTrit′)$_2$(THF) Complexes; (Ln = Y, 23; Lu, 24)

The compounds were obtained as white solids. They are soluble in hydrocarbon as well as ether-type solvents. They are sensitive to air and moisture but thermally stable under an inert atmosphere. The complexes were characterized by NMR spectroscopy, elemental analysis and in the case of **24**, single crystal X-ray

173

diffraction.

The room-temperature ^{1}H and ^{13}C{^{1}H} NMR spectra are consistent with their formulation as the bis-alkynide complex with the alkynide ligands in terminal disposition. The ^{1}H NMR spectra of compounds **23** and **24** display subtle differences based on the metal size. The lutetium complex appears to be rigid in solution with a ^{1}H NMR spectrum which approximates that expected for a six-coordinate octahedral complex with facially coordinated tripodal pyrazolylborate ligand exhibiting C_s symmetry; it shows two sets of signals for the pyrazolyl ring substituents in 2:1 ratio, but the alkynide ligands give one set of broad signals for both the aromatic protons and the ^{t}Bu groups, Fig 4.10. The ^{13}C{^{1}H} NMR spectrum exhibited similar features.

The room temperature ^{1}H NMR spectrum of the yttrium compound, **23** in C_6D_6 indicates a degree of dynamic solution behavior. The signal due to the methyl groups in the 3 position of the pyrazolyl rings appear in the expected 2:1 ratio, although with broadening. The signal for the methyl groups on the 5-position of the pyrazolyl rings appear as a slightly broadened singlet, whereas the 4-hydrogen gives a single sharp signal, Figure 4.11. The latter observation may be the result of accidental overlap of the two signals expected for these groups as seen in the case of the starting dialkyl complexes, **8a** and **14a**.[19] However, ^{13}C NMR spectrum of **23** displays one set of signals for the pyrazolylborate ligand as well as the alkynide ligands; although the pyrazolylborate signals are rather broad. Also, the Y-C chemical shift and coupling constants are consistent with the values reported for other terminal alkynide complexes, Table 4.1.
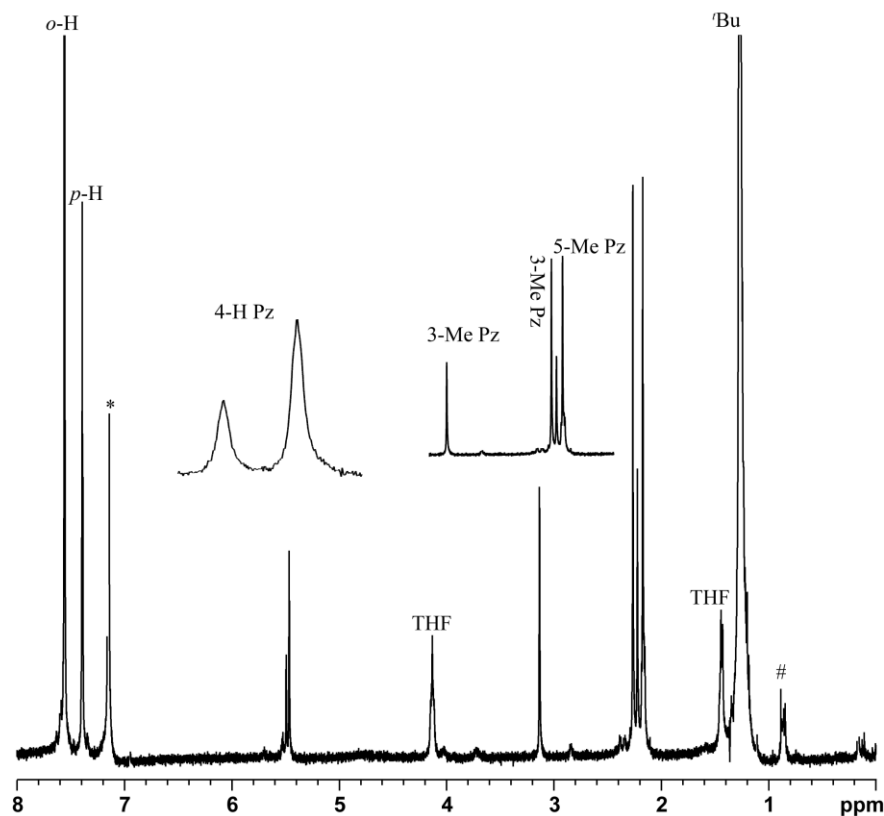
Figure 4.10: ^{1}H NMR Spectrum (400 MHz, C$_6$D$_6$) of (Tp^{Me2})Lu(C≡CTrit′)$_2$(THF) (**24**).

Despite the bulk of the alkyne substituent, compounds **23** and **24** still retained a molecule of THF coordinated to the lanthanide center even in the case of the smaller lutetium center, an indication that although the very bulky C$_\beta$ substituent successfully prevent dimer formation, this does not translate into bulking up the vicinity of the electron deficient lanthanide center which is then compensated by a THF solvent coordination.

Compound **24** crystallizes in the monoclinic space group with four mole-cules in the unit cell. The lutetium center is coordinated by three nitrogen atoms of the pyrazolylborate ligand in the classical κ^3 bonding mode, two carbon atom of
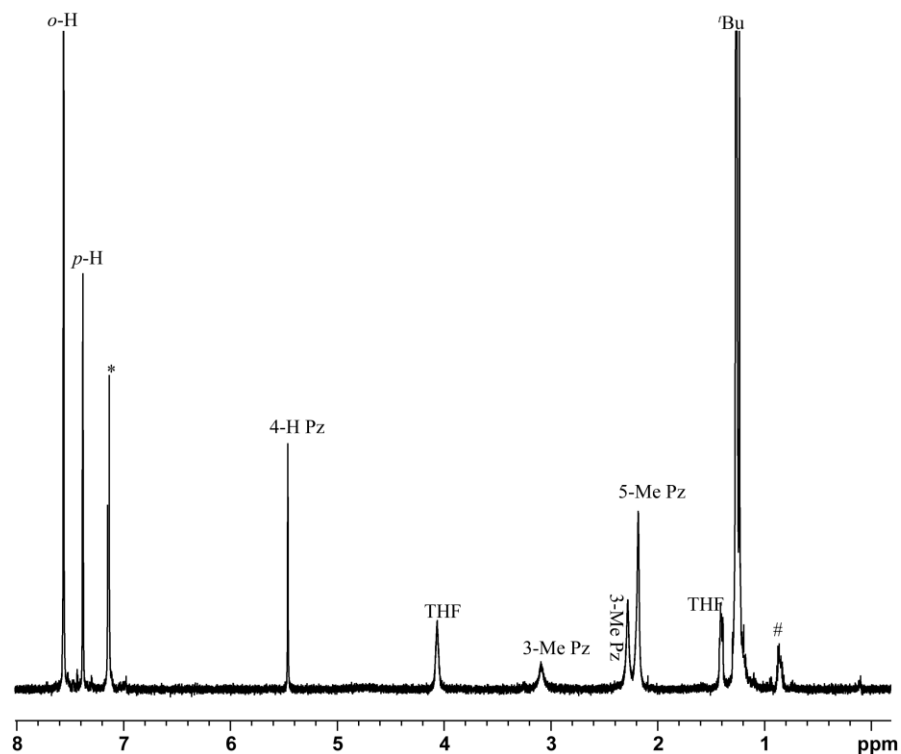
Figure 4.11: ^{1}H NMR Spectrum (400 MHz, C_6D_6) of $(Tp^{Me2})Y(C≡CTrit')_2(THF)$ **(23)**.

the alkynide unit as well as the oxygen atom of the coordinated THF molecule in a distorted octahedral arrangement, Figure 4.12.

Similar to the starting dialkyl complex, **8a**, the molecular symmetry approaches C_s, with O of the THF ring, Lu, B, and pyrazole (N11, N12) almost in a plane, and renders the two alkynide moieties and the other two pyrazole rings equivalent, consistent with the solution NMR data. The Lu-N (Lu-N12 2.443(5); Lu-N22 2.401(4) and Lu-N32 2.362(4) Å) and Lu-C bond lengths (Lu-C1 2.358(6) and Lu-C4 2.328(6) Å) in **24** are comparable to the corresponding distances in **8a**, as are the N-Lu-N intra-ligand angles, which ranges from 77.09(16)-82.84(15). The C-Lu-C inter-ligand angle of 101.50° is larger than the expected
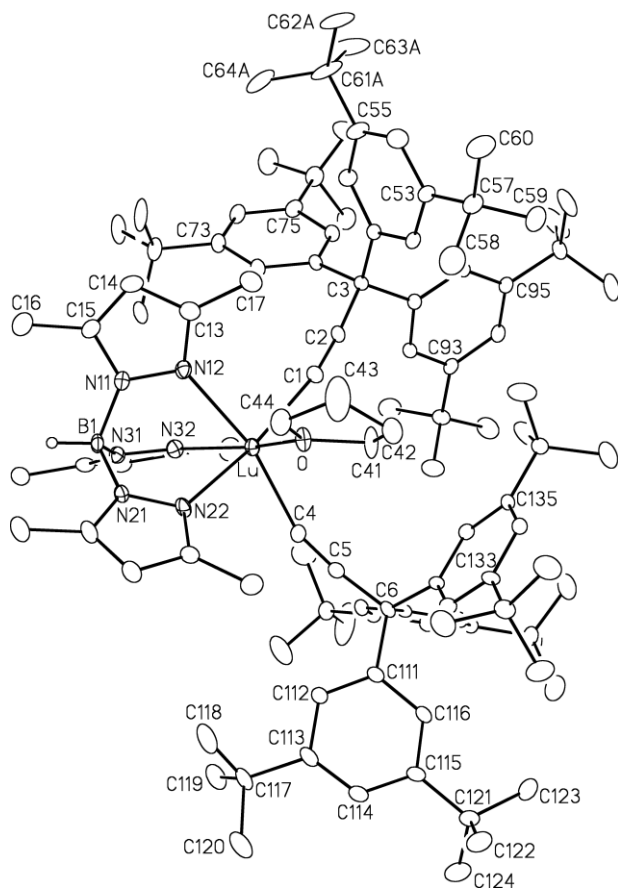
Figure 4.12: ORTEP View of $(Tp^{Me2})Lu(C\equiv CTrit')_2(THF)$ (**24**).

90°. The deviation of this angle from the ideal 90° may be attributed to the steric requirements of the bulky trityl substituents on the alkynide ligands. The Lu-C_α-C_β angles of 169.5(5)° and 159.4(5)° in **24** are comparable to the corresponding values of 162.9(3)° and 169.3(3)° in **22**. Also, the C_α-C_β-C_x angles of 174.7(6)° and 172.6(6)° and 177.2(4)° and 173.2(4)° in **24** and **22** respectively, are similar. The similarity of these values despite the differences in the coordination number may be attributed to the steric bulk of the alkynide substituent in **24**.

177

4.4.4 (Tp^{tBu,Me})Lu(C≡CPh)$_2$ (Ln = Y, 26; Lu, 27)

Attempts to grow single crystals of these compounds were unsuccessful, hence the compounds were characterized in solution by NMR spectroscopy and based on their NMR signatures can be formulated as the terminal alkynide species (Tp^{tBu,Me})Lu(C≡CPh)$_2$ (Ln = Y, **26**; Lu, **27**), free of any other coordinated ligand. The proton NMR spectra consist of a single set of signals for the pyrazolylborate protons as well as for the alkynide units. The ^{13}C{^{1}H} NMR spectra also show one set of signals for each unique carbon. In the case of the yttrium complex, (Tp^{tBu,Me})Y(C≡C-Ph)$_2$, **26**, both the α and β C-atoms show coupling to the yttrium center, Figure 4.13.
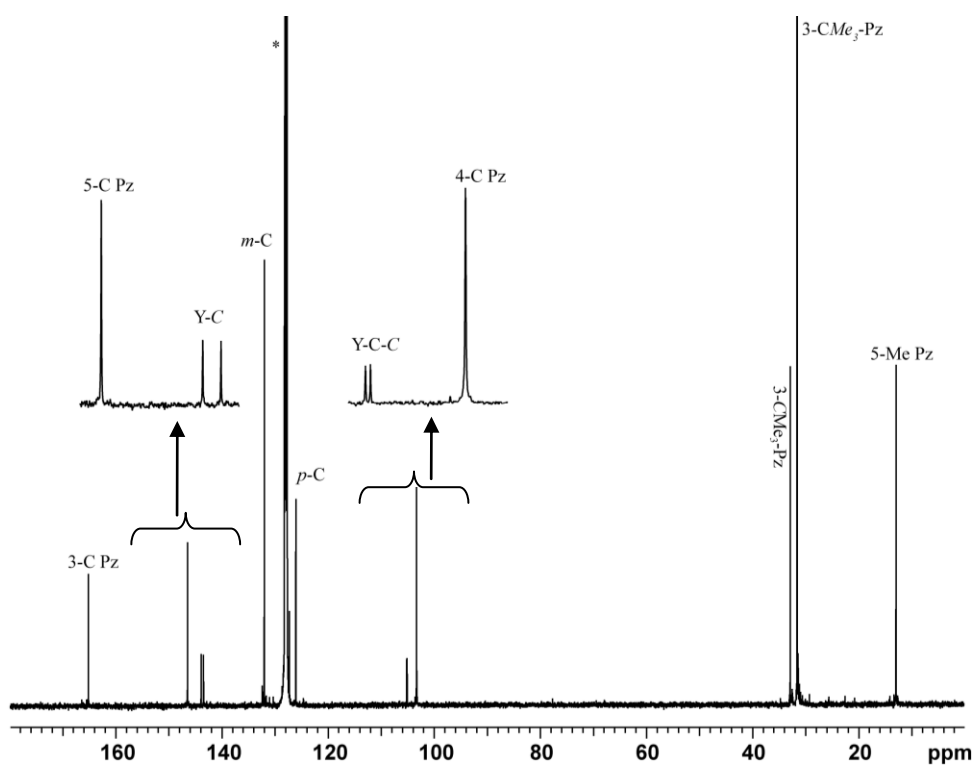
Figure 4.13: ^{13}C{^{1}H} NMR Spectrum (100 MHz, C$_6$D$_6$) of (Tp^{tBu,Me})Y(CCPh)$_2$ (**26**).

4.5 Protonolysis of Lanthanide Bis-Alkynide Dimers, [(Tp^{Me2})Ln(CCR″)$_2$]$_2$

To investigate whether the coupled alkynide unit could be liberated intact, protonolysis of compounds **15**, **17**, **19** and **21** was examined. In the case of **19** and **20**, formation of free enyne would provide complementary evidence to the NMR data for the presence of the coupled alkynide unit as these complexes lack solid state structural data. Treatment of **15**, **17**, **19** and **21** with 2,4,6-trimethylphenol (HOMes) resulted in quantitative formation of the corresponding lanthanide aryl oxides (Tp^{Me2})Y(OMes)$_2$ (Mes = 2,4,6-Me$_3$-C$_6$H$_2$). The other products of the reaction are a 2:1 mixture of free alkyne and *Z*-1,4-disubstituted 1-butene-3-yne, Scheme 4.4. In the case of **19** and **21**, the protonolysis reaction is less selective giving the lanthanide aryl oxide, 2 moles of free alkynes and two coupled products, *Z*-1,4-disubstituted 1-butene-3-yne (80%) and 1,4-disubstituted butatriene (20%), presumably the *Z*-isomer, Scheme 4.5.

Scheme 4.5: Protonolysis of [(Tp^{Me2})Ln(CCR″)$_2$]$_2$ Dimers.

179

The nature of the liberated cumulenes was deduced based on previously established NMR signatures. The titanium(III) complex of Nakamura and co-workers, $(C_5Me_5)_2TiCl_2/i$-PrMgBr[36] was reported to catalyze the exclusive dimerization of phenyl acetylene to give the head-to-tail dimer, 2,4-diphenyl-3-buten-1-yne with the coupling constant established as 8.0 Hz. Yi and Liu[38] showed that the ruthenium hydride complexes, $C_5Me_5Ru(L)H_3$ (L = PPh_3, PCy_3, PMe_3), catalyzed the dimerization of various terminal alkynes to give the head-to head Z- and E-1,4-disubstituted enynes, head-to-tail 2,4-disubstituted enynes as well as butatrienes depending on the catalysts and the alkyne substituents. The pattern of substitution and stereochemistry of the cumulenes were assigned based on chemical shift and coupling constant values. The data are in agreement with those reported by Teuben $et\ al.$[14] and Berg $et\ al.$,[9] Table 4.7 lists the ^1H NMR data for the olefinic protons of several dimerized alkyne products.

Analysis of the ^1H NMR spectra of the protonolysis products shows the presence of a distinct pair of doublets between 5 and 7 ppm with coupling constants consistent with the formation of Z-1,4-disubstituted-butenynes. For example, protonolysis of **15** gave two doublets at 6.41 and 5.79 ppm, respectively with J_{HH} = 12.1 Hz, in addition to the acetylenic proton signals at ca. 2.90 ppm. The exclusive formation of enynes in the case of **15** and **17**, although in line with the nature and geometry of the coupled alkynide unit in the solid state, is nevertheless noteworthy. The results are similar to those obtained by Teuben $et\ al.$ with $(C_5Me_5)Ln(\mu\text{-}MeC=C=C=CMe)$[14] and Berg $et\ al.$ with $[(DAC)Y(\mu\text{-}PhC=C=C=CPh)]$,[9] who also observed the exclusive formation of the

Table 4.7: ^{1}H NMR Data for the Olefinic Protons of Disubstituted Alkyne Dimers.

Product[§§]	Stereo.	δ	Assign.	mult.	J_{HH}	Ref
1,4-diphenyl	Z	5.79	=C*H*	d	12	37
		6.40	=C*H*(Ph)	d	12	
1,4-diphenyl	E	6.30	=C*H*	d	16	37
		7.04	=C*H*(Ph)	d	16	
2,4-diphenyl	germinal	5.74	=C*H*	d	8	36
		4.95	=C*H*	d	8	
1,4-(TMS)$_2$	Z	6.00	=C*H*	d	14.7	38
		6.23	=C*H*(TMS)	d	14.7	
1,4-(TMS)$_2$	E	6.01	=C*H*	d	15.5	38
		6.25	=C*H*(TMS)	d	15.5	
2,4-(TMS)$_2$	germinal	5.54	=C*H*	d	3.4	38, 39
			=C*H*	d	3.4	
1,4-(^{t}Bu)$_2$	Z	5.47	=C*H*	d	12	14, 38
		5.56	=C*H*(CMe$_3$)	d	12	
1,4-(^{t}Bu)$_2$	E	5.49	=C*H*	d	16	14, 38
		6.14	=CH(CMe$_3$)	d	16	
2,4-(^{t}Bu)$_2$	germinal	5.12	=C*H*	d	1.5	38
		5.36	=C*H*	d	1.5	
1,4-(^{t}Bu)$_2$		5.55	=C=CH	s	na[***]	14, 37

[§§] enynes, except the last entry which is a butatriene

[***] not applicable

corresponding enynes.

In the case of **19** and **21**, in addition to the free alkyne and the *Z*-enyne, formation of 1,4-disubstuted butatriene was also observed. Although no solid state structural information is available for **19** and **20**, the formation of enyne and free alkyne is as expected from the similarity in structures with other complexes based on spectroscopic evidence.

Formation of the observed products could be rationalized by the reaction sequence given in Scheme 4.6, similar to previous observations made by Teuben *et al.*[14] in their systems.

Protonation of C_4 of the bridging enyne unit gives a metallated butatriene (**A**) as the first product of protonolysis. This species may either undergo a second protonolysis reaction to give the corresponding 1,4-disubstituted butatriene or
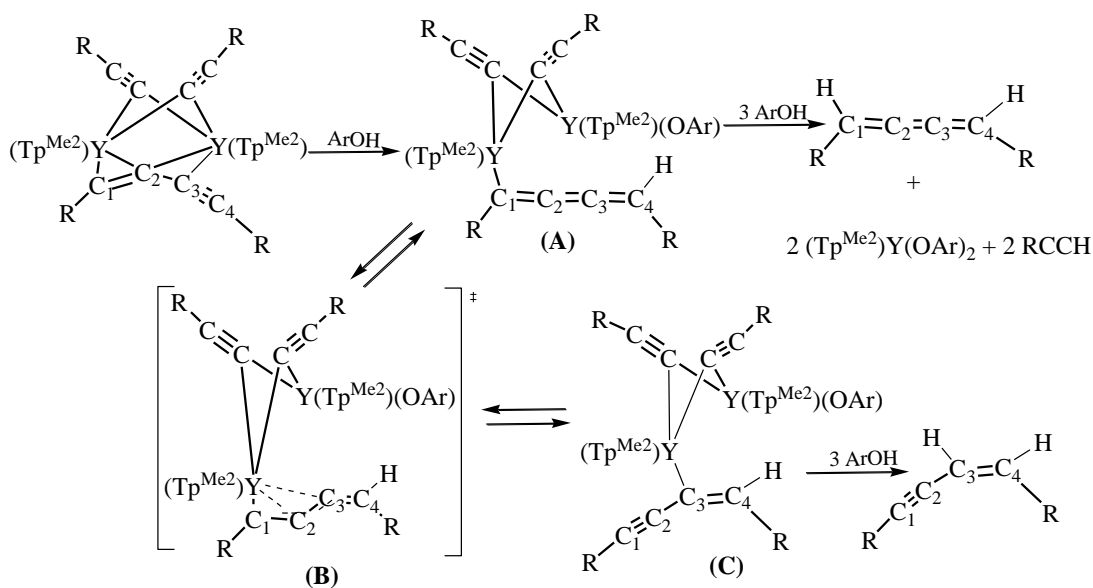
Scheme 4.6: Plausible Scenario for the Formation of *Z*-Enynes and *Z*-Butatrienes.

182

rearrange via a 1,3-metal shift to give the metallated enyne (**C**) through the intermediate (**B**). Further reaction of the metallated enyne with another proton gives the corresponding 1,4-disubstituted enyne. Similar rearrangement was observed by Teuben *et al.*[14] and Berg *et al.*[9,37] in their systems. The rearrangement is not unexpected since theoretical studies have shown that butatrienyl species is less stable than the corresponding enyne by about 80 kJ/mol.[40]

As was previously pointed out by Teuben, the relative rates of the second protonolysis and 1,3-metal shift in this system determines the enyne/butatriene ratio. In the case of compounds **15** and **17**, the results obtained suggest that rearrangement is much faster than protonolysis, thus accounting for the exclusive formation of enynes. The formation of a mixture of enynes and butatrienes in the case of **19** and **21** can be explained on the basis of relief of steric crowding. In the metallated butatriene (**A**), there will be unfavorable steric interaction between the substituent, R on C_1 and the pyrazolyl substituent of the ligand. Thus, in order to relieve this unfavorable steric interaction, (**A**) can either undergo a second protonolysis reaction or undergo a 1,3-metal shift to give the metallated enyne (**B**). Given that the rate of rearrangement is slower with bulky substituents, the second protonolysis is more competitive with the 1,3-metal shift. Therefore, the observation of butatriene formation in only **19** and **21** supports the fact that the rearrangement is slower for the more bulky alkyl groups, *t*Bu and adamantyl.

4.6 Catalytic Oligomerization of Terminal Alkynes.

As briefly mentioned in the introduction, lanthanide alkynide complexes are precursors for the atom economic[1] dimerization of terminal alkynes to enynes.[2,3,4] There are only a few reports of catalytic dimerization by dialkyl complexes and bis-alkynide complexes, and these are mostly focused on phenyl acetylene.[22] It was therefore of interest to carry out catalytic dimerization of terminal alkynes with our lanthanide dialkyl $(Tp^{Me2})Ln(CH_2SiMe_3)_2(THF)_{1/0}$, and bis-alkynide complexes, $[(Tp^{Me2})Ln(CCR)_2]_2$.

The reaction of $(Tp^{Me2})Ln(CH_2SiMe_3)_2(THF)$ (Ln = Y, **14a**; Lu, **8a**) with an excess of phenyl acetylene in benzene at 80°C results in the stereo- and regioselective formation of the head-to-head Z-isomer, 1,4-diphenyl-1-butene-3-yne, and trace amounts of trimers, albeit in low yields and slow conversion; with **8a** and phenyl acetylene, only 40% of the alkyne was consumed after about 72 hrs at 80°C. Both the reaction rate and conversion is slower with the corresponding yttrium compound, **15**, only about 25% of the alkyne was consumed under the same reaction condition. In all cases studied, formation of higher oligomers was not observed, i.e. the highest m/z observed corresponds to that of the trimer. Using the preformed alkynide complexes **15** and **17**, the same reactivity pattern was observed, albeit marginally faster and with improved conversion when compared to starting with the corresponding dialkyl complexes. For example, with **17** and (trimethylsilyl) acetylene, the exclusive formation of the head- to-head E-isomer as well as trace amount of the trimer, was observed, as shown by analysis of the reac-

tion solution by GC-MS. In this case about 50% of the alkyne was consumed after 48 hrs at 80°C.

4.7   Conclusions

The availability of scorpionate supported lanthanide dialkyl complexes, $(Tp^{R,Me})Ln(CH_2SiMe_3)_2(THF)_n$ (R = ^tBu, n = 0; R = Me, n = 1; Ln = Y, Lu) has provided entry into the preparation of lanthanide bis-alkynide complexes, "$(Tp^{R,Me})Ln(CCR'')_2$" via protonolysis of the corresponding dialkyl with an appropriate terminal alkyne, HC≡CR'' (R'' = Ph, Si Me_3, ^tBu, Ad, Trit'). The structures adopted by the complexes depend on the steric size of the $(Tp^{R,Me})$ ligand as well as the alkynide substituent.

With Tp^{Me2} as ligand, dimeric bis-alkynide complexes of the type $[(Tp^{Me2})Ln(CCR'')_2]$ were obtained for R'' = Ph, SiMe_3, ^tBu and Ad. The compounds were characterized by ^1H and $^{13}C\{^1H\}$ NMR spectroscopy and in the solid state for R'' = Ph, SiMe_3 and Ad. The solid state structure revealed two types of alkynide moieties bonded to the lanthanide centers; bridging as well as coupled alkynide units. The bonding within each alkynide unit varies as a function of the alkynide substituents and also the lanthanide metal size. Protonolysis of the dimeric complexes with 2,4,6-trimethyl phenol cleanly gave the aryloxide, 1 mole of 1,4-disubstituted-Z-enynes and 2 moles of free alkynes in the case of R'' = Ph, SiMe_3. With R'' = ^tBu and Ad, in addition to the above products, formation of small amounts of 1,4-disubstituted butatriene was also observed. The dimeric complexes as well as their dialkyl precursors were able to effect the catalytic

185

dimerization of terminal alkynes to exclusively give the head to head dimers. The stereoselectivity of the product however depend on the alkyne substituent.

Although the dimers break down in THF to give the corresponding THF adducts, "(Tp^{Me2})Ln(CCR″)(THF)", the dimeric form is preferred in the solid state and in non-coordinating solvents, so these complexes were characterized in solution as the THF-d_8 adducts. In the presence of the stronger donor ligand, 2,2′-bipyridine, the monomeric complex (Tp^{Me2})Lu(CC^{t}Bu)$_2$(2,2′-bipy) was obtained. The compound was characterized by standard spectroscopic techniques and single crystal X-ray studies confirmed its structure as the monomeric complex with both alkynide units terminal. In the case of the very bulky terminal alkyne, HC≡CTrit′, the compounds obtained, (Tp^{Me2})Ln(CCTrit′)$_2$(THF) (Ln = Y, Lu) have both alkynide ligands in a terminal disposition.

In the case of the bulky Tp^{tBu,Me} ligand, reaction of the dialkyl complexes (Tp^{tBu,Me})Ln(CH$_2$SiMe$_3$)$_2$ (Ln = Y, Lu) with phenyl acetylene gave the corresponding lanthanide bis-alkynide complexes, (Tp^{tBu,Me})Ln(CCPh)$_2$ in which the two alkynide units are in a terminal disposition. In addition, the bulk of the Tp^{tBu,Me} ligand prevented further solvent coordination. Although attempts to grow crystal of these complexes were not successful, both their ^{1}H and ^{13}C{^{1}H} NMR signatures support their formulation as the terminal bis-alkynide complexes.

4.8 Experimental Section

4.8.1 General Techniques, Solvents and Physical Measurements

As in Chapter 2. Products of protonolysis and catalytic reactions were analyzed by NMR spectroscopy and GC-MS.

4.8.2 Starting Materials and Reagents

$(Tp^{Me2})Ln(CH_2SiMe_2)_2(THF)$ (Ln = Y, **14a**; Lu, **8a**) were prepared as previously reported.[19] The alkynes, phenyl acetylene (PhCCH), *tert*-butyl acetylene (^tBuCCH) and trimethylsilyl acetylene (Me_3SiCCH), were obtained from Aldrich and used without further purification. Adamantyl acetylene (AdCCH) and tris(3,5-di-tertbutylphenyl) acetylene (Trit′CCH) were received as gifts from Wes Chalifoux of this Department. 2,4,6-trimethylphenol was purchased from Aldrich and used as received.

4.8.3 Synthesis of the Compounds

$(Tp^{Me2})_2Y_2(\mu-C\equiv CPh)_2(\mu-PhCCCCPh)$ (15)

To a colorless toluene solution $(Tp^{Me2})Y(CH_2SiMe_3)_2(THF)$, **14a** (0.10g, 0.158 mmol) was added 2 equiv. of phenyl acetylene (0.032g, 0.316 mmol) in drops. The solution immediately turned to an intense red color. The solution was kept at RT for ca. 24 h, layered with pentane and then cooled to -40°C overnight. Bright red microcrystalline material formed, the supernatant was decanted and the crystals were dried in vacuum to obtain 0.085g, 0.266 mmol of the title compound

as the toluene solvate in 84% isolated yield. Single crystals suitable for X-ray crystallographic studies were obtained by layering a toluene solution with pentane and cooling to -30°C. Anal. Calc. for $C_{69}H_{72}B_2N_{12}Y_2$ (**15**·C_7H_8) C,65.32; H, 5.72; N, 13.25. Found C, 64.97; H, 5.93; N, 13.19.

^{1}H NMR (400 MHz, C_6D_6, 27°C ; assigned by HMQC and HMBC) δ 6.95 (4H t, $^3J_{HH}$ = 8.0Hz, coupled alkynide *m*-H), 6.90 (4H, dd, $^3J_{HH}$ = 8.0 Hz,2.0 Hz, bridging alkynide *o*-H), 6.85 (2H, tt $^3J_{HH}$ = 8.0 Hz, 2.0 Hz, coupled alkynide *p*-H), 6.79 (4H, dd, $^3J_{HH}$ = 8.0 Hz, 2.0 Hz, coupled alkynide *o*-H), 6.68-6.63 (6H, overlapped multiplet bridging alkynide *m*-& *p*-H), 5.63 (2H, s, 4-*H* Pz), 5.43 (s, 4H, 4-*H* Pz), 2.99 (s, 6H, 3-*Me* Pz), 2.45 (s,12H, 3-*Me* Pz), 2.25 (18H, s, 5-*Me* Pz). $^{13}C\{^1H\}$ NMR (100 MHz, C_6D_6, 27°C ; assigned by HMQC and HMBC) δ 181.12 (d, $^1J_{YC}$ = 17 Hz, Ph-*C*=C coupled alkynide), 151.48 (3-*C* Pz), 150.89 (3-*C* Pz), 144.88 (5-*C* Pz), 144.40 (5-*C* Pz), 143.84 (t, $^1J_{YC}$ = 22.3 Hz, Y-*C*≡C bridging alkynide), 136.50 (*ipso*-C coupled alkynide), 133.91 (d, $^2J_{YC}$ = 5.7 Hz, Ph-C=*C* coupled alkynide), 132.34 (*ipso*-C bridging alkynide), 131.11 (*o*-C Ph bridging alkynide), 128.84 (*o*-C Ph coupled alkynide), 127.88 (*m*-C Ph bridging alkynide), 127.60 (*m*-C Ph coupled alkynide), 127.11 (*p*-C Ph bridging alkynide), 125.92 (*p*-C Ph coupled alkynide) 120.76 (t, $^2J_{YC}$ = 3.9Hz, Y-C≡*C* bridging alkynide), 106.11 (4-*C* Pz), 105.67 (4-*C* Pz), 15.87 (3-*Me* Pz), 13.77 (3-*Me* Pz), 13.28 (5-*Me* Pz), 13.01 (5-*Me* Pz). $^{11}B\{^1H\}$ (128 MHz, C_6D_6, 27°C) -8.93.

(Tp^{Me2})_2Lu_2(μ−C≡CPh)_2(μ-PhCCCCPh) (16)

Following a procedure analogous to **15** using (Tp^{Me2})Lu(CH_2SiMe_3)_2(THF), **8a**, (0.1g, 0.139 mmol) and phenyl acetylene (0.028g, 0.278 mmol), **16** was obtained as a bright red microcrystalline solid (0.09g, 0.125 mmol) in 90% isolated yield. X-ray quality crystals were obtained as described for **15**. Anal. Calc. for $C_{69}H_{72}B_2N_{12}Lu_2$ (**16**·C_7H_8) C, 57.51; H, 5.04; N, 11.60. Found C, 57.49; H, 5.02; N, 11.30.

^{1}H NMR (400 MHz, C_6D_6, 27°C; assigned by HMQC and HMBC) δ 6.96 (4H t, $^3J_{HH}$ = 8.0 Hz, coupled alkynide m-H), 6.85 (2H, t, $^3J_{HH}$ = 8.0 Hz, coupled alkynide p-H), 6.83 (4H, d, $^3J_{HH}$ = 8.0 Hz bridging alkynide o-H), 6.78 (4H, d, $^3J_{HH}$ = 8.0 Hz, coupled alkynide o-H), 6.70-6.62 (6H, overlapped multiplet coupled alkynide m-& p-H), 5.64 (2H, s, 4-H Pz), 5.46 (s, 4H, 4-H Pz), 2.99 (s, 6H, 3-Me Pz), 2.49 (s,12H, 3-Me Pz), 2.26 (18H, s, 5-Me Pz). ^{13}C{^{1}H} NMR (100.7 MHz C_6D_6, 27°C; assigned by HMQC and HMBC) δ 184.88 (Ph-C=C coupled alkynide), 151.94 (3-C Pz),151.33 (3-C Pz), 148.60 (Lu-C≡C bridging alkynide), 144.76 (5-C Pz), 144.25 (5-C Pz), 137.19 (*ipso*-C coupled alkynide), 134.72 (Ph-C=C coupled alkynide), 132.34 (*ipso*-C bridging alkynide), 131.45 (*o*-C aryl bridging alkynide), 128.97 (*o*-C aryl coupled alkynide), 128.75 (*p*-C aryl bridging alkynide), 128.50 (*m*-C aryl coupled alkynide), 127.50 (*m*-C aryl bridging alkynide), 125.73 (*p*-C aryl bridging alkynide), 122.71 (Lu-C≡C bridging alkynide), 106.35 (4-C Pz), 105.85 (4-C Pz), 16.11 (3-Me Pz), 14.03 (3-Me Pz), 13.25 (5-Me Pz), 12.99 (5-Me Pz). ^{11}B{^{1}H} (159.8 MHz C_6D_6, 27°C) -8.41.

(Tp^{Me2})$_2$Y$_2$(μ−C≡CSiMe$_3$)$_2$(μ-SiMe$_3$CCCCSiMe$_3$) (17)

To a colorless toluene solution of (Tp^{Me2})Y(CH$_2$SiMe$_3$)$_2$(THF), **14a**, (0.10g, 0.158 mmol) was added 2 equiv. of Me$_3$SiCCH (0.0310g, 0.316 mmol) in drops. The solution slowly turned to an intense red color. The solution was kept at RT for ca. 24 h, layered with pentane and then cooled to -40°C overnight. A small amount of bright red solid formed, the solvent was stripped under reduced pressure and the resulting red oily residue was triturated with hexane to obtain a red solid. The solid was re-dissolved in 2mL pentane, concentrated to about 1mL and kept at -30°C to obtain 0.086g, 0.296 mmol of **17** (80% isolated yield) as red solid. X-ray quality crystals were grown by cooling concentrated hexane solution of **17** to -30°C for several days to afford **17**·½C$_6$H$_{14}$. Anal. Calc. for C$_{53}$H$_{87}$B$_2$N$_{12}$Si$_4$Y$_2$ (**17**·½C$_6$H$_{14}$)C, 52.87; H, 7.28; N, 13.96. Found C, 52.93; H, 7.32; N, 13.94.

^{1}H NMR (400 MHz C$_6$D$_6$, 27°C ; assigned by HMQC and HMBC) δ 5.93 (2H, s, 4-*H* Pz), 5.59 (s, 4H, 4-*H* Pz), 3.10 (s, 6H, 3-*Me* Pz), 2.48 (s,12H, 3-*Me* Pz), 2.27 (12H, s, 5-*Me* Pz). 2.22 (6H, s, 5-*Me* Pz), -0.05 (18H, s, SiMe$_3$), -0.22 (18H, s, SiMe$_3$). ^{13}C{^{1}H} NMR (100 MHz C$_6$D$_6$, 27°C ; assigned by HMQC and HMBC) δ 204.00 (d, $^1J_{YC}$ = 14.9 Hz, Me$_3$Si-*C*=C coupled alkynide), 173.07 (t, $^1J_{YC}$ = 21.7 Hz, Y-*C*≡C bridging alkynide), 158.28 (d, $^2J_{YC}$ = 4.6 Hz, Me$_3$Si-C=*C* coupled alkynide), 150.66 (3-*C* Pz), 149.95 (3-*C* Pz), 144.60 (5-*C* Pz), 144.33 (5-*C* Pz), 128.00 (hidden under C$_6$D$_6$ peaks, Y-C≡*C* bridging alkynide), 105.83 (4-*C* Pz), 105.50 (4-*C* Pz), 16.82 (3-*Me* Pz), 14.63 (3-*Me* Pz), 13.14 (5-*Me* Pz), 12.96 (5-*Me* Pz), -0.42 (SiMe$_3$), -0.59 (SiMe$_3$.) ^{11}B{^{1}H} (159.8 MHz, C$_6$D$_6$, 27°C) δ

-8.92.

(Tp^{Me2})$_2$Lu$_2$(μ−C≡CSiMe$_3$)$_2$(μ-SiMe$_3$CCCCSiMe$_3$) (18)

Following a procedure analogous to **17** using (Tp^{Me2})Lu(CH$_2$SiMe$_3$)$_2$(THF), **8a**, (0.137g, 0.190 mmol) and Me$_3$SiCCH (0.0370g, 0.380 mmol) affords **18** (98% isolated yield) as a red solid. Attempt to grow X-ray quality crystals by cooling a concentrated hexane solution of **18** to -30°C for several days gave poor quality crystals. Anal. Calc. for C$_{53}$H$_{87}$B$_2$N$_{12}$Si$_4$Lu$_2$ (**18**·½C$_6$H$_{14}$) C, 46.25; H, 6.37; N, 12.21. Found C, 46.24; H, 6.21; N, 11.85.

^{1}H NMR (400 MHz, C$_6$D$_6$, 27°C; assigned by HMQC and HMBC) δ 5.68 (2H, s, 4-*H* Pz), 5.61 (s, 4H, 4-*H* Pz), 3.11 (s, 6H, 3-*Me* Pz), 2.54 (s, 12H, 3-*Me* Pz), 2.27 (12H, s, 5-*Me* Pz). 2.22 (6H, s, 5-*Me* Pz), -0.04 (18H, s, SiMe$_3$), -0.26 (18H, s, SiMe$_3$). ^{13}C{^{1}H} NMR (100 MHz, C$_6$D$_6$, 27°C ; assigned by HMQC and HMBC) δ 204.99 (Me$_3$Si-*C*=C coupled alkynide), 177.67 (Lu-*C*≡C bridging alkynide), 155.61 (Me$_3$Si-C=*C* coupled alkynide), 151.13 (3-*C* Pz), 150.49 (3-*C* Pz), 144.55 (5-*C* Pz), 144.25 (5-*C* Pz), 128.00 (hidden under C$_6$D$_6$ peaks, Lu-C≡*C* bridging alkynide), 105.98 (4-*C* Pz), 105.77 (4-*C* Pz), 16.87 (3-*Me* Pz), 14.78 (3-*Me* Pz), 13.08 (5-*Me* Pz), 12.94 (5-*Me* Pz), -0.63 (SiMe$_3$), -0.66 (SiMe$_3$). ^{11}B{^{1}H} (159.8 MHz, C$_6$D$_6$, 27°C) δ -8.95.

(Tp^{Me2})₂Y₂(μ−C≡C^tBu)₂(μ-^tBuCCCC^tBu) (19)

To a colorless toluene solution (Tp^{Me2})Y(CH$_2$SiMe$_3$)$_2$(THF), **14a**, (0.058g, 0.092 mmol) was added 2 equiv. of ^{t}BuCCH (0.015g, 0.184 mmol) in drops. The solution slowly turned to a yellow color. The solution was kept at RT for ca. 24 h. Solvent was stripped in vacuum to obtain a pale yellow residue which was extracted with about 2mL hexane, concentrated to about 1mL and then cooled to -30°C overnight to obtain a pale yellow solid which was dried in vacuum to give 0.038g , 0.069 mmol of the **19** as a yellow powder in 77% isolated yield. Anal. Calc. for C$_{54}$H$_{80}$B$_2$N$_{12}$Y$_2$ C, 59.14; H, 7.35; N, 15.33. Found C, 58.04; H, 7.50; N, 15.04.

^{1}H NMR (400 MHz, C$_6$D$_6$, 27°C; assigned by HMQC and HMBC) δ 5.76 (2H, s, 4-*H* Pz), 5.67 (s, 4H, 4-*H* Pz), 3.13 (s, 6H, 3-*Me* Pz), 2.59 (s, 12H, 3-*Me* Pz), 2.25 (12H, s, 5-*Me* Pz). 2.19 (6H, s, 5-*Me* Pz), 0.94 (18H, s, C(CH$_3$)$_3$-coupled), 0.884 (18H, s C(CH$_3$)$_3$-bridging). ^{13}C{^{1}H} NMR (100 MHz, C$_6$D$_6$, 27°C ; assigned by HMQC and HMBC) δ 195.50 (d, ^{1}J$_{YC}$ = 17.2 Hz, ^{t}Bu-*C*=C coupled alkynide), 150.60 (3-*C* Pz), 149.90 (3-*C* Pz), 144.45 (5-*C* Pz), 144.38 (5-*C* Pz), 127.02 (t, ^{1}J$_{YC}$ = 23.6 Hz, Y-*C*≡C bridging alkynide), *β*-C of bridging alkynide not observed (hidden under benzene peak) 126.66 (dd, ^{2}J$_{YC}$ = 8.5 Hz, 1.5 Hz, ^{t}Bu-C=*C* coupled alkynide), 105.72 (4-*C* Pz), 105.21 (4-*C* Pz), 36.02 (*C*(CH$_3$)$_3$-coupled), 30.81 (C(*C*H$_3$)$_3$-coupled), 29.83 (C(*C*H$_3$)$_3$-bridging) 28.54 (*C*(CH$_3$)$_3$-bridging), 17.04 (3-*Me* Pz), 14.97 (3-*Me* Pz), 13.22 (5-*Me* Pz), 13.00 (5-*Me* Pz). ^{11}B{^{1}H} (128.32 MHz, C$_6$D$_6$, 27°C) δ -8.53.

(Tp^{Me2})$_2$Lu$_2$(μ−C≡C^{t}Bu)$_2$(μ-^{t}BuCCCC^{t}Bu) (20)

Following a procedure analogous to that for **19** using (Tp^{Me2})Lu(CH$_2$SiMe$_3$)$_2$(THF), **8a**, (0.10g, 0.139 mmol) and (0.023g, 0.278 mmol) ^{t}BuCCH, 0.074g, 0.255 mmol of **20** was obtained as a yellow powder in 80% isolated yield. ^{1}H NMR (400 MHz, C$_6$D$_6$, 27°C; assigned by HMQC and HMBC) δ 5.76 (2H, s, 4-H Pz), 5.69 (4H, s, 4-H Pz), 3.14 (6H, s, 3-Me Pz), 2.64 (12H, s, 3-Me Pz), 2.26 (12H, s, 5-Me Pz), 2.20 (6H, s, 5-Me Pz), 0.94 (18H, s, coupled C(CH$_3$)$_3$), 0.22 (18H, s, bridging C(CH$_3$)$_3$). ^{13}C{^{1}H} NMR (100 MHz, C$_6$D$_6$, 27°C ; assigned by HMQC and HMBC) δ 198.80 (^{t}Bu-C=C coupled alkynide), 150.99 (3-C Pz), 150.36 (3-C Pz), 144.36 (5-C-Pz), 144.22 (5-C Pz), 132.47 (Lu-C≡C bridging alkynide), 130.21 (^{t}Bu-C=C coupled alkynide), 128.52 (Lu-C≡C bridging alkynide), 105.89 (4-C Pz), 105.37 (4-C Pz), 36.05 (C(CH$_3$)$_3$-coupled), 30.70 (C(CH_3)$_3$-bridging), 29.66 (C(CH$_3$)$_3$-coupled), 28.50 (C(CH_3)$_3$-bridging), 17.34 (3-Me Pz), 15.26 (3-Me Pz), 13.20 (5-Me Pz), 12.99 (5-Me Pz), ^{11}B{^{1}H} (128.32 MHz, C$_6$D$_6$, 27°C) δ -9.10. Anal. Calc. for C$_{61}$H$_{88}$B$_2$N$_{12}$Lu$_2$ (**20**·C$_7$H$_8$) C, 53.83; H, 6.52; N, 12.35. Found C, 53.35; H, 6.34; N, 12.18.

(Tp^{Me2})$_2$Y$_2$(μ-C≡CAd)$_2$(μ-AdCCCCAd) (21)

To a colorless toluene solution (Tp^{Me2})Y(CH$_2$SiMe$_3$)$_2$(THF), **14a**, (0.10g, 0.158 mmol) in about 2 mL of toluene was added a solution of adamantyl acety-lene (0.051g, 0.316 mmol) in the same solvent. The solution slowly turned yellow. The solution was left to stand at RT for ca. 4 h during which time crystalline solid was deposited in the bottom of the vial, supernatant was decanted and the solid

washed with pentane and dried in vacuum to give a bright yellow crystalline solid. Solvent was stripped in vacuum from the decanted supernatant to obtain a yellow oily residue which upon trituration with pentane gave **21** as a yellow powder (0.92 g, 1.30 mmol) in 84 % combined yield. X-ray quality crystals were grown by allowing a dilute solution of adamantyl acetylene to slowly diffuse into a dilute solution of $(Tp^{Me2})Y(CH_2SiMe_3)_2(THF)$ in an NMR tube kept at room temperature for about 24 h and then cooling the resultant pale yellow solution to -30°C for several days. Anal. Calc. for $C_{92}H_{120}B_2N_{12}Y_2$ (**21**·$2C_7H_8$) C, 70.93; H, 7.59; N, 10.55. Found C, 70.11; H, 7.92; N, 10.65.

^{1}H NMR (400.4 MHz, C_6D_6, 27°C) δ 5.83 (2H, s, 4-*H* Pz), 5.74 (s, 4H, 4-*H* Pz), 3.25 (s, 6H, 3-*Me* Pz), 2.69 (s, 12H, 3-*Me* Pz), 2.26 (12H, s, 5-*Me* Pz). 2.20 (12H, s, 5-*Me* Pz), 1.93(8H, m, J_{HH} = 2.8 Hz, adamantyl), 1.72 (12H, m, adamantyl), 1.65 (12H, d, J_{HH} = 2.8 Hz, adamantyl), 1.57 (18H, s, adamantyl), 1.38 (12H, s, adamantyl) $^{13}C\{^1H\}$ NMR (100.7 MHz, C_6D_6, 60°C) δ 150.81 (3-*C* Pz), 150.25 (3-*C* Pz), 144.51 (5-*C* Pz), 105.74 (4-*C* Pz), 105.22 (4-*C* Pz), 43.29, 42.89, 41.55, 38.73, 37.72, 36.72, 29.82, 28.52 (adamantyl carbons atoms), 17.49 (3-*Me* Pz), 15.46 (3-*Me* Pz), 13.10 (5-*Me* Pz), 12.85 (5-*Me* Pz). $^{11}B\{^1H\}$ (C_6D_6, 27°C, 159.8 MHz) -8.92.

$(Tp^{Me2})Lu(CCPh)_2(THF\text{-}d_8)$

Dissolution of bright red solid **16** in THF-d_8 led gradually to a change in color from bright red to pale red/orange to yellow orange and finally to yellow. ^{1}H

NMR monitoring showed gradual disappearance of the signals due to **16** and the appearance of those due to the monomeric product. After about 2 h at room temperature, **16** had completely converted to $(Tp^{Me2})Lu(CCPh)_2(THF-d_8)$.

^{1}HNMR (400 MHz, THF-d_8, 27°C) δ 7.28 (4H, dd, $^3J_{HH}$ = 7.2 Hz, 1.6 Hz, o-H phenyl), 7.11 (4H, tt, $^3J_{HH}$ = 7.2 Hz, 1.6 Hz, m-H phenyl), 7.04 (2H, tt, $^3J_{HH}$ = 7.2 Hz, 1.6 Hz, p-H phenyl), 5.77 (3H, s, 4-H Pz), 2.66 (9H, s, 3-CH_3 Pz), 2.40 (9H, s, 5-CH_3 Pz). ^{13}C{^{1}H} (100.58 MHz, THF-d$_8$, 27°C) δ 154.51 (C≡C-Ph), 151.56 (3-C Pz), 145.84 (5-C Pz), 132.73 (*ipso* C phenyl), 132.27 (*o*-C phenyl), 128.31 (*m*-C phenyl), 125.97 (*p*-C phenyl), 106.39 (4-C Pz), 105.85 (C≡C-Ph), 14.34 (3-CH_3 Pz), 12.96 (5-CH_3 Pz).^{11}B{^{1}H} (160 MHz, THF-d_8, 27°C) δ -10.77.

$(Tp^{Me2})Y(CCSiMe_3)_2(THF-d_8)$.

Dissolution of deep red solid **17** in THF-d_8 led gradually to a change in color from deep red to pale red/orange to orange and finally to pale-pink. ^{1}H NMR monitoring shows gradual disappearance of the signals due to **17** and the appearance of those due to the monomeric product. After about 2 h at room temperature, **17** had completely converted to $(Tp^{Me2})Y(CCSiMe_3)_2(THF-d_8)$.

^{1}HNMR (500 MHz, THF-d_8, 27°C) δ 5.70 (3H, s, 4-H Pz), 2.56 (9H, s, 3-CH_3 Pz), 2.37 (9H, s, 5-CH_3 Pz). 0.02 (18H, s, SiMe$_3$). ^{13}C{^{1}H} (125.3 MHz, THF-d_8, 27°C) δ 170.26 (d, $^1J_{YC}$ = 53.50 Hz, C≡C-SiMe$_3$), 150.95 (3-C Pz), 145.64 (5-C Pz), 106.98 (d, $^2J_{YC}$ = 10.15 Hz, C≡C-SiMe$_3$), 106.19 (4-C Pz), 14.73 (3-CH_3 Pz), 12.95 (5-CH_3 Pz), 1.29 (SiMe$_3$). ^{11}B{^{1}H} (160 MHz, THF-d_8, 27°C) δ -9.30.

(Tp^Me2^)Lu(CC^t^Bu)₂(2,2′-Bipy) (22)

To a colorless toluene solution of $(Tp^{Me2})Lu(CH_2SiMe_3)_2(THF)$, **8a** (0.140g, 0.20 mmol) was added 1 equiv. of 2,2′-bipyridine (0.30g) in about 1 mL toluene. The solution turned red immediately. To the red solution was then syringed 2 equiv. of *tert*-butyl acetylene (0.034g, 0.40 mmol) in drops. The solution slowly turned to orange-yellow and the resulting solution was kept at RT for ca. 24 h. Solvent was stripped under vacuum to obtain a pinkish oily residue which was triturated with pentane to obtain a pink solid. Cooling a dilute toluene solution to -30°C for several days afforded pale pink crystals suitable for X-ray studies as the benzene solvate. Anal. Calc. for $C_{37}H_{48}BN_8Lu$ C, 56.21; H, 6.12; N, 14.17. Found C, 56.42; H, 6.34; N, 13.35.

^{1}H NMR (400 MHz, C_6D_6, 40°C) δ 10.77 (1H, s, Bipy), 7.27 (1H, ddd, $^{2}J_{HH}$ = 8.0 Hz, 2.4 Hz, 0.8 Hz, bipy), 7.12-6.99 (4H, overlapping multiplets, bipy), 6.78 (1H. dt, $^{2}J_{HH}$ = 8.0 Hz, 1.6Hz, bipy), 6.03 (1H, dt, $^{2}J_{HH}$ = 8.0 Hz, 1.2 Hz, bipy), 5.78 (1H, s, 4-*H* Pz), 5.56 (2H, s, 4-*H* Pz), 3.57 (3H, s, 3-*Me* Pz), 2.27 (6H, s, 5-*Me* Pz), 2.24 (3H, s, 5-*Me* Pz). 2.07 (6H, s, 3-*Me* Pz), 1.22 (18H, s, C(C*H₃*)₃). ^{13}C{^{1}H} NMR (100.7 MHz, C_6D_6, 40°C) δ 157.18 (bipy), 155.45 (bipy), 152.08 (3-*C* Pz), 151.95 (bipy), 149.34 (3-*C* Pz), 143.65 (Lu-*C*≡CC(CH₃)₃), 142.58 (5-*C* Pz), 141.97 (5-*C* Pz), 138.83 (bipy), 138.09 (bipy), 125.64 (bipy), 124.23 (bipy) 123.90 (bipy), 119.75 (bipy), 119.32 (bipy), 113.32 (Lu-C≡*C*C(CH₃)₃), 106.05 (4-*C* Pz), 105.82 (4-*C* Pz), 33.09 (*C*(CH₃)₃, 32.94 C(*C*H₃)₃, 16.76 (3-*Me* Pz), 14.68 (3-*Me* Pz), 14.33 (5-*Me* Pz), 13.09 (5-*Me* Pz). ^{11}B{^{1}H} (159.8 MHz, C_6D_6, 27°C) δ -8.92.

(Tp^{Me2})Y(CCTrit′)$_2$(THF) (23)

To a colorless toluene solution (Tp^{Me2})Y(CH$_2$SiMe$_3$)$_2$(THF), **14a**, (0.063g, 0.10 mmol) in about 2 mL of toluene was added a pale pink solution of Trit′CCH (0.012g, 0.20 mmol) in the same solvent. The mixture became pale pink. The solution was left to stand at RT overnight (ca. 19 h). Solvent was stripped under vacuum to obtain a pale pink oily residue which upon trituration with pentane gave a pale pink solid. Recrystallization of the solid from pentane afforded **23** as a white powder (0.128g, 0.80 mmol) in 77 % recrystallized yield. Anal. Calc. for C$_{109}$H$_{156}$BN$_6$YO C, 78.57; H, 9.44; N, 5.04. Found C, 78.43; H, 9.45; N, 4.32.

^{1}H NMR (500 MHz, C$_6$D$_6$, 27°C) δ 7.57 (12H, d, $^3J_{HH}$ = 1.6 Hz, o-H Ar″), 7.39 (6H, t, $^3J_{HH}$ = 1.6 Hz, p-H Ar″), 5.47 (3H, s, 4-H Pz), 4.07 (br, s, THF), 3.10 (3H, s, 3-CH_3 Pz), 2.26 (6H, s, 3-CH_3 Pz), 2.19 (9H, s, 5-CH_3 Pz), 1.43 (4H, br s, THF), 1.27 (108H, s, C(CH_3)$_3$), ^{13}C{^{1}H} (125.3 MHz, C$_6$D$_6$, 27°C) δ 150.36 (3-C Pz), 149.26 (m-C Ar″), 148.22 (ipso-C Ar″), 144.84 (5-C Pz), 136.89 (d, $^1J_{YC}$ = 58.9 Hz, Y-C≡C-C-Ar″), 124.87 (o-C Ar″), 119.19 (p-C Ar″), 106.87 (d, $^2J_{YC}$ =12.0 Hz, Y-C≡C-C-Ar″), 106.01 (4-C Pz), 70.79 (THF), 58.25 (Y-C≡C-C-Ar″), 35.00 (C(CH$_3$)$_3$), 31.78 (C(CH_3)$_3$), 25.49 (THF), 14.61 (3-CH$_3$ Pz),12.93 (5-CH$_3$ Pz). ^{11}B{^{1}H} (160 MHz, C$_6$D$_6$, 27°C) δ -9.15.

(Tp^{Me2})Lu(CCTrit′)$_2$(THF) (24)

Following a procedure analogous to that for **23** using (Tp^{Me2})Lu(CH$_2$SiMe$_3$)$_2$(THF) (0.072g, 0.100 mmol) and Trit′CCH (0.121g, 0.200

mmol), 0.134g, 0.080 mmol of **24** was obtained as a white powder in 77% isolated yield. X-ray quality crystals were obtained by keeping a concentrated pentane solution at room temperature for several days. Anal. Calc. for $C_{109}H_{156}BN_6LuO$ C, 74.72; H, 8.97; N, 4.80. Found C, 74.36; H, 9.12; N, 4.49.

^{1}H NMR (500 MHz, C_6D_6, 27°C) δ 7.56 (12H, d, $^3J_{HH}$ = 2.0 Hz, o-*H* Ar″), 7.39 (6H, t, $^3J_{HH}$ = 2.0 Hz, *p*-H Ar″), 5.49 (1H, s, 4-*H* Pz), 5.47 (2H, s, 4-*H* Pz), 4.13 (br, THF), 3.13 (3H, s, 3-C*H₃* Pz), 2.26 (6H, s, 3-C*H₃* Pz), 2.22 (3H, s, 5-C*H₃* Pz), 2.17 (6H, s, 5-C*H₃* Pz), 1.45 (4H, br THF), 1.27 (108H, s, C(C*H₃*)₃). ^{13}C{^{1}H} (100.5 MHz, C_6D_6, 27°C) δ 151.66 (3-*C* Pz), 150.88 (3-*C* Pz), 149.25 (*m*-C Ar″), 148.19 (*ipso*-C Ar″), 147.11 (Lu-C≡C-C-Ar″), 144.67 (5-*C* Pz), 144.47 (5-*C* Pz), 124.90 (*o*-C Ar″), 119.21 (*p*-C Ar″), 109.83 (Lu-C≡*C*-C-Ar″), 106.16 (4-*C* Pz), 105.87 (4-*C* Pz), 71.33 (THF), 58.29 (Lu-C≡C-*C*-Ar″), 35.00 (*C*(CH₃)₃), 31.78 (C(*C*H₃)₃), 25.63 (THF), 15.17 (3-*C*H₃ Pz), 14.65 (3-*C*H₃ Pz), 12.88 (5-*C*H₃ Pz), 12.65 (5-*C*H₃ Pz). ^{11}B{^{1}H} (128 MHz, C_6D_6, 27°C) -9.14.

(Tp*^{tBu,Me}*)Y(CCPh)₂ (26)

To a colorless THF solution (Tp*^{tBu,Me}*)Y(CH₂SiMe₃)₂, **25a**, (0.010g, 0.145 mmol) was added 2 equiv. of PhCCH (0.030g, 0.290 mmol) in drops. The solution gradually changed color from colorless to pale yellow, then deep orange-yellow and finally to a light brown color. The solution was kept at RT for ca. 24 h. Solvent was stripped under reduced pressure to obtain an oily residue which was triturated with hexane to obtain a yellow orange solid with a greenish tint. The solid was washed several times with hexane until the supernatant was colorless. The

solid was dried in vacuum to obtain 0.073g, 1.022 mmol of **26** (71% isolated yield) as a yellow solid. Attempts to grow X-ray quality crystals proved unsuccessful. Anal. Calc. for $C_{40}H_{50}BN_6Y$ C, 67.23; H, 7.05; N, 11.76. Found C, 66.53; H, 7.06; N, 11.24.

^{1}H NMR (500 MHz, C_6D_6, 27°C) δ 7.57 (4H, d, $^3J_{HH}$ = 7.66 Hz, o-*H* Ph), 7.01 (4H, t, $^3J_{HH}$ = 7.66, Hz, *m*-H Ph), 6.92 (2H, t, $^3J_{HH}$ = 7.66 Hz, *p*-H Ph), 5.61 (3H, s, 4-*H* Pz), 2.00 (9H, s, 5-C*H*$_3$ Pz), 1.70 (27H, s, 3 (C*H*$_3$)$_3$ Pz). ^{13}C{^{1}H} (125.53 MHz, C_6D_6, 27°C) δ 165.25 (3-*C* Pz), 146.55 (5-*C* Pz), 143.77 (d, $^1J_{YC}$ = 59.3 Hz, *C*≡C-Ph), 132.09 (*o*-C Ph), 128.29 (*m*-C Ph) 127.36 (*ipso* C Ph), 126.15 (*p*-C Ph), 102.22 (d, $^2J_{YC}$ = 12.2 Hz C≡*C* Ph), 103.39 (4-*C* Pz), 32.99 (*C*(CH$_3$)$_3$-Pz), 31.69 (C(*C*H$_3$)$_3$-Pz), 13.05 (5-*C*H$_3$ Pz). ^{11}B{^{1}H} (160 MHz, C_6D_6, 27°C) δ -8.26.

(Tp^{tBu,Me})Lu(CCPh)$_2$ (27)

Following a procedure analogous to **26** using (Tp^{Me2})Lu(CH$_2$SiMe$_3$)$_2$ (0.072g, 0.100 mmol) and phenyl acetylene (0.021g, 0.200 mmol) affords (0.086g, 0.296 mmol) of **27** as a yellow solid in 80% isolated yield. Attempts to grow X-ray quality crystals proved unsuccessful. Anal. Calc. for $C_{40}H_{50}BN_6LuC$, 60.01; H, 6.29; N, 10.50. Found C, 60.35; H, 5.69; N, 9.71.

^{1}H NMR (500 MHz, C_6D_6, 27°C) δ 7.57 (4H, d, $^3J_{HH}$ = 8.0 Hz, o-*H* Ph), 7.01 (4H, t, $^3J_{HH}$ = 8.0, Hz, *m*-H Ph), 6.91 (2H, t, $^3J_{HH}$ = 8.0 Hz, *p*-H Ph), 5.64 (3H, s, 4-*H* Pz), 1.97 (9H, s, 5-C*H*$_3$ Pz), 1.74 (27H, s, 3 (C*H*$_3$)$_3$ Pz). ^{13}C{^{1}H}

(125.53 MHz, C_6D_6, 27°C) δ 165.99 (3-C Pz), 155.81 ($C{\equiv}C$-Ph), 146.57 (5-C Pz), 132.10 (*ipso* C Ph), 132.27 (*o*-C Ph), 126.75 (*p*-C Ph), 126.17 (*m*-C Ph), 108.20 ($C{\equiv}C$-Ph), 103.84 (4-C Pz), 32.93 ($C(CH_3)_3$-Pz), 31.51 ($C(CH_3)_3$-Pz), 13.03 (5-CH_3 Pz). $^{11}B\{^1H\}$ (160 MHz, C_6D_6, 27°C) δ -8.33.

4.8.4   Protonolysis

General Procedure

Benzene solution of the appropriate bis-alkynide dimer was treated with 4 equiv. of 2,4,6-trimethylphenol in the same solvent. The ^1H NMR spectrum of the solution taken after about 30 mins showed quantitative formation of the yttrium aryloxide, $(Tp^{Me2})Y(OMes)_2$ in addition to 2 equiv. of free alkyne and 1 mole of the corresponding 1,4-disubstituted-Z- enyne. Protonolysis of **15** and **19** are given below as representative examples.

NMR Tube Reaction of $[(Tp^{Me2})Y(CCPh)_2]_2$ (15) With 2,4,6-trimethylphenol

2,4,6-trimethylphenol (5 mg, 34 μmol) dissolved in ca. 0.3 mL of C_6D_6 was added to an NMR tube containing 10 mg (8.4 μmol) of **15** in the same solvent. The solution changed immediately to pale pink and then to colorless. ^1H NMR of the solution after about 30 mins showed formation of 2 equiv. of the aryloxide, $(Tp^{Me2})Y(OMes)_2$, 1 equiv. of 1,4-*Z*-diphenyl-butenyne as well as two equivalent of free phenyl acetylene.

^1H and $^{13}C\{^1H\}$ NMR data of $(Tp^{Me2})Y(OMes)_2$ are listed below. The spectral data for the coupled products are listed at the end of the next section.

^{1}H NMR (400 MHz, C$_6$D$_6$, 27°C) δ 6.90 (4H, s, m-*H* Ph), 5.44 (3H, s, 4-*H*

Pz), 2.27 (6H, s, *p*-Me Ph), 2.24 (12H, s, *o*-Me Ph), 2.08 (9H, s, 3-C*H$_3$* Pz), 2.06,

(9H, s, 5-C*H$_3$* Pz). ^{13}C{^{1}H} (100 MHz, C$_6$D$_6$, 27°C) δ 159.53 (d, J_{YC} = 5.0 Hz,

ipso-C Ph), 151.16 (3-*C* Pz), 145.93 (5-*C* Pz), 129.09 (*m*-C Ph), 125.42 (*o*-C Ph)

125.13 (*p*-C Ph), 106.03 (4-*C* Pz), 20.89 (*p*-Me Ph), 17.84 (*o*-Me Ph), 13.17 (3-

C*H$_3$* Pz), 12.87 (5-C*H$_3$* Pz).

NMR Tube Reaction of [(Tp^{Me2})Y(CC^{t}Bu)$_2$]$_2$ (19) With 2,4,6-trimethylphenol

The same approach was used as for **15**, with 5 mg (36.4 μmol) of 2,4,6-

trimethylphenol and 10 mg (9.1 μmol) of **19**. The color of the solution changed to

very pale yellow and then to colorless after sitting at room temperature for about

30 mins. The ^{1}H NMR taken at this time showed formation of 2 equiv. of the ary-

loxide, (Tp^{Me2})Y(OMes)$_2$, 2 equiv. of free *tert*-butyl acetylene as well as a mixture

of 1,4-*Z*-(^{t}Bu)$_2$-butenyne (80%) and 1,4-(^{t}Bu)$_2$-butatriene (20%).

^{1}H and ^{13}C{^{1}H}NMR data for (Tp^{Me2})Y(OMes)$_2$ is as listed above.

4.8.5   General Procedure for Catalytic Dimerization of Terminal Alkynes

All reactions were carried out on an NMR scale. To a C$_6$D$_6$ solution of the

bis-alkynide complex in an NMR tube was syringed an excess of the correspond-

ing terminal alkyne. The NMR tube was flamed sealed and heated in an oil bath at

80°C for 72 h with periodic monitoring of the reaction by ^{1}H NMR spectroscopy.

4.8.6 NMR Tube Reaction for Catalytic Dimerization of HC≡CSiMe₃ by [(Tp^{Me2})Y(CCSiMe₃)₂]₂ (17)

In an NMR tube, HC≡CSiMe₃ (70μL, 0.50 mmol) was added by syringe to a C_6D_6 solution of the yttrium bis-alkynide complex **17** (12 mg, 10 μmol). The tube was flame sealed and heated in an oil bath at 80°C for 72 h while periodically monitoring the reaction by ¹H NMR spectroscopy. After 72 h of heating, about 50% of the free alkyne was converted to the dimer as seen in the ¹H NMR spectrum. Analysis of the reaction solution by GC-MS showed the formation of the dimer, 1,4-E-(SiMe₃)₂-butenyne, as well as trimers.

4.8.7 Spectroscopic Data for Dimeric Products

***Z*-Ph-CH=CHC≡C-Ph:** ¹H NMR (400 MHz, C_6D_6, 27°C): δ 7.92 (1H, d (br), J_{HH} = 7.57 Hz, Ph), 7.43 (1H, dd, J_{HH} = 7.57 Hz, 1.82, Ph), 6.97-6.87 (8H, m, Ph), 6.41 (1H, d, J_{HH} = 12.07 Hz, =C*H*Ph), 5.79 (1H, d, J_{HH} = 12.07, = C*H*C≡CPh). ¹³C{¹H} NMR (100 MHz, C_6D_6, 27°C): δ 139.33 (=*C*HPh), 137.29, 131.95, 129.47, 128.91, 128.74, 124.21 (Ph carbons), 107.89 (=*C*HC≡CPh), 96.85 (=CH*C*≡CPh), 89.14 (=CHC≡*C*Ph). GC-MS: m/z = 204 (M⁺).

***E*-Me₃Si-CH=CHC≡C-SiMe₃:** ¹H NMR (400 MHz, C_6D_6, 27°C): δ 6.51 (1H, d, J_{HH} = 19.20 Hz, =C*H*SiMe₃), 5.99 (1H, d, J_{HH} = 19.20, = C*H*C≡CSiMe₃) 0.20, -0.09 (9H, 9H, SiMe₃). ¹³C{¹H} NMR (100 MHz, C_6D_6, 27°C): δ 145.33 (=*C*HSiMe₃), 124.89 (=*C*HC≡CSiMe₃), 107.0 (=CH*C*≡CSiMe₃), 95.0 (=CHC≡*C*SiMe₃). GC-MS: m/z = 196 (M⁺).

***Z*-Me₃Si-CH=CHC≡C-SiMe₃:** ^{1}H NMR (400 MHz, C₆D₆, 27°C): δ 6.25 (1H, d,

J_{HH} = 15.2 Hz, =C*H*SiMe₃), 6.01 (1H, d, J_{HH} = 15.2 Hz = C*H*C≡CSiMe₃) 0.25,

0.17 (9H, 9H, SiMe₃). ^{13}C{^{1}H} NMR (100 MHz, C₆D₆, 27°C): δ 145.92

(=*C*HSiMe₃), 125.31 (=*C*HC≡CSiMe₃), 106.03 (=CHC≡*C*SiMe₃), 98.60

(=CH*C*≡CSiMe₃) -0.30, -1.02 (SiMe₃). GC-MS: *m/z* = 196 (M^{+}).

***Z*-^{t}Bu-CH=CHC≡C-^{t}Bu:** ^{1}H NMR (400 MHz, C₆D₆, 27°C): δ 5.56 (1H, d, J_{HH} =

12.0 Hz, =C*H*CMe₃), 5.47 (1H, d, J_{HH} = 12.0 Hz = C*H*C≡CCMe₃) 1.25, 1.19 (9H,

9H, CMe₃). ^{13}C{^{1}H} NMR (125 MHz, C₆D₆, 27°C): δ 150.27 (=*C*HCMe₃),

118.57 (=*C*HC≡CCMe₃), 107.28 (=CHC≡*C*CMe₃), 67.45 (=CHC≡*C*Me₃) 29.90

(C(*C*H₃)₃), 27.31 (*C*Me₃).

^{t}BuCH=C=C=CH-^{t}Bu: ^{1}H NMR (C₆D₆, 400 MHz): δ 5.55 (2H, s, =CH), 1.08

(18H, s, CMe₃) ^{13}C{^{1}H} NMR (C₆D₆, 125 MHz): δ 160.24 (=C=*C*HCMe₃),

118.57 (=*C*HCMe₃), 35.12 (*C*(CH₃)₃), 29.70 (CMe₃).

4.8.8   X-ray Structure Determinations

The crystals were handled as described in previous Chapters. Complete X-ray structure determinations for other compounds were carried out by Dr R. McDonald and Dr. M. J. Ferguson at the X–ray Crystallographic Laboratory, Department of Chemistry University of Alberta.

Summary of data collection and structure refinement are given in the Structure Reports; **15** (TAK 0411); **16** (TAK 0506); **17** (TAK 0730); **21** (TAK 0731); **22** (TAK 0738); **24** (TAK 0915).

4.9   References

1. Trost, B. M. *Acc. Chem. Res.* **2002**, *35*, 695-705.

2. Heeres, H. J. Teuben, J. H. *Organometallics* **1991**, *10*, 1980-1986.

3. Evans, W. J.; Keyer, R. A.; Ziller, J. W. *Organometallics* **1993**, 12, 2618-2633.

4. Nishiura, M.; Hou, Z.; Wakatsuki, Y.; Yamako, T.; Miyamoto, T. *J. Am. Chem. Soc.* **2003**, *125*, 1184-1185.

5. (a) Atwood, J. L.; Hains, C. F.; Tsutsui, M.; Gebala, E. *J. Chem. Soc. Chem. Commun.* **1973**, 452-453. (b)Tsutsui, M.; Ely, N. *J. Am. Chem. Soc.* **1974**, *96*, 4042-4043. (c) Evans, W. J.; Wayda, A. L. *J. Organomet. Chem.* **1980**, 202, C6-C8. (d) Edelmann, F. T. In *Comprehensive Organometallic Chemistry* III; Crabtree, R. H.; Mingos, D. M. P., Eds.; Elsevier, Oxford, *Vol. 401*, **2006**, pp. 1–199. (e) Nast, R. *Coord. Chem. Rev.* **1982**, *47*, 89-124.

6. Evans, W. J.; Bloom, I.; Hunter, W. E.; Atwood, J. L. *Organometallics* **1983**, *2*, 709-714.

7. Atwood, J. L.; Hunter, W. E. Wayda, A. L.; Evans, W. J. *Inorg. Chem.* **1981**, *20*, 4115-4119.

8. Shen, Q.; Zheng, D.; Lin, L.; Lin, Y. *J. Organomet. Chem.* **1990**, *391*, 307-312.

9. Lee, L.; Berg, D. J.; Bushnell, G. W. *Organometallics* **1995**, *14*, 5021-5023.

10. Sun, J. The Synthesis and Characterization of Lanthanide Complexes with

Phenalenide and Aromatic-Fused Cyclopentadienyls as Ligands. Ph.D

Thesis University of Victoria, British Columbia, Canada. **2007**.

11. Duchateau, R.; van-Wee, C. T.; Teuben, J. H. *Organometallics* **1996**, *15*, 2291-2302.

12. Ren, J.; Hu, J.; Lin, Y.; Xing, Y.; Shen, Q. *Polyhedron* **1996**, *15*, 2165-2169.

13. (a) Evans, W. J.; Keyer, R. A.; Ziller, J. W. *Organomtallics* **1990**, *9*, 2628-2631. (b) Evans, W. J.; Keyer, R. A.; Ziller, J. W. *Organomtallics* **1993**, 12, 2618-2633.

14. Heeres, H. J.; Nijhoff, J.; Teuben, J. H.; Rogers, R. D. *Organometallics* **1993**, *12,* 2609-2617.

15. Forsyth, C. M.; Nolan, S. P.; Stern, C. L.; Marks, T. J.; Rheingold, A. L. *Organometallics* **1993**, *12*, 3618-3623.

16. Evans, W. J.; Ulibarri, T. A.; Chamberlain, L. R.; Ziller, J. W.; Alvarez, D., Jr. *Organometallics* **1990**, *9*, 2124-2130.

17. (a) den Haan, K. H.; Wielstra, Y.; Teuben, J. H. *Organometallics* **1987**, 6, 2053-2060. (b) Duchateau, R.; Brussee, E. A. C.; Meetsma, A.; Teuben, J. H. *Organometallics* **1997**, *16*, 5506-5516.

18. Lin, G. Y.; McDonald, R.; Takats, J. *Organometallics* **2000**, *19*, 1814-1816.

19 . Cheng, J.; Saliu, K.; Kiel, G.; Ferguson, M. J.; McDonald, R.; Takats, J. *Angew. Chem. Int. Ed.* **2008**, *47*, 4910-4913.

20. Tazelaar, C. G. J.; Bambirra, S.; van Leusen, D.; Meetsma, A.; Hessen, B.;

Teuben, J. H. *Organometallics* **2004**, *23*, 936-939.

21. Cameron, T. M.; Gordon, J. C.; Scott, B. L. *Organometallcs* **2004**, *23*, 2995-3002.

22. Ge, S.; Meetsma, A.; Hessen, B. *Organometallics* **2009**, *28*, 719-726.

23. Shannon, R. D. *Acta Crystallogr*. *A32*, 751-767.

24. Liu, B.; Liu, X.; Cui, D.; Liu, L. *Organometallics* **2009**, *28*, 1453-1460.

25. Emslie, D. J. H.; Piers, W. E.; Parvez, M.; McDonald, R. *Organometallics* **2002**, 21, 4226-4240. (b) Emslie, D. J. H.; Piers, W. E.; MacDonald, R. *J. Chem. Soc. Dalton Trans*. 2002, 293.

26. Zhang, W-X.; Nishiura, M.; Zhaomin, H. *J. Am. Chem. Soc*. **2005**, *127*, 16788-16789.

27. Evans, W. J.; Bloom, I.; Hunter, W. E.; Atwood, J. L. *Organometallics* **1983**, *2*, 709-714.

28. Atwood, J. L.; Hunter, W. E. Wayda, A. L.; Evans, W. J. *Inorg. Chem*. **1981**, *20*, 4115-4119.

29. Cox, P. A.; Ewart, I. C.; Stigliani, W. M. *J. Chem. Soc., Faraday Trans. 2* **1975**, 504.

30. Stucky, G.D.; McPherson, A. M.; Rhine, W. E.; Eisch, J. J.; Considine, J. L. *J. Am. Chem. Soc*. **1974**, *96*, 1941-1942.

31. Korolev, A. V.; Guzei, I. A.; Jordan R. F. *J. Am. Chem. Soc*. **1999**, *121*, 11605-11606.

32. Trofimenko, S.; Calabrese, J. C. Kochi, J. K.; Wolowiec, S.; Hulsbergen, F. B.; Reedijk, J. *Inorg. Chem*. **1992**, *31*, 3943-3950.

33. Roitershtein, D.; Domingos, A.; Pereira, L. C. J.; Ascenso, J. R.; Marques, N. *Inorg. Chem*. **2003**, *42*, 7666-7673.

34. Sun,C-D.; Wong, W. T. *Inorg. Chim. Acta* **1997**, *255*, 355-360.

35. Liu, S-Y.; Maunder, G.H.; Sella, A.; Stevenson, M.; Tocher, D. *Inorg. Chem*. **2003**, *42*, 7666-7673.

36 Akita, M.; Yasuda, H.; Nakamura, A. *Bull. Chem. Soc. Jpn*. **1984**, *57*, 480-487.

37. Lee, L. Deprotonated Aza-Crown as Simple and Effective Alternatives to C_5Me_5 in Group 3, 4 and Lanthanide Chemistry. Ph.D Thesis, University of Victoria, British Columbia, Canada. **1997**.

38. Yi, C. S.; Liu, N. *Organometallics* **1996,** *15,* 3968-3971.

39. Haskel, A.; Straub, T.; Dash, A. K.; Eisen, M. S. *J. Am. Chem. Soc*. **1999**, *121*, 3014-3124.

40. Wakatsuki, Y.; Yamazaki, H.; Kumegawa, N.; Satoh, T.; Satoh, J. Y. *J. Am. Chem. Soc*. **1991**, *113*, 9604-9610.

Chapter 5

Lanthanide Benzyl Complexes; Lutetium Tribenzyl[*] and Scorpionate Supported Lanthanide Dibenzyl Complexes

5.1   Introduction

The limited reactivity of the lanthanide dialkyl complexes reported in Chapter 3, which may be attributed to steric congestion around the lanthanide center, led to the exploration of other possibilities with reduced steric congestion without compromising the stability of the resulting dialkyl complexes. As briefly discussed in Chapter 3, the first approach taken to achieve this was by the use of the unsubstituted tris(pyrazolyl)borate ligand, Tp. This approach was rather limited in value since only the lutetium compound, $(Tp)Lu(CH_2SiMe_3)_2(THF)$, was found to have sufficient thermal stability. Although the yttrium and ytterbium analogues could be isolated, they proved to be much more delicate. A second approach is the use of less bulky alkyl groups which may permit a higher reactivity at the lanthanide center. As was shown in Chapter 3, both the protonolysis and alkyl abstraction protocols require the availability of the homoleptic lanthanide trialkyls, $LnR_3(THF)_n$. To this end, there have been searches for other alternative alkyl ligands that have the ability to satisfy the large ionic radii of the lanthanides either due to their steric bulk or by multihapto bonding, the latter being the more

---

[*] A brief account of the synthesis and structures of $Lu(CH_2Ph)_3(THF)_{3/2}$ along with their scandium analogues has appeared; Meyer, N.; Roesky, P. W.; Bambirra, S.; Meetsma, A.; Hessen, B.; Saliu, K.; Takats, J. *Organometallics* **2008**, *27*, 1501-1505.

desirable property. A potential candidate is the benzyl ligand, PhCH$_2$-, and thus there has been considerable interest in the synthesis of homoleptic lanthanide tribenzyls as precursors for the synthesis of (Ligand)Ln(CH$_2$Ph)$_2$ complexes.

Initial attempts to isolate homoleptic lanthanide tribenzyl complexes Ln(CH$_2$Ph)$_3$(THF)$_x$ (Ln = Y and Nd and La)[1,2] presented no conclusive evidence that the homoleptic lanthanide tribenzyls were actually made. The lanthanum complex was reported to effect the ring opening reaction of a THF molecule to give a benzyl hydrido vinyloxide lanthanum complex of composition C$_6$H$_5$CH$_2$La(H)(OCH=CH$_2$)(THF)$_2$,[1] whereas for Y and Nd, decomposition to the alkylidene species, "C$_6$H$_5$CH=LnCH$_2$C$_6$H$_5$" was proposed.2 However, by using the intramolecularly coordinating *ortho*-N,N-dimethylaminobenzyl ligand, (CH$_2$C$_6$H$_4$NMe$_2$-*o*), Manzer reported the synthesis and characterization of Sc(CH$_2$C$_6$H$_4$NMe$_2$-*o*)$_3$[3] and almost three decades later, Harder reported the synthesis, characterization and the reactivity of the yttrium and lanthanum analogues.[4] Recently, Hessen and co-workers have successfully prepared the lanthanum tribenzyl complexes, La(CH$_2$Ph-4-R)$_3$(THF)$_3$ (R = H, Me) and showed that they can serve as a convenient starting material for LLa(CH$_2$Ph-4-R)$_2$ complexes (L = ArN=CPhNAr, N-{2-pyrolidin-1-ylethyl}-1,4-diazepan-6-amido ligand).[5,6] This synthesis has been extended to include other lanthanide metals such as Sc and Lu.[7,8]

5.2 Synthesis of Lutetium Tribenzyl Complexes

5.2.1 Lu(CH$_2$Ph-4-R)$_3$(THF)$_3$ (R = H, Me)

Treatment of an *in-situ* generated THF suspension of LuCl$_3$(THF)$_3$ with 3 equiv. of the appropriate potassium benzyl reagent, KCH$_2$Ph-4-R (R = H, Me) in THF at low temperature, followed by slow warming to room temperature over about 2 h affords a pale yellow mixture. The mixture was centrifuged to obtain a pale yellow solution and colorless gelatinous precipitate, containing KCl. The solution was concentrated, layered with hexanes and cooled to -30°C overnight to afford pale-yellow powders of the presumed complexes, Lu(CH$_2$Ph–4–R)$_3$(THF)$_3$ (R = H, **28a**; R = Me, **28b**) Scheme 5.1.
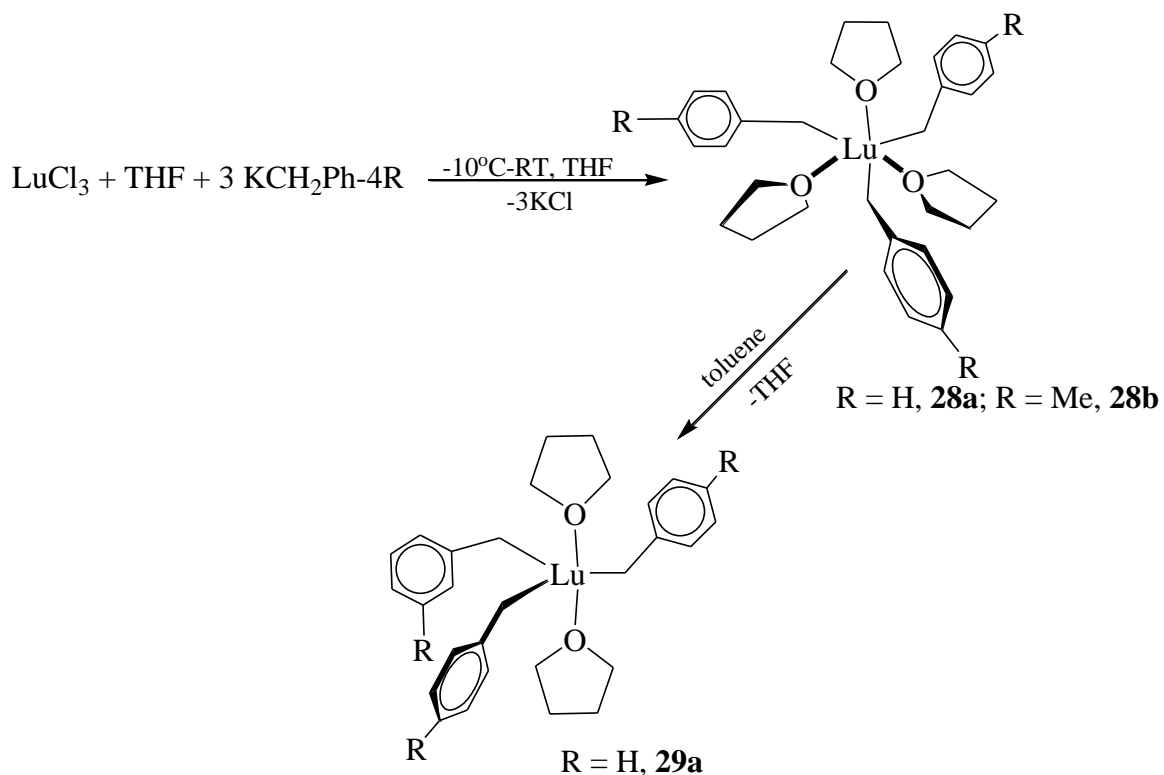
Scheme 5.1: Synthesis of Lu(CH$_2$Ph-4-R)$_3$(THF)$_3$ (R = H, **28a**; R = Me, **28b**) and Lu(CH$_2$Ph)$_3$(THF)$_2$ (**29a**).

Subsequently, extensive variable temperature NMR studies in THF-d_8 revealed that the first products of the reaction contained variable amounts of the "ate" complexes, K[Lu(CH$_2$Ph-4-R)$_4$(THF)$_n$], **30** (Section 5.4). Analytically pure samples of the tri-benzyl complexes could however be obtained by one of three ways: (i) repeated recrystallization from THF/hexanes, with substantial loss of material (ii) recrystallization from THF/ toluene/ pentane, also with significant material loss (see Experimental Section) or (iii) addition of THF to a toluene solution of Lu(CH$_2$Ph)$_3$(THF)$_2$ (Section 5.2.2).

5.2.2   Lu(CH$_2$Ph)$_3$(THF)$_2$ (29a)

Similar to the observation made on the analogous scandium tribenzyl complex Sc(CH$_2$Ph)$_3$(THF)$_3$,[7] repeated trituration of the pale yellow solid from the Lu-tribenzyl preparation with toluene at room temperature resulted in the ready loss of one THF molecule. Extraction of the so obtained orange-yellow solid with toluene followed by crystallization gave Lu(CH$_2$Ph)$_3$(THF)$_2$, **29a**, as orange blocks in high yield, Scheme 5.1. A small amount of a pale yellow solid, later identified as K[Lu(CH$_2$Ph-4-R)$_4$(THF)$_n$], **30a**, was left behind from the extraction (*vide infra*). The difference between compounds **28a** and **29a** is obviously the number of THF molecules attached to the metal center, as with the previously observed analogous Y(CH$_2$SiMe$_3$)$_3$(THF)$_2$ and Y(CH$_2$SiMe$_3$)$_3$(THF)$_3$ complexes.[9] The latter complex with three coordinated THF could only be obtained by recrystallization in the presence of THF, but in hexanes, it loses one of the coordinated THF very readily.

5.3 Characterization of Lutetium Tribenzyl Complexes

5.3.1 General Observations

The compounds are all air, moisture and thermally sensitive. At ambient temperature, a solution of $Lu(CH_2Ph)_3(THF)_3$, **28a** gradually decompose to give free toluene, bibenzyl and other unidentified species. This decomposition appears to be solvent dependent and of all solvents used, it is fastest in dichloromethane. The compounds are more stable in the solid state. However, after being kept at -30°C for a prolonged period, ^1H NMR of samples of the compounds showed formation of toluene or p-xylene and bibenzyls, the radical decomposition products, this being more pronounced with **29a**. The complexes have been characterized by standard spectroscopic techniques and their structures were confirmed by single-crystal X-ray diffraction in the solid state in the case of $Lu(CH_2Ph)_3(THF)_3$, **28a** and $Lu(CH_2Ph)_3(THF)_2$, **29a**.

5.3.2 $Lu(CH_2Ph-4-R)_3(THF)_3$ (R = H, 28a; R = Me, 28b)

Compound **28a** is very soluble in THF, slightly soluble in aromatic hydrocarbon solvents and diethyl ether but insoluble in hydrocarbon solvents. Compound **28b** on the other hand, is very soluble in THF and aromatic hydrocarbon solvents, slightly soluble in diethyl ether but insoluble in hydrocarbon solvents.

In solution, the room temperature ^1H and $^{13}C\{^1H\}$ NMR spectra of the complexes show one set of signals for the benzyl methylene and phenyl protons in accordance with the observed symmetrical *fac*-octahedral solid state structure of

Lu(CH$_2$Ph)$_3$(THF)$_3$, **28a** (*vide infra*) which is also expected for Lu(CH$_2$Ph-4-Me)$_3$(THF)$_3$, **28b**.

For compound **28a**, the NMR spectra recorded in C$_6$D$_6$ and THF-d_8 show some differences, Figure 5.1. Although no significant shift in the benzyl methylene signal was observed by changing the solvents, (δ(C$_6$D$_6$) 1.62 ppm
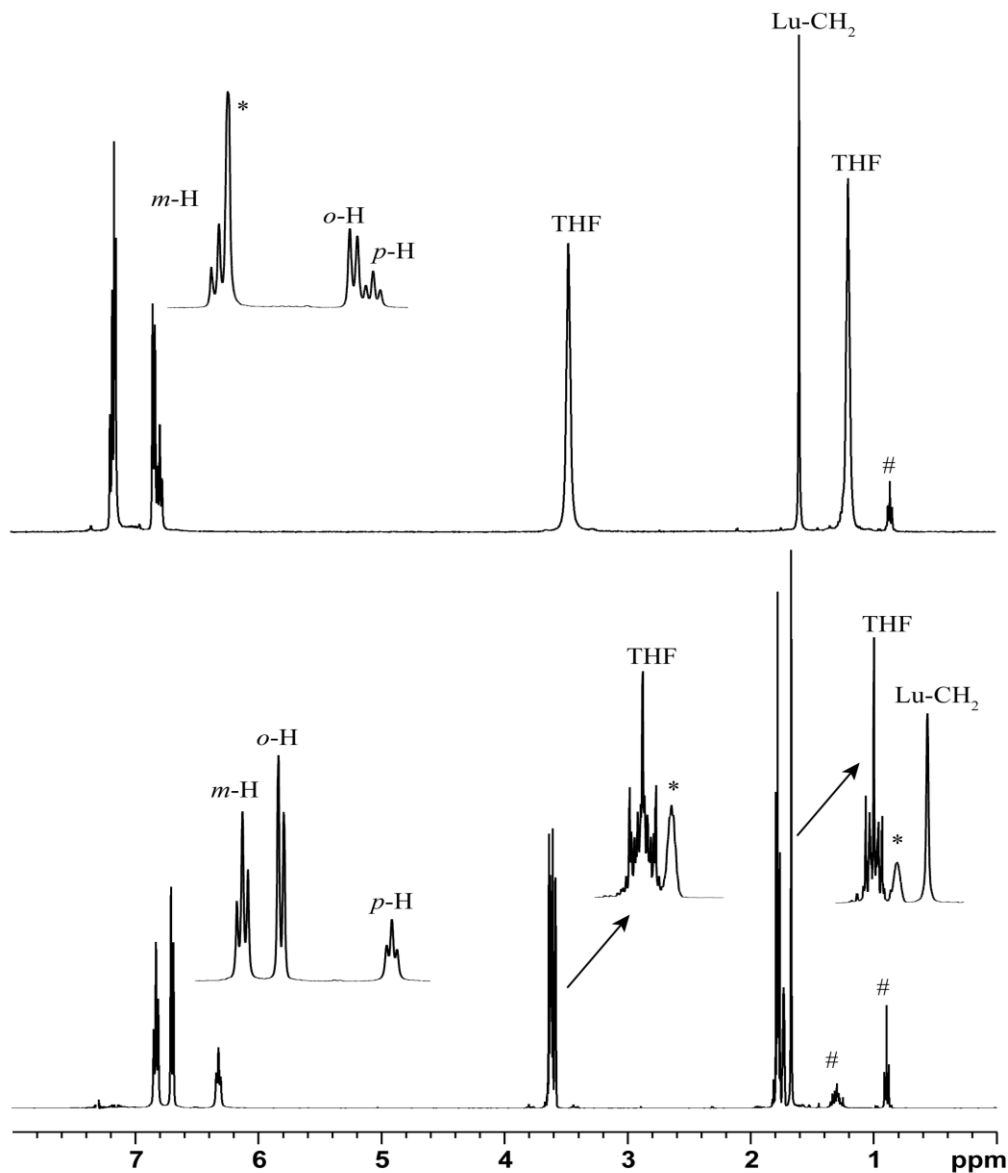
Figure 5.1: Room Temperature ^{1}H NMR Spectra of Lu(CH$_2$Ph)$_3$(THF)$_3$ (**28a**) : C$_6$D$_6$ (top); THF-d_8 (bottom).

Vs. δ(THFd_8) 1.67 ppm), the shift positions of the aromatic proton signals are however affected by the solvent change. In C_6D_6, the signals are well resolved triplet, doublet and triplet for the meta, ortho and para protons, respectively. In THF-d_8, these peaks are all shifted slightly upfield. The benzyl methylene $^{13}C\{^1H\}$ NMR resonances are at $\delta$($C_6D_6$) 59.3 ppm and δ(THF-d_8) 59.5 ppm. Again, there is no significant solvent influence on the position of the methylene signal. In the case of Lu(CH$_2$Ph-4-Me)$_3$(THF)$_3$, **28b**, the benzyl methylene protons show a more pronounced solvent dependence on going from the more polar THF to benzene (δ(C_6D_6) 1.25 ppm vs δ(THFd_8) 1.54 ppm). The aromatic proton signals shows similar behavior to those of Lu(CH$_2$Ph)$_3$(THF)$_3$, **28a**.

Compound **28a** crystallizes in the monoclinic space group *Cc* having four molecules in the unit cell. The solid state structure consist of a metal center bonded to three benzyl groups and three THF molecules in a facial-octahedral arrangement, Figure 5.2, although the coordination polyhedron is somewhat distorted from octahedral.

The Lu-O bond distances, which range from 2.352(2) Å (Lu-O1) to 2.381(3) Å (Lu-O2), fall within the range of other known Lu-O bond distances.[10,11,12] The O-Lu-O angles range from 78.04(10)-80.70(10)°, the deviation of these angles from the expected 90° may be attributed to the steric requirements of the benzyl ligand. The corresponding C-Lu-C angles are slightly larger than the ideal 90° octahedral angles, ranging from 91.14(16)° (C10-Lu-C30) to 94.93(14)° (C10-Lu-C20). Since this is the first structurally characterized lutetium benzyl complex, there are no other Lu-C$_{benzyl}$ bond distances
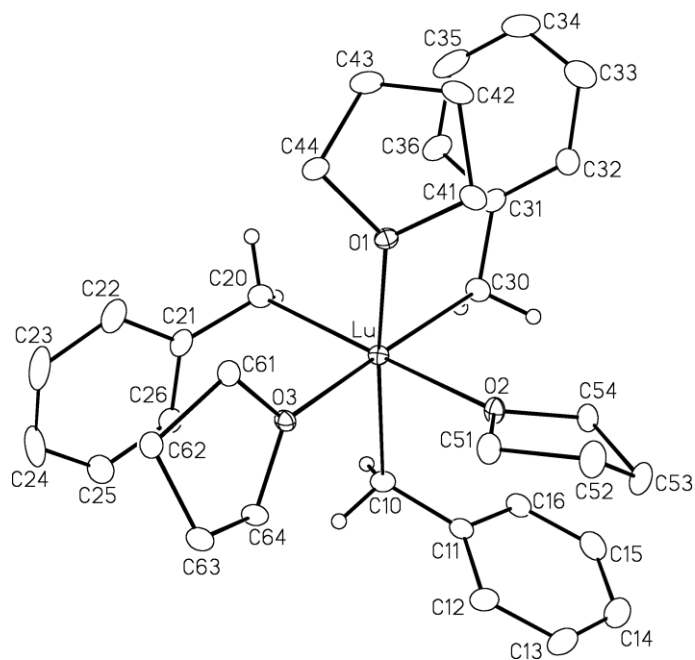
Figure 5.2: ORTEP View of Lu(CH$_2$Ph)$_3$(THF)$_3$ (**28a**).

that can be compared with those in Lu(CH$_2$Ph)$_3$(THF)$_3$, **28a**. The average Lu-C

bond distance of 2.403(5) Å is however in the range of Lu-C bond distances found

in other Lu-C bearing species: 2.376(3) Å in (Tp^{Me2})Lu(CH$_2$SiMe$_3$)$_2$(THF);[10]

2.361(3) Å in Lu(CH$_2$SiMe$_3$)$_3$(THF)$_2$[12] and 2.332(4) Å in

(C$_5$Me$_5$)Lu(CH$_2$SiMe$_3$)$_2$(THF).[11]

The Lu-C$_{ipso}$ bond distances, which range from 3.267(3) Å to 3.434(4) Å,

are too long for any significant interaction between the ipso carbon and the lute-

tium center. Also, the average Lu-CH$_2$-C$_{ipso}$ angle of 118.6(3)° is too large, thus

providing additional evidence for the absence of any significant η^2 interaction be-

tween the lutetium and the benzyl ligands. This is similar to the structure of the

scandium analogue.[7] In contrast to the η^1 bonding mode observed in **28a**, the pre-

viously reported lanthanum tribenzyl complex, La(CH$_2$Ph)$_3$(THF)$_3$,[5] adopts a

structure in which the benzyl ligands are all η^2 bonded to the metal center. This structural differences is a reflection of the smaller ionic radii of lutetium and scandium compared with that of lanthanum.[13]

5.3.3 Lu(CH₂Ph)₃(THF)₂ (29a)

Compound **29a** is more soluble than compound **28a**; it is very soluble in aromatic hydrocarbon solvents, slightly soluble in diethyl ether and insoluble in hydrocarbon solvents. In THF, it readily converts to $Lu(CH_2Ph)_3(THF)_3$, **28a**.

At room temperature, the ^1H and $^{13}C\{^1H\}$ NMR spectra show one set of well resolved signals for the benzyl as well as THF ligands. The observation of a single set of signal for $Lu(CH_2Ph)_3(THF)_2$, **29a**, is consistent with a symmetrical trigonal bipyramidal structure, (tbp) where the two THF ligands occupy axial position, or a less symmetrical fluxional solution structure. Cooling a toluene solution of $Lu(CH_2Ph)_3(THF)_2$, **29a** to -80°C did not result in any line broadening, but was accompanied by a low field shift of the para- and the meta-H triplets, Figure 5.3. Although the appearance of the phenyl region is better at -80°C, the lack of any line broadening is either an indication of a symmetrical tbp structure or a very low energy fluxional motion.

$Lu(CH_2Ph)_3(THF)_2$, **29a**, crystallizes in the triclinic space group $P\bar{1}$ with two molecules in the unit cell. The Lu center is coordinated by two oxygen atoms of the THF molecules and three carbon atoms of the benzyl groups, Figure 5.4. The two THF molecules are almost linear with O1-Lu-O2 angle of 177.18(7)°, thus suggestive of a tbp structure with the two THF molecules occupying the axial sites and
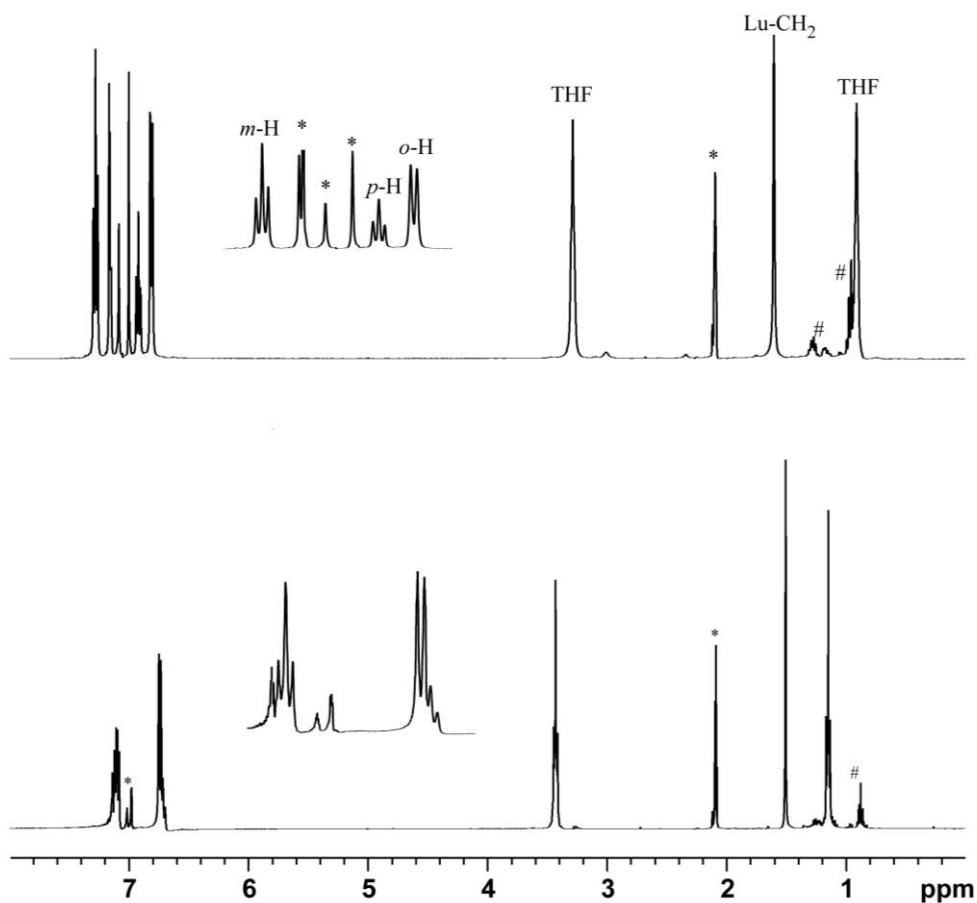
Figure 5.3: ^{1}H NMR Spectra of Lu(CH$_2$Ph)$_3$(THF)$_2$ (**29a**) in C$_7$D$_8$; -80°C (top), RT (bottom).

the benzyl groups in the equatorial positions, consistent with the observed solution behavior. The equatorial C-Lu-C angles, although close to the expected value of 120° (C10-Lu-C20 121.70(11)°, C10-Lu-C30 123.94(10)°, and C20-Lu-C30 114.31(11)°), show some deviation from the ideal value. This deviation can be attributed to the presence of an additional interaction from the ipso carbon of one of the benzyl ligands, as reflected in the Lu-C$_{ipso}$ distances and Lu-C-C$_{ipso}$ angles; Lu-C11 2.920(3) Å cf. 3.315(3) Å and 3.270(3) Å, for Lu-C21 and Lu-C31,
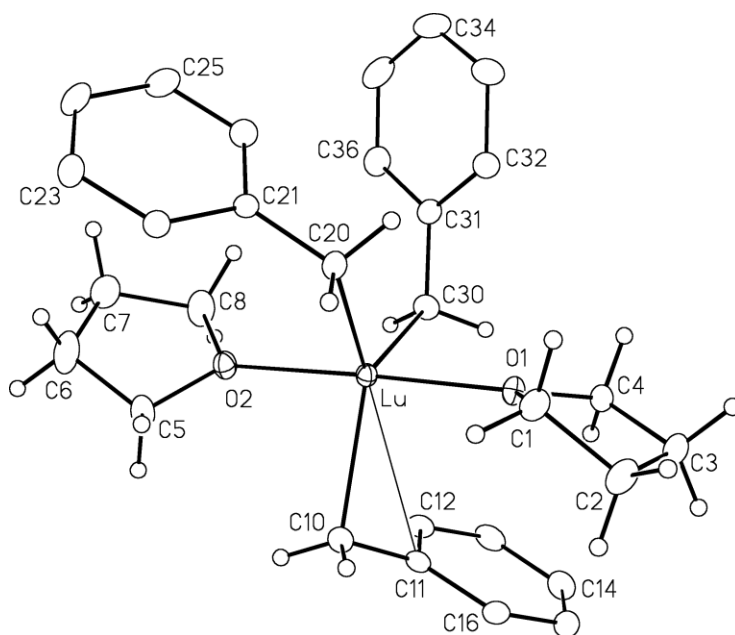
Figure 5.4: ORTEP View of $Lu(CH_2Ph)_3(THF)_2$ (**29a**).

respectively, and Lu-C10-C11 94.99(18)° cf. Lu-C20-C21 116.79(19)° and Lu-C30-C31 112.82(19)°. Thus, in contrast to the structure of $Lu(CH_2Ph)_3(THF)_3$, **28a**, in which all the benzyl ligands adopts η^1 bonding, one benzyl group in $Lu(CH_2Ph)_3(THF)_2$, **29a**, is η^2 bonded and the other two remain η^1 bonded. In $Sc(CH_2Ph)_3(THF)_2$ the three benzyl ligands are also η^1 bound. The additional interaction and increased coordination number at the lutetium center compared to the scandium analogue, $Sc(CH_2Ph)_3(THF)_2$[7] is consistent with the larger ionic radius of lutetium compared with that of scandium.[13] Consistent with the pseudo six-coordinate geometry of $Lu(CH_2Ph)_3(THF)_2$, **29a** the average Lu-C bond distance of 2.396(8) Å in $Lu(CH_2Ph)_3(THF)_2$ is comparable to the value of 2.405(5) Å in $Lu(CH_2Ph)_3(THF)_3$, **28a**. Also, the Lu-O distances of 2.284(2) Å and 2.290(2) Å in **29a** are similar to those in **28a**. The additional interaction however is evidently

rather weak based on the observation of a single set of signals in the NMR spectrum, even down to -80°C.

5.4 On the Trail of the Lu-benzyl ′ate′ Complexes: Variable Temperature NMR Studies of a Sample from an Early Lu-benzyl Preparation

Due to the relatively low solubility of $Lu(CH_2Ph)_3(THF)_3$, **28a** in aromatic solvent, it was of concern that the ^1H and $^{13}C\{^1H\}$ NMR spectra in C_6D_6 was not representative of the bulk material, thus the NMR spectra of an early, once recrystallized sample (from THF / hexane) was recorded in THF-d_8. In contrast to the well-resolved, sharp signals seen in C_6D_6, the benzyl signals were broad, seemingly indicative of some dynamic solution behavior, Figure 5.5. This was in contrast to the case of the scandium[7] and lanthanum[5] complexes which display well resolved and sharp signals for the benzyl moiety.

In an effort to slow down the process and to obtain a well-resolved ^1H NMR spectrum, a VT NMR study in THF-d_8 was undertaken. It was surprising that instead of sharpening the peaks broadened and, already at 0°C, the benzyl *p*-H signal resolved into two broad signals. Lowering the temperature resulted in sharpening of the resonances and, at -80 °C, two sets of well-resolved benzyl aryl-H and Lu-CH$_2$ signals were observed, with an intensity ratio of 2:1, Figure 5.5. Two sets of benzyl signals were also seen in the ^{13}C NMR spectrum at low temperature.
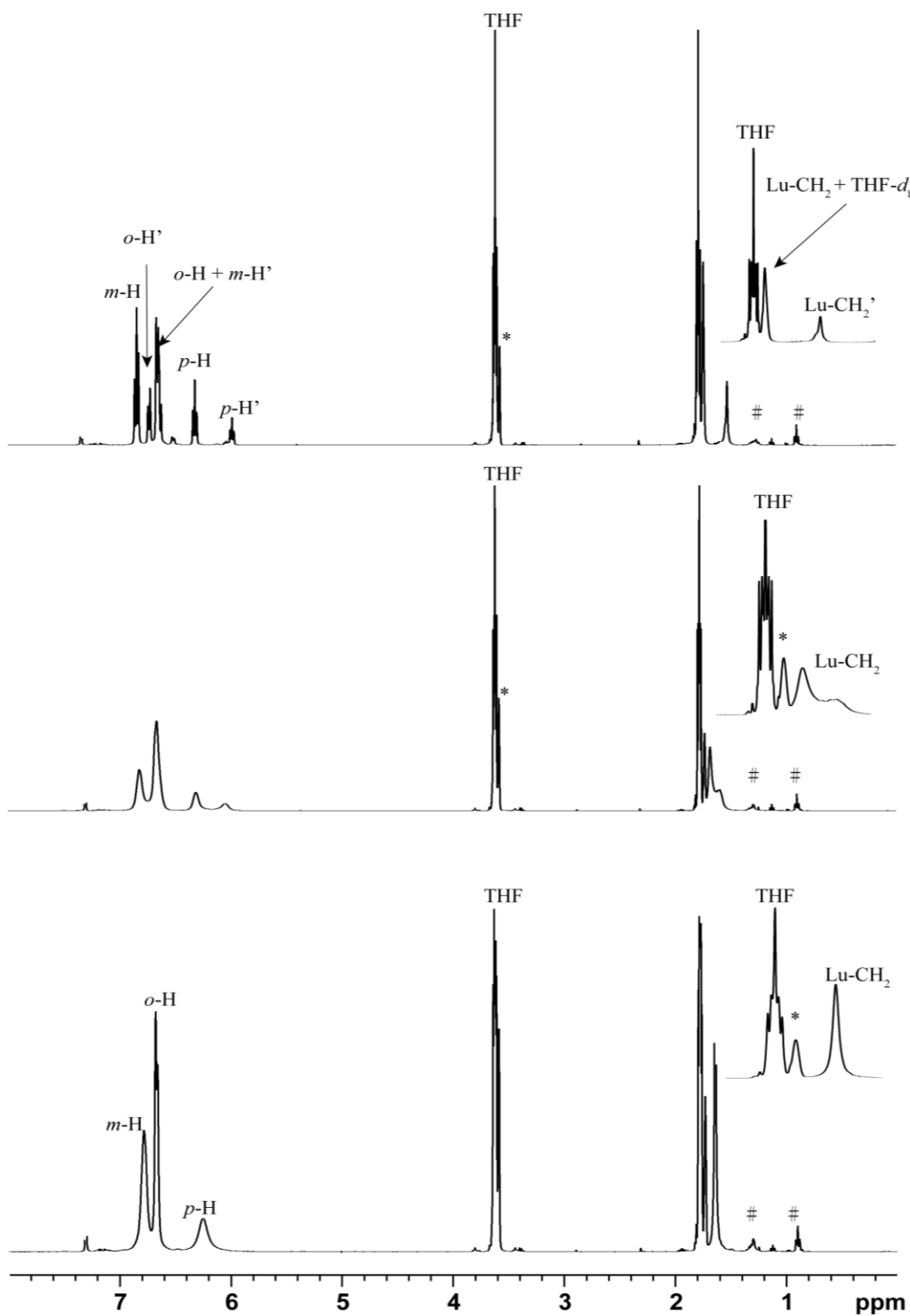
Figure 5.5: Variable Temperature ^{1}H NMR Spectra of a Sample from an Early Preparation of $Lu(CH_2Ph)_3(THF)_3$ in THF-d_8. Only the -80°C (top), 0°C (middle) and room temperature (bottom) spectra are shown.

The observation of two sets of NMR signals was puzzling but the 2:1 ratio could be accounted for by unexpected *fac*-to *mer*-isomerization in the polar THF solution. The fact that the proposed *fac*-to *mer*-isomerization was not observed in benzene was attributed to lack of THF dissociation / re-association in this less polar solvent, Scheme 5.2.
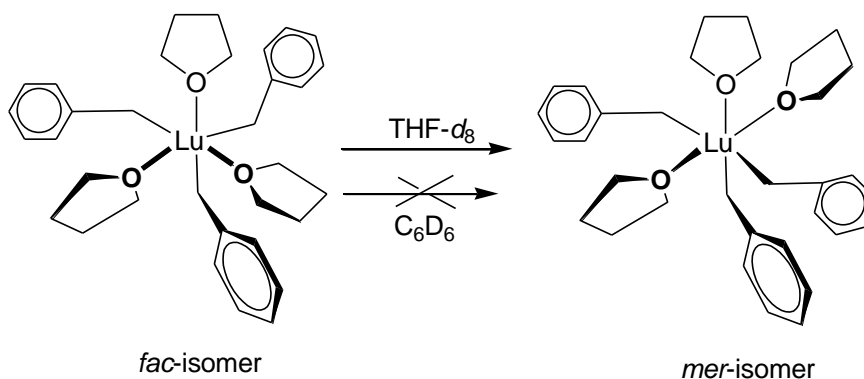
Scheme 5.2 Possible *Fac*- to *Mer*-Isomerization of
$Lu(CH_2Ph)_3(THF)_3$ (**28a**) in THF.

To gain more evidence, the yttrium compound $Y(CH_2Ph)_3(THF)_3$ was investigated. Again, two sets of signals were seen at low temperature, but the ratio was 4:1.[14] A similar observation was made on the ^1H and $^{13}C\{^1H\}$ NMR of the yttrium analogue of **28b**, $Y(CH_2Ph-4-Me)_3(THF)_3$. The NMR spectra in THF-d_8 showed a broad signal for the benzyl methylene proton and carbon at room temperature. At low temperature however, two sets of peaks were observed, also with intensity ratio of about 4:1. This intensity ratio is not consistent with the existence of a *fac*-to-*mer*-isomerization. In addition, only one of the two peaks shows well resolved Y-C coupling in the $^{13}C\{^1H\}$ as a result of coupling to yttrium (^{89}Y, I =

½), the other was just a broad peak.[15] A similar observation was seen in the $^{13}C\{^1H\}$ NMR spectrum of $Y(CH_2Ph)_3(THF)_3$.

Based on the observations made on the yttrium complexes, a repeat of the VT studies on the same sample of **28a** in THF-d_8 was deemed necessary. The experiment was repeated using long relaxation delay (d1) values in order to avoid possible errors in integration value, which often occur as a result of using too short relaxation delays. This time the ratio of the peaks was 2.7:1, clearly different from 2:1 and thus ruling out the possibility of a solvent-induced *fac*-to-*mer*-isomerisation in THF.

To rule out the unlikely possibility that the two sets of signals in the low temperature spectra was due to the presence of a mixture of $Lu(CH_2Ph)_3(THF)_3$, **28a** and $Lu(CH_2Ph)_3(THF)_2$, **29a**, the ^1H NMR spectrum of **29a** was obtained in THF-d_8, starting from low temperature (-80°C). The assumption was this: Should THF addition to **29a** at low temperature occur slowly, it might be possible to detect signals due to **29a** prior to its conversion to **28a**. Thus, pre-cooled THF-d_8 (-78°C) was syringed into an NMR tube containing **29a** maintained at the same temperature. The ^1H NMR spectrum obtained immediately at -80°C displayed one set of signals which corresponded to the major species in the -80°C spectrum of the sample from an early preparation of $Lu(CH_2Ph)_3(THF)_3$, **28a** in THF-d_8, Figure 5.5, and the spectrum remained the same upon warming to room temperature, Figure 5.6. The observation of one, temperature invariant set of signals was clearly not in accord with the assumption of slow THF addition at low temperature rather it was indicative of rapid THF addition to **29a** to produce **28a**. This

thus identifies the major set of signals as belonging to **28a** and ruled out the minor

set as belonging to **29a**; the nature of the minor set still remaining a mystery.
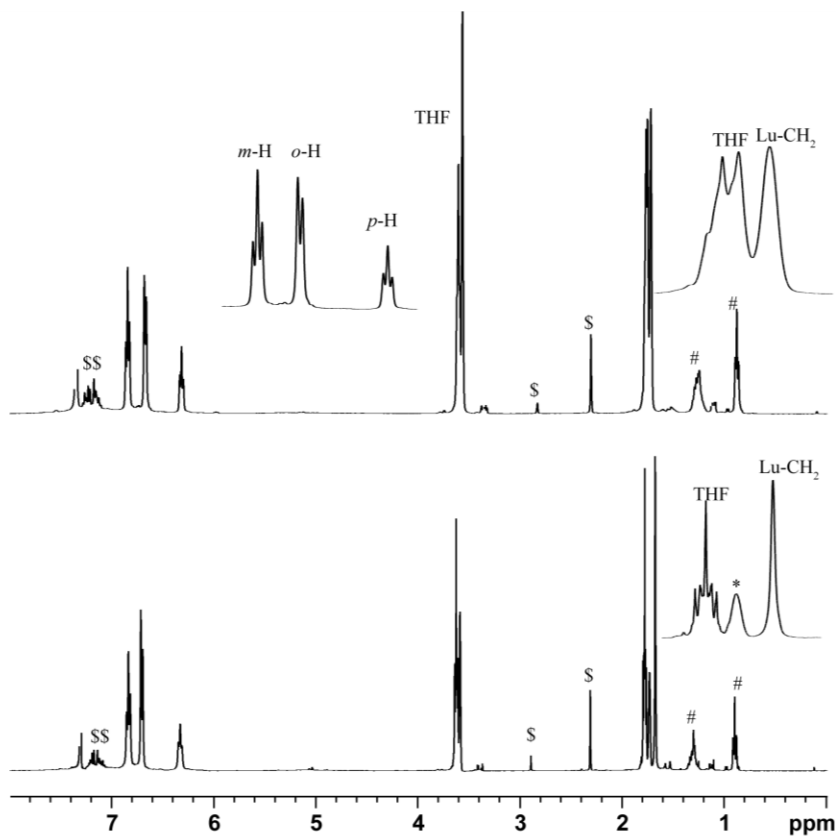
Figure 5.6: ^{1}H NMR Spectra of Lu(CH$_2$Ph)$_3$(THF)$_2$ (**29a**) in THF-d_8
at -80°C (top) and RT (bottom). The spectra corresponds to that of
Lu(CH$_2$Ph)$_3$(THF)$_3$ (**28a**). $$ denotes the decomposition products
(toluene and bibenzyl) of the compound.

Albeit rather late, the other species observed in the THF-d_8 spectra was fi-

nally suggested as possibly being due to one of the ′ate′ complexes

[Lu(CH$_2$Ph)$_{4/5}$].[1,2] This would be more in line with the fact that the signal ratio

between the two species, seen in the NMR spectra recorded in THF-d_8,

varied between different preparations of Lu(CH$_2$Ph)$_3$(THF)$_3$, **28a**; a recently pre-

pared sample showed 4:1 ratio. It would also be consistent with the observation of

an insoluble residue remaining when the reaction product from the preparation of **28a** was triturated and extracted with toluene to obtain **29a**. To corroborate this, ^{1}H and ^{13}C{^{1}H} NMR spectra were obtained on this residue in THF-d_8. The signals at -80°C matched that of the minor species seen in theTHF-d_8 NMR spectrum of the "early" sample of **28a**, Figure 5.5. The room temperature spectrum is however slightly different in the aromatic region, with the peaks order as *meta*, *ortho* and *para*, respectively, as opposed the order *ortho*, *meta* and *para* observed at -80°C. In order to identify which 'ate' complex, mono- or di-anionic, this species is, an NMR preparation of each compound was carried out by sequential addition of KCH$_2$Ph to pure **28a** in THF-d_8. Addition of 1 equiv. of potassium benzyl to pure **28a** quantitatively generated a species whose NMR signature, Figure 5.7 matches that of the insoluble species, and corresponds to the minor species in the NMR spectra of the early sample of "**28a**". This identifies the insoluble species as the mono-anionic compound, K[Lu(CH$_2$Ph)$_4$(THF)$_n$], **30a**.

Addition of a second equiv. of KCH$_2$Ph to the NMR tube generates a second species that could be assigned to the di-anionic complex K$_2$[Lu(CH$_2$Ph)$_5$(THF)$_n$]. The second equivalent of KCH$_2$Ph was however not completely consumed and thus the ^{1}H NMR spectrum was a complex mixture of signals from K[Lu(CH$_2$Ph)$_4$(THF)$_n$], **30a**, K$_2$[Lu(CH$_2$Ph)$_5$(THF)$_n$], and un-reacted KCH$_2$Ph.

Figure 5.7: ^{1}H NMR Spectra of K[Lu(CH$_2$Ph)$_4$(THF)$_n$)] (**30a**); -80°C (top), Room Temperature (bottom).

In conclusion, the preparation of Lu(CH$_2$PH)$_3$(THF)$_3$, **28a** may be accompanied by formation of variable amount of K[Lu(CH$_2$Ph)$_4$(THF)$_n$], **30a**. In solution, the compounds are in equilibrium and this accounts for the broad NMR signals seen at room temperature in THF. In aromatic solvents, the ′ate′ complex is insoluble and therefore only compound **28a** is present in solution, thus explaining the sharp, characteristic NMR signals of this complex seen in C$_6$D$_6$. To avoid any complication due to the ′ate′ complex by-product, possibly, the most reliable

method of obtaining pure **28a** is by extracting the reaction product with toluene and convert the obtained **29a** to **28a** by addition of THF.

5.5 Synthesis of $(Tp^{tBu,Me})Ln(CH_2Ph-4-R)_2$ and $(Tp^{Me2})Ln(CH_2Ph-4-R)_2(THF)$ (Ln = Y, Lu; R = H, Me) Compounds

The synthesis was attempted both via alkyl abstraction, using $Tl(Tp^{R,R`})$, and protonolysis employing the acid form, $H(Tp^{R,R`})$. The alkyl abstraction method was of particular interest since preparation of $H(Tp^{Me2})$ is problematic.

Unfortunately, the alkyl abstraction protocol, according to eq. 5.1, did not work. Reaction of $Ln(CH_2Ph-4-R)_3(THF)_3$ with $Tl(Tp^{Me2})$ consistently produced black precipitate as opposed to Tl shot. No pure product could be isolated from these reactions. All attempts to crystallize the crude reaction products continuously gave black precipitate and unidentified products.

$$Ln(CH_2Ph-4-R)_3(THF)_3 \xrightarrow[Tl(Tp^{R,R`})]{-TlCH_2Ph-4-R} (Tp^{R,R`})Ln(CH_2Ph-4-R)_2(THF)_{1/0} \qquad 5.1$$

As mentioned in Chapter 3, the by-product of the thallium abstraction reaction, in this case thallium(I) benzyl, could decompose in one of two ways: (i) disproportionation into thallium metal and thallium(III) benzyl, eq. 5.2 and (ii) decomposition into thallium metal and products of the benzyl radical eq. 5.3.[16] The observation of a small amount of bibenzyl in the NMR mixture suggests that the initially formed Tl(I) benzyl decomposed by eq. 5.3. However, failure to isolate a clean reaction product in this case may be explained on the basis of the

greater stability of Tl(CH$_2$Ph). This stability is attributable to interactions between the thallium ion and the aromatic ring.

$$3\ Tl(CH_2Ph) \longrightarrow 2\ Tl^0 + Tl(CH_2Ph)_3 \qquad 5.2$$

$$2\ Tl(CH_2Ph) \longrightarrow 2\ Tl^0 + PhCH_2\text{-}CH_2Ph \qquad 5.3$$
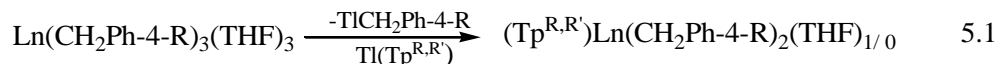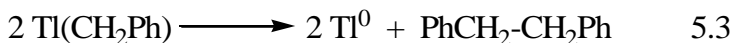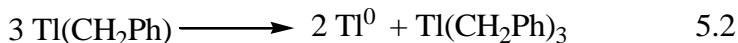
Multihapto interactions between thallium metal and aromatic rings is well documented and it has been shown to be one of the contributing factors for the unusual stability of low coordination number complexes of this metal in the absence of other interactions such as thallophilic interactions, hydrogen bonding etc.[17,18]

Since alkyl abstraction is not practicable, only the protonolysis protocol worked for the synthesis of the scorpionate dibenzyl complexes, (Tp^{R,Me})Ln(CH$_2$Ph-4-R)$_2$(THF)$_{1/0}$.

5.5.1 Synthesis via Protonolysis Reaction

Reaction of the acid form of the ligand, H(Tp^{tBu,Me}) with one equiv. of the lanthanide tribenzyl complexes Ln(CH$_2$Ph-4-R)$_3$(THF)$_3$ (Ln = Y, Lu) in THF at RT affords the lanthanide dibenzyl complexes, (Tp^{tBu,Me})Ln(CH$_2$Ph-4-R)$_2$, (Ln = Y, R = Me **31b**; Ln = Lu, R = H, **32a** ;Me, **32b**) as white powders in good to excellent yields, Scheme 5.3. Although the reaction of H(Tp^{Me2}) with one equivalent of yttrium tribenzyl complex, Y(CH$_2$Ph-4-Me)$_3$(THF)$_3$ affords the dibenzyl compound (Tp^{Me2})Ln(CH$_2$Ph-4-Me)$_2$(THF), **33a** as a pale yellow solid, purity of the compounds is an issue possibly due to problems encountered in the preparation of HTp^{Me2} (Chapter 3).

Ln(CH$_2$Ph-4-R)$_3$(THF)$_3$ $\xrightarrow[\text{-CH}_3\text{Ph-4-R}]{\text{H(Tp}^{\text{R',Me}})}$

Ln = Y, Lu
R = H, Me

R' = CH$_3$, n = 1
R' = ^{t}Bu, n = 0
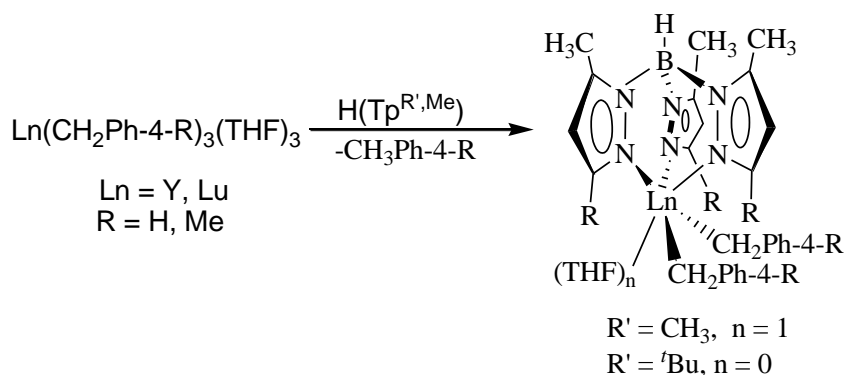
Scheme 5.3: Synthesis of (Tp$^{\text{R',Me}}$)Ln(CH$_2$Ph-4-R)$_2$(THF)$_{1/0}$ by Protonolysis.

5.6 Characterization of (Tp$^{\text{R,Me}}$)Ln(CH$_2$Ph-4-R)$_2$(THF)$_{0/1}$

5.6.1 (Tp$^{t\text{Bu,Me}}$)Ln(CH$_2$Ph-4-R)$_2$ Complexes

The compounds are soluble in hydrocarbon as well as ether-type solvents and they are both air and moisture sensitive. The compounds were characterized by NMR spectroscopy, elemental analysis and their structures were determined in the solid state by single crystal X-ray crystallography. At room temperature, the ^{1}H NMR spectra of (Tp$^{t\text{Bu,Me}}$)Lu(CH$_2$Ph)$_2$, **32a** and (Tp$^{t\text{Bu,Me}}$)Lu(CH$_2$Ph-4-Me)$_2$, **32b** show a single set of peaks for the pyrazolylborate ligand in the appropriate 27:9:3 ratio. The benzyl protons also show one set of peaks, albeit broad, and no resolved coupling was seen for the aromatic signals. The ^{13}C{^{1}H} NMR spectrum also showed one set of signals. The room temperature ^{1}H NMR spectrum of the yttrium complex **31b** shows a single set of peaks for the pyrazolylborate ligand as well as the benzyl ligands, for the benzyl signals however, only the *meta*-H appeared as a well resolved doublet. The *ortho*-H signal and the benzyl methylene

228

peak both appeared as broad singlets. The $^{13}C\{^1H\}$ NMR spectrum also showed one set of signals, with the benzyl methylene signal appearing as a doublet at ca. 59.0 ppm with $^1J_{YC}$ = 37.0 Hz. As with other $(Tp^{tBu,Me})$Ln dialkyl compounds the simple NMR spectra are indicative of rapidly fluxional 5-coordinate structures.

Single crystals suitable for X-ray diffraction studies were obtained for **31b**, **32a** and **32b** by cooling a dilute hexane solution to -40°C for several days. ORTEP drawings of **31b** and **32a** are shown in Figures 5.8 and 5.9, respectively. Important metric parameters are listed in Table 5.1.

In the solid state, the structure of $(Tp^{tBu,Me})Lu(CH_2Ph)_2$, **32a** is very similar to those of $(Tp^{tBu,Me})Ln(CH_2Ph-4-Me)_2$ (Ln = Y, **31b**; Lu, **32b**) which are isostructural. The compounds all are five-coordinate and adopt a structure similar to that found in the closely related (trimethylsilyl)methyl analogues, $(Tp^{tBu,Me})Ln(CH_2SiMe_3)_2$ (Ln = Sc, Y, Nd, Sm, Yb, Lu).[10,19] The metal center is coordinated by the three nitrogen atoms of the pyrazolylborate ligand in the classical κ^3 bonding mode and the two carbon atoms of the benzyl moieties to give an overall coordination number of 5. However, unlike in the case of the five coordinate homoleptic benzyl complex, $Lu(CH_2Ph)_3(THF)_2$, **29a**, in which one of the benzyl adopts a η^2 coordination mode to give an overall coordination number of six, the bulky nature of the $Tp^{tBu,Me}$ ligand[20] prevents further interaction between the benzyl ligand and the lanthanide center as shown by the $Ln-C_{ipso}$ distances ranging from 3.303 Å to 3.403 Å; the corresponding $Ln-CH_2-C_{ipso}$ angle ranges from 113.90° to 120.88°. The coordination geometry around the metal center is

best described as a distorted trigonal bipyramidal with N12 and C1 occupying the axial sites and N22, N32 and C2 in the equatorial sites.

Similar to the lanthanide dialkyl complexes, $(Tp^{tBu,Me})Ln(CH_2SiMe_3)_2$ and other five coordinate complexes supported by $Tp^{tBu,Me}$ ligand,[21] the Ln-N (equatorial) bond distances are shorter than Ln-N12 (axial) bond length by ca.0.15-0.2 Å.

In the yttrium complex, **31b**, the observed equatorial Y-C1 distance of (2.426(3) Å) is shorter, whereas the axial Y-C2 distance of (2.471(3) Å) is in the range of Y-C bond distances in other yttrium benzyl compounds such as $Li[PhC(NSiMe_3)N(CH_2)_2-NMe_2]_2Y(CH_2Ph)_2$ (2.490(8) and 2.463(6) Å), [22] $[PhC(NSiMe_3)N(CH_2)_2-NMe_2]_2YCH_2Ph$ (2.487(6) Å)[22] and $(L)Y(CH_2Ph)_2$ (L = N-{2-pyrolidin-1-ylethyl)-1,4-diazepan-6-amido ligand) (2.491(3) and 2.544(3) Å).[6] The Lu-C1 and Lu-C2 bond distances of 2.387(6) Å and 2.403(5) Å in **32a** and 2.386(4) Å and 2.374(4) in **32b**, respectively are similar to the 2.403(5) Å in the tribenzyl complex **28a**,[7] respectively and 2.396(8) Å in the pseudo six-coordinate lutetium tribenzyl, **29a**. The Ln-C bond distances in these complexes are however longer than those found in the corresponding dialkyl complexes, $(Tp^{tBu,Me})Ln(CH_2SiMe_3)_2$.[10]

The axial benzyl ligands in compounds **31b, 32a** and **32b** sits in the cleft formed by the two ^tBu substituents of the equatorial pyrazolyl groups, for example in the lutetium compound, **31b**, (C1-Lu---B = 98 cf. C2-Lu---B = 173), thus opening up the equatorial N22-Lu-N32 bite angle to 103.49(10)° and resulting in the tightening of the other two angles, with values of 75.28(10)° and 74.52(10)° for
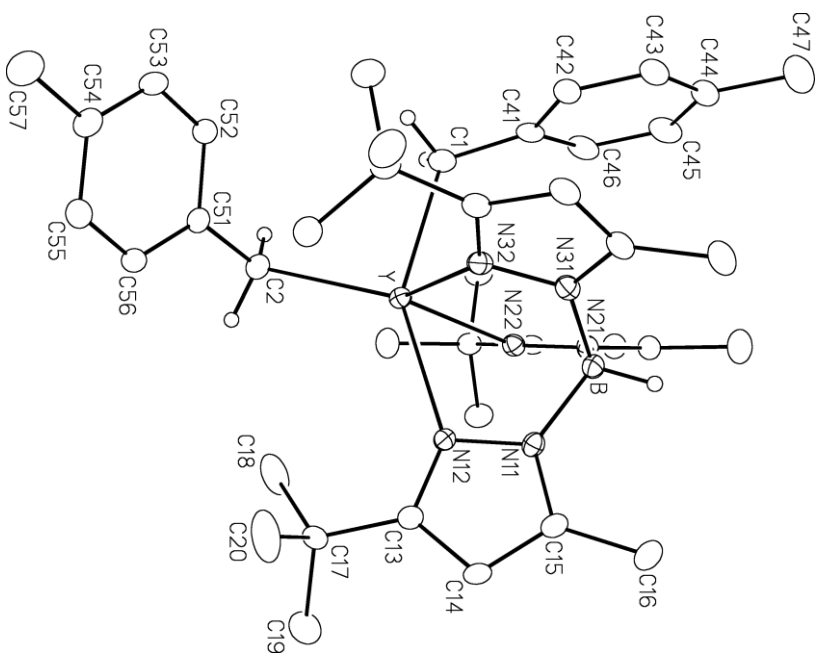
Figure 5.8: ORTEP View of (Tp^{tBu,Me})Y(CH$_2$Ph-4-Me)$_2$, **31b**.
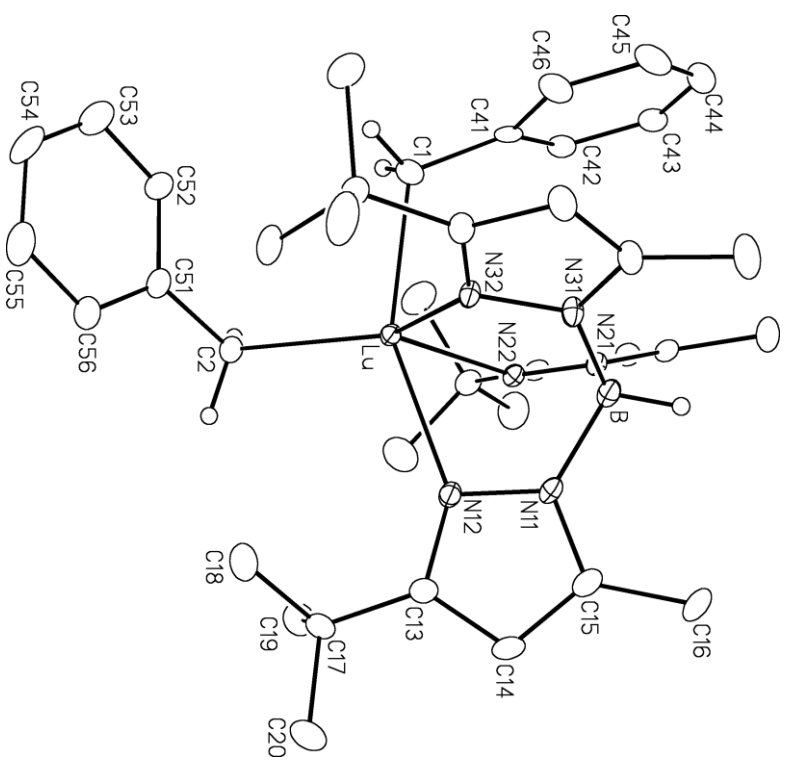
Figure 5.9: ORTEP View of (Tp^{tBu,Me})Lu(CH$_2$Ph)$_2$, **32a**.

231

Table 5.1 Selected Bond Lengths (Å) and Angles (deg.) for $(Tp^{tBu,Me})Y(CH_2Ph\text{-}4\text{-}Me)_2$ (**31b**), $(Tp^{tBu,Me})Lu(CH_2Ph)_2$ (**32a**) and $(Tp^{tBu,Me})Lu(CH_2Ph\text{-}4\text{-}Me)_2$ (**32b**).

	31b	32a	32b
		Distances	
Ln-N12	2.510(2)	2.463(4)	2.478(3)
Ln-N22	2.367(2)	2.351(4)	2.303(3)
Ln-N32	2.397(2)	2.324(4)	2.323(3)
Ln-C1	2.426(3)	2.387(6)	2.386(4)
Ln-C2	2.471(3)	2.403(5)	2.374(4)
Ln---C41	3.433	3.333	3.340
Ln---C51	3.403	3.303	3.390
		Angles	
N12-Ln-N22	74.01(7)	74.69(14)	75.28(10)
N12-Ln-N32	73.05(8)	75.83(15)	74.52(10)
N12-Ln-C1	147.48(9)	153.76(18)	153.69(12)
N12-Ln-C2	123.91(9)	110.23(7)	108.18(12)
N22-Ln-N32	97.42(8)	103.46(6)	103.49(10)
N22-Ln-C1	128.50(9)	89.87(18)	87.11(12)
N22-Ln-C2	84.99(10)	119.79(18)	133.65(14)
N32-Ln-C1	85.69(9)	87.67(18)	91.21(13)
N32-Ln-C2	132.99(9)	136.56(18)	122.27(13)
C1-Ln-C2	88.59(11)	95.8 (2)	98.13(13)

N12-Lu-N22 and N12-Lu-N32, respectively.

5.6.2 $(Tp^{Me2})Y(CH_2Ph–4–Me)_2(THF)$ (33b)

Protonolysis of $Y(CH_2Ph-4-Me)_3(THF)_3$ with HTp^{Me2} in toluene appeared to proceed, however, only a small amount of crystals could be harvested that was used to determine the solid state structure. Further attempts to obtain spectroscopically and analytically pure material from this reaction for further characterization were unsuccessful. Repeating the reaction in THF at low temperature produced a material that resulted in a more satisfactory ^1H and $^{13}C\{^1H\}$ NMR spectra, but still with unidentified peaks.

In the solid state, the compound is six-coordinate and has similar structure as the corresponding $(Tp^{Me2})Ln(CH_2SiMe_3)_2(THF)$ complexes,[10] Figure 5.10. The yttrium center is coordinated to a κ^3 bonded (Tp^{Me2}) ligand, two carbon atoms of the benzyl ligands and the oxygen of THF ligand in a distorted octahedral geometry, the distortion from the ideal can be attributed to the constraint of the tripodal Tp^{Me2} ligand. The Y-N (2.465(1), 2.529(2) and 2.402(2) (Å) and Y-C (2.464(2) and 2.488(2) Å) bond lengths in **33b** are longer than the corresponding values in **31b**, as expected for the increased coordination number. Both benzyl ligands in **33b** are η^1 coordinated to the yttrium center. This is in contrast to observation in $(L)Y(CH_2Ph)_2$ (L = N-{2-pyrolidin-1-ylethyl)-1,4- diazepan-6-amido ligand), in which one of the benzyl ligands is η^2 coordinated while the other one remains η^1 coordinated.[6] Also, in the mono-benzyl scandium complex supported by a
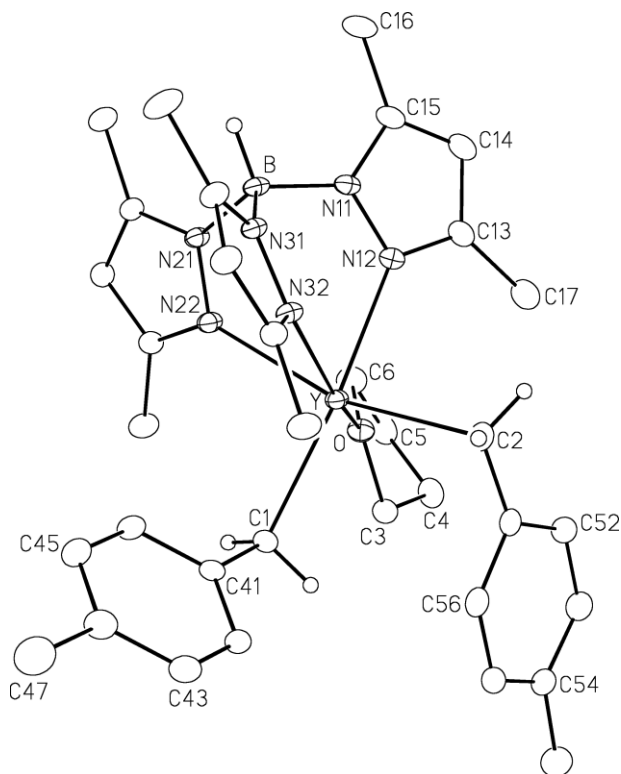
Figure 5.10: ORTEP View of $(Tp^{Me2})Y(CH_2Ph\text{-}4\text{-}Me)_2(THF)$ (**33b**).

ferrocenyl ligand, $Sc(fc[NSi(t\text{-}Bu)Me_2]_2)(CH_2Ph\text{–}3,5\text{–}Me_2)(THF)$ (fc = 1,1′-ferrocenylene), the benzyl ligand is η^2 coordinated to the scandium center.[8] The differences in the bonding modes of the benzyl ligands in these complexes may be attributed to the differences in the steric bulk of the respective ancillary ligands.

The average Y-N bond distance of 2.47(4) Å in **33b** is comparable to the value of 2.47(2) Å in $(Tp^{Me2})Y(CH_2SiMe_3)_2(THF)$.[10] The corresponding Y-C bond distances of 2.48(1) Å in **33b** is however slightly longer than 2.42(1) Å in $(Tp^{Me2})Y(CH_2SiMe_3)_2(THF)$.[10]

5.7 Conclusions

Salt metathesis reaction between $LuCl_3$ and 3 equiv. of KCH_2Ph-4-R (R = H, Me) gives the corresponding lutetium tribenzyl complexes, $Lu(CH_2Ph$-4-R)(THF)$_3$ (R = H, **28a**; Me, **28b**) in moderate yields, however, the complexes are obtained contaminated with various amounts of the anionic ′ate′ complex $K[Lu(CH_2Ph$-4-R)$_4$(THF)$_n$], **30**.[†] Trituration of **28a** with toluene followed by re-crystallization affords $Lu(CH_2Ph)_3$(THF)$_2$, **29a**. Addition of THF to **29a** gives pure **28a**. The anionic complex, **30** can be prepared independently by addition of 1 equiv. of KCH_2Ph to **28a**.

Unlike in the case of the lanthanide dialkyl complexes, the alkyl abstraction protocol failed to yield any isolable product, possibly due to the higher stability of the thallium(I) benzyl compared with the corresponding thallium(I) alkyl by- product. Only the protonolysis approach is applicable to the synthesis of the $Tp^{R,R'}$ lanthanide dibenzyl complexes. Protonolysis of the tribenzyl complexes **28a** and **28b** and the yttrium analogue of **28b** with $HTp^{tBu,Me}$ gave the corresponding $(Tp^{tBu,Me})Ln(CH_2Ph$-4-R)$_2$ (Ln = Y, R = Me **31b**; Ln = Lu, **32, R = H, Me**) complexes in good yields. Protonolysis of $Y(CH_2Ph$-4-Me)$_3$(THF)$_3$ with HTp^{Me2} proved problematic in toluene and furnished only small amount of the structurally characterized $(Tp^{Me2})Y(CH_2Ph$-4-Me)$_2$(THF), **33b**. Carrying out the reaction in

[†] The by-product in the synthesis of $Lu(CH_2Ph)_3$(THF)$_3$, **28a** has been identified, however it is not yet clear why the by-product forms. Experiments designed to identify the problem are underway and a correction to the synthesis and solution behaviour of $Lu(CH_2Ph)_3$(THF)$_3$, **28a** which appeared in *Organometallics* **2008**, *27*, 1501-1505, will be submitted to the same journal.

THF at low temperature afforded $(Tp^{Me2})Y(CH_2Ph-4-Me)_2(THF)$, **33b,** in a moderate yield albeit with some impurities as shown by NMR spectroscopy.

5.8 Experimental Section

5.8.1 General Techniques, Solvents and Physical Measurements

As in Chapter 2.

5.8.2 Starting Materials and Reagents

Anhydrous $LnCl_3$ (Ln = Y, Lu) were purchased from Strem Chemicals Ltd. $KCH_2Ph-4-R$ (R = H, Me) were prepared by a modification of the published procedure[23] (see below). The compounds $Tl(Tp^{tBu,Me})$, $Tl(Tp^{Me2})$,[24] $H(Tp^{tBu,Me})$ and $H(Tp^{Me2})$ [25,26] were prepared by literature procedures.

5.8.3 Synthetic Aspects

$KCH_2Ph-4-Me$

To a suspension of potassium tert-butoxide (3.0g, 2.67 mmol) in a mixture of *p*-xylene (50 mL) and hexanes (20 mL) was slowly added n-butyllithium (15 mL, 37.5 mmol) over about 20 mins. During addition, the color of the suspension changed to yellow, deep yellow-orange and finally deep orange and the suspension became a thick emulsion. The resulting emulsion was stirred for additional 3 h at RT and then filtered to obtain a bright orange solid which was washed several

times with p-xylene (50mL), hexanes (100mL) and pentane (150mL) followed by drying in vacuum to obtain the compound as a bright orange solid (3.6g, 24.95 mmol) in 93% isolated yield.

Lu(CH$_2$Ph)$_3$(THF)$_3$ (28a)

(a) **Example of an early preparation**

A suspension of anhydrous LuCl$_3$ (1.07 g, 3.80 mmol) was stirred overnight in THF (ca. 14 h). The suspension was cooled to -10°C with stirring for another 1 h. A cold THF solution of KCH$_2$Ph (1.48 g, 11.4 mmol) was slowly added to the suspension over about 10 min. During addition, the bright orange red color of the KCH$_2$Ph disappeared and LuCl$_3$ suspension dissolved giving a very pale yellow emulsion-like mixture, which was stirred at this temperature for a further 2 h. The mixture was centrifuged to remove KCl (centrifugation has to be done for a long time because the precipitate does not settle very well). The precipitate was further extracted with about 20 mL THF. The combined mother liquor and extract were concentrated to about 10 mL, layered with Et$_2$O, and kept at -30°C overnight to obtain a pale yellow solid, which was dried under vacuum to obtain 1.52g of once crystallized product.

This sample was shown to be contaminated by ca. 22% of the ′ate′ complex K[Lu(CH$_2$Ph)$_4$(THF)$_n$], **30a**. Although contaminated, X-ray quality crystals of pure **28a** were grown from THF/Et$_2$O solvent mixture.

An analytically pure sample was obtained by careful, repeated crystalliza-

tion of the originally obtained mixture of **28a** and **30a** from THF/Et$_2$O or

THF/hexane solvent mixtures, but with significant loss of material. Anal. Calcd

for C$_{33}$H$_{45}$O$_3$Lu: C, 59.63; H, 6.82. Found: C, 59.40; H, 6.78.

Alternatively, a spectroscopically pure sample of **28a** can be obtained from

the once crystallized material by trituration and extraction with toluene to convert

it to **29a** (*vide infra*) which is then converted back to **28a** by addition of THF. The

so obtained **28a** (95% yield) from **29a** is satisfactory for further reaction, but a

sample for elemental analysis was further recrystallized from THF/hexane with

minimal loss.

(b) **Example of a later preparation using a modified isolation procedure**

Following the same procedure as above using anhydrous LuCl$_3$ (0.70 g,

2.44 mmol) in 15 mL THF and KCH$_2$Ph (0.96 g, 7.38 mmol) in 15 mL THF re-

sulted in the formation of a pale yellow emulsion-like mixture, which was stirred

for another 2 h while slowly raising the temperature. After the reaction, 20 mL

toluene was added to the mixture which was stirred at room temperature for an-

other 30 mins. The mixture was centrifuged to remove KCl (centrifugation has to

be done for a long time because the precipitate does not settle very well). Solvent

was stripped in vacuum from the solution to obtain a pale-yellow sticky solid

which was triturated with 3 X 5 mL pentane followed by removal of solvent under

vacuum each time, to give 1.06 g of a pale-yellow solid.

A variable temperature NMR study on the solid obtained showed that the material is contaminated by 16% of the 'ate' complex $K[Lu(CH_2Ph)_4(THF)_n]$, **30a**. Recrystallization of this solid from a THF / toluene/ pentane solvent mixture gave 0.31g of a spectroscopically pure very pale yellow (almost colorless) crystalline solid of **28a**.

^1H NMR (400 MHz, C_6D_6, 27°C): δ 7.17 ("t", $^3J_{HH}$ 7.6 Hz, 6H, Ph m-H), 6.85 (d, $^3J_{HH}$ = 7.6 Hz, 6H, Ph o-H), 6.78 (t, $^3J_{HH}$ = 7.6 Hz, 3H, Ph p-H), 3.48 (s br, 12H, α-THF), 1.62 (s, 6H, $LuCH_2$), 1.20 (s br, 12H, β-THF). $^{13}C\{^1H\}$ NMR (100.58 MHz, C_6D_6, 27°C): δ 152.3 (Ph C_{ipso}), 129.0 (Ph m-CH), 124.3 (Ph o - CH), 118.3 (Ph p-CH), 69.7 (α-THF), 59.3 (Lu-CH_2), 25.3 (β-THF).

^1H NMR (400 MHz, THF-d_8, 27°C): ^1H NMR (500 MHz, THF-d_8, 27 °C): δ 6.83 ("t", $^3J_{HH}$ = 7.4 Hz, 6H, Ph m-H), 6.69 (d, $^3J_{HH}$ = 7.2 Hz, 6H, Ph o-H), 6.32 (t, $^3J_{HH}$ = 7.6 Hz, 3H, Ph p-H), 3.62 (m, 12H, α-THF), 1.78 (m, 12H, β-THF), 1.67 (s, 6H, Lu-CH_2). $^{13}C\{^1H\}$ NMR (125.58 MHz, THF-d_8, 27°C): δ 156.39 (Ph C$ipso$), 128.15 (Ph m-C), 124.29 (Ph o-C), 116.34 (Ph p-C), 68.22 (α-C THF), 59.48 (Lu-CH_2), 26.36 (β-C THF).

$Lu(CH_2Ph-4-Me)_3(THF)_3$ (28b)

Same procedure as for $Lu(CH_2Ph)_3(THF)_3$, using anhydrous $LuCl_3$ (1.07g, 3.80 mmol) and KCH_2Ph-4-Me (1.59g, 11.03 mmol) yielded 1.54g, of a pale yellow solid. The product obtained is a mixture of $Lu(CH_2Ph-4-Me)_3(THF)_3$, **28b** and another species, presumably the corresponding 'ate' complex, $K[Lu(CH_2Ph$-4-Me$)_4(THF)_x]$, **30b** as shown by variable temperature ^1H NMR study in THF-d_8.

The material however was successfully used for the synthesis of $(Tp^{tBu,Me})Lu(CH_2Ph-4-Me)_2$.

^{1}H NMR (500 MHz, C_6D_6, 27°C): δ 7.01 (d, $^{3}J_{HH}$ = 8.0 Hz, 6H, *m*-H Ph), 6.78 (d, $^{3}J_{HH}$ = 8.0 Hz, 6H, Ph *o*-H), 3.51 (s br, 12, α-H THF), 2.29 (s, 9H, *p*-CH$_3$ Ph), 1.58 (s, 6H, Lu-CH$_2$), 1.11 (s br, 12H, *β*-H THF). ^{13}C{^{1}H} NMR (125.30 MHz, C_6D_6, 27°C): δ 149.0 (s, *ipso* C Ph), 129.6 (s, *m*-C Ph), 126.7 (s, *p*-C Ph), 124.4 (s, *o*-C Ph), 69.6 (s, α-C THF), 58.6 (s, Lu-CH$_2$), 25.3 (s, *β*-C THF), 20.8 (s, *p*-CH$_3$ Ph).

^{1}H NMR (400 MHz, THF-d_8, 27°C): δ 6.66 (d, $^{3}J_{HH}$ = 8.0 Hz, 6H, Ph *m*-H), 6.59 (d, $^{3}J_{HH}$ = 8.0 Hz, 6H, Ph *o*-H), 3.61 (m, α-THF), 2.14 (s, 9H, *p*-CH$_3$ Ph), 1.76 (m, *β*-THF), 1.57 (s, 6H, Lu-C*H*$_2$). ^{13}C{^{1}H} NMR (100.58 MHz, THF-d_8, 27°C): δ 153.2 (Ph C*ipso*), 128.8 (Ph *m*-C), 124.4 (Ph *o*-C), 68.2 (α-C THF), 59.0 (Lu-CH$_2$), 26.4 (β-C THF), 20.8 (s, *p*-CH$_3$ Ph).

Lu(CH$_2$Ph)$_3$(THF)$_2$ (29a)

A suspension of 0.30 g (0.45 mmol) of Lu(CH$_2$Ph)$_3$(THF)$_3$ in 15 mL of toluene was stirred at room temperature for 1.5 h. During stirring, the color of the suspension became orange-yellow. After 1.5 h, the solvent was stripped under vacuum to obtain an orange-yellow solid. The above procedure was repeated once more to obtain a yellow-orange solid after stripping the solvent in vacuum. The solid was extracted 3 times with about 25 mL of toluene (2 X 10mL and 5mL), until the extract was colorless, to obtain a yellow orange solution and a small amount of a pale yellow solid (later identified as compound **30a**, see later). Sol-

vent was stripped under vacuum to obtain a yellow orange solid. The solid was dried under vacuum for another 2 h to obtain 0.23 g (0.39 mmol, 85%) of **29a** as a yellow-orange solid. X-ray quality crystals were obtained from a dilute toluene solution cooled to -30°C for several days. Anal. Calcd for $C_{29}H_{37}O_2Lu$ (592.58): C, 58.78; H, 6.29. Found: C, 58.85; H, 6.26.

^{1}H NMR (400 MHz, C_7D_8, 27°C): δ 7.10 ("t", $^3J_{HH}$ = 7.6 Hz, 6H, Ph m-H), 6.74 (d, $^3J_{HH}$ = 7.2 Hz, 6H, Ph o-H), 6.71 (t, $^3J_{HH}$ = 7.2 Hz, 3H, Ph p-H), 3.43 (m, 8H, α-THF), 1.50 (s, 6H, Lu- CH_2), 1.15 (m, 8H, β-THF). ^{1}H NMR (400 MHz, C_7D_8, -80°C): δ 7.28 ("t", $^3J_{HH}$ = 7.4 Hz, 6H, Ph m-H), 6.92 (t, $^3J_{HH}$ = 7.2 Hz, 3H, Ph p-H), 6.81 (d, $^3J_{HH}$ = 7.6 Hz, 6H, Ph o-H), 3.29 (s, br 8H, α-THF), 1.60 (s, br 6H, Lu-CH_2), 0.94 (s, br 8H, β-THF). $^{13}C\{^1H\}$ NMR (100.58 MHz, C_7D_8, 27°C): δ 152.1 (Ph C$ipso$), 129.0 (Ph o/m-CH), 124.3 (Ph o/m- CH), 118.3 (Ph p-CH), 71.0 (α-THF), 59.5 (Lu-CH_2), 25.1 (β- THF). $^{13}C\{^1H\}$ NMR (100.58 MHz, C_7D_8, -80°C): δ 152.1 (Ph C$ipso$), 129.6 (Ph m-CH), 124.3 (Ph o-CH), 118.4 (Ph p-CH), 71.4 (α-THF), 58.5 (Lu-CH_2), 25.4 (β- THF).

Conversion of Lu(CH$_2$Ph)$_3$(THF)$_2$ (29a) to Lu(CH$_2$Ph)$_3$(THF)$_3$ (28a)

Lu(CH$_2$Ph)$_3$(THF)$_2$, **30** (0.22g, 0.37 mmol) was dissolved in about 2 mL of toluene and about 0.5 mL THF was added in drops. There was immediate forma-tion of a pale-yellow precipitate. The mixture was kept at -30°C after the addition of THF. After about 30 mins, there was formation of more pale-yellow crystalline solid. Supernatant was removed and the solid was washed with pentane, then dried under vacuum to obtain **28** as a pale yellow crystalline solid in 95% yield

(0.23g, 0.35 mmol). Low temperature and VT ^{1}H and ^{13}C{^{1}H} NMR spectra are consistent with that of the major species in the NMR spectra of a sample from the early preparation of **28a**, pages 240-241. Anal. Calcd. for $C_{33}H_{45}O_3Lu$: C, 59.63; H, 6.82. Found: C, 59.72; H, 6.72.

K[Lu(CH₂Ph)₄(THF)ₙ] (30a)

In a small vial, solid **28a** (33.0 mg, 50 μmol) and KCH₂Ph (6.0 mg, 50 μmol) were mixed together and dissolved in 0.6 mL of THF-d_8 at room temperature. An orange-red solution formed immediately and was transferred into an NMR tube. NMR spectroscopy showed clean conversion to **30a**. The NMR signals correspond to the minor species in the NMR spectra of an early reaction product sample of **28a**.

^{1}H NMR (400 MHz, THF-d_8, 27°C): δ 6.69 (″t″, $^3J_{HH}$ = 7.5 Hz, Ph *m*-H), 6.61(d, $^3J_{HH}$ = 8.0 Hz, Ph *o*-H), 6.07 (t, $^3J_{HH}$ = 7.5 Hz, Ph *p*-H), 3.61 (m, THF), 1.77 (m, THF), 1.59 (s, Lu-C*H₂*). ^{1}H NMR (400 MHz, THF-d_8, -80°C): δ 6.74 (d, $^3J_{HH}$ = 7.5 Hz, Ph *o*-H), 6.65 (″t″, $^3J_{HH}$ = 7.5 Hz, Ph *m*-H), 5.98 (t, $^3J_{HH}$ = 7.0 Hz, Ph *p*-H), 3.61 (m, THF), 1.78 (m, THF), 1.53 (s, Lu-C*H₂*).

^{13}C{^{1}H} NMR (100.58 MHz, THF-d_8, 27°C): δ 158.87 (Ph C*ipso*), 127.72 (Ph *m*-C), 123.26 (Ph *o*-C), 113.25 (Ph *p*-C), 68.26 (α–C THF), 56.71 (Lu-CH₂), 26.36 (β–C THF). ^{13}C{^{1}H} NMR (100.58 MHz, THF-d_8,-80°C): δ 159.17 (Ph C*ipso*), 127.64 (Ph *m*-C), 122.49 (Ph *o*-C), 112.13 (Ph *p*-C), 68.23 (α–C THF), 53.45 (Lu-CH₂), 26.39 (β–C THF).

**Variable temperature NMR studies in THF-d_8**

a) Once-crystallized material from early preparation of Lu(CH$_2$Ph)$_3$(THF)$_3$

VT NMR study on the material obtained from the preparation described on pages 234-235 showed two sets of resonances at low temperature. The two sets of resonances at LT are in a 2.7:1 ratio, minor peaks marked with prime; the major set is due to **28a**, while the minor is K[Lu(CH$_2$Ph)$_4$(THF)$_x$], **30a** (ca. 22%).

^{1}H NMR (400 MHz, THF-d_8, 27°C): δ 6.78 (s br, 6H, Ph *m*-H), 6.67 (d, $^3J_{HH}$ = 7.2 Hz, 6H, Ph *o*-H), 6.25 (s br, 3H, Ph *p*-H), 3.62 (m, 12H, α-THF), 1.77 (m, 12H, *β*-THF), 1.64 (s, 6H, Lu-C*H$_2$*). ^{1}H NMR (400 MHz, THF-d_8, -80 °C): δ 6.84 (″t″, $^3J_{HH}$ = 7.6 Hz, Ph *m*-H), 6.73 (d, $^3J_{HH}$ = 7.6 Hz, Ph′ *o*-H), 6.67–6.62 ((doublet overlapping with a triplet and other minor peaks) d, $^3J_{HH}$ = 7.6 Hz, Ph *o*-H; ″t″, $^3J_{HH}$ = 7.2 Hz, Ph′ *m*-H), 6.32 (t, $^3J_{HH}$ = 7.4 Hz, Ph *p*-H), 5.98 (t, $^3J_{HH}$) 7.0 Hz, Ph′ *p*-H), 3.62 (m, 12H, α-THF), 1.78 (m, 12H, *β*-THF), 1.73 (s, (partially buried under THF-d_8 solvent peak) Lu-C*H$_2$*), 1.52 (s br, Lu′-C*H$_2$*).

^{13}C{^{1}H} NMR (100.58 MHz, THF-d_8, 27°C): δ 156.9 (Ph C*ipso* v br.), 128.0 (Ph *o/m*-CH), 124.0 (Ph *o/m*-CH), 115.9 (Ph *p*-CH v br), 68.3 (THF), 59.0 (Lu-CH$_2$ v br), 26.3 (THF). ^{13}C{^{1}H} NMR (100.58 MHz, THF-d_8, -80 °C): δ 159.2 (Ph′ C*ipso*), 156.3 (Ph C*ipso*), 128.4 (Ph *o/m*-CH), 127.8 (Ph′ *o/m*-CH), 123.9 (Ph *o/m*- CH), 122.6 (Ph′ *o/m*-CH), 116.0 (Ph *p*-CH), 112.3 (Ph′ *p*-CH), 70.7 (br, THF), 68.4 (α-THF), 59.3 (Lu-CH$_2$), 53.5 (Lu′-CH$_2$), 26.5 (*β*- THF).

b) Once-crystallized material from early preparation of

   Lu(CH$_2$Ph-4-Me)$_3$(THF)$_3$
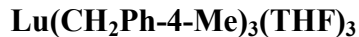
In this case, both **28b** and **30b** are soluble in aromatic solvents, thus making the detection of the ′ate′ complex difficult at the initial stage. However, VT NMR study in THF-d_8 on the material obtained from the preparation described on pages 237-238 showed two sets of resonances at low temperature. The two sets of resonances at LT are in a 2.9:1 ratio i.e. it contained ca. 21% of K[Lu(CH$_2$Ph-4-Me)$_4$(THF)$_x$], **30b**.

^{1}H NMR (400 MHz, THF-d_8, 27°C): δ 6.62 (s br, 6H, Ph m-H), 6.57 (s br, 6H, Ph o-H), 3.62 (m, α-H THF), 2.13 (s, 9H, Ph p-CH$_3$), 1.78 (m, β-H THF), 1.54 (s, 6H, Lu-CH_2). ^{1}H NMR (400 MHz, THF-d_8, -80 °C): δ 6.67 (d, $^3J_{HH}$ = 8.0 Hz, Ph m-H), 6.65 (d, $^3J_{HH}$ = 8.0 Hz, Ph′ m-H), 6.56 (d, $^3J_{HH}$ = 8.0 Hz, Ph o-H), 6.47 (d, $^3J_{HH}$ = 8.0 Hz, Ph′ p-H), 3.62 (m, α-H THF), 2.14 (s, Ph p-CH$_3$), 2.05 (s, Ph′ p-CH$_3$), 1.78 (m, β-H THF), 1.62 (s, Lu-CH_2), 1.40 (s br, Lu′-CH_2).

^{13}C{^{1}H} NMR (100.58 MHz, THF-d_8, 27°C): δ 153.4 (Ph C$ipso$ v br.), 129.0 (Ph m-CH), 124.2 (Ph o-CH), 118.5 (Ph p-CH v br), 68.3 (THF), 58.8 (Lu-CH$_2$ v br), 26.4 (THF), 20.8 (p-CH$_3$ Ph). ^{13}C{^{1}H} NMR (100.58 MHz, THF-d_8, -80 °C): δ 156.1 (Ph′ C$ipso$), 153.0 (Ph C$ipso$), 128.8 (Ph m-CH), 128.2 (Ph′ m-CH), 123.9 (Ph p-CH), 123.8 (Ph o-CH), 122.5 (Ph′ o-CH), 119.6 (Ph′ p-CH), 70.5 (br, THF), 68.2 (α-THF), 58.6 (Lu-CH$_2$), 52.4 (Lu′-CH$_2$), 26.5 (β- THF), 21.1 (Ph′ p-CH$_3$), 21.0 (Ph p-CH$_3$).

Synthesis of Y(CH$_2$Ph-4-Me)$_3$(THF)$_3$

Following the same procedure as used for **28a**, using anhydrous YCl$_3$ (0.87g, 4.46 mmol) and KCH$_2$Ph-4-Me 1.93g, 13.4 mmol) to obtain (1.62g, 2.61 mmol) of Y(CH$_2$Ph-4-Me)$_3$(THF)$_3$ as a yellow orange solid in 59% isolated yield. ^{1}H NMR (500 MHz, C$_6$D$_6$, 27°C): δ 6.99 (d, $^3J_{HH}$ = 7.7 Hz, 6H, *m*-H Ph), 6.71 (d, $^3J_{HH}$ = 7.6 Hz, 6H, Ph *o*-H), 3.49 (s, br 12, α-H THF), 2.26 (s, 9H, *p*-CH$_3$ Ph), 1.75 (s, 6H, Y-C*H$_2$*), 1.27 (s, br 12H, β-H THF). ^{13}C{^{1}H} NMR (125.3 MHz, C$_6$D$_6$, 27°C): δ 148.79 (*ipso* C Ph), 130.29 (*m*-C Ph), 123.52 (*o*-C Ph), 115.10 (*p*-C Ph), 69.21 (α-C THF), 51.82 (br Y-C*H$_2$*), 25.42 (β-C THF), 20.88 (*p*-CH$_3$ Ph).

Synthesis of (Tp^{tBu,Me})Ln(CH$_2$Ph-4-R)$_2$(THF)$_{1/0}$ Complexes

(Tp^{tBu,Me})Y(CH$_2$Ph-4-Me)$_2$ (31b)

At room temperature, a colorless THF solution of HTp^{tBu,Me} (0.239g, 0.560 mmol) was added slowly to a pale yellow THF solution of Y(CH$_2$Ph-4-Me)$_3$(THF)$_3$ (0.350g, 0.560 mmol). The solution gradually became lighter in color and finally resulted in a clear, pale yellow, almost colorless solution. The resulting pale yellow solution was stirred for another 4 h at RT. Solvent was removed under reduced pressure to obtain a sticky colorless solid which was triturated with pentane to obtain a white powder after removing solvent in vacuum. The resulting powder was extracted with hexanes (7 mL) to obtain a colorless solution and leaving behind a small amount of an insoluble residue. The colorless solution was concentrated to about 2 mL and cooled down to -30°C to obtain the compound as a pale-yellow crystalline solid in 75% isolated yield (0.304g, 0.421 mmol) after

drying under vacuum. X-ray quality crystals were obtained by cooling a concentrated hexane solution to -30°C. Anal. Calcd. for $C_{40}H_{58}N_6BY$ (**31b**): C, 66.48; H, 8.09 N, 11.63. Found: C, 66.58; H, 8.28; N, 10.78.

^{1}H NMR (400 MHz, C_6D_6, 27°C): δ 6.94 (d, $^3J_{HH}$ = 8.0 Hz, 4H, *m*-H Ph), 6.72 (s, br 4H, *o*-H Ph), 5.55 (s, 3H, 4-*H*-Pz), 4.50 (br, 1H, *H*-B), 2.29 (s, 6H, *p*-CH$_3$ Ph), 2.11 (s, br Y-C*H*$_2$), 2.01 (s, 9H, 5-*Me*-Pz), 1.34 (s, 27H, 3-(C*H$_3$*)$_3$C-Pz). ^{13}C{^{1}H} NMR (100 MHz, C_6D_6, 27°C): δ 164.35 (s, 5-*C*-Pz), 150.32 (s, 3-C-Pz), 147.00 (s, *ipso*-C Ph), 128.65 (s, *m*-C Ph), 125.91 (s, *p*-C Ph), 124.71 (s, *o*-C Ph), 103.41 (s, 4-*C*-Pz), 58.48 (d, $^1J_{YC}$ = 37.3 Hz Y-*C*H$_2$), 32.30 (s, 3-(CH$_3$)$_3$*C*-Pz), 31.60 (s, 3-(*C*H$_3$)$_3$C-Pz), 21.01 (s, *p*-CH$_3$ Ph), 13.03 (s, 5-*Me*-Pz). ^{11}B NMR (128 MHz, C_6D_6, 27°C): δ -8.21.

(Tp^{tBu,Me})Lu(CH$_2$Ph)$_2$ (32a)

A procedure analogous to **31b** using Lu(CH$_2$Ph)$_3$(THF)$_3$ (0.510g, 0.767 mmol) and HTp^{tBu,Me} (0.326g, 0.767 mmol) gave **32a** (0.455g, 0.583 mmol, 76% yield) as a white solid. Anal. Calcd. for $C_{41.50}H_{58}N_6BLu$ (**32a·½ C$_7$H$_8$**): C, 60.08; H, 7.09 N, 10.16. Found: C, 59.84; H, 7.46; N, 10.23.

^{1}H NMR (400 MHz, C_6D_6, 27°C): δ 7.14 (s, br, 4H, *m*-H Ph,), 7.00-6.50 (br, 6H, *o*- & *p*-H Ph), 5.57 (s, 3H, 4-*H*-Pz), 4.50 (br, 1H, *H*-B), 2.07 (s, 9H, 5-*Me*-Pz), 1.96 (s, br Lu-C*H*$_2$), 1.35 (s, 27H, 3-(C*H$_3$*)$_3$C-Pz). ^{13}C{^{1}H} NMR (100 MHz, C_6D_6, 27°C): δ 164.85 (s, 5-*C*-Pz). 153.63 (s, 3-C-Pz), 147.16 (s, *ipso*-C Ph), 128.53 (s, *m*-C Ph), 125.23 (s, *o*-C Ph), 118.31 (s, *p*-C Ph), 103.96 (s, 4-*C*-Pz), 65.51 (s, Lu-*C*H$_2$), 32.36 (s, 3-(CH$_3$)$_3$*C*-Pz), 31.49 (s, 3-(*C*H$_3$)$_3$C-Pz), 13.01 (s, 5-

Me-Pz). ^{11}B NMR (128 MHz, C$_6$D$_6$, 27°C): δ -8.40.

(Tp$^{t\text{Bu,Me}}$)Lu(CH$_2$Ph-4-Me)$_2$ (32b)

A procedure analogous to **31b** using Lu(CH$_2$Ph-4-Me)$_3$(THF)$_3$ (0.260g, 0.368 mmol) and HTp$^{t\text{Bu,Me}}$ (0.156g, 0.368 mmol) gave **32b** (0.221g, 0.273 mmol, 74% yield) as a pale-yellow solid. Anal. Calcd. for C$_{40}$H$_{58}$N$_6$BLu (**32b**): C, 59.41; H, 7.23 N, 10.39. Found: C, 59.77; H, 7.26; N, 10.38.

^{1}H NMR (400 MHz, C$_6$D$_6$, 27°C): δ 6.93 (s, 4H, *m*-H Ph), 6.65 (s, br 4H, *o*-H Ph), 5.58 (s, 3H, 4-*H*-Pz), 4.50 (br, 1H, *H*-B), 2.32 (s, 6H, *p*-CH$_3$ Ph), 2.03 (s, br Lu-C*H*$_2$), 1.97 (s, 9H, 5-*Me*-Pz), 1.37 (s, 27H, 3-(*CH*$_3$)$_3$C-Pz). ^{13}C{^{1}H} NMR (100 MHz, C$_6$D$_6$, 27°C): δ 164.83 (s, 5-*C*-Pz), 150.41 (s, 3-C-Pz), 147.02 (s, *ipso*-C Ph), 128.12 (s, *m*-C Ph), 126.38 (s, *o*-C Ph), 125.28 (s, *p*-C Ph), 103.93 (s, 4-*C*-Pz), 65.50 (s, Lu-*CH*$_2$), 32.23 (s, 3-(CH$_3$)$_3$*C*-Pz), 31.53 (s, 3-(*CH*$_3$)$_3$C-Pz), 20.94 (s, *p*-CH$_3$ Ph), 12.98 (s, 5-*Me*-Pz). ^{11}B NMR (128 MHz, C$_6$D$_6$, 27°C): δ -8.41.

(Tp$^{\text{Me2}}$)Y(CH$_2$Ph-4-Me)$_2$(THF) (33b)

Method 1: Toluene Reaction

To an orange-yellow toluene solution (10 mL) of Y(CH$_2$Ph-4-Me)$_3$(THF)$_2$ (0.21g, 0.34 mmol) was added a colorless solution of HTp$^{\text{Me2}}$ in the same solvent (0.10g, 0.34 mmol). The resulting yellow mixture was stirred at room temperature for another for 4 h. Solvent was stripped under vacuum to obtain an orange- yellow sticky solid. Trituration of the sticky solid with pentane followed by removal of solvent in vacuum affords an orange-yellow solid. ^{1}H NMR of the crude prod-

uct in C_6D_6 showed a mixture of compounds. The solid was re-dissolved in toluene, centrifuged and concentrated to about 1 mL, layered with pentane, and kept at -30°C overnight to give some pale-yellow flaky solid. Supernatant was decanted and attempts to dry the solid gave oily material which did not yield any solid upon several triturations. Solvent was removed from the supernatant to obtain a pale-yellow solid. The ^{1}H NMR of this solid in C_6D_6 still showed a mixture of compounds. The solid was re-dissolved in toluene, centrifuged, layered with hexanes and cooled to -30°C for several days to obtain pale-yellow crystals from which the solid state, X-ray structure was obtained.

Method 2: THF Reaction

To a pale-yellow THF solution (10 mL) of $Y(CH_2Ph\text{-}4\text{-}Me)_3(THF)_3$ (0.26g, 0.41 mmol) cooled to -30°C was added solid HTp^{Me2} (0.12g, 0.41 mmol). The resulting yellow mixture was allowed to warm up to room-temperature over 4 h. Solvent was stripped under vacuum to obtain an orange- yellow sticky solid. Trituration of the sticky solid with pentane followed by removal of solvent in vacuum afforded an orange-yellow solid. The solid was re-dissolved in THF and centrifuged to obtain an orange-yellow solution. The solution was concentrated to about 1 mL, layered with pentane, and kept at -30°C overnight to give 0.18g of an orange-yellow solid. ^{1}H and [13]{^{1}H} NMR showed it signals assignable to **33b** but still with other unidentified peaks.

^{1}H NMR (400 MHz, C_6D_6, 27°C): δ 7.13 (d, J_{HH} = 8.0 Hz, 4H, *m*-H Ph) 7.04 (d, J_{HH} = 8.0 Hz, 4H, *o*-H Ph) 5.55 (s, br, 3H, 4-*H*-Pz), 4.85 (br, 1H, *H*-B),

3.52 (br, 4H, THF), 2.33 (br, 6H, 4-Me Ph), 2.31 (s, 9H 3-*Me*- Pz), 2.20 (br, 4H Y-C*H$_2$*), 2.09 (s, 9H, 5-*Me*-Pz), 1.20 (br, 4H, THF). ^{13}C NMR (100 MHz, C$_6$D$_6$, 27°C): δ 151.43 (s, 5-*C*-Pz), 150.34 (s, *ipso*-C Ph), 145.40 (s, 3-C-Pz), 129.15 (s, *m*-C Ph), 125.40 (s, *p*-C Ph), 124.61 (s, *o*-C Ph), 106.24 (s, 4-*C*-Pz), 70.32 (s br, THF), 55.81 (d, J$_{YC}$ = 34.7 Hz, Y-C*H$_2$*), 25.19 (s, THF), 22.99 (s, *p*-CH$_3$ Ph), 14.29 (s, 3-*Me*-Pz), 12.98 (s, 5-*Me*-Pz). ^{11}B NMR (128 MHz, C$_6$D$_6$, 27°C): δ -8.99.

5.8.4   X-ray Structure Determinations

The crystals were handled as described in previous chapters. Data for compound **28a** was collected by Mr. David O. Miller at the Department of Chemistry, Memorial University of Newfoundland. Data refinement and structural solution of **28a** was carried out by Dr. M. J. Ferguson. Complete X-ray structure determinations for other compounds were carried out by Dr R. McDonald and Dr. M. J. Ferguson at the X–ray Crystallographic Laboratory, Department of Chemistry University of Alberta

Summary of data collection and structure refinement are given in the Structure Reports; **28a** (TAK 0607); **29a** (TAK 0802); **31b** (TAK 0724); **32a** (TAK 0725); **32b** (TAK 0723); **33b** (TAK 0728).

5.9 References

1. Dolgoplosk, B. A.; Tinyakova, E. I.; Guzman, I. Sh.; Vollerstein, E. L.; Chigir, N. N.; Bondarenko, G. N. Sharaev, O. K.; Yakovlev, V. A. *J. Organomet. Chem.* **1980**, *201*, 249-255.

2. Thiele, K.-H.; Unverhau, K.; Geitner, M. Jakob K. *Z. Anorg. Allg. Chem.* **1987**, *548*, 175-179.

3. Manzer, L. E. *J. Am. Chem. Soc.* **1978**, *100*, 8068-8073.

4. Harder, S. *Organometallics* **2005**, *24*, 373-379.

5. Bambirra, S.; Meetsma, A.; Hessen, B. *Organometallics* **2006**, *25*, 3454-3462.

6. Ge, S.; Meetsma, A.; Hessen, B. *Organometallics* **2009**, *28*, 719-726.

7. Meyer, N.; Roesky, P. W.; Bambirra, S.; Meetsma, A.; Hessen, B.; Saliu, K.; Takats, J. *Organometallics* **2008**, *27*, 1501-1505.

8. Carver, C. T.; Montreal, M. J.; Diaconescu, P. L. *Organometallics* **2008**, *27*, 363-370.

9. Evans, W. J.; Brady, J. C.; Ziller, J. W. *J. Am. Chem. Soc.* **2001**, *123*, 7711-7712.

10. Cheng, J.; Saliu, K.; Kiel, G. Y.; Ferguson, M. J.; McDonald, R.; Takats, J. *Angew. Chem. Int. Ed.* **2008**, *47*, 4910-4913.

11. Cameron, T. M.; Gordon, J. C.; Scott, B. L. *Organometallics* **2004**, *23*, 2995-3002.

12. Schumann, H.; Freckmann, D. M. M.; Dechert, S. *Z.Anorg. Allg. Chem.* **2002**, *628*, 2422-2426.

13. Shannon, R. D. *Acta Crystallogr.* **1976**, *A32*, 751-767.

14. Kiel, G.; Takats, J. Unpublished Results

15. Bambirra, S. Personal Communications.

16. (a) Lee, A. G. *Q. Rev., Chem. Soc.* **1970**, *24*, 310–329. (b) Schwerdtfeger, P.; Boyd, P.D. W.; Bowmaker, G. A.; Mack, H. G.; Oberhammer, H. *J. Am. Chem. Soc.* **1989**, *111*, 15–23.

17. (a) Askarinejad, A; Morsali, A. *Helv. Chim. Acta* **2006**, *89*, 265-269. (b) Askarinejad, A; Morsali, A. *J. Organomet. Chem.* **2006**, *691*, 3563–3566.

18. Wiesbrock, F.; Schmidbaur, H. *J. Am. Chem. Soc.* **2003**, 125, 3622-3630.

19. Blackwell, J,; Lehr, C.; Sun, Y. M.; Piers, W. E.; Pearce-Batchilder, S. D.; Zaworotko, M. J.; Young, V. G. *Can. J. Chem.* **1997**, *75*, 702–711.

20. Trofmenko, S.; Calabrese, J. C.; Kochi, J. K.; Wolowiec, S.; Hulsbergen, F. B.; Reedijk, J. *Inorg. Chem.* **1992**, *31*, 3943.

21. Hasinoff, L.; Takats, J.; Zhang, X. W. ; Bond, A. H.; Rogers, R. D. *J. Am. Chem. Soc.,* **1994**, *116,* 8833–8834. (b) Maunder, G. H.; Sella, A.; Tocher, D. A. *J. Chem. Soc. Chem. Commun.* **1994**, 2689–2690.

22. Bambirra, S.; Brandsma M. J. R.; Brusse, E. A. C.; Meetsma, A.; Hessen, B.; Teuben, J. H. *Organometallics* **2000**, 19 (16), 3197-3204.

23. Schlosser, M.; Hartmann, J. *Angew. Chem., Int. Ed. Engl.* **1973**, *12*, 508-509.

24. Trofmenko, S.; Calabrese, J. C.; Kochi, J. K.; Wolowiec, S.; Hulsbergen, F. B.; Reedijk, J. *Inorg. Chem.* **1992**, *31*, 3943–3950.

25. (a) Trofimenko, S.; *J. Am. Chem. So*c. **1967**, *89*, 3170–3177.

251

(b) Kresinski, R. A.; *J. Chem. Soc., Dalton Trans*. 1999, 401–406.

26. Kisko, J. L.; Hascall, T.; Kimblin, C.; Parkin, G. *J. Chem. Soc. Dalton Trans*. **1999**, 1929–1935.

Chapter 6

Conclusions and Future Works

6.1   Conclusions

The goal of this thesis was to further explore the chemistry of organolanthanide complexes supported by tris(pyrazolyl)borate ligands, $Tp^{R,R'}$. The focus of the main subject is on trivalent lanthanide chemistry, but divalent ytterbium complexes were first explored as a means of introducing the author to organolanthanide chemistry. The rest of the thesis was thus devoted exclusively to the synthesis, characterization and reactivity studies on trivalent lanthanide complexes bearing lanthanide-carbon σ-bonds. Interest in these complexes arose due to their usefulness for a variety of transformations; stoichiometric and catalytic. Although, this area has been dominated by bis-cyclopentadienyl mono alkyl type complexes, (Cp_2LnR), there has been a lot of recent interest in the isolation of mono-ligand dialkyl complexes of the type $(Ligand)LnR_2L_n$ bearing two reactive lanthanide-carbon sigma bonds.[1,2] Apart from the works of Hessen[3] and Hou,[1,4] work in this area has mostly been limited to the group 3 metals and the smaller, late lanthanides. This is due to the fact that such complexes with the early, large lanthanide centers tend to undergo facile ligand redistribution as a result of insufficient steric protection for the large lanthanide centers.

The tris(pyrazolyl)borate ligands, $Tp^{R,R'}$ have proved very effective for lanthanide metals due to the combination of hard nitrogen donor atoms and their bulky nature.[5]

253

Divalent ytterbium borohydride complexes, $(Tp^{tBu,Me})Yb(BH_4)(THF)_{1/0}$ were successfully synthesized and characterized. The first isolation of $(Tp^{tBu,Me})Yb(BH_4)(THF)$ was from the crystallization of $(Tp^{tBu,Me})Yb(BH_4)$ obtained from the reaction of $[(Tp^{tBu,Me})YbH]_2$ with BH_3NH_3. Its preparation by salt metathesis is solvent, reaction time and MBH_4 (M = K, Na) dependent. However, an optimum condition was found using a $NaBH_4/MeCN$ combination. In solution, the compounds display dynamic behavior as shown by the presence of one set of signals for the pyrazolylborate ligands as well as the tetrahydroborate ligand. In the solid state, $(Tp^{tBu,Me})Yb(BH_4)(THF)$ is monomeric with the ytterbium center coordinated by one $Tp^{tBu,Me}$ ligand, a BH_4 ligand and one coordinated THF molecule. Both the $Tp^{tBu,Me}$ and BH_4 ligand are coordinated in κ^3 fashion to the ytterbium center. Although all attempts to obtain X-ray quality crystals of $(Tp^{tBu,Me})Yb(BH_4)$ proved fruitless, its formulation as the solvent free analogue of $(Tp^{tBu,Me})Yb(BH_4)(THF)$ is in accord with spectroscopic evidence. The κ^3-bonding mode of the BH_4 ligand in $(Tp^{tBu,Me})Yb(BH_4)$ was inferred from IR data.

A series of mono-$Tp^{R,R'}$ lanthanide dialkyl complexes, $(Tp^{R,R'})Ln(CH_2SiMe_2R'')_2(THF)_{1/0}$ (R = R' = H, Me, n = 1 ; R = ^{t}Bu, R' = Me, n = 0; R'' = Me, Ph; Ln = Yb, Lu) were successfully isolated from the homoleptic $Ln(CH_2SiMe_3)_3(THF)_2$ (Ln = Yb, Lu) complexes via two alternative and complementary methods; alkyl abstraction and protonolysis. The complexes are remarkably stable with no tendency for ligand redistribution. The structures of $(Tp^{tBu,Me})Ln(CH_2SiMe_2Ph)_2$ complexes were determined in the solid state. They consist of five coordinate lanthanide centers with κ^3-pyrazolylborate ligands and

two carbon atoms of the alkyl ligands coordinated in a distorted trigonal bipyramidal geometry. In solution, the room temperature ^{1}H NMR spectra of $(Tp^{tBu,Me})Lu(CH_2SiMe_2R'')_2$ complexes showed that the compounds are fluxional. At low temperature however, the expected number of signals were obtained in ratio appropriate for the C_s symmetric trigonal bipyramidal structure. The $(Tp^{Me2})Ln(CH_2SiMe_2R'')_2(THF)$ (R'' = Me, Ph; Ln = Yb, Lu) compounds were all characterized in solution as well as in the solid state. The solid state structures of the six-coordinate $(Tp^{Me2})Ln(CH_2SiMe_2R'')_2(THF)$ complexes is distorted octahedral with κ^3-pyrazolylborate ligands, two carbon atoms of the alkyl ligands and an oxygen atom of a coordinated THF molecule coordinated to the lanthanide centers.[6] In solution, the lutetium complexes, $(Tp^{Me2})Lu(CH_2SiMe_2R'')_2(THF)$, display a certain degree of dynamic behaviour due to the dissociation and recoordination of the coordinated THF ligand, the process is however solvent dependent. For the ytterbium complexes, $(Tp^{Me2})Yb(CH_2SiMe_2R'')_2(THF)$, the room temperature ^{1}H NMR spectra approximate the observed solid state structure with well separated peaks which are shifted due to the effect of the paramagnetic ytterbium center.

Hydrogenolysis of the dialkyl complexes, $(Tp^{Me2})Ln(CH_2SiMe_3)_2(THF)$, afforded the corresponding dihydrides, "$(Tp^{Me2})LnH_2$" (Ln = Yb, Lu) which proved to be tetrameric in the solid state and in solution. For the ytterbium compound, although the conversion was successful, attempts to recrystallize the compound was complicated by disproportionation and ligand redistribution with formation of the highly insoluble divalent compound, $(Tp^{Me2})_2Yb$ and other unidenti-

fied products. Hydrogenolysis of (Tp)Yb(CH$_2$SiMe$_3$)$_2$(THF) gave the hexanuclear hydride [(Tp)YbH$_2$]$_6$. Thus, the nuclearity of the hydride cluster is dependent on the steric size of the ancillary scorpionate ligand.

The dialkyl complexes (Tp^{Me2})Lu(CH$_2$SiMe$_3$)$_2$(THF) also react with a variety of terminal alkynes giving the bis-alkynide complexes, "(Tp^{R,Me})Ln(C≡CR″)$_2$" (R = Me, ^{t}Bu, R″ = Ph, ^{t}Bu, SiMe$_3$, Ad and Trit′; Ln = Y, Lu). The structures of the complexes depend on the steric sizes of both the substituent on position 3 of the pyrazolyl group of the ligand as well as the R″ group on the alkyne. With the Tp^{Me2} ligand and R″ = Ph, ^{t}Bu, SiMe$_3$, Ad, the compounds obtained were dimeric bis-alkynide complexes of the form [(Tp^{Me2})Ln(μ-C≡CR″)$_2$]$_2$(μ-R″CCCCR″) with both bridging and coupled alkynide units. These complexes are in equilibrium with the monomeric THF adduct (Tp^{Me2})Ln(C≡CR″)$_2$(THF) in THF. In the presence of bipyridine, (Tp^{Me2})Lu(C≡C^{t}Bu)$_2$(2,2′-bipy) was obtained and characterized. In the case of R″ = Trit′, monomeric (Tp^{Me2})Ln(C≡CTrit′)$_2$(THF) were obtained. Reaction of the dialkyl complexes supported by the more bulky ancillary Tp^{tBu,Me} ligand, (Tp$^{tBu,Me′}$)Ln(CH$_2$SiMe$_3$)$_2$ (Ln = Y, Lu) with phenyl acetylene afforded the bis-alkynide complexes (Tp^{tBu,Me})Ln(C≡CPh)$_2$, which are both monomeric and without further solvent or additional ligand coordination. Both the dialkyl [(Tp^{Me2})Ln(CH$_2$SiMe$_3$)$_2$ complexes and the bis-alkynide [(Tp^{Me2})Ln(μ-C≡CR″)$_2$]$_2$(μ-R″CCCCR″) (R″ = Ph, SiMe$_3$) were found to catalytically dimerize terminal alkynes giving either the *cis*- or *trans*-head-to-head dimers, depending on the system, albeit in low yield and with low conversion.

In search of more reactive lanthanide dialkyl system, lutetium tribenzyl complexes $Lu(CH_2Ph\text{-}4\text{-}R)_3(THF)_3$, (R = H, Me) were synthesized. The isolation of these complexes was accompanied by formation of variable amounts of the corresponding 'ate' complexes, $K[Lu(CH_2Ph\text{-}4\text{-}R)_4(THF)_n]$. Pure samples of the compounds $Lu(CH_2Ph\text{-}4\text{-}R)_3(THF)_3$ were obtained by extracting the crude reaction products with toluene. Trituration of $Lu(CH_2Ph)_3(THF)_3$ with toluene followed by extraction and recrystallization from toluene afforded $Lu(CH_2Ph)_3(THF)_2$. Protonolysis reaction with $HTp^{R,Me}$ afforded the corresponding dibenzyl complexes, $(Tp^{R,Me})Ln(CH_2Ph\text{-}4\text{-}R)_2(THF)_{1/0}$.

6.2   Future Works

Further research in this area should include development of an alternative approach to the isolation of the scorpionate supported lanthanide dialkyl complexes which does not involve the use of poisonous thallium reagents. This is especially important for the Tp^{Me2} and Tp supported complexes which rely solely on this approach. A potential candidate is the reaction of the potassium or sodium salts of these ligands with the readily available and thermally robust cationic dialkyl complexes, $[Ln(CH_2SiMe_2R'')_2(THF)_n][Anion]$, eq. 6.1 .[7] This method should also allow the extension of the synthesis to other $Tp^{R,R'}$ ligands with substituents of

$$Ln(CH_2SiMe_2R'')_2(THF)_n^+ + M(Tp^{R,R'}) \longrightarrow (Tp^{R,R'})Ln(CH_2SiMe_2R'')_2(THF)_{1/0} + M^+ \qquad 6.1$$
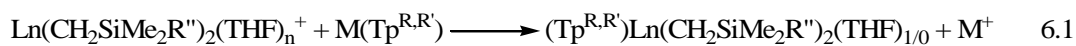
different steric and electronic demands, so as to allow for structural comparison with the complexes described herein and to determine the effect of these substituents on the course of further reactions of the resulting dialkyl complexes.

The dialkyl and dihydride complexes described here are potential starting materials for the preparation of the corresponding cationic complexes, which, as mentioned in the introduction to chapter 3, are believed to be more active than their neutral counterparts for ethylene polymerization. Furthermore, the bulk of the ancillary $Tp^{R,R'}$ ligands might be expected to help stabilize the initial product of ethylene insertion into the Ln-C or Ln-H bonds. Isolation of putative intermediates in ethylene polymerization would be of great value to offer further insights to the mechanism of the reaction.
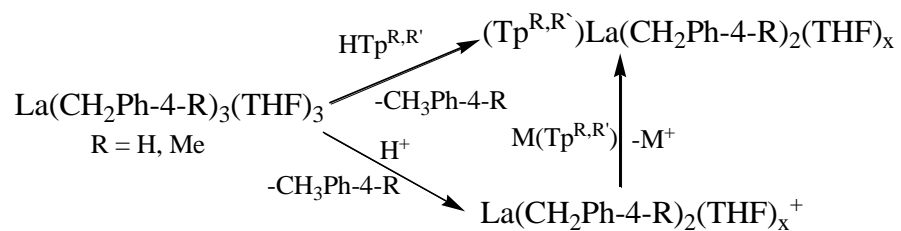
The reaction of terminal alkynes with $(Tp^{Me2})Ln(CH_2SiMe_3)_2(THF)$ (Ln = Y, Lu) complexes provided yet another illustration of the ability of the $Tp^{R,R'}$ ligands to steer reaction in different directions. Coupling of terminal alkynes by metals have been observed before,[8,9,10,11] but formation of coupled alkynide unit with a Z-enyne bonding motif is unprecedented. So far only the effect of the steric size of the alkyne substituents on the course of the reaction was investigated. To probe the effect of electronic factors on alkynide coupling, it is essential to carry out the reaction of $(Tp^{Me2})Ln(CH_2SiMe_3)_2(THF)$ complexes (Ln = Y, Lu) with terminal alkynes having substituents with distinctly different electronic properties, similar to what was done by Lee[12] using phenyl acetylene with different para-substituents. In the above study, it was observed that electron withdrawing groups favor the formation of coupled alkynide products. It is intriguing to speculate that

258

perhaps electron donor groups might prevent coupling and lead to further examples of monomeric "$(Tp^{R,R'})Ln(C{\equiv}CAr\text{-}X)_2$" (X = electron donating group) complexes with terminal alkynide ligands.

Furthermore, it is essential to improve the catalytic performance of both the dialkyl and the preformed bis-alkynide complexes for the dimerization of terminal alkynes. The exclusive formation of head-to-head coupled alkyne dimers by these complexes is rather fascinating and it is in contrast to previously known systems in which either exclusive formation of head-to tail or a mixture of head-to-head and head-to-tail dimers are formed.[13] Since the preformed alkynide dimers are known to exist as monomers in THF, carrying out the reactions in this solvent may potentially increase the rate of the reaction thus improving the catalytic performance of these complexes.

Lastly, the synthesis of the elusive lanthanum dialkyl and dihydride complexes, $(Tp^{R,R'})La(CH_2R'')_2(THF)_x$ (R'' = $SiMe_3$, $SiMe_2Ph$, Ph) and "$(Tp^{R,R'})LaH_2$" are still of interest given the paucity of the dialkyl and especially the dihydride complexes of this largest lanthanide. The large ionic radius of lanthanum is expected to be an advantage when it comes to reactivity studies. A possible way of achieving this goal is by starting from the known lanthanum tribenzyl complexes, $La(CH_2Ph\text{-}4\text{-}R)_3(THF)_3$. Protonolysis of these complexes was shown to give the corresponding dibenzyl complexes, $LLa(CH_2Ph\text{-}4\text{-}R)_2(THF)_x$ (L = ArN=CPhNAr, N-{2-pyrolidin-1-ylethyl)-1,4-diazepan-6-amido ligand).[14,15] Similar protonolysis with $HTp^{R,R'}$ is a potential route to the preparation of the corresponding $(Tp^{R,R'})La(CH_2Ph\text{-}4\text{-}R)_2(THF)_x$ complexes, Scheme 6.1. Alternatively converting

the tribenzyl complexes to the monocation, $La(CH_2Ph\text{-}4\text{-}R)_2^+$,[14] followed by reac-

tion with the alkali metal salt of the ligand is another potential route, Scheme 6.1.

$La(CH_2Ph\text{-}4\text{-}R)_3(THF)_3$
$R = H, Me$

$HTp^{R,R'}$ $-CH_3Ph\text{-}4\text{-}R$ → $(Tp^{R,R`})La(CH_2Ph\text{-}4\text{-}R)_2(THF)_x$

H^+ $-CH_3Ph\text{-}4\text{-}R$ → $La(CH_2Ph\text{-}4\text{-}R)_2(THF)_x^+$

$M(Tp^{R,R'})$ $-M^+$

Scheme 6.1 Possible Synthetic Routes for the Isolation of
$(Tp^{R,R'})La(CH_2Ph\text{-}4\text{-}R)_2(THF)_x$ Complexes

6.3 References

1. Cui, D. M.; Nishiura, M. Hou, Z. *Macromolecules* **2005**, *38*, 4089-4095.

2 . Lyubov, D. M.; Fukin, G. K.; Trifonov, A. A. *Inorg. Chem.* **2007**,*46*, 11450-11456, and references therein.

3. Bambirra, S.; Bouwkamp, M. W.; Meetsma, A.; Hessen, B. *J. Am. Chem. Soc.* **2004**, *126*, 9182–9183.

4. (a) Luo, Y. J.; Nishiura, M.; Hou, Z. *J. Organomet. Chem.* **2007**, *692*, 536-544.

5. (a) Carvalho, A.; Domingos, A.; Gaspar, P.; Marques, N.; Pires de Matos, A.; Santos, I. *Polyhedron* **1992**, *11*, 1481–1488. (b) Santos, I.; Marques, N.; *New   J. Chem*. **1995,** *19*, 551–571. (b) Marques, N.; Sella, A.; Takats, J. *Chem. Rev*. **2002**, *102*, 2137–2160.

6 . Cheng, J.; Saliu, K.; Kiel, G. Y.; Ferguson, M. J.; McDonald, R.; Takats, J. *Angew. Chem. Int. Ed.* **2008**, *47*, 4910-4913.

7. (a) Arndt, S.; Spaniol, T. P.; Okuda, *Chem. Commun.* **2002**, 896-897. (b) Arndt, S.; Spaniol, T. P.; Okuda, J. *Angew. Chem., Int.Ed* .**2003**, *42*, 5075-5079.

8. (a) Evans, W. J.; Keyer, R. A.; Ziller, J. W. *Organomtallics* **1990**, *9*, 2628-2631. (b) Evans, W. J.; Keyer, R. A.; Ziller, J. W. *Organomtallics* **1993**, 12, 2618-2633.

9. Heeres, H. J.; Nijhoff, J.; Teuben, J. H.; Rogers, R. D. *Organometallics* **1993**, *12,* 2609-2617.

10. Forsyth, C. M.; Nolan, S. P.; Stern, C. L.; Marks, T. J.; Rheingold, A. L. *Organometallics* **1993**, *12*, 3618-3623.

11. Lee, L.; Berg, D. J.; Bushnell, G. W. *Organometallics* **1995**, *14*, 5021-5023.

12. Lee, L. Deprotonated Aza-Crown as Simple and Effective Alternatives to C_5Me_5 in Group 3, 4 and Lanthanide Chemistry. Ph.D Thesis, University of Victoria, British Columbia, Canada. **1997**.

13. (a) Heeres, H. J. Teuben, J. H. *Organometallics* **1991**, *10*, 1980-1986. (b) Evans, W. J.; Keyer, R. A.; Ziller, J. W. *Organometallics* **1993**, 12, 2618-2633. (c) Nishiura, M.; Hou, Z.; Wakatsuki, Y.; Yamako, T.; Miyamoto, T. *J. Am.Chem. Soc.* **2003**, *125*, 1184-1185. (d) Akita, M.; Yasuda, H.; Nakamura, A. *Bull. Chem. Soc. Jpn*. **1984**, *57*, 480- 487. (e) Yi, C. S.; Liu, N. *Organometallics* **1996,** *15,* 3968-3971.

14. Bambirra, S.; Meetsma, A.; Hessen, B. *Organometallics* **2006**, *25*, 3454-3462.

15. Ge, S.; Meetsma, A.; Hessen, B. *Organometallics* **2009**, *28*, 719-726.